

STOCHASTIC FINITE ELEMENT ANALYSIS
APPLIED TO SOIL MEDIA WITH UNCERTAIN
MATERIAL PROPERTIES

CENTRE FOR NEWFOUNDLAND STUDIES

**TOTAL OF 10 PAGES ONLY
MAY BE XEROXED**

(Without Author's Permission)

TERRY KEITH HODDINOTT



STOCHASTIC FINITE ELEMENT ANALYSIS APPLIED TO SOIL MEDIA
WITH UNCERTAIN MATERIAL PROPERTIES

BY

* Terry Keith Hoddinott, B.Eng.

A thesis submitted to the School of Graduate
Studies in partial fulfillment of the
requirements for the degree of
Master of Engineering

Faculty of Engineering and Applied Science
Memorial University of Newfoundland

December, 1986

St. John's

Newfoundland

Canada

Permission has been granted
to the National Library of
Canada to microfilm this
thesis and to lend or sell
copies of the film.

The author (copyright owner)
has reserved other
publication rights, and
neither the thesis nor
extensive extracts from it
may be printed or otherwise
reproduced without his/her
written permission.

L'autorisation a été accordée
à la Bibliothèque nationale
du Canada de microfilmer
cette thèse et de prêter ou
de vendre des exemplaires du
film.

L'auteur (titulaire du droit
d'auteur) se réserve les
autres droits de publication;
ni la thèse ni de longs
extraits de celle-ci ne
doivent être imprimés ou
autrement reproduits sans son
autorisation écrite.

ISBN: 0-315-37022-X

ABSTRACT

This thesis examines how material uncertainty influences the short term settlements and stresses of foundations. Expressing the uncertainty of material strength in terms of elastic modulus, the foundation and layered-soil-medium interaction is analyzed. Two soil models are examined: (i) an elastic, single phase, layered soil medium with undrained material properties and (ii) a piecewise linear elastic, single phase, layered soil medium approximating the nonlinear behaviour of soil. For the piecewise linear approximation, two shear-strain-dependent soil modulus relationships are included to differentiate between clays and sands.

Utilizing a two-dimensional plane strain triangular element, a stochastic finite element solution is formulated.

The procedure incorporates the elastic modulus variation by considering a linear two term Taylor series expansion of the equilibrium equations.

To limit the extent of errors induced by the omission of second order terms, the coefficient of variation (C.O.V.) for elastic modulus is assumed to be less than 30%. To model the degrees of interdependency between finite elements, a decaying exponential correlation distance function in

terms of the scalar distance between elements is used. Based on the definition of covariance combined with the linear two-term expansion for elastic modulus, the covariance of nodal displacements and the variance of element stresses are derived.

To model the stochastic finite element procedure, a FORTRAN computer code is developed for both linear and piecewise linear material elasticity. The displacements and stresses obtained from the plane strain analysis are considered as the mean values. Using the covariance of displacements and variance of stresses computed for selected nodes and elements, the resulting coefficients of variation are determined for actual displacements, relative displacements and stresses. A parametric analysis is carried out to establish the sensitivity of the stochastic finite element procedure to correlation distance, modulus C.O.V. and soil models. This type of analysis is defined as an upper bound due to its maximizing the material uncertainty. Also the random variation of material properties and its influence on displacements and stresses are examined by including a procedure to randomly vary the modulus C.O.V. from zero to maximum.

Two ocean structure cases are examined to verify the stochastic finite element formulation, viz., (i) the ~~Exocet~~

Tank and (ii) the Mobile Arctic Caisson (M.A.C.). The Ekofisk Tank is examined for gravitational loads and quasi-static wave loads representative of an actual storm. Gravitational forces and design ice forces are applied to the M.A.C. structure. In both cases, numerical results compare very well with those published in literature for the prototype structures, differing by less than 10% for most conditions.

The main conclusions from the parametric study of the stochastic finite element procedure for soil-structure interaction are:

- (i) The effect of elastic modulus uncertainty is more pronounced in the uncertainty of stresses than the displacements.
- (ii) As the correlation distance factor becomes large (greater than 10), the variation of displacements or stresses attributed to local material uncertainty is smaller. Under this condition the soil continuum is highly correlated.
- (iii) The proportion of uncertainty in results are insensitive to the varying loading conditions.

- (iv) The piecewise linear soil model provides closer agreement with the published data for prototype structures and yields lower coefficients of variation for displacements and stresses than the elastic model.

ACKNOWLEDGEMENTS

The author wishes to acknowledge the valued guidance and support received during the programme for the degree of Master of Engineering at Memorial University of Newfoundland. I am very grateful for the excellent guidance, continuous encouragement and financial support of my supervisor, Dr. A.S.J. Swamidas and former supervisor, Dr. M. Arockiasamy, Department of Ocean Engineering, Florida Atlantic University. I also wish to thank Dr. A.J. Christian for his early assistance, financial aid and his continued interest. The financial support provided through the NSERC (Natural Sciences and Engineering Research Council of Canada) and University fellowships are greatly appreciated, without which my studies would not have been possible.

Special thanks are due to Dr. K. Munaswamy who provided enormous help with computer programs and his experience in finite element analysis. Also, thanks are due to Mr. V. Neelakantan, who provided the graphics package used in generating many of the figures.

I wish to acknowledge the motivation and leadership shown by Dr. F.A. Aldrich, Dean of Graduate Studies, Dr. G.R. Peters, Dean of Engineering, and Dr. T.R. Chari,

Associate Dean of Engineering. I also wish to thank the University for providing many useful facilities during my graduate programme. The accessibility and quality of computer and library facilities on campus are especially noteworthy.

I thank Mr. Terry Dyer and Mrs. Margaret Michalak for their drafting work. Thanks are due to Mrs. Mary Brown for her careful typing of the draft and final manuscript.

Finally, I am especially grateful to my wife, Rennie, whose understanding and sacrifices made it possible to complete this thesis.

TABLE OF CONTENTS

	Page
ABSTRACT	ii
ACKNOWLEDGEMENTS	vi
TABLE OF CONTENTS	viii
LIST OF TABLES	xi
LIST OF FIGURES	xii
LIST OF SYMBOLS	xvi
CHAPTER 1 INTRODUCTION	1
CHAPTER 2 LITERATURE REVIEW	4
2.1 Concrete Gravity Platforms	5
2.1.1 Caisson Retained Islands	17
2.2 Platform Soil Foundation-Interaction	21
2.2.1 Foundation Sliding	22
2.2.2 Stability Modeling	26
2.2.2.1 Semi-Empirical Formulae for Bearing Capacity	26
2.2.2.2 Analytical Modeling of Stability	28
2.2.2.3 Comparison of Some Bearing Capacity Procedures	28
2.2.3 Deformation Modeling	28
2.2.3.1 Simple Settlement Relationships	29
2.2.3.2 Centrifuge Model Testing	29
2.2.3.3 Finite Element Method	31
2.2.3.4 Boundary Element Method	33
2.2.4 Effects of Material Uncertainty in Physical Models	34
2.2.4.1 Soil Uncertainty	36
2.2.4.2 Stability Models	42
2.2.4.3 Deformation Models	43
2.3 Proposed Research	50
CHAPTER 3 STOCHASTIC FINITE ELEMENT FORMULATION	54
3.1 Formulation of Nodal Displacement Covariance	56

3.1.1	Derivation of Covariance of Displacement	60
3.1.2	Correlation Coefficient Function	63
3.1.3	Variance of Relative Settlement	69
3.2	Formulation of Normal and Shear Stress Variance	72
3.3	Procedure for Soil Nonlinearity Model	77
3.3.1	Constitutive Laws for Soil Media	77
3.3.2	Stress-Strain Relationship	80
3.3.3	Numerical Implementation of Soil Nonlinearity	83
3.3.3.1	Fundamental Relationships	87
3.3.3.2	Piecewise Linear Analysis	88
3.4	Procedure for Random Stochastic Analysis	93
3.5	Computer Implementation of Stochastic Finite Element	97

CHAPTER 4 STOCHASTIC FINITE ELEMENT ANALYSIS OF SOIL-FOUNDATION INTERACTION FOR A CONCRETE GRAVITY PLATFORM 109

4.1	Introduction	109
4.2	Ekofisk Tank Description	111
4.2.1	Ekofisk Site Conditions	111
4.2.2	Finite Element Representation	115
4.2.2.1	Mean Material Properties for Finite Element Model	120
4.2.3	Load-Cases for Analysis of Platform	125
4.3	Linear Elastic Analysis	130
4.3.1	Vertical Displacement Results	133
4.3.1.1	Effect of Coefficient of Variation for Elastic Modulus	137
4.3.1.2	Effect of Correlation Distance Factor	143
4.3.2	Relative Displacement	148
4.3.3	Vertical Stress Distributions	156
4.3.3.1	Effect of Coefficient of Variation for Elastic Modulus	163
4.3.3.2	Effect of Correlation Distance Factor	169
4.3.4	Shear Stress Distributions	175
4.3.4.1	Effect of Coefficient of Variation for Elastic Modulus	178
4.3.4.2	Effect of Correlation Distance Factor	181
4.3.5	Random Stochastic Analysis	186
4.4	Piecewise Linear Elastic Analysis	195
4.4.1	Vertical Displacement Results	200
4.4.2	Vertical Stress Distributions	208
4.4.3	Shear Stress Distributions	215

CHAPTER 5 STOCHASTIC FINITE ELEMENT ANALYSIS OF SOIL-FOUNDATION INTERACTION FOR A CAISSON RETAINED ISLAND	222
5.1 Introduction	222
5.2 Mobile Arctic Caisson Island Description	225
5.2.1 Finite Element Representation	227
5.2.2 Mean Material Properties	229
5.2.3 Load Cases for Analysis	232
5.3 Linear Elastic Analysis	238
5.3.1 Nodal Displacement Analysis	240
5.3.2 Vertical Stress Distribution	246
5.3.3 Horizontal Stress Distribution	254
5.3.4 Random Stochastic Analysis	259
CHAPTER 6 CONCLUSIONS AND RECOMMENDATIONS	266
6.1 Conclusions	266
6.2 Contributions	269
6.3 Recommendations for Future Research	269
CHAPTER 7 REFERENCES	271
APPENDIX I Taylor Series Approximation of Nodal Displacement	283
APPENDIX II Taylor Series Approximation of Element Stresses	285
APPENDIX III Main Programs for Stochastic Finite Element Analysis	287
APPENDIX IV Subroutines for Stochastic Finite Element Analysis	312
APPENDIX V Gross Moment of Inertia for Ekofisk's Raft Foundation	374
APPENDIX VI Nodal Forces for Combined Gravity and Wave Loading at Ekofisk	377

LIST OF TABLES

Table	Title	Page
2.1	Gravity Structures in the North Sea (1973-1988)	6
2.2	Coefficients of Variation for Selected Soil Parameters	40
2.3	Coefficients of Variation for Stability Analysis of Gravity Platform	41
3.1	Strain-Compatible Soil Properties	86
3.2	Pseudo-Random Number Sequences Between 0,1	96
3.3	Main Computer Programs for Stochastic Finite Element Foundations	98
3.4	Outline of Main Program ELASTC.FTN	99
3.5	Outline of Main Program ELRAND.FTN	101
3.6	Outline of Main Program NONLIN.FTN	103
3.7	Outline of Main Program CAISON.FTN	105
3.8	Outline of Main Program RAND.FTN	107
4.1	Mean Material Properties at Platform Site	123
4.2	Calculation of Average Modulus of Elasticity for Upper 100 m of Seabed at Ekofisk	124
4.3	Nodal Forces for Piecewise Linear Analysis	196
5.1	Mean Material Properties at Tarsit P-45 Site	233

LIST OF FIGURES

Figure	Title	Page
2.1	Design Wave Heights for the North Sea	9
2.2	Ekofisk Tank (Doris)	10
2.3	Statfjord A (Condeep)	11
2.4	Cormorant A (Sea Tank)	12
2.5	Dunlin A (Andoc)	13
2.6	Maureen (Techomare)	14
2.7	Plan View of Gravity Platform Foundation Skirt Designs	15
2.8	Section View of Gravity Platform Foundation Skirt Designs	16
2.9	Single Steel Drilling Caisson (Dome)	19
2.10	Caisson Retained Island (Esso Resources)	19
2.11	Mobile Arctic Caisson (Gulf)	20
2.12	Possible Foundation Failure Modes	23
2.13	Principal Failure Modes for Sliding of Foundation	24
2.14	Foundation Sliding Failure Complicated by Local Site Conditions and Foundation Design	25
3.1	Random Variation of Soil Property about a Constant Mean	55
3.2	Autocorrelation Functions for Scalar Random Fields	65
3.3	Relative Settlement at Soil-Foundation Interface	70
3.4	Types of Stress-Strain Behaviour	79
3.5	In-Situ Shear Moduli for Saturated Clays	82
3.6	Typical Reduction of Shear Modulus with Shear Strain for Saturated Clays	84
3.7	Variation of Shear Modulus with Shear Strain for Sands	85
4.1	Ekofisk Tank; Horizontal and Vertical Sections	112
4.2	Grain-Size Distributions of Sand Samples from North Sea Platform Sites	114
4.3	In-situ Soil Profile, Ekofisk	116
4.4	Finite Element Mesh for Two-Dimensional Model	118
4.5	Load Cases for Platform	126
4.6	Load Forces on Nodes of Finite Element Representation of Tank Foundation	128
4.7	Correlation Coefficient Function for Ekofisk Tank	132
4.8	Mean Vertical Displacement of Soil-Foundation Interface	134
4.9	Vertical Displacement at Various Depths	136
4.10	Statistical Parameters for Vertical Displacement Due to Gravity Load	138

4.11	Statistical Parameters for Vertical Displacement Due to Gravity and Wave Loads	139
4.12	95% Confidence Interval for Vertical Displacement Due to Gravity Load	141
4.13	95% Confidence Interval for Vertical Displacement Due to Gravity and Wave Loads	142
4.14	Statistical Parameters for Vertical Displacement Due to Gravity Load	144
4.15	Statistical Parameters for Vertical Displacement Due to Gravity and Wave Loads	145
4.15a	Comparison of Stochastic Settlement Analysis	147
4.16	95% Confidence Intervals for Vertical Displacement Due to Gravity Load	149
4.17	95% Confidence Intervals for Vertical Displacement	150
4.18	Relative Settlement at Center: Gravity Load	152
4.19	Relative Settlement at Edge: Gravity Load	152
4.20	Relative Settlement at Center: Combined Load	154
4.21	Relative Settlement at Left Edge: Combined Load	154
4.22	Relative Settlement at Right Edge: Combined Load	155
4.23	Mean Vertical Stress at Soil-Foundation Interface	157
4.24	Vertical Stress at Various Depths	159
4.24a	Vertical Stress Variation at Center	161
4.24b	Vertical Stress Variation at Edge	162
4.25	Statistical Parameters for Vertical Stress Due to Gravity Load	164
4.26	Statistical Parameters for Vertical Stress Due to Gravity and Wave Loads	165
4.27	95% Confidence Interval for Vertical Stress Due to Gravity Load	167
4.28	95% Confidence Interval for Vertical Stress Due to Gravity and Wave Loads	168
4.29	Statistical Parameters for Vertical Stress Due to Gravity Load	170
4.30	Statistical Parameters for Vertical Stress Due to Gravity and Wave Loads	171
4.31	95% Confidence Intervals for Vertical Stress Due to Gravity Load	173
4.32	95% Confidence Intervals for Vertical Stress Due to Gravity and Wave Loads	174
4.33	Mean Shear Stress at Soil-Foundation Interface	176
4.34	Shear Stress at Various Depths	177
4.35	Statistical Parameters for Shear Stress Due to Gravity Load	179
4.36	Statistical Parameters for Shear Stress Due to Gravity and Wave Loads	180
4.37	Statistical Parameters for Shear Stress Due to Gravity Load	182
4.38	Statistical Parameters for Shear Stress Due to Gravity and Wave Loads	183
4.39	95% Confidence Intervals for Shear Stress Due to Gravity Load	184

4.40	95% Confidence Intervals for Shear Stress Due to Gravity and Wave Loads	185
4.41	Statistical Parameters for Vertical Displacement Due to Gravity Load	188
4.42	Statistical Parameters for Vertical Displacement Due to Gravity and Wave Loads	189
4.43	Statistical Parameters for Vertical Stress Due to Gravity Load	190
4.44	Statistical Parameters for Vertical Stress Due to Gravity and Wave Loads	191
4.45	Statistical Parameters for Shear Stress Due to Gravity Load	192
4.46	Statistical Parameters for Shear Stress Due to Gravity and Wave Loads	193
4.47	Elements Attaining EMIN Moduli Values for 100% Gravity Load	197
4.48	Elements Attaining EMIN Moduli Values for 100% Gravity and Wave Loads	198
4.49	Mean Vertical Displacement for Gravity Loads	201
4.50	Mean Vertical Displacement for Gravity and Wave Loads	202
4.51	Statistical Parameters for Vertical Displacement Due to 100% Gravity Load	204
4.52	Statistical Parameters for Vertical Displacement Due to 100% Gravity and Wave Loads	206
4.53	95% Confidence Intervals for Vertical Displacement	207
4.54	Mean Vertical Stress for Gravity Load	209
4.55	Mean Vertical Stress for Gravity and Wave Loads	210
4.56	Statistical Parameters for Vertical Stress Due to 100% Gravity Loads	211
4.57	Statistical Parameters for Vertical Stress Due to 100% Gravity and Wave Loads	212
4.58	95% Confidence Intervals for Vertical Stress	214
4.59	Mean Shear Stress for Gravity Load	216
4.60	Mean Shear Stress for Gravity and Wave Loads	217
4.61	Statistical Parameters for Shear Stress Due to 100% Gravity Load	218
4.62	Statistical Parameters for Shear Stress Due to 100% Gravity and Wave Loads	219
4.63	95% Confidence Intervals for Shear Stress	220
5.1	M.A.C. Schematic Cross-Section	226
5.2	Finite Element Mesh for Two-Dimensional Model	228
5.3	Loadings on Mobile, Arctic Caisson	230
5.4	Nodal Forces Representing Platform Live Load	236
5.5	Nodal Forces Representing Lateral Ice Force	237
5.6	Correlation Coefficient Function for M.A.C.	239
5.7	Mean Vertical and Horizontal Displacements at Datum Level	241
5.8	Vertical Displacements at Various Depths	243

5.9	Statistical Parameters for Vertical Displacement Due to Gravity Load	244
5.10	Statistical Parameters for Vertical Displacement Due to Ice and Gravity Loads	245
5.11	95% Confidence Interval for Vertical Displacement Due to Ice and Gravity Loads	247
5.12	Mean Vertical Stress at Datum Level	248
5.13	Vertical Stress at Various Depths	250
5.14	Statistical Parameters for Vertical Stress Due to Ice and Gravity Loads	251
5.15	95% Confidence Interval for Vertical Stress Due to Ice and Gravity Loads	253
5.16	Horizontal Stress at Datum Level	255
5.17	Statistical Parameters for Horizontal Stress Due to Gravity Load	257
5.18	Statistical Parameters for Horizontal Stress Due to Ice and Gravity Loads	258
5.19	95% Confidence Interval for Horizontal Stress Due to Ice and Gravity Loads	260
5.20	Statistical Parameters for Vertical Displacement Due to Ice and Gravity Loads	262
5.21	Statistical Parameters for Vertical Stress Due to Ice and Gravity Loads	264
5.22	Statistical Parameters for Horizontal Stress Due to Ice and Gravity Loads	265
V.1	Subdivisions of Raft Foundation	375
VI.1	Vertical Nodal Force Derivation	378

LIST OF SYMBOLS

a	coefficient for correlation function dependent upon in-situ soil conditions
A	net foundation area
B	platform or foundation width
[B]	strain displacement matrix dependent on element geometry
BEM	boundary element method
c	soil cohesion
c	distance from extreme fibre to bending axis
CDF	correlation distance factor
c.o.v.	coefficient of variation, ratio of standard deviation to the mean
Cov(E _i , E _j)	covariance of elastic moduli between elements i and j
Cov(U _i , U _j)	covariance of displacement between any two nodal displacements, U _i and U _j
[D]	elastic constituent matrix
D _s	skirt depth
E, E _i	elastic modulus, modulus of element i
\bar{E}	mean elastic modulus
E _j	updated elastic modulus for iteration j
E _{min}	minimum expected elastic modulus
E _o	initial elastic modulus for piecewise linear analysis
(F)	external force vector
f'c	average concrete compressive strength

FEM	finite-element method
G	shear modulus
G_j	modified shear modulus for iteration j
G_0	initial shear modulus based on E_0
G_u	undrained shear modulus
H	horizontal force
$(H)_{ij}$	predefined function denoting the difference between actual stress and expected stress vectors
I	gross moment of inertia
I.F.	influence factor
$[K], [\bar{K}]$	stiffness matrix, mean stiffness matrix
L	product of correlation distance factor and foundation width
M	overturning moment
M.A.C.	Mobile Arctic Caisson
N	total number of elements (or nodes) in the discretized domain
N_c, N_q, N_g	bearing capacity factors for soil cohesion, surcharge and effective soil weight and foundation width, respectively
P	distributed soil pressure
$p(E_i, E_j)$	joint probability density function for moduli, E_i and E_j
$p(U_i, U_j)$	joint probability density function for displacements, U_i and U_j
q	uniform surcharge around foundation
q_u	ultimate bearing capacity
r, r_{ij}	scalar distance between two element centroids of elements i and j

R_i	random number between zero and unity
RF	reduction factor as per Table 3.1
(S)	stress vector, $(\sigma_x, \sigma_y, \tau_{xy})$
S_0	starting value for pseudo-random number generator
s_u	undrained shear strength
S.F.	safety factor
t	soil layer thickness
(U), $\langle U \rangle$	nodal displacement vector, mean nodal displacement vector
V	vertical force
Var(U_i)	variance of displacement at node i
Var($\sigma_x, \sigma_y, \tau_{xy}$)	variance of normal stresses and shear stress
γ'	effective soil weight
γ_{max}	maximum shear strain
γ_{xy}	shear strain in cartesian coordinates
δ_{ij}	Dirac delta function
ϵ_x, ϵ_y	normal strains in cartesian coordinates
ϵ_1, ϵ_2	principal strains (maximum, minimum)
(ϵ)	strain vector
λ	modulus coefficient of variation
μ	statistical mean value
ν	Poisson's ratio
$E_i E_j$	correlation coefficient of elastic moduli between elements i and j
σ, σ_{E_i}	standard deviation, e.g. standard deviation of elastic modulus for element i
σ^2	variance

σ_x, σ_y normal stresses in cartesian coordinates

σ_1, σ_2 principal stresses (maximum, minimum)

τ_{\max} maximum shear stress

τ_{xy} shear stress in cartesian coordinates

ϕ angle of internal friction

Δu_{ij} relative settlement between nodes i and j

CHAPTER 1

INTRODUCTION

The advancement of new technologies can usually be attributed to a couple of principal proponents, establishing the necessary impetus and funding to support such research. The achievements in the space industry through the backing of major governments have created numerous spin-off technologies in its wake; some of those being computer hardware systems, robotics and materials science breakthroughs. Similarly the oil industry has been the chief driving force of new developments in marine offshore structures. With depleting land based sources of hydrocarbons and minerals, the exploration and extraction of these resources from subsea sites is necessary for society to maintain its present standard of living.

Recent exploration and development of offshore energy and mineral resources in increasingly deeper waters has required larger offshore gravity structures. To make similar developments in northern frontiers like the Beaufort Sea feasible, structural designers are required to produce fixed year-round drilling and production platforms, such as caisson retained islands. The novelty of these types of construction projects has meant limited availability of information on soil-structure interaction behaviour. These

structures are subjected to more hostile environmental forces which are nonperiodic in nature, thereby increasing the level of uncertainty in their design. Uncertainties arise from several sources, (i) the unpredictable wave, wind and, in some instances, ice or pack ice loadings; (ii) the lack of understanding and experience of the physical response mechanisms of these novel systems; and (iii) the variation of actual material properties from the design values. This latter problem is especially relevant to uncertainty and spatial variation of geotechnical properties in the offshore, leading to increased uncertainties inherent with the foundation design. Furthermore, physical limitations and large expenses associated with obtaining detailed geotechnical properties at deep sea or Arctic drill sites, restricts the amount and quality of test results available to the designer. To make the most use of the limited data, the offshore structural designs should incorporate probabilistic procedures.

The previous design procedure has been to assign a large factor of safety to compensate the inadequate understanding of the soil-structure interaction. However, this practice could lead to structural members or the soil medium being overstressed under actual loadings. Therefore, the designer must identify the significant sources of uncertainty and properly assess the effect on structural re-

sponse. One of the more significant sources of uncertainty is the randomness associated with the material characteristics. The proposed research shall be restricted to analysing the influence of this type of uncertainty on the stresses and deformation on the soil. The application of procedures developed herein are equally valid for other sources of uncertainty such as loadings.

CHAPTER 2

LITERATURE REVIEW

The need to address randomness of material properties is especially relevant to offshore structures. With the high costs and risks associated with these projects, it is prudent to investigate the effects of material uncertainty on the structural performance. One of the more significant sources of uncertainty is the variation of soil properties.

In this chapter, a general overview of concrete gravity platforms and caisson retained islands is provided. The current procedures for investigating the soil-structure interaction (i.e. foundation sliding, stability modeling, deformation modeling) are summarized. A state-of-the-art review of methods of measuring the uncertainties and how it relates to the structural stability analysis is examined. This is followed by an outline of the proposed research.

2.1 Concrete Gravity Platforms

The first modern fixed offshore platform was a steel template (jacket) type installed in the Gulf of Mexico during 1947. The soft clayey sediments in the Gulf of Mexico had made it mandatory for pile support to prevent excessive settlement of the platform during operation. With the 1969 discovery of the Ekofisk oil field in the North Sea, the beginning of a new category of fixed offshore platforms was initiated. In regions where hard soil conditions existed and pile driving was more difficult, the concrete gravity structures were preferred. This alternate form of fixed offshore platform was designed to remain on location by virtue of self-weight. The favourable soil conditions of the North Sea contributed to the selection of concrete gravity base structures for most production sites (Eide and Andersen [1], Dawson [2], Bech and Haugsden [3], and Hoeg [4]).

Recent reviews of the concrete gravity platform development have been prepared by Eide and Andersen [1], Graff [5] and Graff and Chen [6]. The majority of deep water gravity structures are located in the North Sea. Table 2.1 shows a list of these platforms installed in the northern sector of the North Sea from 1973 to 1984. As indicated in Table 2.1, two additional Condeep platforms are

TABLE 2.1 Gravity Structures in the North Sea (1973-1988)

Type	Name	Water Depth (m)	Submerged Weight (10^6 kN)	Foundation Area (m^2)	Soil Properties
Doris	Ekofisk	70	1.9	7,400	Fine dense silty sand
Condeep	Beryl A	120	1.7	6,200	Fine dense silty sand (0-10 m) overlying very stiff silty clay
Condeep	Brent B	140	1.7	6,200	Stiff silty clay with interbedded sand layers
Doris	Frigg CDP-1	98	1.8	5,600	Fine dense silty sand (8 m) overlying stiff silty clay
Sea Tank	Frigg TP-1	104	1.8	5,600	Fine dense silty sand (3-7 m) overlying stiff silty clay
Doris	Frigg Manifold	94	1.8	5,600	Fine dense silty sand
Condeep	Brent D	140	1.8	6,300	Stiff silty clay with interbedded sand layers
Condeep	Statfjord A	145	2.0	7,800	Stiff silty clay with 2-10 cm sand cover
Andoc	Dunlin A	153	2.0	10,600	Stiff silty clay with interbedded sand layers

TABLE 2.1 (continued)

Type	Name	Water Depth (m)	Submerged Weight (10^6 kN)	Foundation Area (m^2)	Soil Properties
Condeep	Frigg TCP-2	102	1.6	9,300	Fine dense silty sand (3-6 m) overlying stiff silty clay
Doris	Ninian Central	136	3.2	15,400	Stiff silty clay with interbedded sand layers
Sea Tank	Cormorant A	150	2.3	9,700	Stiff silty clay with interbedded sand layers
Sea Tank	Brent C	140	1.6	10,100	Stiff silty clay with interbedded sand layers
Condeep	Statfjord B	145	3.7	18,200	Stiff clay with 0.2-1.5 m sand cover
Tecnomare	Maureen	96	1.5	4,350	Stiff clay with 2-6 m sand cover
Condeep	Statfjord C	146	3.9	12,770	Stiff clay with 0-3 m sand cover
Condeep	Gullfaks A	133	3.9	11,000	3 m moraine material above stiff clay
Condeep	Gullfaks B	143	3.0	8,700	Dense sand

planned for 1986 and 1988. These gravity structures are all located in favourable foundation soils, ranging from dense sand to very stiff clays. The depth of water ranges from 70 m for the Ekofisk Tank to 153 m for Dunlin A. The maximum design wave heights vary from 24 m for the Ekofisk Tank to 31.2 m for Ninian Central (Figure 2.1).

From the over twenty platform concepts envisioned by engineers, there are basically four concrete designs (Doris, Condeep, Sea Tank, Andoc) and one steel design (Tecnmare) presently operating in the North Sea. The fundamental shapes of these five designs are indicated in Figures 2.2 to 2.6. The concrete platforms are constructed almost entirely of various shells of large dimensions known as caissons with two, three or four hollow-concrete towers that support prefabricated deck facilities.

Another feature to distinguish the four main designs is the caisson base shape. The principal source of this distinction is the skirt design. As indicated in Figures 2.7 and 2.8, the skirt system selected will vary from type of platform site and soil conditions. With the exception of Ninian Central, the Doris platforms are flat slabs with virtually no skirts.



FIGURE 2.I DESIGN WAVE HEIGHTS FOR THE NORTH SEA

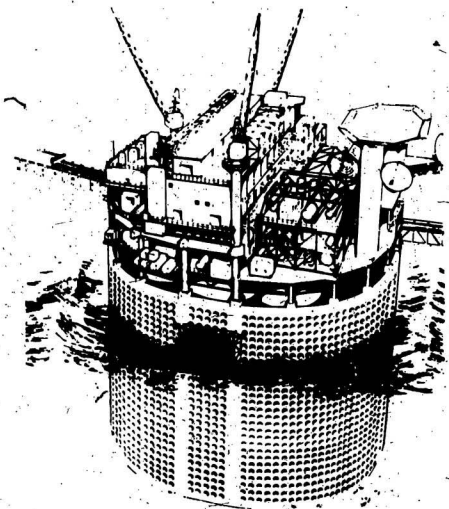


FIGURE 2.2 EKOISK TANK (Doris)

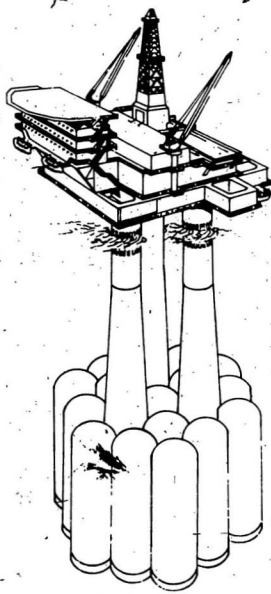


FIGURE 2.3 STATFJORD A (Condeep)

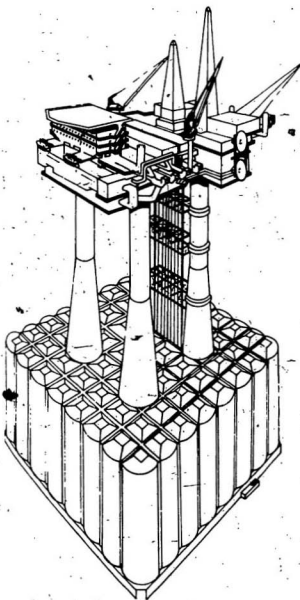


FIGURE 2.4 CORMORANT A (Sea Tank)

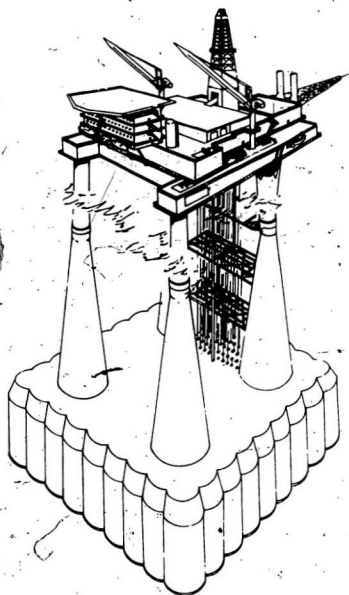


FIGURE 2.5 DUNLIN A (Andoc)

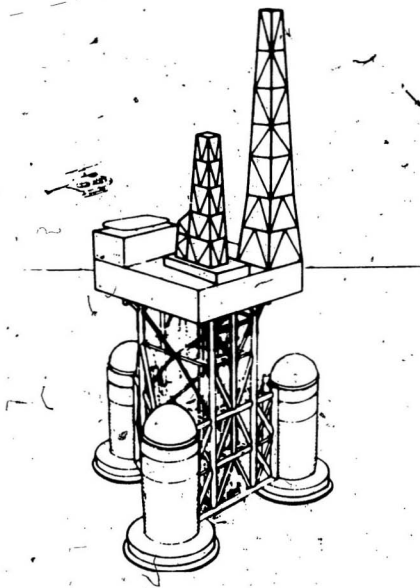
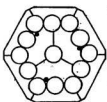
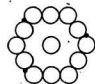


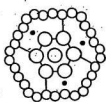
FIGURE 2.6 MAUREEN (Tecnómare)



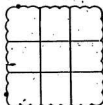
Condeep Frigg TCP2



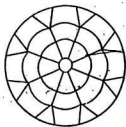
Condeep Beryl A
Condeep Brent B
Condeep Brent D



Condeep Statfjord A



Andoc Dunlin A

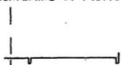


Howard-Doris
Ninian Central

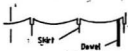
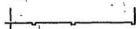
• dowel location

FIGURE 2.7 PLAN VIEW OF GRAVITY PLATFORM FOUNDATION SKIRT DESIGNS

Centerline of Platforms



Sea Tank: Frigg TP-1

Condeep: Beryl A
Brent B and D

Doris: Ekofisk Tank

Doris: Frigg Manifold
Frigg CDP-1

Condeep: Statfjord A



Condeep: Frigg TCP-2

Sea Tank: Brent C
Cormorant A

Andoc: Dunlin A



Doris: Ninian Central



FIGURE 2.8 SECTION VIEW OF GRAVITY PLATFORM FOUNDATION SKIRT DESIGNS

2.1.1 Caisson Retained Islands

During the 1960's, oil and gas exploration in the Beaufort Sea had been successful in finding hydrocarbon deposits of commercial potential. The Beaufort Sea - MacKenzie Delta Environmental Impact Statement (volume 2) [7] summarized the development systems proposed and currently in operation in the Beaufort Sea. Hnatiuk and Felzien [8] presented a brief up-to-date review of the Arctic offshore activity. Several techniques were used to drill wells in the Beaufort Sea such as artificial islands, ice-reinforced drillships and conical drilling units (e.g. Kulluk). Discussion here will be limited to artificial islands.

In 1973, the first alternative to seasonal drilling was the construction of a gravel-filled man-made island in a water depth of 3 m. By the end of 1984, twenty-two surface piercing islands had been constructed in the Beaufort, to a maximum of 18 m water depth. But this type of facility is restricted to shallow water depths with abundant borrow material in the vicinity. The high construction cost for an artificial island above a 20 m height is the primary reason for this restriction.

To make exploration and production feasible in deeper waters year-round, a new technology had to be developed. The caisson retained island is a sound solution to this problem, being the next logical hybrid artificial island structure. The caisson island is mainly for water depths ranging from 15 m to 40 m. The caisson is essentially a continuous steel or concrete annulus resting on a carefully constructed sand berm. The interior of the caisson is filled with sand which will provide a substantial portion of the lateral resistance to ice forces. The caisson structure itself is used for ballasting the structure and for supporting the deck carrying production and drilling facilities. The main criterion for making the caisson concept feasible is the requirement of being able to re-use the caissons at several other locations once the work is completed at the present site.

The construction of caisson islands began in 1982 with Dome's SSDC - Single Steel Drilling Caisson (Brophy [9]), 1983 with Esso's prestressed concrete CRI - Caisson-Retained Island (Mancini et al. [10]) and 1984 with Gulf's M.A.C. - Mobile Arctic Caisson (Jeffries et al. [11]). Dome's SSDC, Esso's CRI and Gulf's M.A.C. are shown in Figures 2.9, 2.10 and 2.11 respectively.

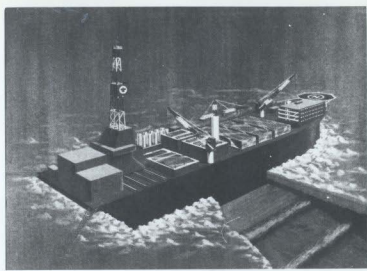


FIGURE 2.9 SINGLE STEEL DRILLING CAISSON (DOME)

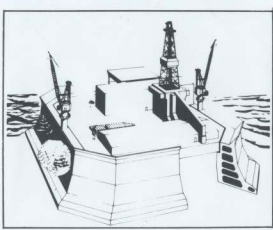


FIGURE 2.10 CAISSON-RETAINED ISLAND
(ESSO RESOURCES)

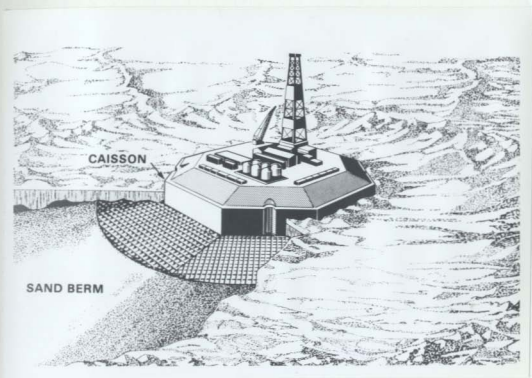


FIGURE 2.11 MOBILE ARCTIC CAISSON (GULF)

2.2 Platform Soil-Foundation Interaction

Concrete gravity structures depend upon single or multiple raft foundations bearing on the unprepared ocean floor to provide stability against the maximum environmental loads imposed on the structures. These structures rely principally on their submerged self-weight and skirt designs for resistance to vertical and horizontal forces. In the same manner, caisson retained islands depend on their large mass and horizontal shear resistance of the core and berm materials for stability. For analytical purposes the caisson retained island's soil-foundation interaction can be considered to fundamentally behave as the concrete gravity structures. How a foundation interacts with the seabed is of primary importance in evaluating a platform's performance. The foundation design must have adequate capacity for the following possible failure modes: (i) sliding failure of the base along the soil surface, (ii) sliding failure of soil foundation at subsurface sand-clay layer interfaces, (iii) actual bearing capacity failure of the soil with a ruptured boundary beneath the foundations, (iv) failure of the soil through cyclic loadings such as wave or seismic affecting platform performance through rocking motions or soil liquefaction of sand deposits, (v) instability of the foundation due to excessive scouring of the soil, and (vi) unacceptable deformation of the soil either

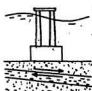
in total or differential settlements (Figure 2.12). The necessity of accurate and reliable geotechnical models to describe these various failure modes have challenged design and geotechnical engineers. During the past half century, especially the past two decades, much research has been performed on these topics. Several scientific procedures have been utilized to gain insight into these failure mechanisms, such as: semi-empirical formulae, elasticity and plasticity theories, centrifuge model testing, finite element analysis and boundary element procedures.

2.2.1 Foundation Sliding

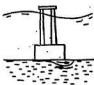
Young et al. [12] summarized the main types of foundation failure for gravity platforms resulting from insufficient sliding resistance. The potential failure mode, depended primarily on the skirt height and shape, the net vertical force, and the soil profile's strength properties. The principal failure modes were passive wedge failure, deep passive failure and sliding base failure (Figure 2.13). Site conditions and skirt designs would complicate the failure pattern as shown in Figure 2.14. Eide [13] provided simple formulae for evaluating the safety factor for horizontal sliding for sand and clay deposits.



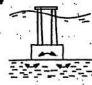
(1) Sliding along base



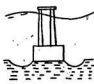
(2) Sliding at sand-clay layer



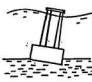
(3) Ruptured Soil boundary



(4) Rocking

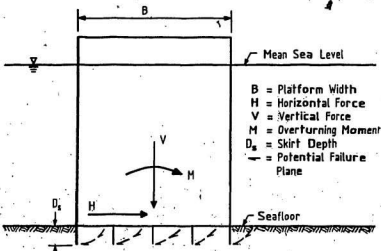


(5) Excessive scouring



(6) Large differential settlements

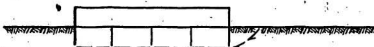
FIGURE 2.12 POSSIBLE FOUNDATION FAILURE MODES



(1) Passive Wedge Failure

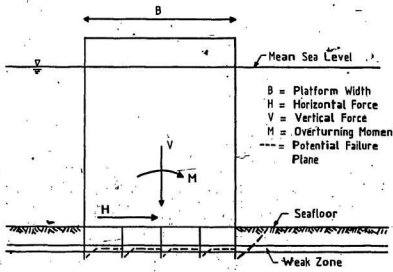


(2) Deep Passive Failure

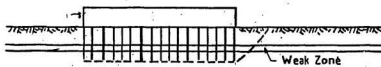


(3) Sliding Base Failure

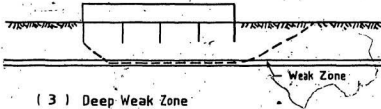
FIGURE 2.13 PRINCIPAL FAILURE MODES FOR SLIDING OF FOUNDATION



(1) Shallow Weak Zone With Widely Spaced Skirts



(2) Closely Spaced Skirts to Avoid Failure in Shallow Weak Zone



(3) Deep Weak Zone

FIGURE 2.14 FOUNDATION SLIDING FAILURE COMPLICATED BY LOCAL SITE CONDITIONS & FOUNDATION DESIGN

2.2.2 Stability Modeling

The stability analysis and foundation design of a gravity platform are vital in ensuring safety and convenient operation on site. The preliminary designs are based on the classical bearing capacity and settlement theories. Once stability is assured, more elaborate analyses by complex geotechnical principles are performed.

2.2.2.1 Semi-Empirical Formulae for Bearing Capacity

The most accepted model is the semi-empirical model using superposition of cohesive, overburden, and frictional resistances, based partly on theoretical work and partly on empirical research. This superposition method had been initially proposed by Terzaghi [14] and later developed by Terzaghi and Peck [15]. An ultimate bearing capacity equation for a vertically and concentrically loaded strip foundation supported on a homogeneous soil had been given as,

$$q_u = N_c c + N_q q + 0.5B\gamma'N_f \quad (2.1)$$

where

q_u = ultimate bearing capacity

c = soil cohesion

q = uniform surcharge around foundation

B = foundation width

γ' = effective soil weight

N_c, N_q, N_s = bearing capacity factors

Modifications of this formula were proposed by Meyerhof [16], Vesic [17], Hansen [18], and Bjerrum [19].

Meyerhof [20] investigated the ultimate bearing capacity of footings situated on layered soil media. Similar investigations of bearing capacity of layered soil systems were considered by Reddy and Srinivasan [21], Brown and Meyerhof [22], and Mitchell et al. [23].

Vesic [24] provided a "state-of-the-art" review of the bearing capacity of shallow foundations on homogeneous soils, loaded centrally and vertically. A presentation of all the major contributors to the subject prior to 1971 was given with a commentary on best solutions, appropriate factors and coefficients for bearing capacity formulae, and shortcomings of available theories.

2.2.2.2 Analytical Modeling of Stability

As the amount and quantity of geotechnical information improves, the need for stability analysis by more sophisticated theories is realized. The method of slices is the basis for a number of procedures. Typically, these methods assume several trial failure surfaces and determine the one with the lowest factor of safety. Several versions of method of slices are available, with the main differences being in the treating of the physical system's indeterminacy (Janbu et al. [25] and Murff and Miller [26]).

2.2.2.3 Comparison of Some Bearing Capacity Procedures

Lauritzen and Schjetne [27] presented a general discussion of bearing capacity stability calculations for offshore gravity structures placed on clay deposits. Saxena et al. [28] examined the available methods for the prediction of the ultimate bearing capacity of large offshore gravity structures on layered subsoils.

2.2.3 Deformation Modeling

Another important aspect of soil-structure interaction is the deformation modeling of the soil surface. Total settlement, differential settlement, short term settlement,

shakedown phenomenon, storm induced settlement and consolidation behaviour, all have to be considered for the offshore gravity platforms. Excessive unpredicted displacements can lead to serious overstressing of the raft foundation, tilting of the structure affecting performance level, and possible fracture of connecting equipment such as pipelines. The procedures available range from the simple elastic formulae to the complex centrifuge model tests and the numerical finite element method.

2.2.3.1 Simple Settlement Relationships

Prediction formulae for vertical, horizontal and rotational movements based on the elastic properties of modulus of elasticity and Poisson's ratio for the soil medium were proposed by Young et al. [12]. Poulos and Davis [29] summarized other solutions including the effects of a layered soil system, soil anisotropy and foundation shape. Baecher et al. [30] reviewed some of the simple settlement formulae for immediate settlements that assume rapid, complete drainage.

2.2.3.2 Centrifuge Model Testing

The absence of foundation performance data for large offshore gravity platforms make the research on model

testing an important information source. Models at a fraction of the prototype size, provide clues as to how the actual platform will respond to complex and varied loadings and soil conditions. It is a means for the designer to verify the prototype design or to make modifications that will improve performance.

For modeling procedures to accurately predict the prototype behaviour, the model system must have geometric, kinematic, and dynamic similarity with the prototype. To achieve all three types of similitude in a one-gravity model is not possible. Many of these problems can be overcome through multi-gravity modeling in a centrifuge. This centrifuge model is particularly adaptable for geotechnical simulation of cyclic loading, using model soil that will behave with the same stress-strain properties as the in-situ soil. Most of the model soils are limited to the undrained state.

Jean H. Prevost at the California Institute of Technology, U.S.A., and P.W. Rowe at Manchester University, U.K., are two of the foremost researchers in centrifuge modeling. Both have independently conducted centrifuge model tests of offshore gravity platforms. Prevost et al. [31, 32] utilized both analytical calculations and centrifuge model tests in examining the soilstructure

interaction problem for offshore gravity structures placed on normally consolidated clay deposits. Rowe and Craig [33] presented some of the results of centrifugal model tests of four gravity structures, two resting on overconsolidated clay with an intercalated weaker layer close to the seabed level, and two situated on normally consolidated sand.

Anderson et al. [34] reported on the combined experimental efforts of centrifuge model testing at Manchester University and the analytical experience of the Norwegian Geotechnical Institute.

2.2.3.3 Finite Element Method

The finite element method plays an important role in foundation design of offshore gravity platforms. Its versatility in geotechnical applications makes the finite element method a valuable asset in predicting platform foundation behaviour under a wide range of conditions. The procedure is equally applicable to static - dynamic situations, two-dimensional or three-dimensional problems, linear - nonlinear material properties, homogeneous-heterogeneous soil conditions, and simple - complex foundation shapes.

Young et al. [12] presented a summary of a two-dimensional nonlinear finite element method analysis of a platform foundation. They compared the results of FEM with and without a weak soil layer to elastic theory for both soil profiles. Typically, the foundation movements computed by finite elements were smaller than those computed by elastic theory.

Zienkiewicz et al. [35] examined a range of factors to be considered in the application of the finite element method to the solution of elasto-plastic static and transient soil mechanics problems. Their work included stability analysis and settlement, both immediate and time-dependent, for offshore gravity platforms considering drained and undrained soil conditions. The effects of cyclic loading and consolidation were found to be important in foundation analysis and were examined by Andersen et al. [36].

The soil-foundation interaction behaviour of various types of offshore structures could be illustrated with the numerical techniques of FEM. Broughton [37] modeled a concrete gravity platform and a hybrid steel jacket platform with cellular concrete raft foundation, both being subjected to gravity loads and design storm wave forces. The wave loadings were treated in a quasi-static manner through the

application of maximum horizontal thrust and maximum overturning moment associated with the storm wave. The analysis consisted of the contact stresses of the structure and soil due to both gravity and wave forces, as well as model displacements including short term "elastic" settlements, long term consolidated settlements under gravity loads, and immediate storm settlements resulting from wave action. Other researchers have utilized FEM in the analysis of gravity structure foundations (Vaughan et al. [38], Prevost et al. [39], and Whitman [40]).

2.2.3.4 Boundary Element Method

The boundary element method, BEM, also known as the boundary integral equation method, is a powerful numerical procedure with applications in many branches of science and engineering. The basis for this procedure lies in the integral equation formulation of a given boundary value problem, originating from applications of Green's functions in mathematics. Rather than discretization of the entire domain of the body as in FEM, only the boundary or surface discretization is required for BEM. Crouch and Starfield [41] applied BEM to problems in rock mechanics and geological engineering, such as rock joints, stratified media, underground excavations, and mining operations in faulted ore deposits.

Hobbs et al. [42] described the main numerical methods for foundation analysis with special application to offshore structures. In addition to the simple "desk-top" studies of semi-empirical formulae and limit equilibrium procedures, detailed analyses were performed through computer models such as finite element and boundary element methods. Comparison of FEM and BEM for a plane strain analysis of a footing on uniform soil with a vertical load, provided reasonable agreement.

2.2.4 Effects of Material Uncertainty in Physical Models

The need to incorporate material uncertainties into deterministic analysis procedures has been realized over the past three decades. The analysis of structural response to random excitations is now well established with the development of both stochastic and spectral analysis techniques. But the study of physical systems with random material characteristics is still being developed. It has long been realized that due to the inability to precisely define physical parameters of materials, a range of values indicating the degree of variation expected, would more adequately describe the possible system behaviour. One of the earliest studies on this topic was the work of Samuels and Eringen [43]. Using a perturbation solution procedure, linear stochastic differential equations with small randomly

varying parameters were examined for statistical properties of mean and autocovariance. Two other special cases were also investigated, (i) equations with slowly varying random coefficients, and (ii) equations containing only one random coefficient.

Collins and Thomson [44] considered the problem of treating as deterministic, dynamic systems which do not have well-defined material properties. The random nature of these properties could produce significant variations in the system performance from the mean value response. Collins and Thomson examined an undamped free vibration multi-degree-of-freedom system in matrix form. In applying a perturbation of the eigenvalues and eigenvectors, the system elements were expressed in terms of a covariance matrix, permitting the statistical correlation of elements to be included throughout the formulation. The matrix approach permitted the application of the procedure to a broader class of eigenvalue and eigenvector problems.

Chen and Soroka [45] investigated the response of a single-degree-of-freedom system of a harmonic oscillator with random parameters. Using a perturbation method, the impulse response function of the second-order random differential equation of motion was examined. In the procedure, the natural frequency was analyzed as a random

parameter represented by a mean value plus a perturbation portion having a random distribution with zero mean. Chen and Soroka [46] applied the same perturbation technique to multi-degree-of-freedom dynamic systems with statistical properties. Second-order statistical moments of the response solution were found to be correlated to the variations in eigenvalues and eigenvectors which in turn were dependent on the variance of the system properties. A numerical example using a random earthquake loading as the exciting force was applied to the procedure. Their analysis indicated that the probabilistic response resulted in larger response values than the standard deterministic response.

2.2.4.1 Soil Uncertainty

The application of stochastic material properties to soil foundation problems has been receiving recent research attention. Christian [47] prepared a state-of-the-art review of probabilistic soil dynamics. Christian categorized the study of probabilistic soil problems into four major areas, (i) random vibration in soil-structure interaction, (ii) sensitivity analysis, parameter evaluation and reliability determination of analytical procedures, (iii) studies of field behaviour of soils and (iv) probabilistic description of load and material properties. Baecher et al. [30] compiled a comprehensive review of geotechnical

reliability studies of offshore gravity platforms. They provided discussions on the various sources of uncertainty in offshore design including quantitative estimates of the uncertainty for environmental loads, soil exploration programs, and geotechnical models. The study indicated that although complete probabilistic analysis was not possible, the current techniques of risk and reliability analysis did provide a strong analytical framework for making rational decisions in design and implementation.

Examination of soil property variation by Lumb [48] indicated that a Gaussian statistical distribution will adequately model the material randomness. Four natural soils were discussed, these being a soft marine clay, an alluvial sandy clay, a residual silty sand, and a residual clayey silt. Atterberg limits, grain size, strength and compressibility characteristics were shown to follow normal, log-normal or bi-normal distributions.

Engineering problems involving probabilistic analysis of stability and deformation of soil foundations and embankments were discussed by Cornell [49]. Cornell noted three significant sources of soil uncertainty, (i) variation in the soil properties attributed to the natural spatial variation, (ii) discrepancies between the soil property measured and the actual value due to sample disturbance and

errors of the testing procedure, and (iii) uncertainty in the engineering theory applied to the problem. He provided a formulation for practical first-order uncertainty analysis using approximate means and variances for both two and three dimensional spatial variation of material properties. Cornell proposed an exponential decay correlation function which was dependent on spatial scalar distance between location points and a correlation distance parameter.

Vanmarcke [50] examined the use of a probabilistic soil profile description to simulate the natural variability of the soil both horizontally and with depth. The natural soil heterogeneity could be the result of different mineral composition, changing stress history, varying water contents, as well as different geologic formations. For a probabilistic soil profile, the profile characteristics were treated as a random function in the three principal directions. Vanmarcke suggested the use of three parameters to describe the random nature: average value, standard deviation and scale of fluctuation which measures the distance within which the soil property shows a relatively strong correlation between neighboring points. Using a procedure of averaging a soil property over a volume, similar to Cornell's work, Vanmarcke investigated the relationships between parameters such as size of variation or fluctuation from the mean trend and the types of correl-

ation functions for describing the soil medium's random, nature.

In studying the process of parameter variability in foundation engineering, Tang [51] applied Bayesian statistical concepts. This method of systematically combining various sources of information leading to the estimation of a parameter would provide more accurate predictions with minimum cost. Tang explained the proper usage of the Bayesian approach through several illustrative examples.

Meyerhof [52] stated that in the absence of premature soil failure, the safety factors in offshore foundation design were controlled primarily by the degree of variability and uncertainty in the applied loads and soil resistance, as well as the assumptions and simplifications of the stability analysis. Meyerhof estimated the following coefficients of variation (C.O.V.): (i) for maximum wave and wind-loads, a C.O.V. of about 0.2, (ii) for static cone penetration tests on sand or clay, a C.O.V. ranging from 0.2 to 0.3, (iii) for undrained shear strength of clay at shallow depth, a C.O.V. of 0.3 and (iv) for undrained shear strength of clay at great depth a C.O.V. of 0.4. With large-scale tests, Meyerhof suggested that these coefficients were likely to be smaller. In Table 2.2 other researchers indicated the expected ranges of C.O.V. for some

TABLE 2.2: Coefficients of Variation for Selected Soil Parameters

Soil Type	Property	C.O.V. (%)	Reference
Clay	liquid limit	6.0	Lumb [53]
	plastic limit	2.0	
Residual Soils	cohesion (D)	13.5	
Undisturbed	cohesion (CU)	19.9	
	cohesion (UU)	18.8	
	$\tan \phi$ (D)	1.6	
	$\tan \phi$ (CU)	9.8	
	$\tan \phi$ (UU)	22.3	
Residual Soils	cohesion (D)	24.0	
(compacted)	cohesion (CU)	26.9	
	cohesion (UU)	25.5	
	$\tan \phi$ (D)	2.1	
	$\tan \phi$ (CU)	6.8	
	$\tan \phi$ (UU)	5.4	
Glacial Tills (various)	unconfined strength	14.7 31.0	Morse [54]
Gravelly Sand	porosity	18.8	
	void ratio	29.6	
	$\tan \phi$	7.3	
Coarse Sand	porosity	9.8	
	void ratio	16.0	
Medium Sand	porosity	10.1	
	void ratio	17.5	
Fine Sand	porosity	8.0	
	void ratio	13.3	
Clay	water content	12.9	
	liquid limit	22.1	
	plastic limit	15.7	
	coefficient of modulus of compressibility	28.4	
Marine Clay	cohesion	18.4	
London Clay	cohesion	16.2	
Silty Sand	$\tan \phi$ (drained)	13.8	
Ottawa Sand (dense)		12.5	
Coulomb c- ϕ Soils	liquid limit	6-11	
	plastic limit	8-11	
	water content	6-29	
	dry density	2-4	

TABLE 2.2: (Continued)

Soil Type	Property	C.O.V. (%)	Reference
Inorganic Clay	cohesion (UU)	15.0	Singh [56]
(High Plasticity)	ϕ (UU)	56.0	
	cohesion (DS)	63.0	
	ϕ (DS)	10.4	
Inorganic Clay	cohesion (UU)	22.0	
(Low Plasticity)	ϕ (UU)	19.0	
Fine Sand	ϕ (DS)	3.0	
	ϕ (UU)	12.0	
	ϕ (DS)	2.5	
Fine Sand	$\tan \phi$	5-13	Schultze [57]
Coarse Sand	$\tan \phi$	8-14	
Glacial Till	cohesion	~31	Kraft and
London Clay	cohesion	19-32	Murff [58]
Bangkok Clay	cohesion	11-35	
Notes:	ϕ = angle of internal friction		
	D = drained triaxial test		
	CU = consolidated-undrained triaxial test		
	UU = undrained triaxial test		
	DS = direct shear test		

TABLE 2.3: Coefficients of Variation for Stability Analysis of Gravity Platforms

Source of Uncertainty	C.O.V. (%)	Overall Uncertainty (%)
(1) Loads	24.0	13.0
(2) Undrained Shear Strength	26.0	83.2
(3) Cyclic Loading	2.0	0.5
(4) Depth of Embedment	4.0	2.0
(5) Conductor Effect	1.0	0.1
(6) Erosion Effect	1.0	0.1
(7) Model Uncertainty	3.0	1.1

Based on results from Tang et al. [59]

soil parameters. Tang et al. [59] summarized the sources of uncertainty in a stability analysis of a gravity platform (Table 2.3).

2.2.4.2 Stability Models

Work on the foundation stability problem with probabilistic applications were published by Singh [56] with reference to earth structures. Considering the variability of soil strength parameters, Singh computed the confidence limits of the factor of safety for varying foundation problems. Singh concluded from his analysis that traditional approach of safety factors produced inconsistent reliability in earth structures, resulting in possible unsafe designs being accepted. This was primarily due to ignoring the effect of soil parameter variation in the design.

Tang et al. [59] developed a procedure for probabilistic stability analysis of offshore gravity platforms utilizing the Norwegian Geotechnical Institute's slip surface stability model as described by Lauritzen and Schjøthe [27]. To illustrate the analysis method, an example using a Condeep platform design was provided. The analysis assumed statistical independence between all variables and the events of stability failure under various

conditions to be mutually exclusive events. The results indicated that the principal sources of uncertainty were the loads and the undrained shear strength with coefficients of variation of 0.24 and 0.26, respectively (Table 2.3). Although the C.O.V.'s were approximately the same, / the undrained shear strength contributed 83.2% of the uncertainty whereas the load contributed only 13.0%. This revealed that the safety factor was more sensitive to changes in soil shear strengths than in wave loads.

Høeg and Tang [60] published an overview of soil stability models as applied to offshore gravity structures. They examined the use of probability and statistics in the various geotechnical aspects related to gravity platforms. Their analysis revealed that uncertainty levels associated with different methods of analysis vary widely. Høeg and Tang suggested that reliability levels associated with resulting designs could vary widely unless load and material safety factors were re-evaluated for each procedure. Kraft and Murff [58] also presented a procedure for probabilistic analysis of offshore gravity structure foundations.

2.2.4.3 Deformation Models

The uncertainty of soil properties affects the reliability of the total and differential settlements obtained

from deformation models, whether it be simple theoretical methods or elastic-elastoplastic numerical models. The extent to which the geotechnical uncertainty has affected the results was explored by some researchers.

One-dimensional stochastic settlement models were proposed by Resendiz and Herrera [61], Hilldale [62] and Diaz and Vanmarcke [63]. Resendiz and Herrera analyzed the probability distributions of settlement and rotation of rectangular foundations on randomly compressible, layered soils. Both rigid and flexible foundations were discussed, considering all variations in soil compressibility to occur within sublayers in the horizontal direction. This model was based on the assumption of independence in soil layers and constant variance within layers. Expressions were derived for the average settlement mean and variance for each sublayer. Hilldale treated the soil elastic modulus as a second-order stationary stochastic process. Based on stress levels obtained from deterministic analysis, one-dimensional (e.g. vertical) deformations for footings in sand were calculated. The stochastic settlements were then determined by integrating these deformations over the layer depth. Diaz and Vanmarcke developed a probabilistic soil-structure interaction model with autocorrelated properties within soil layers. The second-moment analysis yielded "first-order" values for means, standard deviations

and correlation coefficients for consolidated settlements in terms of uncertainty of input parameters of loads and soil continuum. A sensitivity analysis was performed to ascertain the relative importance of the component uncertainty. This parametric study examined the horizontal and vertical correlation distance and the coefficient of variation of each random variable (e.g., overburden pressure, recompression indices, virgin compression indices, initial void ratio, layer thickness, member load, and maximum effective past pressure). The correlation distances ranged from 10 to 50 Feet (3 to 15 m) and the C.O.V. from 0% to 15%.

These one-dimensional models considered the spatial variation of the soil strata through second-order stationary stochastic process. The soil profiles were assumed to be independent between layers and to have constant variance within layers. Cornell [49] provided a formulation for practical first-order uncertainty analysis using approximate means and variances of material properties for two and three dimensional analysis of the elastic continuum. Similar models were proposed by Baecher et al. [30] and Vanmarcke [50].

Dendrou and Houstis [64] presented an uncertainty finite element model for dynamic analysis based on a perturbation technique. The model considered the spatial

distribution density function for the mean and variance of the elastic modulus, Poisson's ratio and density of the soil continuum. The spatial uncertainty was implemented by using a linearly varying plane strain triangular element. This procedure required an inference scheme to be coupled with a perturbation technique. The results of Dendrou and Houstis' analysis showed the mean and variance of the displacements and stresses of an earth structure to be in agreement with observed field values. Dendrou and Houstis [65] modeled field problems using semi-stochastic finite elements. The estimation of physical parameters were inferred from experimental data based on a concept of correlated random fields. Coupling this procedure with a Ritz-Galerkin method, the level of uncertainty was computed. Comparison showed a correlative-finite element model to give superior results than a regression finite element model.

Su et al. [66] incorporated the variation in rock properties of elastic modulus and Poisson's ratio in the stress analysis of underground tunnels. From their experience in rock mechanics, they noted that the properties of the rock medium were not single-valued but form some distribution that was associated with the rock material and not with the testing procedure. A linear plane strain finite element analysis with an isotropic, homogeneous, elastic rock continuum to model a long circular tunnel was

selected as an example. The elastic moduli and Poisson's ratio varied randomly from element to element according to an assumed frequency distribution utilizing a probabilistic Monte-Carlo simulation. Su et al. proposed that this procedure of considering the variation of the stresses, permitted a more meaningful safety factor to be determined for the underground opening. Similarly, Cambou [67] applied a first-order uncertainty analysis in finite element methods to soil mechanics utilizing autocorrelation among properties. Using linear elasticity theory, means, variances and covariances of nodal displacements and element stresses were determined.

Statistical concepts and finite element method were applied to slope stability analysis of a soil medium composed of linear isotropic but statistically heterogeneous elastic material by Kraft and Yeung [68]. The uncertainty of the soil deformations was simulated with a random distribution of moduli properties for the elements following a log-normal probability distribution. The results of the study provided a quantitative measure of the influence of soil heterogeneity, as measured by the coefficient of variation of the modulus of elasticity, on slope deformation. Kraft and Yeung's results indicated that the slope geometry, Poisson's ratio and earth pressure coefficients

had a minor influence on the statistical variation as compared to the modulus.

Baecher and Ingra [69] developed a two-dimensional finite element second-moment short term settlement analysis procedure using plane strain elements. The stochastic finite element model assumed that the statistical properties of the soil were spatially constant and the spatial variability in the soil profile could be considered as random fluctuations about the mean trend (Cornell [49]). In the actual model, the uncertainty was simulated by a Monte-Carlo algorithm for element property selection, which in this case was the elastic modulus. Baecher and Ingra used the first two terms of a Taylor series expansion to approximate the expected total settlement. This first-order approximation of settlement was required for estimation of the variance and covariance of the nodal displacements in the discretized domain. A formulation for relative settlements was also provided. Comparison of the settlement predictions from one and two dimensional uncertainty models showed this second-order stochastic finite element technique to be more realistic. The study examined the effect of isotropic and anisotropic correlation functions on the displacements and stresses within the soil.

Munaswamy and Arockiasamy [70] extended the work of Baecher and Ingra. Short term settlement analysis of gravity platform foundation using stochastic finite elements was presented considering the spatial variability of element moduli. Variance and covariance of settlements and differential settlements as well as element stresses were determined due to wave forces and gravity loading. Plane strain stochastic finite element method was used to model the spatial variability of soil properties. The short term settlements and stress variation were computed for a sample gravity platform foundation.

2.3 Proposed Research

Foundation design for gravity platforms and caisson retained islands requires the determination of total and differential settlement, vertical stress distribution beneath the structures and within the layered soil medium, and maximum shear stresses in the soil. Deterministic procedures using sensitivity analysis have been developed earlier to quantify the effect of statistical uncertainty in material properties. Yet, these procedures have not assessed the effect of spatial variability of soil parameters on settlement and stress distribution. Finite element analysis is a popular deterministic procedure used in foundation design to study soil-structure interaction. The possibility of incorporating two-dimensional probabilistic spatial variability of soil properties in a finite element procedure has been already demonstrated by earlier researchers. As noted in Section 2.2.4.3, researchers such as Su et al. [66], Cambou [67], Kraft and Yeung [68], Baecher and Ingra [69], and Munaswamy and Arockiasamy [70], have developed such probabilistic FEM models for an isotropic elastic soil medium. The present research shall consider the variation in soil strength of a layered foundation by spatially varying the element moduli. In addition to this, the present study will incorporate the nonlinear soil behaviour into the stochastic finite element

model, and generate the randomness in properties through computer software implementations instead of Monte-Carlo simulation techniques used by other researchers.

The soil and structure foundation is approximated as a two-dimensional plane strain continuum using triangular elements with six degrees of freedom. Two soil models are utilized in the analysis, (i) a layered, elastic, single phase, soil medium with undrained soil properties and (ii) a piecewise linear, elastic, single phase, layered soil medium approximating the nonlinear behaviour of soil. A shear strain dependent soil modulus is considered in the piecewise linear approximation of nonlinear soil behaviour.

In Chapter 3, a two-dimensional plane strain stochastic finite element solution is formulated considering two terms in the Taylor series expansion of the equilibrium equations, incorporating the variation of soil properties. Instead of assuming synthetic soil properties as earlier researchers have done, the soil properties are obtained from results of prototype in-situ measurements. Computer programs in the FORTRAN language are developed to simulate the derived theory (Appendices III and IV). The means and covariances of short term displacements of the nodal points of the discretized model of the soil strata are obtained. Normal

and shear stresses of the soil continuum are examined in terms of mean values and variances.

Sensitivity studies of changes in the coefficient of variation of elastic moduli, the correlation distance factors in the covariance functions and comparisons of soil models are included. Analyses with fixed parameter values maximize the material C.O.V. as expressed through the elastic moduli, ensuring that upper bound solutions for displacement and stress uncertainty are obtained. In purely stochastic analyses wherein the elastic moduli vary in a random manner, the resulting displacement and stress coefficients of variation will be substantially lower than the upper bound values. The computer software has been modified to perform this purely stochastic analysis by utilizing a pseudo-random number generator, in addition to the upper bound values.

In the analysis, the coefficient of variation of elastic modulus is assumed to be less than 30.0%, restricting the degree of variability of the soil layers. This restriction is acceptable since most soil parameters have coefficients of variation below this value, as indicated in Table 2.2. For larger coefficients of variation to be included, some additional nonlinear term in the Taylor series expansion will have to be incorporated into the

formulation and the programs. For the present study, the linear approximation of the Taylor series will be used.

To indicate the procedure, two physical examples are modeled and comparisons made with the measured response of these structures. For the first illustration given in Chapter 4, a prestressed concrete gravity structure placed in the North Sea is selected. The structure is examined with gravity loads and with additional forces of overturning moment and horizontal thrust of an actual storm (Hoddinott et al. [71]). The second example given in Chapter 5 considers a caisson retained island subjected to ice loadings in the Beaufort Sea (Hoddinott et al. [72]). These two problems are presented in depth.

Chapter 6 gives the salient conclusions of this study and outlines further lines of investigation for extending this study.

CHAPTER 3

STOCHASTIC FINITE ELEMENT FORMULATION

In traditional deterministic quasi-static analysis of offshore foundations, the soil properties are assumed to be constant. But in actual situations these properties vary spatially, as indicated from both laboratory and in-situ tests. This uncertainty in soil properties and its effect on the system response may be quantified by considering stochastic variability in a finite element model. The soil variability is modeled as one realization of a second-order stationary random field. Following standard practice in geological modeling, the assumption is made that the statistical properties of the soil are spatially constant (i.e. horizontally) and that this spatial variability is introduced by a random fluctuation about the mean, as shown in Figure 3.1. The random fluctuation is characterized by a point variance and autocorrelation function.

The two-dimensional model developed in this study uses a finite element discretization of a linear elastic subsurface, and uses the first two terms of Taylor series expansions to calculate means, variances and covariances of nodal displacements.

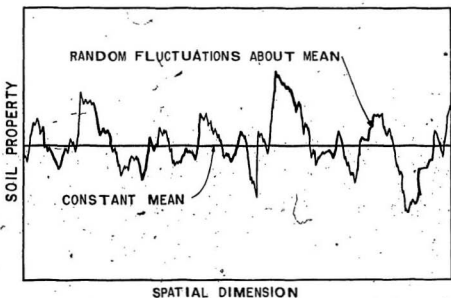


FIGURE 3.1 RANDOM VARIATION OF SOIL PROPERTY
ABOUT A CONSTANT MEAN

3.1 Formulation of Nodal Displacement Covariances

For a continuum discretized into a number of elements, the static equilibrium of the soil-foundation system can be written as,

$$[K] (U) = (F) \quad (3.1)$$

wherein $[K]$ denotes stiffness matrix, (U) is displacement vector and (F) is external load vector.

For a given set of material properties of the elements in the continuum, the mean value of displacements can be determined by solving the linear system of equations given by Eq. (3.1). Using the mean values of the material properties for each element, the expected value of the stiffness matrix $[K]$ can be obtained. Rearranging Eq. (3.1) to solve for the displacement vector, the expected displacement vector can be determined using the mean stiffness matrix \bar{K} .

$$(\bar{U}) = [\bar{K}]^{-1} (F) \quad (3.2)$$

In this derivation, the uncertainty in soil strength is considered to be expressed in terms of the elastic modulus, E . Therefore, a Taylor series expansion of the displacement

vector (\mathbf{U}) expanded with respect to the elastic modulus, will represent the actual displacement in terms of the mean displacement ($\bar{\mathbf{U}}$) and the spatially varying displacement terms (Appendix I).

$$\mathbf{U} = \bar{\mathbf{U}} + \sum_{i=1}^N \frac{\partial(\mathbf{U})}{\partial E_i} (E_i - \bar{E}_i) + \frac{1}{2!} \sum_{i=1}^N \frac{\partial^2(\mathbf{U})}{\partial E_i^2} (E_i - \bar{E}_i)^2 + \dots \quad (3.3)$$

Neglecting second order and higher derivatives in Eq. (3.3), the expansion can be written in the linearized form by,

$$\mathbf{U} = \bar{\mathbf{U}} + \sum_{i=1}^N \frac{\partial(\mathbf{U})}{\partial E_i} (E_i - \bar{E}_i) \quad (3.4)$$

where i denotes the element number in the discretized domain and N is the total number of elements.

This simplifying assumption will restrict the formulation to small variations about the element means of the elastic modulus. A statistical measurement of variation in the elastic modulus of soil is the coefficient of variation, defined as the ratio of standard deviation to the mean. Baecher and Ingra [69] report that if the point variance of the modulus is large with a coefficient of variation greater

than 0.30, a better approximation of the elemental displacement would include the first three terms of the Taylor series expansion. Baecher et al. [30], Kraft and Murff [58] and Tang et al. [59] have indicated that for soil properties, most of the coefficients of variation lie below the 0.30 level, making this simplification acceptable.

Considering one nodal displacement degree of freedom U_k , the difference between the actual displacement and the expected displacement can be expressed as,

$$(U_k - \bar{U}_k) = \sum_{i=1}^N \frac{\partial U_k}{\partial E_i} (E_i - \bar{E}_i) \quad (3.5)$$

Partial derivatives of displacement with respect to the element moduli can be obtained from Eq. (3.1) as,

$$[K] \frac{\partial (U)}{\partial E_i} + \frac{\partial [K]}{\partial E_i} (U) = \frac{\partial (F)}{\partial E_i} \quad (3.6)$$

Since (F) is independent of element moduli (i.e. $\frac{\partial (F)}{\partial E_i} = 0$),

Eq. (3.6) yields,

$$\frac{\partial(U)}{\partial E_i} = -[K]^{-1} \frac{\partial[K]}{\partial E_i} (U) \quad (3.7)$$

Evaluating Eq. (3.7) at mean values, one obtains

$$\frac{\partial(U)}{\partial E_i} = -[\bar{K}]^{-1} \frac{\partial[\bar{K}]}{\partial E_i} [\bar{K}]^{-1} (F) \quad (3.8)$$

The partial derivatives of displacements with respect to the individual element moduli are arranged in a $n \times m$ matrix whereby n is the number of nodal degrees of freedom or displacements and m is the number of finite elements.

$$\begin{bmatrix} \frac{\partial(U_1)}{\partial E_1} & \frac{\partial(U_1)}{\partial E_2} & \frac{\partial(U_1)}{\partial E_3} & \cdots & \frac{\partial(U_1)}{\partial E_m} \\ \frac{\partial(U_2)}{\partial E_1} & \frac{\partial(U_2)}{\partial E_2} & & & \frac{\partial(U_2)}{\partial E_m} \\ \vdots & \vdots & & & \vdots \\ \frac{\partial(U_n)}{\partial E_1} & \frac{\partial(U_n)}{\partial E_2} & & \cdots & \frac{\partial(U_n)}{\partial E_m} \end{bmatrix} \quad (3.9)$$

The differentials in matrix (3.9) are evaluated using the mean material and load properties as suggested by Eq. (3.8). For the two-dimensional plane-strain triangular FEM formulation, the first order partial derivative of displacement with respect to elastic modulus can be easily obtained by noting that E being linear in the elastic constituent matrix, D; is replaced by 1.0.

3.1.1 Derivation of Covariance of Displacement

Using the statistical definition of covariance [44,73], the covariance of displacement between any two displacements, U_k and U_l , is,

$$\text{cov}(U_k, U_l) = \int \int (U_k - \bar{U}_k)(U_l - \bar{U}_l) P(U_i, U_j) dU_i dU_j \quad (3.10)$$

where

$P(U_i, U_j)$ = joint probability density function for U_i and U_j .

Assuming the soil uncertainty in strength to be dependent on modulus of elasticity, the joint probability density function will be determined by the element moduli interdependence. Modeling the soil uncertainty in this manner has

been previously carried out by other researchers [63, 64, 65, 66, 67, 69, 70]. As shown by Cambou [67], the vertical nodal displacements are relatively insensitive to Poisson's ratio. Neglecting the effect of uncertainty in Poisson's ratio will have little effect on results. Thereby, considering only moduli uncertainty, the covariance of displacement is given by

$$\text{Cov}(U_k, U_l) = \int_{-\infty}^{\infty} \int_{-\infty}^{\infty} (U_k - \bar{U}_k)(U_l - \bar{U}_l) P(E_i, E_j) dE_i dE_j \quad (3.11)$$

where

$P(E_i, E_j)$ = joint probability density function for E_i and E_j .

Substituting Eq. (3.5) into Eq. (3.11),

$$\begin{aligned} \text{Cov}(U_k, U_l) &= \int_{-\infty}^{\infty} \int_{-\infty}^{\infty} \left[\sum_{i=1}^N \frac{\partial U_k}{\partial E_i} (E_i - \bar{E}_i) \right] \left[\sum_{j=1}^N \frac{\partial U_l}{\partial E_j} (E_j - \bar{E}_j) \right] \\ &\quad \cdot P(E_i, E_j) dE_i dE_j \quad (3.12) \end{aligned}$$

Rearranging Eq. (3.12) and assuming linearity of operations,

$$\text{Cov}(U_k, U_l) = \sum_{i=1}^N \sum_{j=1}^N \frac{\partial U_k}{\partial E_i} \frac{\partial U_l}{\partial E_j} \int_{-\infty}^{\infty} \int_{-\infty}^{\infty} (E_i - \bar{E}_i)(E_j - \bar{E}_j) P(E_i, E_j) dE_i dE_j \quad (3.13)$$

Noting that the definition of covariance of E_i and E_j is expressed in the double integration term, the calculation form of the covariance of displacement is,

$$\text{Cov}(U_k, U_l) = \sum_{i=1}^N \sum_{j=1}^N \frac{\partial U_k}{\partial E_i} \frac{\partial U_l}{\partial E_j} \text{Cov}(E_i, E_j) \quad (3.14)$$

When $k = l$, Eq. (3.14) becomes the variance of the displacement,

$$\text{Var}(U_k) = \sigma_U^2 = \sum_{i=1}^N \sum_{j=1}^N \frac{\partial U_k}{\partial E_i} \frac{\partial U_k}{\partial E_j} \text{Cov}(E_i, E_j) \quad (3.15)$$

The variances and covariances of displacements are determined based on the partial derivatives of displacements with respect to element moduli of the various elements evaluated at the means. The covariance of E_i and E_j can be expressed in terms of correlation coefficient, $r_{E_i E_j}$, and standard deviations of elastic moduli, σ_{E_i} and σ_{E_j} , based on standard statistical relationships.

$$\text{Cov}(E_i, E_j) = \rho_{E_i E_j} \sigma_{E_i} \sigma_{E_j} \quad (3.16)$$

In the present study, the coefficient of variation of modulus is assumed constant for any particular element, thereby making it possible to evaluate the standard deviations of the element moduli. Constant autocorrelation functions are implemented to generate correlation coefficients. These functions are described in greater detail in Section 3.1.2. The correlation coefficient for E_i and E_j ranges in value from 0 to 1.

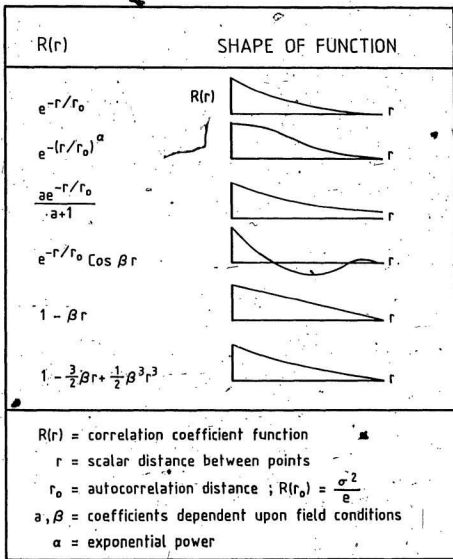
3.1.2 Correlation Coefficient Function

In the stochastic finite element formulation, material properties are assumed based on element means, variances of element means and covariances among element means. The statistical properties are influenced by element size, shape and orientation with respect to the correlation function. Baecher et al. [30], Cornell [49], Vanmarcke [50], Diaz and Vanmarcke [63] and Baecher and Ingra [69] have indicated some procedures for obtaining statistical properties using the autocorrelation functions. The correlation function must show the tendency for points closely spaced to exhibit similar values more than widely spaced points. For soil foundations, the estimation typically involves determining the in-situ soil properties from a finite number of samples.

The spatially varying property ($P(x,y,z)$) in the soil foundation is considered to be a stochastic process with mean value function $\mu P(x,y,z)$ and covariance function $Cov(r)$. The latter function is assumed to be stationary¹ and isotropic for simplicity. Thereby the covariance between the property values at two points in space is a function of only the scalar distance r between the points. When r is zero, the correlation coefficient is unity. As the scalar distance r increases the correlation coefficient decreases until at r approaching infinity, it is zero. Commonly used autocorrelation functions for scalar random fields are presented by Baecher et al. [30] and Vanmarcke [50] (see Figure 3.2). Reasonable choices for the covariance function are $\sigma^2 e^{-ar}$ and $\sigma^2 e^{-ar^2}$ where σ^2 is the variance and e^{-ar} or e^{-ar^2} is the correlation coefficient function which decays with distance r . These exponential and squared exponential correlation coefficient functions have been verified by field observations by Hög and Tang [60].

A parameter 'a' has to be estimated from actual field data. For an uncorrelated process, there is no variability in the spatial average of a finite volume. This assumption

¹Stationary refers to statistical homogeneity when dealing with spatial rather than temporal variables. It describes the nature and degree of local fluctuations of the random variables.



Autocorrelation Functions for Scalar Random Fields

FIGURE 3.2

of lack of correlation is reasonable if the volumes involved are large compared to the cube of the characteristic correlation distance. Cornell [49] has stated that it may be reasonable to use (i) means based on the designer's best estimate of the property, (ii) variances based on measured values in similar situations and under similar specifications with quality control procedures and (iii) spatial correlation as unity. This enables the designer to obtain mean soil property values from the proposed structure site and consider variances from other similar geographic locations to be applicable to this location.

The correlation coefficient of element moduli between any two elements is idealized to be decreasing as a function of their centroidal distance. The following expression in exponential form describes the correlation coefficient,

$E_i E_j$, between any two elements, i and j, viz.,

$$E_i E_j = e^{-\frac{|r_{ij}|}{L}} \quad (3.17)$$

where the centroidal distance r between elements i and j can be determined from the FEM discretization. For this formulation, the parameter 'a' of the correlation function is selected as the reciprocal of the correlation distance, L. The exponential ratio is normalized by the correlation distance, with L being the product of a correlation distance

factor and the diameter or width of the structure's foundation. The correlation distance factor is determined by the degree of soil variability in the region, with lower factors indicating greater variability. The standard deviation of the elastic modulus, σ_E , is estimated as the product of the mean elastic modulus as determined by local soil properties and the coefficient of variation of the material characteristics as measured by the degree of variability in elastic moduli from other sites. This standard deviation value will change from element to element as these parameters of elastic modulus and C.O.V. vary.

For the FEM application, Eq. (3.16) can be written in matrix form

$$[\text{Cov. } (E_i, E_j)] = [\sigma_{E_i}][\rho_{E_i E_j}][\sigma_{E_j}] \quad (3.18)$$

wherein i and j vary from 1 to N, the total number of elements in the discretized model. The matrices are as follows:

68

$$\begin{bmatrix}
 [\rho_{E_1 E_j}] & \\
 & \frac{|r_{12}|}{L} \dots \frac{|r_{1N}|}{L} \\
 & e \quad \dots \quad e \\
 & |r_{21}| \quad \dots \quad |r_{2N}| \\
 & e \quad \dots \quad e \\
 & |r_{N1}| \quad \dots \quad |r_{NN}| \\
 & e \quad \dots \quad e
 \end{bmatrix}$$

(3.19)

$$[\sigma_{E_i}] = [\sigma_{E_j}] = \begin{bmatrix}
 \sigma_{E_1} & 0 & \dots & 0 \\
 0 & \sigma_{E_2} & \dots & 0 \\
 \vdots & \vdots & \ddots & \vdots \\
 0 & 0 & \dots & \sigma_{E_N}
 \end{bmatrix}$$

(3.20)-

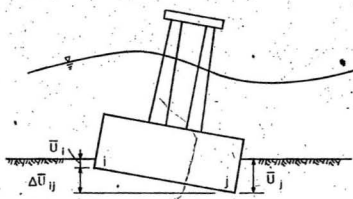
3.1.3 Variance of Relative Settlement

In a discretized soil continuum, the total nodal displacements (vertical and horizontal) are determined by finite element analysis. Considering vertical displacements only, differential and relative settlements can be obtained for nodal points having the same vertical level prior to application of loads. Baecher and Ingra [69] have presented a procedure for estimating the variances of differential (absolute) and relative settlements. For differential settlement analysis, the variances are strongly nonlinear and cannot be approximated by the linear Taylor series formulation unless a distributional assumption is introduced. Relative settlements are not based on any distributional assumption.

With the aid of Figure 3.3, the definition of relative settlement between nodes i and j is,

$$\Delta u_{ij} = (\bar{u}_i - \bar{u}_j) \quad (3.21)$$

The relative settlement, Δu_{ij} , is expressed as the difference between the expected vertical displacements, \bar{u}_i and \bar{u}_j . Recall that the expected displacements are obtained from the finite element analysis using mean elastic moduli.



Relative Settlement \Rightarrow Soil-Foundation Interface

FIGURE 3.3

The variance of the addition of two dependent random variables, x and y , with existing variances is defined by Dwass [74] as,

$$\text{Var}(x+y) = \text{Var}(x) + \text{Var}(y) + 2\text{Cov}(x,y) \quad (3.22)$$

Relative settlement requires the subtraction of two dependent random variables, settlements \bar{U}_i and \bar{U}_j . The variance for relative settlement is expressed by modifying Eq. (3.22) as,

$$\text{Var}(\Delta U_{ij}) = \text{Var}(U_i) + \text{Var}(U_j) - 2 \text{Cov}(U_i, U_j) \quad (3.23)$$

where $\text{Var}(U_i)$ and $\text{Var}(U_j)$ are determined by Eq. (3.15) and $\text{Cov}(U_i, U_j)$ is based on Eq. (3.14).

The displacements, \bar{U}_i and \bar{U}_j , are dependent random variables based on the influence the settlement at one node has on the other. For mutually independent variables, the covariance term in Eqs. (3.22) and (3.23) is zero.

Although attention here has been focused on vertical settlements, variances for horizontal displacements are also calculated in a similar manner.

3.2 Formulation of Normal and Shear Stress Variances

In a manner similar to the displacement variance derivation, the mean and variance of the normal and shear stresses within an element can be determined. The computer implementation uses a plane strain triangular element resulting in constant strains and stresses within the element. The basic strain displacement relationship for an element, i , is written as,

$$(\epsilon)_i = [B]_i(U)_i \quad (3.24)$$

where

$[B]$ = strain displacement matrix dependent on the geometry of the element

$$(\epsilon)_i = [\epsilon_x \epsilon_y \gamma_{xy}]^T$$

wherein ϵ_x , ϵ_y = normal strains in cartesian coordinates

γ_{xy} = shear strain in cartesian coordinates

T = transpose

$(U)_i$ = displacement vector associated with element i , which for the constant strain triangular element will consist of six degrees of freedom

The stress-strain relationship is written as,

$$(S)_i = [D]_i (\epsilon)_i \quad (3.25)$$

where

$[D]_i$ = elastic constituent plane strain matrix
dependent on random element modulus

$$(S)_i = [\sigma_x \ \sigma_y \ \tau_{xy}]_i^T$$

wherein σ_x, σ_y = normal stresses in cartesian coordinates
 τ_{xy} = shear stress in cartesian coordinates

Substituting Eq. (3.24) into Eq. (3.25),

$$(S)_i = [D]_i [B]_i (U)_i \quad (3.26)$$

One can observe that the stresses are dependent on the elastic modulus, E_i , through $[D]_i$ and the displacement vector, $(U)_i$, which are both random variables. Neglecting the second order and higher partial derivatives, the expression for $(S)_i$ is linearized using Taylor series expansion for a function with two variables about their means (Appendix II).

$$(S)_i = (S)_i + \frac{\partial (S)_i}{\partial E_i} dE_i + \frac{\partial (S)_i}{\partial (U)_i} d(U)_i \quad (3.27)$$

The following partial derivatives are determined by substituting Eq. (3.26) for $(S)_i$,

$$\frac{\partial (S)_i}{\partial E_i} = \frac{\partial}{\partial E_i} [[D]_i [B]_i (U)_i]$$

$$= \frac{\partial [D]_i}{\partial E_i} [B]_i (U)_i \quad (3.28)$$

$$\frac{\partial (S)_i}{\partial (U)_i} = \frac{\partial}{\partial U_i} [[D]_i [B]_i (U)_i]$$

$$= [D]_i [B]_i \quad (3.29)$$

The difference between the actual stress and the calculated mean stress is obtained from Eq. (3.27) using Eq. (3.28) and Eq. (3.29) and noting that dE_i can be expressed as $(E_i - \bar{E}_i)$ and $d(U)_i$ as $((U)_i - (\bar{U})_i)$.

$$(S)_i - (\bar{S})_i = \frac{\partial [D]_i}{\partial E_i} [B]_i (U)_i (E_i - \bar{E}_i) + [D]_i [B]_i ((U)_i - (\bar{U})_i) \quad (3.30)$$

Using Eq. (3.5), the $((U)_i - (\bar{U})_i)$ term in Eq. (3.30) may be replaced by the linearized form of the Taylor series expansion for nodal displacements.

$$(S)_i - (\bar{S})_i = \frac{\partial [D]_i}{\partial E_i} [B]_i (U)_i (E_i - \bar{E}_i)$$

$$+ [D]_i [B]_i \sum_{j=1}^N \frac{\partial (U)_i}{\partial E_j} (E_j - \bar{E}_j) \quad (3.31)$$

Define a function $(H)_{ij}$ as follows,

$$(H)_{ij} = \frac{\partial [D]_i}{\partial E_i} [B]_i (U)_i \delta_{ij} + [D]_i [B]_i \frac{\partial (U)_i}{\partial E_j} \quad (3.32)$$

where the Kroenecker delta function,

$$\delta_{ij} = 1 \text{ when } i = j$$

$$\delta_{ij} = 0 \text{ when } i \neq j$$

Substituting $(H)_{ij}$ into Eq. (3.31):

$$(S)_i - (\bar{S})_i = \sum_{j=1}^N (H)_{ij} (E_j - \bar{E}_j) \quad (3.33)$$

Based on the definition of variance, the variance for σ_x, σ_y or r_{xy} of any element i can be evaluated.

$$\text{e.g. Variance } (\sigma_x, \sigma_y, r_{xy}) = \sum_{j=1}^N \sum_{k=1}^N (H)_{ij} (H)_{ik} \text{Cov}(E_j, E_k) \quad (3.34)$$

It is of interest to note that the uncertainties in the predicted stresses depend on both the uncertainty in element moduli and the uncertainty in the nodal displacements. The variances and covariances estimated by Eqs. (3.14), (3.15) and (3.34) indicate that uncertainties in predicted deformations and stresses depend on uncertainties of all the elements and their correlations.

3.3 Procedure for Soil Nonlinearity Model

Soils exhibit material nonlinearity. The stress-strain relations are much more complicated than the simple, linear elastic model assumed in the previous sections. Therefore, to model soil-structure interaction problems realistically, a nonlinear relationship must be applied. The development and application of such relations have been important areas of research in recent years. Christian and Desai [75] have provided a comprehensive review of constitutive models of soil behaviour.

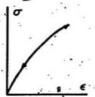
3.3.1 Constitutive Laws for Soil Media

Constitutive relations are those that describe the relationships between physical quantities such as stress, strain and time. Founded upon the theories of solid mechanics, these relationships enable the use of the finite element methods to simulate the soil continuum's behaviour under various loadings. The stress-strain behaviour of the material is required for application of the finite element method to actual problem situations. For elastic behaviour, all the strains are completely recovered when the load is removed. The stress-strain deformation curve is identical for both loading and unloading. If the relationship is linear, the material is linearly elastic. For this special

case where the materials obey linear constitutive laws, the problem solution is straightforward. Only one application of the solution process is required to obtain results for an applied load since the material parameters are constant.

For this simple case, all that is required for the stochastic finite element application are the values of modulus of elasticity, shear modulus and Poisson's ratio of the materials. Therefore the solution to this case can be obtained directly from the theory derived in Sections 3.1 and 3.2. For the nonlinear elastic materials, alternative solution techniques have to be employed. This is especially relevant to geotechnical problems since soil is a nonlinear continuum where the stiffness is not constant but dependent on the state of stress, strain and strain rate. When a portion of the strains are unrecoverable on unloading, the material is said to have experienced plastic behaviour. Several variations of plastic stress-strain curves are realized, such as (i) rigid, perfectly plastic, (ii) elastoplastic showing perfect plasticity, (iii) elastoplastic with strain hardening and (iv) elastoplastic with strain softening. The typical stress-strain curves for these conditions are depicted in Figure 3.4.

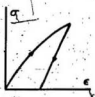
All the above cases involve stresses and strains that occur simultaneously. Materials exhibiting viscous



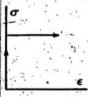
Nonlinearly Elastic



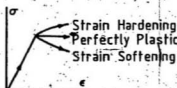
Linearly Elastic



Plastic



Rigid, Perfectly Plastic



Elastoplastic

Note : Arrowheads denote direction of loading.

FIGURE 3.4 TYPES OF STRESS-STRAIN BEHAVIOUR

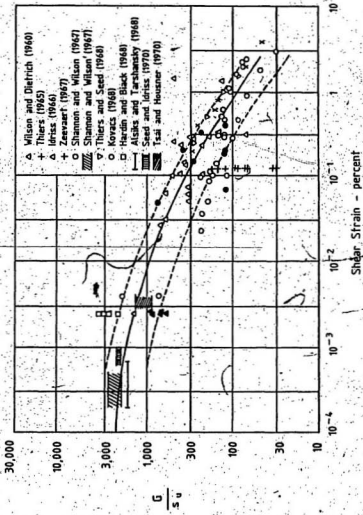
behaviour, that is, stress-strain behaviour that changes over time, are called viscoelastic. Viscoelastic creep is the increase in strain with time as the stress remains constant. Viscoelastic relaxation is the decrease in stress with time as the strain remains constant. For the present analysis, viscous or consolidation effects of the soil strata shall not be investigated. Attention will be restricted to short term deformations using linear elastic and nonlinear elastic models. The models will assume unique relations between stress and strain.

3.3.2 Stress-Strain Relationship

Stress-strain curves are often represented through the use of curve-fitting methods, mathematical functions and interpolation techniques. Duncan and Chang [76,77] used hyperbolic relations to simulate soil behaviour based on previous research by Kondner [78] that the plot of triaxial compression test stress-strain curves resembled hyperbolas. Hardin and Black [79] proposed a formula for the shear modulus as a function of octahedral shearing stress level, soil plasticity index, overconsolidation ratio and void ratio. Hardin and Drnevich [80] examined the usage of stress-strain curves for shear modulus and damping factors for soils as applied to design equations. They introduced three main concepts (i) a reference strain for normalizing

strain, (ii) the simple relationship between shear modulus and damping ratio for cyclic loading and (iii) the variation of modulus and damping with strain amplitude in terms of a stress-strain curve defined by the end points of hysteresis loops.

Seed and Idriss [81] devised a means of modeling large, nonlinear effects of earthquake forces on soil deformations. The equivalent linear method provides an approximate nonlinear solution by using a series of linear analyses with stiffness and damping coefficients based on effective shear strain amplitudes. Idriss et al. [82] established a computer algorithm for the implementation of the equivalent linear procedure. The present research will concentrate on shear modulus and elastic modulus variation only. Dynamic or cyclic effects will be treated as a quasi-static analysis to reduce computational effort. Therefore soil damping and inertial terms are omitted from the analysis. Seed and Idriss [83] developed typical soil deformation curves for both sand and saturated clays relating shear modulus, G , and shear-strain level, γ , of the soil. To assess the influence of strain on the shear modulus of natural clays, Seed and Idriss expressed the experimental results of several researchers graphically (Figure 3.5). The mean normalized ratios of shear modulus at shear strain γ to shear modulus at shear strain 3×10^{-4} percent are plotted against shear



NOTES: (1) Solid line indicates average values
(2) Broken lines indicate range of $\pm 50\%$ of average values

FIGURE 3.5
IN-SITU SHEAR MODULI FOR SATURATED CLAYS
(Reference [83])

strain amplitude in Figures 3.6 and 3.7 for saturated clays and sands respectively. As indicated in Figure 3.7, the results fall within a relatively narrow band. A close approximation to the modulus versus shear strain, for a wide range of sands can be represented by determining field modulus values at low shear strain levels and then reducing this value according to the average stress-strain relationship. A similar procedure can be applied to the results of Figure 3.6 for clays. Utilizing the information from these soil model curves, Lysmer et al. [84] prepared a table of strain-compatible soil properties. For corresponding levels of effective shear-strain, γ , shear modulus reduction factors are presented in Table 3.1 for both sand and clay. These reduction factors are applied to initial shear modulus values (i.e. shear modulus at low strain level taken as 10^{-4} percent) to obtain representative values for shear modulus at higher strains.

3.3.3 Numerical Implementation of Soil Nonlinearity

The nonlinear stress-strain behaviour of soils can be approximated as a piecewise linear curve [75, 82, 83, 84, 85]. For the procedure developed herein, it will be assumed that the stress-strain compatible properties of Lysmer et al. listed in Table 3.1 are representative of clays and

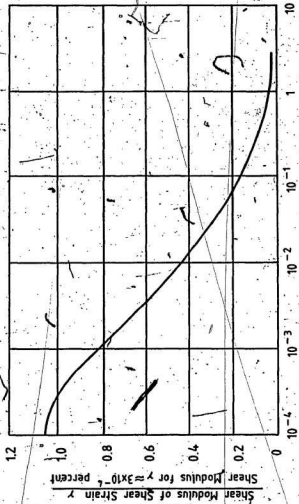


FIGURE 3.6 TYPICAL REDUCTION OF SHEAR MODULUS WITH SHEAR STRAIN FOR SATURATED CLAYS (Reference [83])

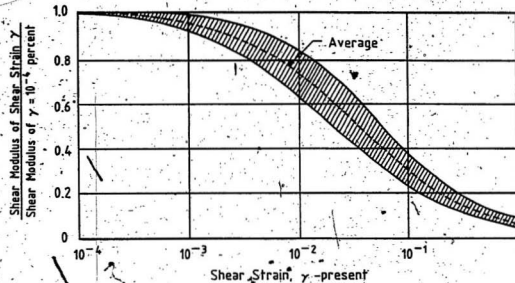


FIGURE 3.7

VARIATION OF SHEAR MODULUS WITH SHEAR STRAIN
FOR SANDS (Reference [83])

Table 3.1: Strain Compatible Soil Properties*

Effective Shear Strain ^{**}	Shear Modulus Reduction Factor	Shear Modulus Reduction Factor
(%)	Clay	Sand
< 0.0001	1.000	1.000
0.000316	0.913	0.984
0.001	0.761	0.934
0.00316	0.565	0.826
0.01	0.400	0.656
0.0316	0.261	0.443
0.1	0.152	0.246
0.316	0.076	0.115
1.0	0.037	0.049
3.16	0.013	0.049
> 10.0	0.004	0.049

*From Lysmer et al. [84]

**Effective shear strain is maximum shear strain times shear strain dependent reduction factor.

sands considered later in the problem applications. The initial shear modulus values taken at low strain levels are to be estimated from the on-site geotechnical testing data. The subroutine used to store the stress-strain relationship can be easily modified to include plastic modulus characteristics or updated to better represent local soil conditions as determined from triaxial testing of the sediments.

3.3.3.1 Fundamental Relationships

To begin, some fundamental relationships have to be established. Using two-dimensional elasticity equations, the principal stresses (σ_1, σ_2) and maximum shear stress (τ_{\max}) for each element are determined from the finite element program using the normal stresses (σ_x, σ_y) and the shear stress (τ_{xy}).

$$\text{e.g. } \sigma_1, \sigma_2 = \frac{\sigma_x + \sigma_y}{2} \pm \left[\frac{\sigma_x - \sigma_y}{2}^2 + \tau_{xy}^2 \right]^{1/2} \quad (3.35)$$

$$\tau_{\max} = \left| \frac{\sigma_1 - \sigma_2}{2} \right| \quad (3.36)$$

From two-dimensional theory of elasticity the principal strains (ϵ_1, ϵ_2) and maximum shear strain are related to the principal stress by,

$$\epsilon_1 = \frac{\sigma_1 - \nu\sigma_2}{E} \quad (3.37)$$

$$\epsilon_2 = \frac{\sigma_2 - \nu\sigma_1}{E} \quad (3.38)$$

$$\gamma_{\max} = \frac{|\epsilon_1 - \epsilon_2|}{2} \quad (3.39)$$

where E = elastic modulus and ν = Poisson's ratio. The basic relationship between elastic modulus, E , shear modulus, G , and Poisson's ratio, ν , for isotropic elements is,

$$E = 2G(1 + \nu) \quad (3.40)$$

3.3.3.2 Piecewise Linear Analysis

The algorithm for the piecewise linear analysis resembles the secant modulus (variable stiffness) method of Cook [85], whereby the stiffness matrix is repeatedly revised. Assuming initially all material is linearly elastic, the displacements, stresses and strains are computed for all nodes and elements. Using the maximum shear strain, γ_{max} , as calculated by Eq. (3.39), the shear modulus reduction factor, RF , is determined by performing a linear interpolation between the appropriate values of Table 3.1. The maximum shear strain value, γ_{max} , is the summation of all previous load step strains plus the incremental strain incurred by the present load increment with uncorrected modulus. The initial shear modulus, G_0 , for low strain rates is obtained by rearranging Eq. (3.40) inputting initial elastic modulus, E_0 , and Poisson's ratio (obtained from field tests).

$$G_0 = \frac{E_0}{2(1 + \nu)} \quad (3.41)$$

To determine the modified shear modulus, the initial shear modulus is reduced by applying the reduction factor, RF,

$$G_j = -RF \cdot G_0 \quad (3.42)$$

where j denotes iteration number in the piecewise linear analysis. Substituting the new reduced value G_j into Eq. (3.40), an updated elastic modulus value E'_j is computed. To achieve faster convergence of moduli, the average of E'_j and E'_{j-1} is used to obtain a new elastic modulus E_j ,

$$E_j = 0.5(E'_j + E'_{j-1}) \quad (3.43)$$

When the difference in the elastic modulus from the previous modulus is less than 5.0%, the modulus is considered to have converged for that element. The following convergence test is applied,

$$\frac{E_{j-1} - E_j}{E_{j-1}} < 0.05, \text{ converged} \quad (3.44a)$$

$$\frac{E_{j-1} - E_j}{E_{j-1}} > 0.05, \text{ un converged} \quad (3.44b)$$

When Eq. (3.44a) governs, the modulus is fixed at this value for the remaining iterations of the load step. Otherwise the un converged element modulus will proceed through another iteration until compatible stress-strain results are obtained. This procedure is repeated for all elements of the finite element model until all or a satisfactory number of element moduli (95%) have converged. Typically, this requires approximately six iterations for the first load step and four or fewer iterations for remaining load steps where each load step provides approximately 10 to 15 percent of total load. If smaller load steps are considered, the number of iterations per load step will be reduced.

To avoid excessive local deformations another criteria is considered. If the new elastic modulus E_j , as calculated by Eq. (3.43), is less than a pre-selected minimum value, the element modulus is fixed at the pre-selected minimum for all remaining iterations and load steps. A minimum modulus, E_{min} , of 20.0% of the original element modulus E_0 is selected for the present analysis.

$$E_j < E_{min}, \quad E_j = E_{min} \quad (3.45)$$

where $E_{min} = 0.2 E_0$ for the element. This criteria also has the benefit of artificially including plastic soil deformation effects into the results.

For the piecewise linear analysis, the total load is reduced to equal fractional loads. These incremental loads are applied to the FEM mesh in load steps. For each load step, convergence of the elastic modulus must be obtained prior to advancing to the next load increment. When all of the elements have converged, the elemental elastic moduli values are stored. The elemental stresses and strains and nodal displacements are accumulated as the summation of all previous load step values plus the incremental terms of the present load step.

The stochastic analysis is conducted using the converged element moduli for the load step. Using the elastic moduli values with the stresses and displacements incurred by the fractional load, the direct application of Eqs. (3.14), (3.15) and (3.34) is made to determine the resulting covariances and variances of selected node displacements and element stresses. To estimate the net effect of the total loads, the covariances and variances of each load step are superimposed. Due to simplifying assumptions in both the stochastic analysis (i.e. linearized Taylor series approximation) and the piecewise linear elastic analysis (i.e.

stress-strain relationship approximation), the cumulative effects of covariances and variances for displacement and stress are additive. With the limitations of the procedure, the simple superposition of results provide the best estimator of material uncertainty. The implementation of this procedure into the analysis, assumes the variance addition of load steps to be mutually independent random variables. The actual nonlinear soil model is expected to have some interdependence within load increments, resulting with a variance formula between load steps similar to Eq. (3.22). The possibility of obtaining an autocorrelation function between the piecewise linear stages warrants further study. The present investigation will assume the independence between stages and provide a basis of comparison for additional research.

3.4 Procedure for Random Stochastic Analysis

The stochastic finite element model developed in Sections 3.1 and 3.2 estimates upper bound solutions for node displacement and element stress uncertainty. The method of analysis uses a constant elastic modulus coefficient of variation (C.O.V.) as the measure of material uncertainty. This constant modulus C.O.V. ensures that maximum effects of soil uncertainty are obtained in the covariance results from the computer analysis.

As previously mentioned, the soil strength variation is assumed to be represented by the changes in element moduli. The covariance function for elastic moduli (3.16) indicates the manner the variation occurs. The modulus C.O.V. determines the standard deviation of elastic modulus, σ_{E_i} , for an element,

$$\sigma_{E_i} = \bar{E}_i \lambda_i \quad (3.46)$$

where \bar{E}_i is the best estimate of the elastic modulus for the element and λ is the modulus C.O.V.

In purely stochastic analysis, the elastic modulus varies in a random manner about the mean modulus. Su et al. [66] and Baecher and Ingra [69] have introduced Monte-Carlo

simulation to generate randomness in their stochastic models. For the present random stochastic analysis, an alternative computer technique is selected. To incorporate this effect, the selection of modulus C.O.V. must range from zero to the maximum or best estimate of the material's C.O.V. This is achieved by making a random selection of the modulus C.O.V. for each element in the finite element model. By introducing a random number, R_i , between the value of zero and one, the elemental standard deviations are modified.

$$\sigma_{E_i} = \bar{\sigma}_i R_i \lambda_i \quad (3.47)$$

Lewis et al. [86] discussed the application of a pseudo-random number generator to usage on an IBM/360 computer system. The number generator is based on the following algorithm. To generate N random numbers between zero and one, select any number, s_0 , between 1 and $(2^{31}-1)$. This starting value, s_0 , will be used to initiate the sequence of random numbers.

$$s_i = 7^5 s_{i-1} \pmod{(2^{31}-1)} \quad (3.48)$$

$$R_i = 2^{-31} s_i \quad (3.49)$$

where $i = 1, 2, \dots, N$ and R_i represents the random numbers generated. The total number of random numbers required is

equal to the total number of elements, thereby obtaining random σ_g values for each element. The modulo function will perform the following steps:

- (i) Divide the first argument by the second,

e.g.
$$\frac{(7^5 S_0)}{(2^{31}-1)}$$

- (ii) Take the integer part of the quotient by truncating it to the next smallest integer (absolute value).
- (iii) Multiply the integer quotient by the second argument, and subtract the product from the first argument.

This process is analogous to the process of long division. For further information on this procedure see Meissner and Organick [87].

The pseudo-randomness is attributed to the same sequence of random numbers being generated when using the same starting value for S_0 . Once the program reaches a steady-state, the same sequence of random numbers are repeated over a bandwidth of 32 as indicated in Table 3.2.

This provides adequate randomness provided that the finite element model does not have layers with the number of elements being multiples of 32. Otherwise, the pseudo-randomness will be very subjective to localized effects, with all vertical lines of elements having the same pseudo-random coefficients. The procedure generates sequences of uniform random numbers with good random characteristics ([86], [87]).

Table 3.2 Pseudo-Random Number Sequences Between 0,1

Starting Value $S_0 = 1000$	Starting Value $S_0 = 123,457$	Starting Value $S_0 = 500,000$
1 0.007826	1 0.966220	1 0.913185
2 0.537781	2 0.260742	2 0.894531
3 0.481445	3 0.293945	3 0.386719
.	.	.
.	.	.
68 0.152344	12 0.152344	7 0.269531
69 0.441406	13 0.441406	8 0.011719
70 0.714844	14 0.714844	9 0.957031
71 0.378906	15 0.378906	10 0.824219
72 0.277344	16 0.277344	11 0.644531
.	.	.
.	.	.
96 0.027344	40 0.027344	30 0.519531
97 0.566406	41 0.566406	31 0.761719
98 0.589844	42 0.589844	32 0.207031
99 0.503906	43 0.503906	33 0.574219
100 0.152344	44 0.152344	34 0.894531
101 0.441406	45 0.441406	35 0.386719
102 0.714844	46 0.714844	36 0.582031
.	.	.
.	.	.

3.5 Computer Implementation of the Procedure

The algorithms and procedures developed in the previous sections have been coded in FORTRAN 77 language and incorporated into computer programs. Table 3.3 indicates the main computer programs developed for the stochastic finite element analysis. Two problem situations are examined: (i) soil-foundation interaction of a concrete gravity platform resting on a layered soil medium, and (ii) response of sea bottom to placement of Mobile Arctic Caisson structure. Three principal types of analysis have been implemented: (i) linear elastic model, (ii) linear elastic model with pseudo-random material properties and (iii) piecewise linear elastic model. The programs utilize several subroutines which are listed in detail in Appendix IV. This format is used since all the programs are essentially modified forms of ELASTC.FTN, having the same basic subroutines with additional and slightly changed subroutines to incorporate the different versions. An outline of the computer logic and subroutines are listed for the main programs in Tables 3.4 to 3.8.

Table 3.3 Main Computer Programs for Stochastic Finite Element Formulations

Type of Analysis	Gravity Platform Foundation	Mobile Arctic Caisson Structure
Linear Elastic	ELASTC.FTN	CAISON.FTN
Linear Elastic with Pseudo-Random Material Properties	ELRAND.FTN	RAND.FTN
Piecewise Linear Elastic	NONLIN.FTN	

NOTE: Programs are listed with descriptions in Appendix III.

Table 3.4 Outline of Main Program ELASTC.FTN

Description	Subroutine
(1) Generate location and numbering of nodal points and triangular elements for a foundation overlying layered soil media.	GGEN
(2) Input material properties, nodal loads, coefficient of variation for elastic moduli and correlation distance factor.	Main Program
(3) Generate elastic constituent matrix of material properties	DMAT
(4) Assemble local stiffness matrix for element which requires the interpolation matrix, [B], as determined in subroutine BDEFIN, to be generated.	ELST BDEFIN
(5) Assemble global stiffness matrix.	ASMB
Repeat steps (3), (4) and (5) for all elements.	
(6) Decompose global stiffness matrix to an upper triangular matrix using Gaussian elimination procedures.	SYMBOL
(7) Generate load vector.	LOAD
(8) Decompose load vector and solve for nodal displacements using backward substitution.	SYMBOL
(9) Determine displacement vector, (U), and element stresses, (S), for each node and element. (Reference: Eq. (3.26))	RDIS
(10) Differentiate displacement with respect to elastic modulus to obtain coefficients used in calculating the covariances of nodal displacements. (Reference: Eq. (3.8)). Requires subroutine SYMBOL to obtain coefficient values through backward substitution.	DUWM SYMBOL

Table 3.4 Outline of Main Program ELASTC.FTN

Description	Subroutine
(11) Determine displacement covariances by solving Eq. (3.14). Use subroutine CTRD to calculate scalar distance between element centroids for correlation function. Call subroutine SCOVE.	DCOVL CTRD SCOVE
(12) Determine variances of stresses by using Eq. (3.34). This requires (H) function values as described by Eq. (3.32) and obtained in subroutine MAT.	MAT

Table 3.5 Outline of Main Program ELRAND.FTN

Description	Subroutine
(1) Generate location and numbering of nodal points and triangular elements for a foundation overlying layered soil media.	GGEN
(2) Input material properties, nodal loads, coefficient of variation for elastic moduli and correlation distance factor.	Main Program
(3) Generate elastic constituent matrix of material properties.	DMAT
(4) Assemble local stiffness matrix for element which requires the interpolation matrix, [B], as determined in subroutine BDEFIN, to be generated.	ELST BDEFIN
(5) Assemble global stiffness matrix. Repeat steps (3), (4) and (5) for all elements.	ASMB
(6) Decompose global stiffness matrix to an upper triangular matrix using Gaussian elimination procedures.	SYMBOL
(7) Generate load vector.	LOAD
(8) Decompose load vector and solve for nodal displacements using backward substitution.	SYMBOL
(9) Determine displacement vector, (U), and element stresses, (S), for each node and element. (Reference: Eq. (3.26)).	RDIS
(10) Differentiate displacement with respect to elastic modulus to obtain coefficients used in calculating the covariances of nodal displacements. (Reference: Eq. (3.8)). Requires subroutine SYMBOL to obtain coefficient values through backward substitution.	DUWM SYMBOL

Table 3.5. Outline of Main Program ELRAND.FTN

Description	Subroutine
(11) Determine displacement covariances by solving Eq. (3.14). Use subroutine CTRD to calculate scalar distance between element centroids for correlation function. Subroutine GGUBS is used to randomly vary the coefficient of variation of the elastic moduli. Call subroutine SCOVE.	DCOV4 CTRD GGUBS
(12) Determine variances of stresses by using Eq. (3.34). This requires (H) function values as described by Eq. (3.32) and obtained in subroutine MAT.	SCOVE MAT

Table 3.6 .Outline of Main Program NONLIN.FTN

Description	Subroutine
(1) Generate location and numbering of nodal points and triangular elements for a foundation overlying a layered soil media.	GGEN
(2) Input material properties, nodal loads, coefficient of variation for elastic moduli and correlation distance factor.	Main Program
(3) Generate elastic constituent matrix of material properties.	DMAT
(4) Assemble local stiffness matrix for element which requires the interpolation matrix, [B], as determined in subroutine BDEFIN, to be generated as based on latest moduli values.	ELST BDEFIN
(5) Assemble global stiffness matrix. Repeat steps (3), (4) and (5) for all elements.	ASMB
(6) Decompose global stiffness matrix to an upper triangular matrix using Gaussian elimination procedures.	SYMBOL
(7) Generate load vector for load stage.	LOADD
(8) Decompose load vector and solve for nodal displacements using backward substitution.	SYMBOL
(9) Determine displacement vector, (U), and element stresses, (S), for each node and element. (Reference: Eq. (3.26)).	RRDIS
(10) Select piecewise linear elastic modulus for each element based on shear modulus and principal strains obtained from latest stiffness analysis.	NLIN
Repeat steps (3) to (10) until all element moduli have converged (Eq. 3.44) or when advancement to next load stage is required.	

Table 3.6 Outline of Main Program NONLIN.FTN

Description	Subroutine
(11) After each load stage, the nodal displacement and element stresses are accumulated.	Main Program
(12) Differentiate displacement with respect to elastic modulus to obtain coefficients used in calculating the covariances of nodal displacements. (Reference: Eq. (3.8)). Requires subroutine SYMBOL to obtain coefficient values through backward substitution.	DUWM SYMBOL
(13) Determine displacement covariances for this load step by solving Eq. (3.14). Use subroutine CTRDD to calculate scalar distance between element centroids for correlation function. Call subroutine SCOVEN.	DCOVE CTRDD
(14) Determine variances of stress for this step by using Eq. (3.34). This requires $(H)_{ij}^{ij}$ function values as described by Eq. (3.32) and obtained in subroutine MAT.	SCOVEN MAT
(15) Accumulate the nodal displacement covariances and elemental stress variances.	Main Program
Repeat steps (3) to (15) until all load steps are completed.	

Table 3.7 Outline of Main Program CAISON.FTN

Description	Subroutine
(1) Input location and numbering of nodal points and triangular elements for a Mobile Arctic Caisson Island resting on the sea floor. Input material properties, nodal loads, coefficient of variation for elastic moduli and correlation distance factor.	Main Program
(2) Generate elastic constituent matrix of material properties.	DMAT
(3) Assemble local stiffness matrix for element which requires the interpolation matrix, [B], as determined in subroutine BDEFIN, to be generated.	ELST BDEFIN
(4) Assemble global stiffness matrix. Repeat steps (2), (3) and (4) for all elements.	ASMB
(5) Decompose global stiffness matrix to an upper triangular matrix using Gaussian elimination procedures.	SYMBOL
(6) Generate load vector.	LOAD
(7) Decompose load vector and solve for nodal displacement using backward substitution.	SYMBOL
(8) Determine displacement vector, (U), and element stresses, (S), for each node and element. (Reference: Eq. (3.26)).	RDIS
(9) Differentiate displacement with respect to elastic modulus to obtain coefficients used in calculating the covariances of nodal displacements. (Reference: Eq. (3.8)). Requires subroutine SYMBOL to obtain coefficient values through backward substitution.	DUMM SYMBOL

Table 3.7 Outline of Main Program CAISON-FTN

Description	Subroutine
(10) Determine displacement covariances by solving Eq. (3.14). Use subroutine CTRD to calculate scalar distance between element centroids for correlation function. Call subroutine SCOVE.	DCOV2 CTRD
(11) Determine variances of stresses by using Eq. (3.34). This requires $\langle H \rangle_{ij}$ function MAT values as described by Eq. (3.32) and obtained in subroutine MAT.	SCOVE

Table 3.8 Outline of Main Program RAND.FTN

Description	Subroutine
(1) Input location and numbering of nodal points and triangular elements for a Mobile Arctic Caisson Island resting on the sea floor. Input material properties, nodal loads, coefficient of variation for elastic moduli and correlation distance factor.	Main Program
(2) Generate elastic constituent matrix of material properties.	DMAT
(3) Assemble local stiffness matrix for element which requires the interpolation matrix, [B], as determined in subroutine BDEFIN, to be generated.	ELST BDEFIN
(4) Assemble global stiffness matrix. Repeat steps (2), (3), and (4) for all elements.	ASMB
(5) Decompose global stiffness matrix to an upper triangular matrix using Gaussian elimination procedures.	SYMBOL
(6) Generate load vector.	LOAD
(7) Decompose load vector and solve for nodal displacement using backward substitution.	SYMBOL
(8) Determine displacement vector, (U), and element stresses, (S), for each node and element. (Reference: Eq. (3.26)).	RDIS
(9) Differentiate displacement with respect to elastic modulus to obtain coefficients used in calculating the covariances of nodal displacements. (Reference: Eq. (3.8)). Requires subroutine SYMBOL to obtain coefficient values through backward substitution.	DUWM SYMBOL

Table 3.8 Outline of Main Program RAND.FTN

Description	Subroutine
(10) Determine displacement covariances by solving Eq. (3.14). Use subroutine CTRD to calculate scalar distance between element centroids for correlation function. Subroutine GGUBS is used to randomly vary the coefficient of variation of the elastic moduli. Call subroutine SCOVE.	DCOV3 CTRD GGUBS
(11) Determine variances of stresses by using Eq. (3.34). This requires (H_{ij}) function values as described by Eq. (3.32), and obtained in subroutine MAT.	SCOVE MAT

CHAPTER 4

STOCHASTIC FINITE ELEMENT ANALYSIS OF SOIL-FOUNDATION FOR A
CONCRETE GRAVITY PLATFORM

4.1 Introduction

The stochastic finite element procedure outlined above can be applied to many structural and geotechnical problems. To indicate the possible usage, an application related to offshore structures is selected. As a result of the offshore oil and gas exploration on the Canadian East Coast, the likelihood of a fixed platform production mode has become a strong possibility. The federal and Newfoundland governments have favoured the use of concrete gravity platforms for the Hibernia oil field and recently, Mobil Oil, the developer of Hibernia, has stated in their development plan at least one concrete gravity platform will be utilized. Much knowledge and expertise in concrete gravity structures is readily available from existing operations in the North Sea. There are many similarities between the marine climates of these two regions. The environmental conditions such as water temperature, air temperature,

extreme wind and wave conditions; all indicate common design criteria².

To make the example more applicable to the local offshore, a North Sea concrete gravity structure located under similar water depth and soil conditions to the Hibernia site is preferred. From Table 2.1, the Ekofisk Tank at 70 m water depth overlying dense sand best resembles the site conditions of Hibernia at 90 m water depth [88]. The Ekofisk Tank, being the first concrete gravity structure placed in the North Sea, has been the subject of several technical papers describing its design, construction, location and on-site performance. With this abundance of information available, the Ekofisk Tank can be examined to determine the soil-foundation interaction. Comparison of the stochastic analysis results and the measured response of the tank foundation as reported in literature is made in this Chapter.

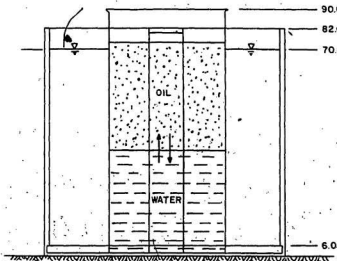
²One notable exception is the presence of seasonable pack-ice and icebergs on the Canadian East Coast which will require special attention.

4.2 Ekofisk Tank Description

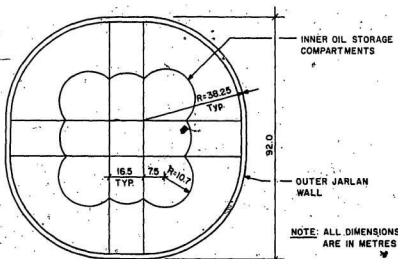
The Ekofisk Tank (Figure 2.2) has been described by Clausen et al. [89] and Gerwick and Hognestad [90]. Based on their descriptions, a plan and section of the Ekofisk Tank is presented in Figure 4.1. The prestressed concrete structure has a large inner concrete section of nine cellular compartments with an overall dimension of 52 m square. Surrounding this central cellular section is an outer perforated breakwater wall of the Jarlan-type [91]. In plan this wall is a 92 m square with corners rounded to a 38.25 m radius of curvature. The platform is resting on the seafloor in 70 m water depth with the deck level 20 m above the ocean surface. The tank foundation covers an area of 7360 square meters.

4.2.1 Ekofisk Site Conditions

Examination of subsurface sediments require more costly sample retrieval methods such as gravity corers and wire-line drive samplers for deep borings. Experimental scatter of results within a boring sample or between several borings in the same vicinity indicate the difficulty of specifying the proper soil strengths. The soil strengths are expressed as the algebraic sum of a mean value and a deviation. The effect of uncertainty on the platform response is examined



Vertical Cross-Section



Horizontal Section

FIGURE 4.1 EKOFISK TANK ; HORIZONTAL & VERTICAL SECTIONS

in a quantitative manner by the stochastic finite element procedure. Using the means and variances of the site conditions published in literature, the analysis is performed.

Typically at the Ekofisk field, the upper 25 m consists of extremely uniform sand. Samples of grain-size distribution from four platform sites, shown in Figure 4.2, indicate the sand composition to be fairly consistent throughout the area (Bjerrum [19]). It is of interest to note that the samples fall within the middle range for sands susceptible to liquefaction. Most sand layers in the North Sea exhibit very dense depositions with 90% to 100% relative density.

The clays encountered beneath the sand are of the Pleistocene age. These clays are heavily over-consolidated. The clays, with the exception of surface deposits, range from stiff to very hard consistency with an average un-drained shear strength of 200 kPa to 500 kPa. Typical clays in the North Sea have medium to high plasticity with a plasticity index of 20-40%. The water content of these clays is close to the plastic limit, usually 20-25%. The sensitivity is on the average 1.0 to 1.5 for this region. It is not uncommon for the clay layers to contain bands of silt and silty clays within the soil matrix. In some

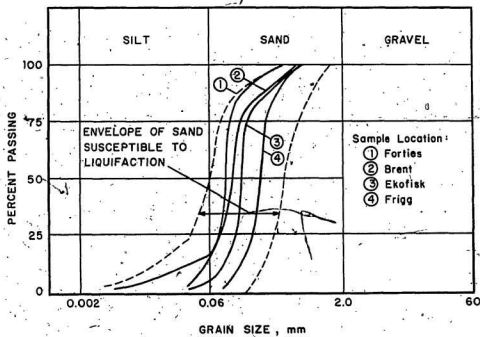


FIGURE 4.2 GRAIN-SIZE DISTRIBUTIONS^a OF SAND SAMPLES FROM NORTH SEA PLATFORM SITES (Bjerrum[19].)

locations, boring samples show a trend in the undrained shear strength of clays as a function of depth [13, 92].

The soil composition at the site is shown in Figure 4.3 [19, 89]. The top 26 m of soil consists of fine uniformly graded sand at a relative density close to 100%. The angle of internal friction for the dense sand layers under drained conditions is $\phi = 42^\circ$. The minimum porosity ($n_{\min.}$) of 34% and the maximum porosity ($n_{\max.}$) of 48% are characteristic of the upper sand layers. Interbedded in this sand layer between 16 m and 18 m depth is a two meter layer of stiff clay with low plasticity and undrained shear strength ≈ 200 kPa. At the depths between 26 m to 40 m, 49 m to 53 m and 80 m to 100 m, extremely hard clay materials are encountered with an average undrained shear strength of 400 kPa. These clay layers are found interbedded with dense sand to dense silty sand layers. Below the 100 m depth, little information is available on material properties for the soils. The unit weight of the soils are consistent within the range of 21.0 to 21.7 kN/m³.

4.2.2 Finite Element Representation

The stochastic finite element formulation developed in Chapter 3 utilizes a two-dimensional plane strain finite element with constant strain triangular elements. To apply

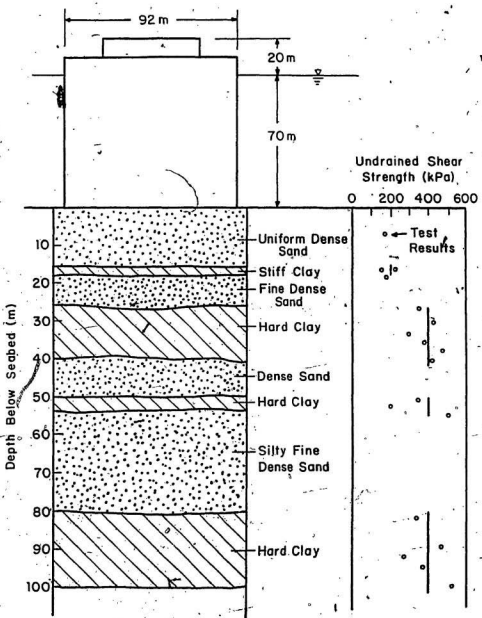


FIGURE 4.3 IN-SITU SOIL PROFILE , EKOFISK

(Bjerrum [19] and Clausen et. al. [89])

this procedure, the problem situation must be represented as a two-dimensional section with all model deformations restricted to this plane. This limitation involves a simplification of most real problems since in reality the materials are free to deform in all three dimensions.

The present model has its own merits in providing useful information on problems. Proper selection of material properties, section locations and load applications will provide a reliable analysis.

The raft foundation of the Ekofisk Tank and the underlying soil continuum have been discretized into triangular elements as shown in Figure 4.4. This model contains 303 nodal points and 536 elements. The basic procedure utilized in arriving at this configuration is presented herein.

The overall dimensions of the finite element model have been made to correspond with the limits suggested by earlier researchers for soil-foundation interaction problems. The horizontal dimension of the model should be within the range of 4 to 6 times the foundation width to ensure reliable results. Similarly, the criterion for vertical overall model dimensions should fall within 3 to 4 times the foundation width.

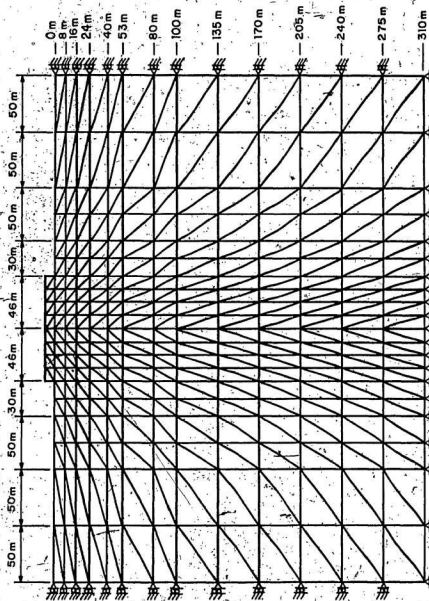


FIGURE 4.4 FINITE ELEMENT MESH FOR TWO-DIMENSIONAL MODEL

Boundary conditions of the model have been selected to best simulate the soil behaviour. At the lower horizontal boundary, the nodes are fixed to represent the diminishing displacements at this extreme location in the mesh. Vertical rollers are used at the two vertical boundaries to permit vertical movement only. Lateral resistance provided by neighbouring soils is considered sufficient to restrain any horizontal nodal displacements at these locations.

Selection of interhal dimensions of the mesh are influenced by primarily two factors, (i) soil stratification and (ii) element aspect ratios (e.g. ratio of long to short dimension of elements). As indicated in Figure 4.3, the soil profile beneath the tank consists of several nearly horizontal strata of differing soil types. To duplicate this effect, the vertical depth of the elements have been selected to correspond to actual in-situ soil layers. But, to obtain permissible aspect ratios, some soil layers have been combined to form a single layer with modified material properties. Reliable finite element results require a large number of smaller elements beneath the highly stressed foundation zone and aspect ratios no greater than five or six. To achieve this latter requirement, a clay layer between elevations 16 m and 18 m has been combined with a sand layer from 18 m to 24 m (see Figure 4.3). Similarly,

the clay layer between 49 m and 53 m has been grouped with the dense sand above it. Consequently, over 95% of the elements conform to the aspect ratio requirement. A small number of elements in both upper corners of the mesh have aspect ratios of 6.25. These elements are situated in a low stress region away from the raft foundation zone, thereby having negligible affect on results.

The published soil borings are limited to the 0 m to 100 m depths. Beyond this limit the material properties are assumed using gradually stiffer materials.

4.2.2.1 Mean Material Properties for Finite Element Model

The concrete raft foundation of the Ekofisk Tank is represented by sixteen elements shown above 0 m level in Figure 4.4. These elements are 6 m in height as indicated in Figure 4.1. The concrete foundation consists of a lean concrete mix (i.e. low strength, high water-cement ratio) poured between a stronger vertical concrete rib network [90]. Using an average concrete compressive strength, f'_c , of 20 MPa, the material properties are estimated.

The modulus of elasticity, E , for normal density concrete can be determined as [93]:

$$E = 4730 \text{ ft}^2/\text{lb}$$
$$= 21,150 \text{ MPa}$$

(4.1)

This elastic modulus is substantially higher than that of soil thereby inducing the concrete foundation to behave as a rigid structure.

For normal density concrete, Poisson's ratio has an expected range of values between 0.15 and 0.25 as suggested by the Canadian Portland Cement Association [94]. Poisson's ratio, ν , will vary according to the aggregate type, moisture condition in the service environment and age of concrete. For this example, a value of 0.20 is selected.

For immediate or short-term settlement analysis, the geotechnical properties must be representative of undrained site conditions. Kjekstad and Lunne [95] have provided undrained elastic moduli values for a North Sea site with dense sand overlying hard clay, similar to Ekofisk. Their results have indicated the undrained modulus, E_u , typically varied from 130 MPa for the upper 10 m, increasing to 160 MPa for the next 35 m, then reaching a maximum of 200 MPa at a depth of 45 m. These values are in good agreement with those given by Bowles [96].

Similarly for clay strata, Kjekstad and Lunne [95] have presented an empirical relationship between undrained shear strength, S_u , and undrained shear modulus, G_u , for cyclic stress levels below 0.25 S_u .

$$G_u = 135 S_u \quad (4.2)$$

For the undrained soil condition, with Poisson's ratio at 0.5, the elastic modulus, E_u , can be approximated as 3 G_u or:

$$E_u = 400 S_u \quad (4.3)$$

Using this relationship, E_u for the stiff clay and hard clay layers, respectively, are estimated at 80 MPa and 160 MPa for the Ekofisk site (see Figure 4.3).

As mentioned in Section 4.2.1, little published information is available on the soil properties below the 100 m level. For the present analysis, 80 to 90% of total soil deformation has occurred in the upper 100 m based on preliminary finite element results. This is comparable to an expected 80% of total settlement beneath a square foundation with homogeneous and laminated soil according to Westergaard [97]. Essentially, soil settlement is primarily determined by the upper soil layers. For the finite element

model, layers below 100 m, the modulus is assumed to gradually increase, to physically represent the expected increase in stiffness with depth.

The mean material properties selected to simulate the soil conditions at the platform site are indicated in Table 4.1. The selection of Poisson's ratio, ν , has been reduced slightly from the 0.5 value for undrained conditions to avoid numerical instability in the finite element analysis. Poisson's ratios have been selected as 0.49 for clays, 0.45 for sands due to its almost immediate drainage action, 0.46 for combined sand and clay strata and 0.30 for typical rock types.

Table 4.1. Mean Material Properties at Platform Site

Depth Range (m)	Material Description	Elastic Modulus (MPa)	Poisson's Ratio
-6 - 0	Concrete	21,150	0.20
0 - 6	Fine Dense Sand	118	0.45
6 - 16	Fine Dense Sand	148	0.45
16 - 26	Dense Clayey Sand	152	0.46
26 - 40	Hard Clay	160	0.49
40 - 53	Dense Clayey Sand	188	0.46
53 - 80	Silty Fine Dense Sand	200	0.45
80 - 100	Hard Clay	160	0.49
100 - 135	Very Dense Sand	500	0.45
135 - 170	Very Soft Rock	1,500	0.30
170 - 205	Soft Rock	3,000	0.30
205 - 240	Medium Rock	5,000	0.30
240 - 275	Medium Rock	7,500	0.30
275 - 310	Hard Rock	10,000	0.30

Table 4.2 Calculation of Average Modulus of Elasticity
for Upper 100 m of Seabed at Ekofisk

Depth Range (m)	Thickness t (m)	E_u per layer (MPa)	Influence Factor (I.F.)	E_u' * per layer (MPa)
0 - 8	8	118	1.3	12.27
8 - 16	8	148	1.2	14.21
16 - 26	10	152	1.1	16.72
26 - 40	14	160	1.0	22.40
40 - 53	13	188	0.9	22.00
53 - 80	27	200	0.8	43.20
80 - 100	20	160	0.7	22.40

$$\Sigma E_u' = 153.20$$

* E_u' = layer contribution to average elastic modulus

$$E_u' = E_u \times I.F. \cdot \left(\frac{t}{100}\right)$$

(Based on Westergaard [97])

Clausen et al. [89] have reported an average elastic modulus of 150 MPa on settlement records of the Ekofisk tank. The average modulus for the top 100 m as calculated in Table 4.2 has been estimated at 153 MPa. Included in the calculating procedure are the effects of layer depth and the decreased influence on the average with increased depth (i.e. influence factor).

4.2.3 Load Cases for Analysis of Platform

To apply the stochastic finite element procedure, two practical load cases are examined for the Ekofisk Tank. The first case is the static load with the gravitational forces of the submerged tank self-weight acting on the soil medium. The second case is the quasi-static wave force of an actual storm combined with the gravity load. Clausen et al. [89] have published numerical values for both conditions as indicated in Figure 4.5.

For the case of a rigid foundation resting on a dense sand layer with modulus of elasticity increasing with depth, the pressure distribution beneath the foundation is maximum at the center and minimum at the edges. However as the foundation dimensions become large, the distribution of contact pressures approach a uniform distribution [98]. Such is the case for the gravity loading of the Ekofisk Tank³. The submerged weight of the ballasted structure has been estimated at 1860 MN. By considering this force to be distributed evenly over the total base area of 7360 m^2 , the expected base contact pressure is 252.7 kPa. Using a one metre wide strip, this pressure is applied as nodal forces

³The modulus of elasticity for the concrete foundation being approximately 180 times that of the uppermost sand layer, the foundation will behave with much more rigidity than the soil.

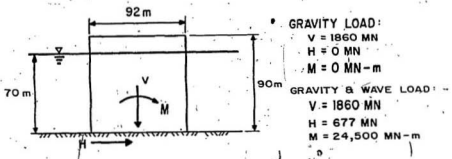


FIGURE 4.5 LOAD CASES FOR PLATFORM

(Clausen et al. [89])

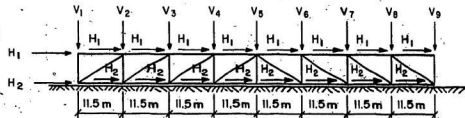
on the finite element mesh of Figure 4.4. These forces which act on the nodes representing the concrete tank foundation are shown in Figure 4.6.

In November 1973, the Ekofisk Tank had been subjected to a North Sea storm creating wave forces at 90% of the 100-year design wave. This storm of five hours duration had an average wave period of twelve seconds and a maximum wave height of 21 m. Estimated storm forces have been obtained from tests on a 1:100 scale model of the Ekofisk Tank at the River and Harbour Laboratory in Trondheim, Norway. Using a 21 m wave with a fifteen second period, the quasi-static forces at the seafloor level were estimated as 677 MN horizontal sliding force and 24,500 MN-m overturning moment. The average vertical load remained unchanged at 1860 MN [89].

The conventional equation for subgrade reaction on a rigid foundation subjected to an eccentric vertical load is used to arrive at the soil pressures and the subsequent nodal loads.

$$P = \frac{V}{A} + \frac{Mc}{I} \quad (4.4)$$

where P = soil pressure



Finite Elements of Tank Foundation

NODAL FORCE	GRAVITY LOAD (MN)	GRAVITY & WAVE LOADS (MN)
H_1	0.00	0.5688
H_2	0.00	0.5688
V_1	1.453	0.048
V_2	2.906	0.6584
V_3	2.906	1.4076
V_4	2.906	2.1568
V_5	2.906	2.9061
V_6	2.906	3.6553
V_7	2.906	4.4045
V_8	2.906	5.1537
V_9	1.453	2.8578

FIGURE 4.6 LOAD FORCES ON NODES OF FINITE ELEMENT REPRESENTATION OF TANK FOUNDATION

- V = vertical force (1860 MN)
A = area of raft foundation (7360 m^2)
M = overturning moment (24,500 MN-m)
c = distance from extreme fibre to bending axis
= $(0.5)(92 \text{ m}) = 46 \text{ m}$
I = gross moment of inertia (see Appendix V)
(4324150 m^4)

The soil pressure ranges from a minimum of -7.9 kPa to a maximum of 513.3 kPa. The nodal forces required to simulate this loading condition are derived in Appendix VI. In Figure 4.6, the resulting nodal forces are indicated.

4.3 Linear Elastic Analysis

Using a linear elastic constitutive relationship for the modulus of elasticity, the stochastic finite element method is applied to the Ekofisk Tank. Using the program ELASTC.FTN (Appendix III), the soil-foundation interaction is examined for the gravity load and the combined gravity and wave load cases. The analysis has examined the vertical displacement, relative settlement, normal stresses and shear stress of the soil foundation as the gravity base is subjected to these loading conditions. To establish the sensitivity of the stochastic procedure to changes in parameters, several versions of the analysis are compared. The parameters to be varied in the computer runs are the coefficient of variation of the elastic modulus, C.O.V. (E), and the correlation distance factor, CDF.

Considering the modulus C.O.V. to represent the degree of material uncertainty, a value is assumed for the computer analysis. This selected modulus C.O.V. is constant for each element during the analysis. The range of values used in the parametric analysis varies from 5% to 25% by 5% increments. This range is representative of typical soil strength uncertainties as suggested in section 2.2.4.1. For this segment of the parametric study, the correlation distance factor is fixed at 50 to remove its influence on the

results. As indicated previously in Section 3.1, the modulus C.O.V. should be less than 30% due to accumulating errors in neglecting second order terms of Eq. (3.3).

The stochastic nature of the analysis is attributed to the correlation function as defined by Eq. (3.17). The correlation function describes the degree of dependency or likelihood of similar material properties occurring as a function of the distance between element centroids, r_{ij} . The rate of exponential decay of the correlation function is established through the correlation distance, L . The correlation distance is simply the product of the width of the foundation (e.g. 9.2 m) and the correlation distance factor. In Figure 4.7, the correlation function is shown for various correlation distances corresponding to correlation distance factors of 0.1, 0.5, 1, 5 and 50. For a correlation distance of 9.2 m, elements separated by more than 50 m are perfectly uncorrelated. For this case, there is little influence of one element's uncertainty on the others. For correlation distance above 4600 m, the soil continuum becomes highly correlated. Under this condition, the uncertainty in elastic moduli of all elements have significant influence on the uncertainty of local displacements and stresses. The effect of different correlation distance factors on results is examined by fixing the modulus C.O.V. at 15%.

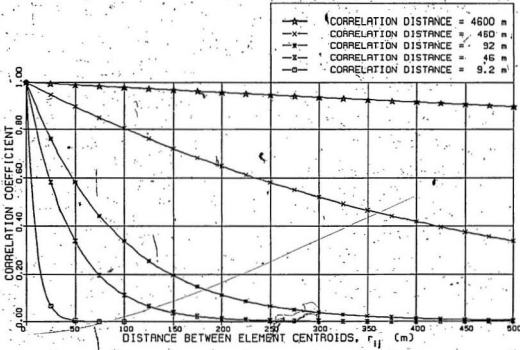


FIGURE 4.7 CORRELATION COEFFICIENT FUNCTION FOR EKOFISK TANK

4.3.1 Vertical Displacement Results

The nodal displacements obtained from the plane strain finite element analysis are selected as the expected mean displacements for the stochastic analysis. In Figure 4.8, the mean vertical displacements at the soil-foundation interface are indicated for both load conditions. The Ekofisk Tank foundation is situated between -46 m and +46 m with zero representing the center of the foundation. The analysis indicates symmetrical settlements for the gravity load. As expected, maximum displacements and differential settlements occur during the combined gravity and storm wave cases. Clausen et al. [89] have published actual field measurements of the tank's performance. Up to the time of ballasting to 1860 MN submerged weight, the foundation settled on average 140 mm. Maximum settlement predicted by the gravity load in Figure 4.8 is .60 mm. Some of this difference can be attributed to consolidation settlement over the two-month installation period and settlement resulting from previous wave loadings being included in the 140 mm figure. But the major factor contributing to the large difference is the neglecting of nonlinear soil effects in the linear elastic model. As shown in Section 4.4, the nonlinear soil model provides a more realistic comparison with the field data. After the storm wave loading, the

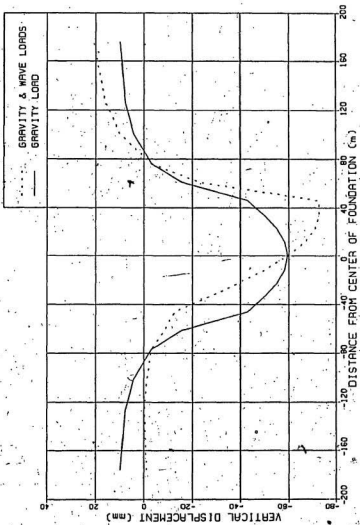


FIGURE 4.8 MEAN VERTICAL DISPLACEMENT AT SOIL-FOUNDATION INTERFACE

total settlement was measured at 220 mm [89]; the elastic finite element model gave an average displacement of 60 mm at the center and a maximum displacement of 73 mm at the edge. The elastic material properties have not been adjusted to account for these discrepancies since these values provide excellent agreement between the nonlinear analysis results and the field data. Nevertheless, the linear elastic analysis will indicate the general behaviour of the structure. A modification factor can be applied to reflect the relative proportion of the actual displacement to the predicted value.

In Figure 4.9, the vertical displacement profiles at different depths are compared. The depths considered are 0 m, 40 m, and 80 m with zero denoting the original seabed level. The results are presented for both load conditions. The settlements are as anticipated with 40% occurring in the 40 m and 35% occurring between the 40 m and 80 m levels. It is observed that as depth increases, the local distortions become less pronounced, indicating the redistribution of applied stresses in the soil.

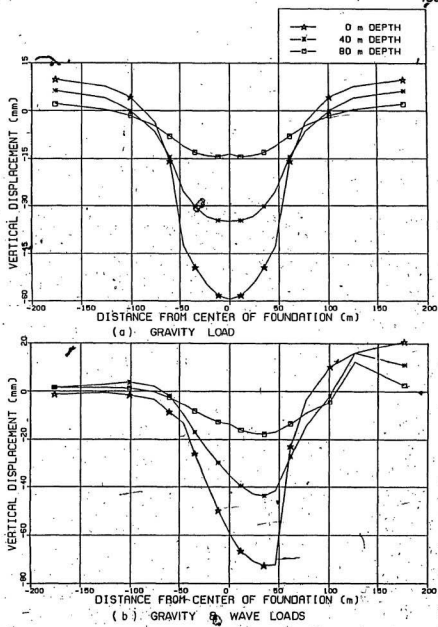


FIGURE 4.9 VERTICAL DISPLACEMENT AT VARIOUS DEPTHS

4.3.1.1 Effect of Coefficient of Variation for Elastic Modulus

The uncertainty in the resulting nodal displacements due to the uncertainty in element moduli is determined through the stochastic analysis. The sensitivity to different coefficients of variation for the elastic modulus is examined first. Using Eq. 3.15, the variance in vertical displacements is computed for each of the nodal points selected for uncertainty analysis. Using the definition of standard deviation as the square root of variance, the results are plotted in Figure 4.10 for the gravity load case. Dividing the standard deviation values by the mean vertical displacements (Figure 4.8), the coefficients of variation for vertical displacement are determined. Similarly, the results for combined gravity and wave loads are shown in Figure 4.11. As expected for both load cases, the standard deviation curves are maximum directly beneath the foundation. The larger standard deviations correspond to regions of greater vertical settlements. The sensitivity of the standard deviation to changes in modulus C.O.V. is a linear relationship. The vertical displacement C.O.V. is fairly constant beneath the foundation for each modulus C.O.V. curve, but it tends to become erratic at the foundation edges due to boundary effects. For the combined load case, the C.O.V. values increase dramatically between -100.m

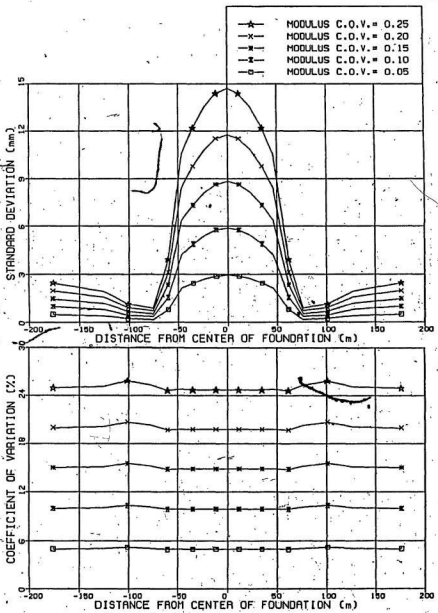


FIGURE 4.10 STATISTICAL PARAMETERS FOR VERTICAL DISPLACEMENT DUE TO GRAVITY LOAD

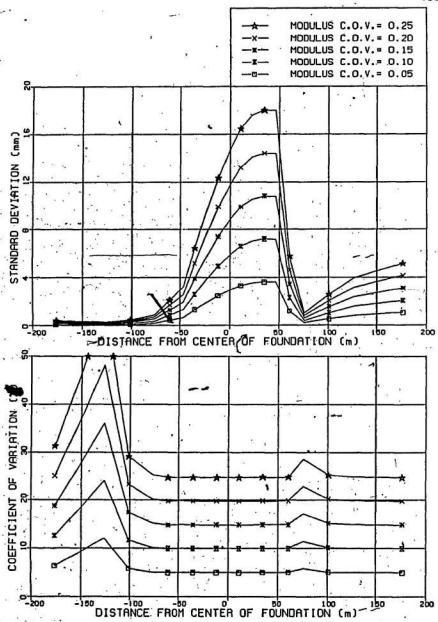


FIGURE 4.11 STATISTICAL PARAMETERS FOR VERTICAL
DISPLACEMENT DUE TO GRAVITY & WAVE LOADS

and -150 m. This anomaly is attributed to the magnified effect on the results when the mean displacement decreases rapidly.

To provide a means of easier physical interpretation of these statistical parameters, confidence intervals are used. For most statistical and design purposes, the 95% confidence limits are most common. The 95% confidence limits are shown for the vertical displacement of the gravity load and combined gravity and wave loads in Figures 4.12 and 4.13, respectively. Based on a material uncertainty of 15% in the elastic modulus and a correlation distance factor of 50, the regions bounded by these limits represent the range of probable settlements for 95% of the time. The upper and lower limits are obtained by adding and subtracting two standard deviations to the mean values [99]. This procedure is based on the assumption that the stochastic results follow a normal distribution. As observed, the bandwidth is widest directly beneath the tank foundation, reaching a maximum of 43 mm at +35 m in Figure 4.13. The observed bandwidths are worst case scenarios since the present analysis assumes a 15% modulus C.O.V. for all elements. In a real soil medium, the modulus uncertainty will vary from location to location. This aspect is addressed in Section 4.3.5. Another contributing factor to the large bandwidth is the correlation distance factor of 50. Under this

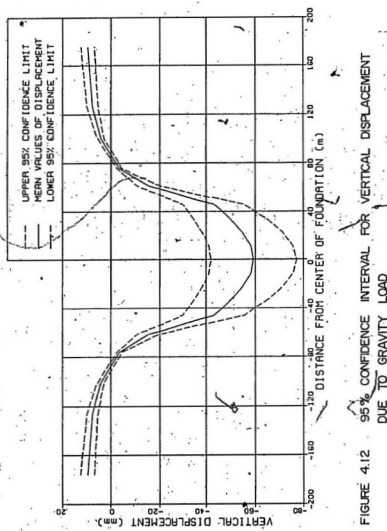


FIGURE 4.12 95% CONFIDENCE INTERVAL FOR VERTICAL DISPLACEMENT DUE TO GRAVITY LOAD

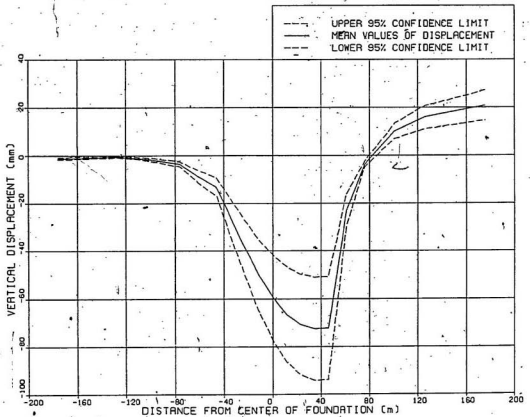


FIGURE 4.13 95% CONFIDENCE INTERVAL FOR VERTICAL DISPLACEMENT DUE TO GRAVITY & WAVE LOADS.

condition, the model becomes highly correlated, increasing the influence of uncertainty in nodal displacements on each other.

4.3.1.2 Effect of Correlation Distance Factor

The correlation distance factor used in evaluating the correlation coefficient between elastic moduli of different elements (Eq. 3.17) is set at 0.1, 0.5, 1, 5 and 50. For this analysis, the elastic modulus C.O.V. is fixed at 15%. The sensitivity to different correlation distance factors is examined in Figures 4.14 and 4.15. Two trends are indicated by these results:

(i) As the correlation distance factor approaches infinity (i.e., for practical purposes, approaches 50), the vertical displacement C.O.V. approaches the elastic modulus C.O.V. In Figures 4.14 and 4.15, for CDF of 50, the C.O.V. curves have attained a value of 15%, equal to the modulus C.O.V. used in the analysis.

(ii) As the correlation distance factor approaches zero, the vertical displacement C.O.V. approaches zero.

These results are anticipated if the exponential decay in the correlation coefficient function of Eq. (3.17) is observed. With larger correlation distance, the correlation coefficient approaches one; with smaller correlation dis-

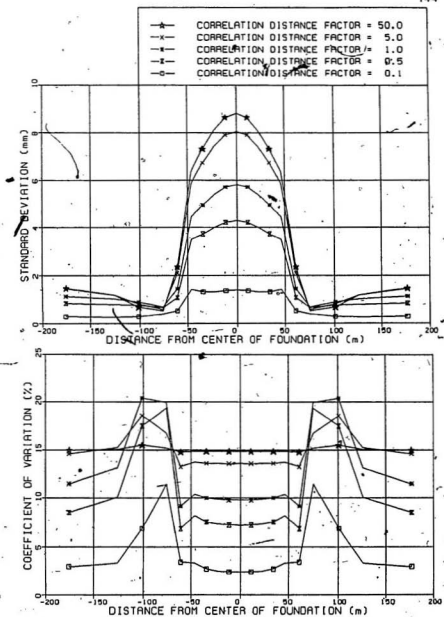


FIGURE 4.14 STATISTICAL PARAMETERS FOR VERTICAL
DISPLACEMENT DUE TO GRAVITY LOAD

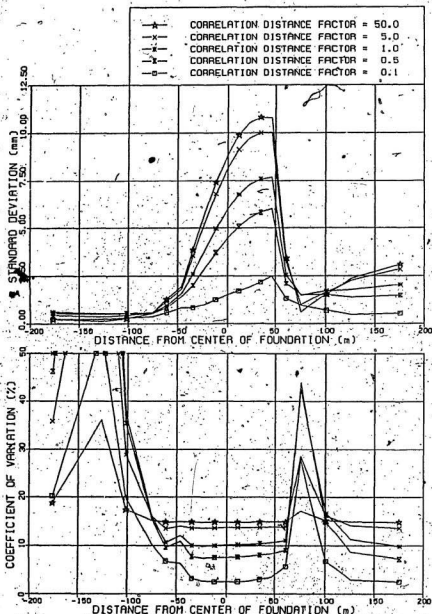


FIGURE 4.15. STATISTICAL PARAMETERS FOR VERTICAL DISPLACEMENT DUE TO GRAVITY & WAVE LOADS

tance, the correlation coefficient approaches zero (Figure 4.7).

The most pertinent information relating to soil displacement relates the behaviour under the structure. Restricting the examination of results to directly beneath the tank foundation (i.e. between -46 m and +46 m), the results indicate essentially the same vertical displacement C.O.V. for both load conditions using the same parameters. This suggests that the vertical displacement C.O.V. is insensitive to load type (e.g., uniform or linearly varying).

To verify the results of the stochastic analysis, the total settlement uncertainties for various correlation distance factors (i.e. normalized autocorrelation distance) are compared to the results of Baecher and Ingra's [69] two-dimensional models with isotropic correlation. In Figure 4.15a, the results of the linear elastic model are compared to the homogeneous and nonhomogeneous soil profiles. The total settlement uncertainty is measured through the ratio of the coefficient of variation of vertical displacement to the coefficient of variation of elastic modulus. The present analysis shows strong correlation with the nonhomogeneous profile results.

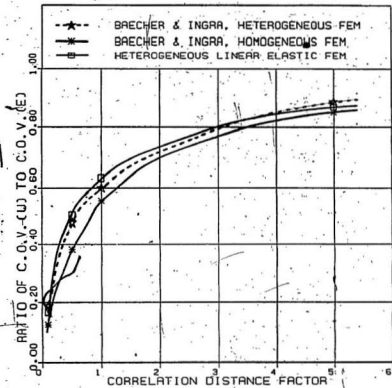


FIGURE 4-15a COMPARISON OF STOCHASTIC SETTLEMENT ANALYSIS

In Figures 4.16 and 4.17, a comparison of 95% confidence intervals for correlation distance factors of 0.5 and 50 is presented. The predictability of short term settlement is greatly enhanced by the CDF of 0.5. The maximum bandwidth reduces from 43 mm for CDF of 50 to 23 mm, indicating a significant reduction in displacement uncertainty. This correlation distance factor is a parameter determined by site soil conditions and foundation width. For practical applications this factor has to be verified by statistical analysis on a grid network of boreholes.

4.3.2 Relative Settlement

Relative settlement, ΔU_{ij} , is expressed as the difference between the expected vertical displacement, U_i and U_j . Using an i-axis to denote the location of node i or the tank foundation, the mean relative displacements for all nodes j are computed relative to the mean vertical displacement at node i, using Eq. (3.21). The variance for these relative settlements are estimated using Eq. (3.23), derived in Section 3.1.3. For each relative settlement, the variance is the summation of the vertical displacement variance at node i and j minus twice the covariance between nodal displacements U_i and U_j .

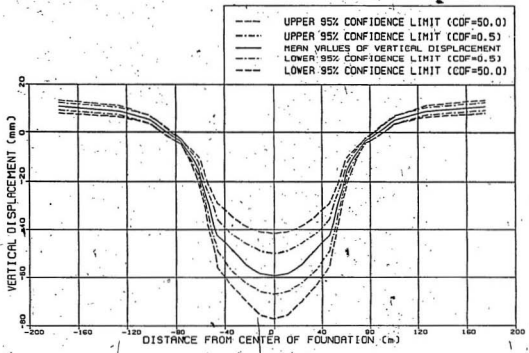


FIGURE 4.16 95 % CONFIDENCE INTERVALS FOR VERTICAL DISPLACEMENT
DUE TO GRAVITY LOAD

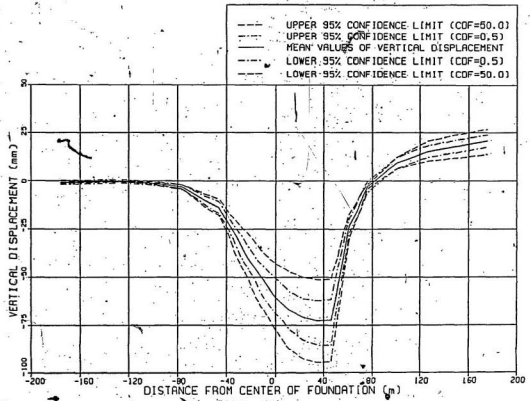


FIGURE 4.17 95% CONFIDENCE INTERVALS FOR VERTICAL DISPLACEMENT DUE TO GRAVITY & WAVE LOADS

The relative settlement at the soil-tank interface only is examined, since it has physical significance. For the present investigation, results are selected from the stochastic analysis in which the coefficient of variation of elastic modulus and correlation distance factor are fixed at 15% and 50, respectively. In Figures 4.18 and 4.19, the results of the gravity load case are compared using 95% confidence intervals. The results are symmetrical about the center of the foundation for both i-axis locations. Defining bandwidth as the range of values between the upper and lower limits, this term is used to describe the curves. Typically, the bandwidth is zero at the i-axis location and gradually increases with distance from node i. Within the vicinity of the foundation, a maximum bandwidth of 10 mm is measured. For 95% confidence, the 16.5 mm mean relative settlement between the center and edge is expected to vary anywhere between 11.5 mm to 21.5 mm. Clausen et al. [89] have reported the tank's differential settlement as less than 20 mm for the gravity load case. This value compares well with the stochastic model simulation. Beyond the foundation to the edges of the finite element model, the covariance term and the variance of node j term become more significant in Eq. (3.23). Both terms decrease in magnitude, with the covariance term gradually taking on a negative value. This explains the large bandwidths beyond ± 50 m.

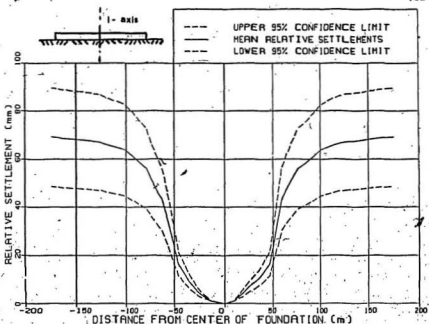


FIGURE 4.18 RELATIVE SETTLEMENT AT CENTER : GRAVITY LOAD

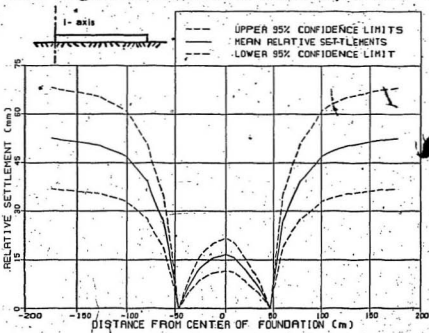


FIGURE 4.19 RELATIVE SETTLEMENT AT EDGE : GRAVITY LOAD

Using the same stochastic parameters, the combined gravity plus storm wave load case results are examined for relative settlement. The information is summarized using confidence intervals as shown in Figures 4.20, 4.21 and 4.22. These curves indicate essentially the same results but plotted from different frames of reference. In Figure 4.20, the difference in settlement of the foundation is more pronounced on the left side of center. After examining the load configuration for the overturning moment (Figure 4.6), this result seems to be reasonable. To observe overall differential settlement, the i-axis is located at the left or right edge of the tank foundation (Figures 4.21 and 4.22). With 95% confidence, the stochastic analysis has suggested the total differential settlement ranging between 41.5 mm and 77.0 mm, with an expected value of 59.5 mm. After removing the effects of the gravity loading, the relative settlement attributed to the storm wave loading is estimated between 30 mm to 55.5 mm with a mean value of 43 mm. This concurs with the observed field settlement of 40 mm [89].

Within the width of the foundation, the bandwidths are still rather large. As mentioned in Section 4.3.1, the stochastic parameters describe a worst case scenario. A reduction in the uncertainty will occur in most practical

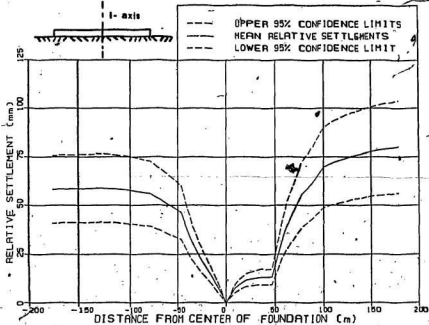


FIGURE 4.20 RELATIVE SETTLEMENT AT CENTER : COMBINED LOAD

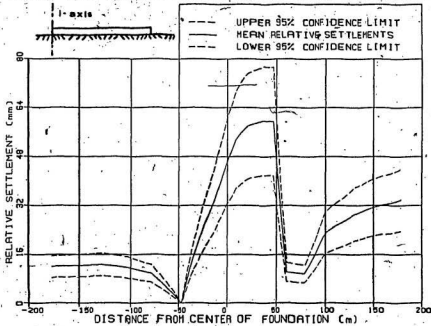


FIGURE 4.21 RELATIVE SETTLEMENT AT LEFT EDGE : COMBINED LOAD

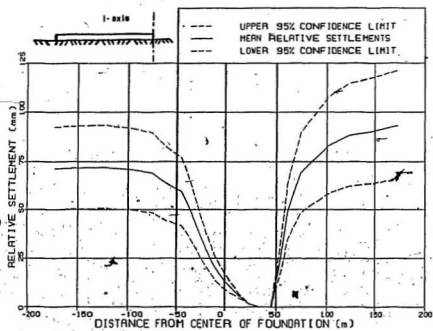


FIGURE 4.22 RELATIVE SETTLEMENT AT RIGHT EDGE:
COMBINED LOAD

problems since the actual soil continuum will have less correlation and the modulus C.O.V. will not be a fixed value but vary between zero and a maximum.

4.3.3 Vertical Stress Distributions

The mean vertical stresses utilized in the stochastic analysis are obtained from the finite element analysis. In Figure 4.23 the variation^s of vertical stress, σ_y , is presented for gravity load and gravity plus storm wave loads on the Ekofisk Tank. The highest vertical stresses occur directly beneath the platform foundation as expected. Lee and Focht [100] have calculated a contact bearing pressure of -267 kPa during static gravity load. In the present analysis, the expected uniform vertical stress is estimated at -253 kPa based on simple footing bearing pressure formulae (Section 4.2.3). Similarly, during the combined loading, the vertical stress variation beneath the foundation is estimated to be linearly distributed with a minimum of +8 kPa and a maximum of -513 kPa. These computed stresses are compatible with the finite element values shown in Figure 4.23. It should be noted that these element stresses represent the average stress at the element centroid depth of 2.67 m for the top 8 m sand layer. These values will reflect the actual soil pressures at the soil-foundation interface with sufficient accuracy.

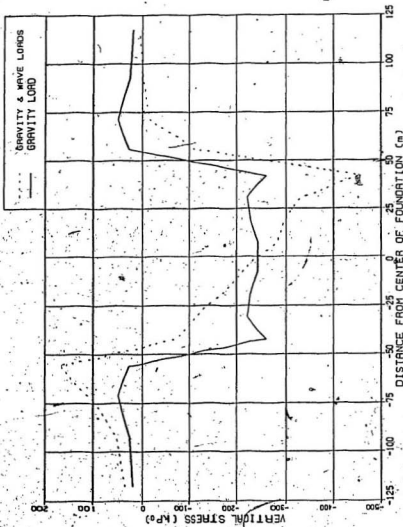


FIG E. 4.23 MEAN VERTICAL STRESS AT SOIL-FOUNDATION INTERFACE

In Figure 4.24, the vertical stress profiles at 3 m, 44 m, and 112 m depth below seabed surface are compared. The vertical stress is greatest at the soil-foundation layer, averaging -250 kPa for the gravity load and varying from -75 kPa to -450 kPa for the combined load. Between the 3 m and 44 m depths, the stress is reduced 35%. At the 112 m depth, the majority of the applied load has dissipated.

To verify the plane strain triangular finite element model used in the present analysis, the vertical stress variations over depth predicted by the finite element model for the gravity load case are compared to some theoretical distributions. These theoretical models are:

- (i) the Boussinesq equivalent square foundation model in a semi-infinite homogeneous elastic solid [97],
- (ii) the Boussinesq infinitesimally long foundation model in a semi-infinite homogeneous elastic solid [97],
- (iii) the Westergaard infinitely long foundation model in a semi-infinite homogeneous thinly stratified material with elastic properties [97], and
- (iv) the simple radial distribution procedure presented by Timoshenko and Goodier [101] for a series of point load distributions on the straight boundary of an infinitely large plate (based on theory of elasticity).

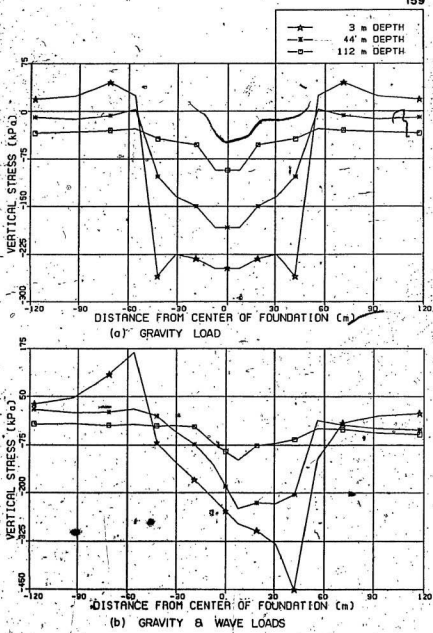


FIGURE 4.24 VERTICAL STRESS AT VARIOUS DEPTHS

The mesh model shown in Figure 4.4 is used with the gravity load nodal forces shown in Figure 4.6. Three linear elastic finite element runs are made using various material properties, namely:

- (i) homogeneous soil profile with elastic modulus of 150 MPa and Poisson's ratio of 0.1,
- (ii) homogeneous soil profile with elastic modulus of 150 MPa and Poisson's ratio of 0.45, and
- (iii) mean material properties as shown in Table 4.1.

The comparisons are presented graphically for vertical stress variation with depth about the center of the foundation (Figure 4.24a) and about the edge of the foundation (Figure 4.26b). There is good agreement between the Boussinesq infinitely long foundation model, the Timoshenko and Goodier model, and the homogeneous finite element model with Poisson's ratio of 0.1. As the finite element model is modified to represent a more complicated soil profile (i.e. varying Poisson's ratios and elastic moduli), the vertical stress distributions digress from the simple theoretical models. The order of magnitude of difference is the same as that predicted by Baecher and Ingra [69].

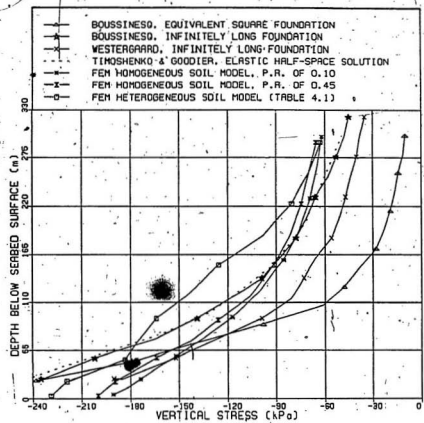


FIGURE 4-24d VERTICAL STRESS VARIATION AT CENTER

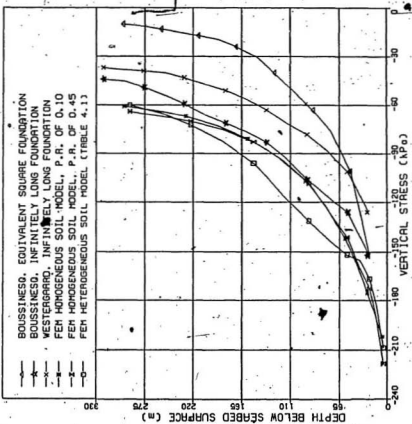


FIGURE 4-24b VERTICAL STRESS VARIATION AT EDGE

4.3.3.1 Effect of Coefficient of Variation for Elastic Modulus

The effect of soil strength uncertainty is investigated through various computer runs with different modulus coefficients of variation. The uncertainty of the vertical stress results are computed in accordance with Eq. (3.34), thereby defining the variance for each element. As with the displacement C.O.V. curves of Section 4.3.1.1, vertical stress C.O.V. values are obtained as the standard deviation divided by the mean vertical stress.

The results of this parametric study are presented in Figures 4.25 and 4.26 for the gravity load and combined loads, respectively. Results of both load cases indicate essentially the same stress C.O.V. for corresponding modulus C.O.V. The only anomaly occurs with the combined load case where the stress value approaches zero, causing an inflated coefficient of variation. The stochastic analysis appears to be insensitive to load case for vertical stress.

The standard deviation curves show a linear relationship with the modulus C.O.V. For equal increments in modulus C.O.V., a corresponding increase in standard deviation is observed. Generally, the shape of the standard

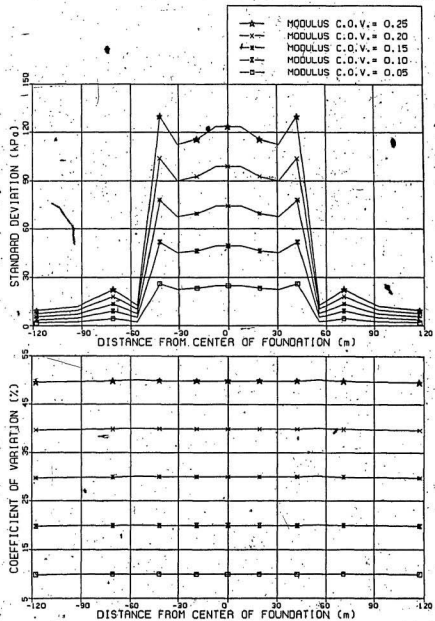


FIGURE 4.25 STATISTICAL PARAMETERS FOR VERTICAL STRESS DUE TO GRAVITY LOAD

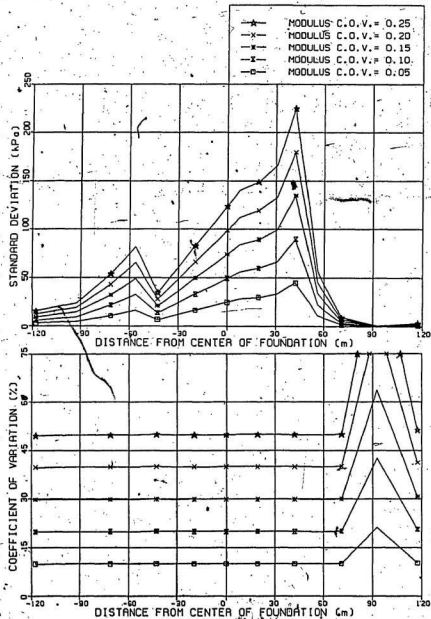


FIGURE 4.26. STATISTICAL PARAMETERS FOR VERTICAL STRESS DUE TO GRAVITY & WAVE LOADS

deviation curves reflect the absolute value of the mean vertical stress curves of Figure 4.23..

The coefficient of variation attains a nearly constant value of approximately twice that of the modulus C.O.V. This suggests that the element stresses are more sensitive to the soil strength uncertainty than the node displacements. By examining Eq. (4.5), this statement can be verified:

$$(H)_{ij} = \frac{\partial [D]_i}{\partial E_j} [B]_i (U)_i \delta_{ij} + [D]_{ij} [B]_i \frac{\partial (U)_i}{\partial E_j} \quad (4.5)$$

The first term estimates the uncertainty contribution from the element stress while the second term determines the effect of uncertainty of all the nodal displacements in the finite element mesh. With the CDF equal to 50, the elements are almost perfectly correlated. The net result is each term attains a coefficient of variation of stress equal to the modulus C.O.V., combining to give twice the modulus C.O.V. percentage.

The 95% confidence limits are shown for the vertical stress due to gravity load and combined gravity and wave loads in Figures 4.27 and 4.28, respectively. Beneath the tank foundation (e.g. between -46 m to 46 m), the bandwidth

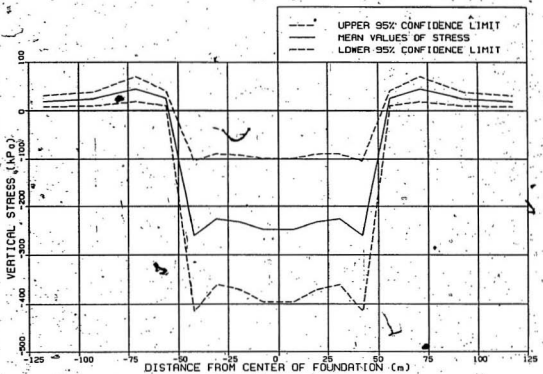


FIGURE 4.27 95% CONFIDENCE INTERVAL FOR VERTICAL STRESS DUE TO GRAVITY LOAD

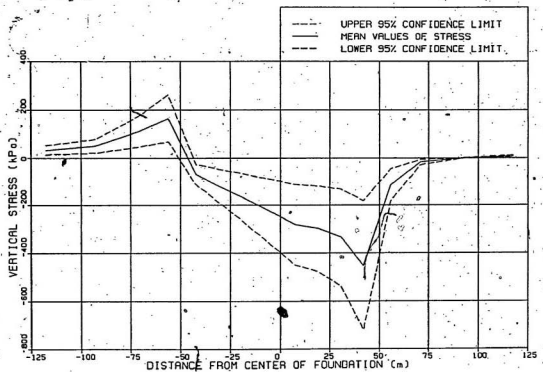


FIGURE 4.28 95% CONFIDENCE INTERVAL FOR VERTICAL STRESS
 DUE TO GRAVITY & WAVE LOADS

is essentially constant at 300 kPa for the gravity load case. For the combined loading, the bandwidth starts at 85 kPa at the left edge of the platform, gradually increasing to a maximum at the right of 540 kPa. As mentioned previously, these curves represent a worst case scenario, with more probable situations having smaller bandwidths.

4.3.3.2 Effect of Correlation Distance Factor

To establish the influence of the correlation function (Eq. 3.17) on the vertical stress results, several computer runs are examined using different correlation distance factors. As with the displacement analysis, the modulus C.O.V. is constant at 15%. The corresponding standard deviation and coefficient of variation curves of the vertical stress distributions are presented in Figures 4.29 and 4.30 for both load cases.

The standard deviation curves reflect the shape of the vertical stress magnitudes, as mentioned in Section 4.3.3.1. For both loading conditions, a 7% increase in standard deviation is observed for an increase in the correlation distance factor from 0.5 to 50.0. For similar CDF change in the vertical displacement analysis, over 25% increase in the standard deviation would result (Section 4.3.1.2). Based on this observation, the vertical stress is not as sensitive to

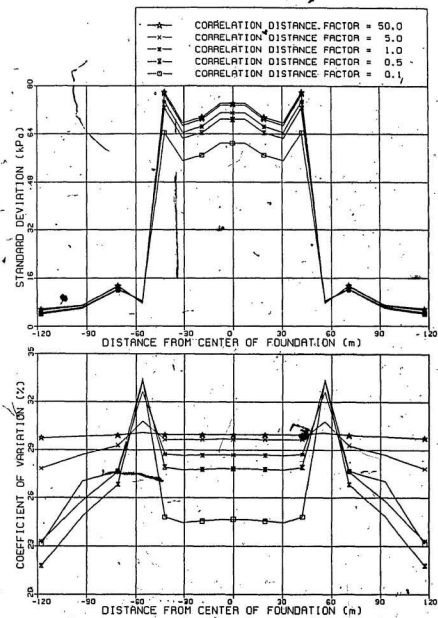


FIGURE 4.29 STATISTICAL PARAMETERS FOR VERTICAL STRESS DUE TO GRAVITY LOAD

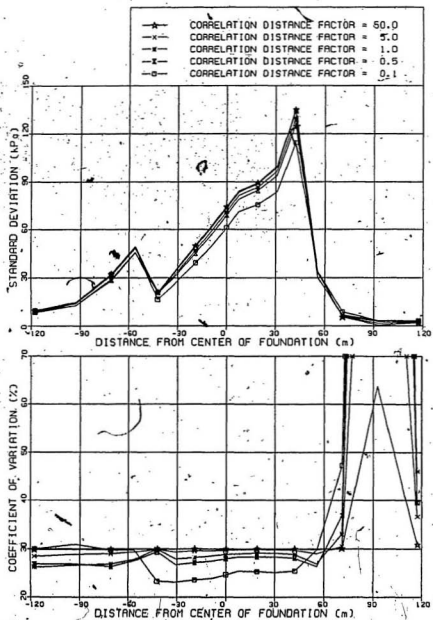


FIGURE 4.30 STATISTICAL PARAMETERS FOR VERTICAL STRESS DUE TO GRAVITY & WAVE LOADS

changes in the correlation distance factor as displacement. The coefficient of variation graphs also indicate the influence of correlation distance is not as significant for stress as for displacement. The following remarks are made in reference to the vertical stress C.O.V. curves:

- (i) As the correlation distance factor approaches infinity (i.e. for practical purposes, approaches 50), the vertical stress C.O.V. attains a value equivalent to twice the modulus C.O.V.
- (ii) As the correlation distance factor approaches zero, the vertical stress C.O.V. approaches zero.

The rate at which these trends occur is not as great as observed in Section 4.3.1.2 for displacement C.O.V.

The 95% confidence intervals of vertical stress (σ_y) are shown in Figures 4.31 and 4.32 for both load passes. Two sets of limits are indicated corresponding to CDF of 0.5 and 50. Comparison of the two sets of limits suggests little difference in the stochastic analysis of vertical stress. This reemphasizes the observation that vertical stress is not as significantly affected by the correlation distance as nodal displacements.

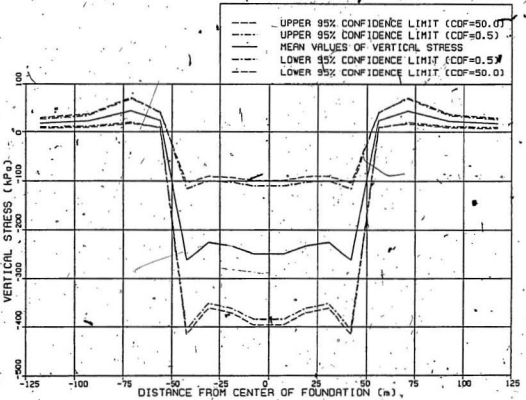


FIGURE 4.31 95% CONFIDENCE INTERVALS FOR VERTICAL STRESS DUE TO GRAVITY LOAD

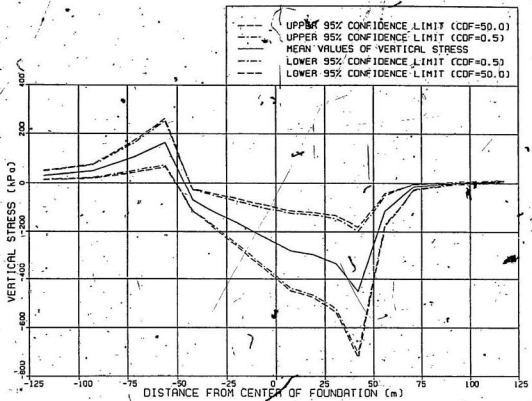


FIGURE 4.32 95% CONFIDENCE INTERVALS FOR VERTICAL STRESS
DUE TO GRAVITY AND WAVE LOADS

4.3.4 Shear Stress Distributions

Although the principal stresses and maximum shear stress are calculated by the computer programs, the application of the stochastic finite element analysis to these forces has not yet been developed. The present analysis will be restricted to the shear stress, τ_{xy} , corresponding to vertical and horizontal stress within each element. In Figure 4.33, the shear stress variation is indicated for both loading conditions. For the gravity load, the largest shear stress, 27.2 kPa, has occurred at the edges of the platform foundation. For the combined wave plus gravity load, the shear stress level in the top sand layer has increased significantly, varying from 83.6 kPa to 41.1 kPa beneath the foundation. This result is attributed to the horizontal force component of the storm wave loading. The maximum shear stress of 87.6 kPa is observed at the right edge of the foundation where increased vertical pressure due to the overturning moment combined with horizontal force has induced larger shearing stresses in the soil continuum.

In Figure 4.34, the shear stress is examined at various depths within the soil. The results are erratic with no obvious trends present. This is partially attributed to not using the maximum shear stresses as associated with the principal stresses.

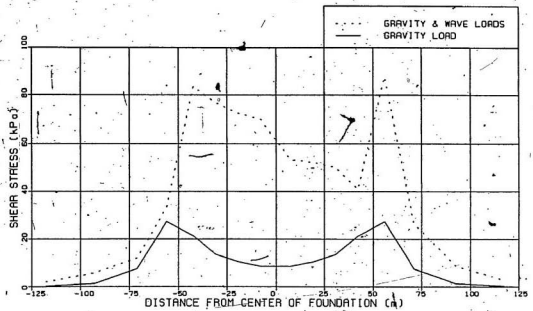


FIGURE 4.33 MEAN SHEAR STRESS AT SOIL-FOUNDATION INTERFACE

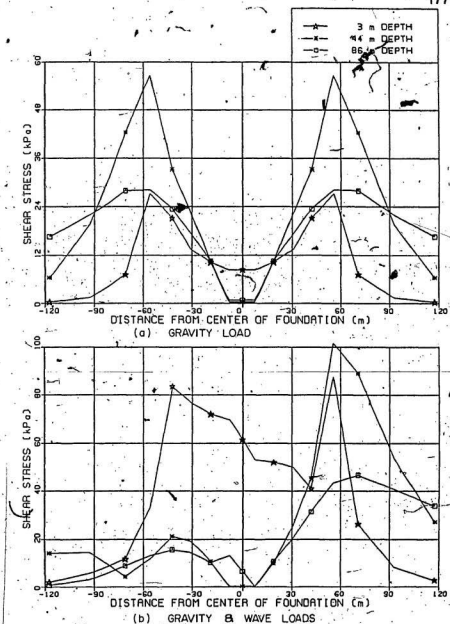


FIGURE 4.34 SHEAR STRESS AT VARIOUS DEPTHS

4.3.4.1 Effect of Coefficient of Variation for Elastic Modulus

As with the previous displacement and stress analysis, the modulus C.O.V. values are altered for several computer runs to establish the sensitivity of stress to soil uncertainty. The variance of shear stress, σ_{xy}^2 , is defined by Eq. (3.34) for each element. Figures 4.35 and 4.36 graphically portray the standard deviations and coefficients of variation for shear stress. The coefficient of variation results very closely resemble the vertical stress results (Figures 4.25 and 4.26). The stress C.O.V. values are practically identical, attaining percentages twice that of the modulus C.O.V. To this effect, the remarks of Section 4.3.3.1 are equally applicable here.

The standard deviation curves for the shear stress have different shapes as compared to the vertical stress plots. The peaking of results at the platform boundaries highlights the increased uncertainty in shear stress at the foundation edges. This is due to the mean shear stress at these locations having larger magnitudes.

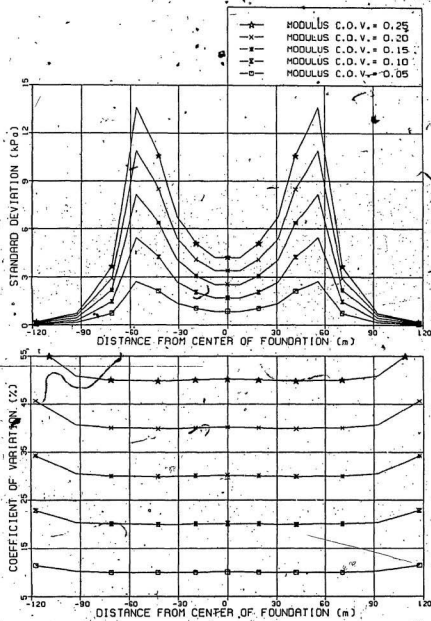


FIGURE 4.35 STATISTICAL PARAMETERS FOR SHEAR STRESS DUE TO GRAVITY LOAD

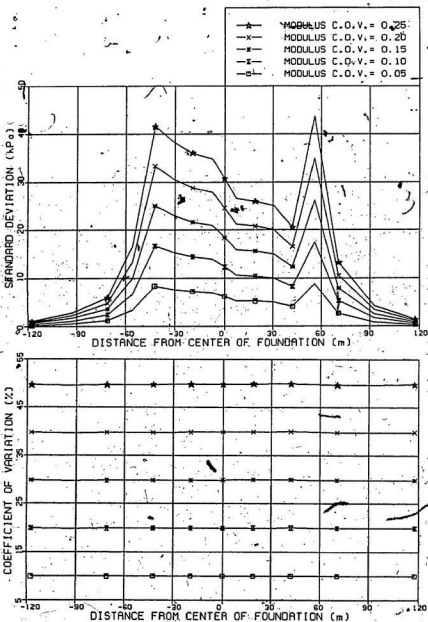


FIGURE 4.36 STATISTICAL PARAMETERS FOR SHEAR STRESS DUE TO GRAVITY & WAVE LOADS.

4.3.4.2 Effect of Correlation Distance Factor

To illustrate the effect of correlation function on shear stress, the stochastic analysis is performed using five different correlation distance factors. The results are shown in Figures 4.37 and 4.38 for both load conditions with 15% modulus C.O.V. The standard deviation curves again show the maximums at the foundation edges (i.e. at -46 m and 46 m). Note that changing the correlation distance factor from 0.5 to 50 does not alter the results very much (i.e. less than 10%). The coefficient of variation curves for shear stress show the same trends as described in Section 4.3.3.2. In Figure 4.38, the stress C.O.V. curves appear more erratic as a result of the plotting scale selected.

The 95% confidence intervals for shear stress, τ_{xy} , are shown in Figures 4.39 and 4.40. Two sets of limits corresponding to 0.5 and 50 CDF values show little effect on range of possible stresses. As with vertical stress, the shear stress is not as significantly affected by correlation distance as nodal displacements. For the gravity load, the bandwidth is maximum at edges with 33 kPa narrowing to 10 kPa at the center. For the combined load, the maximum bandwidth of 105 kPa is observed at +55 m.

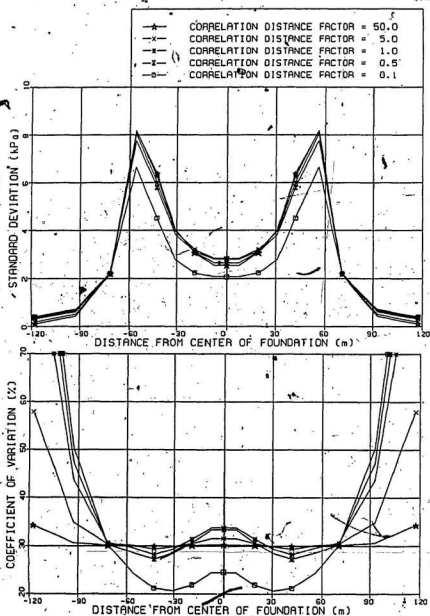


FIGURE 4.37 STATISTICAL PARAMETERS FOR SHEAR STRESS DUE TO GRAVITY LOAD

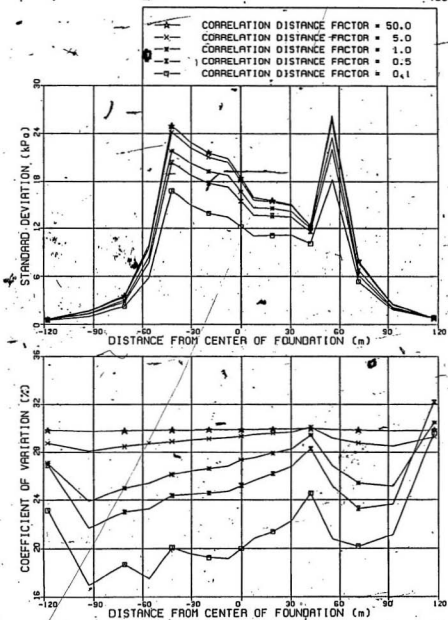


FIGURE 4.38 STATISTICAL PARAMETERS FOR SHEAR STRESS DUE TO GRAVITY & WAVE LOADS

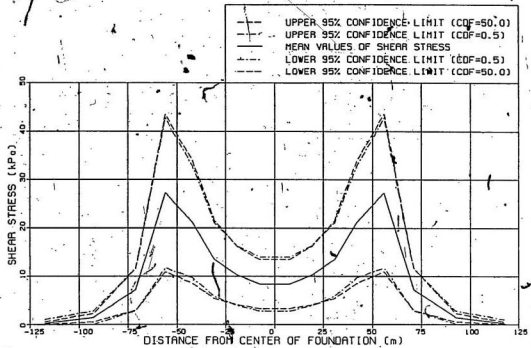


FIGURE 4.39 95% CONFIDENCE INTERVALS FOR SHEAR STRESS DUE TO GRAVITY LOAD

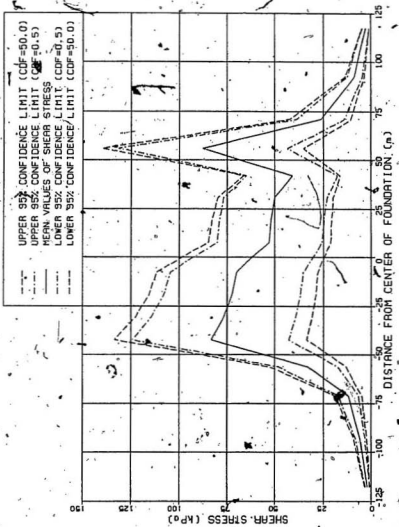


FIGURE 4.40. 95% CONFIDENCE INTERVALS FOR SHEAR STRESS DUE TO GRAVITY & WAVE LOADS

4.3.5 Random Stochastic Analysis

In the previous subsections, the stochastic analysis has assumed the soil continuum to have a fixed coefficient of variation of elastic modulus for all elements. This method of analysis maximizes the uncertainty of the material properties, thereby establishing the upper boundaries of the resulting stresses and displacements. In a purely stochastic analysis, the elastic modulus varies randomly about a constant mean. For more realistic results, the modulus C.O.V. can actually be anywhere between zero and the maximum value anticipated. As outlined in Section 3.4, a pseudo-random number generator is used to create a sequence of thirty-two random numbers between zero and unity. Through the application of Eq. (3.47), a random variation of moduli standard deviations are obtained.

For the Ekofisk Tank problem, the computer program EIRAND.FTN of Appendix III is used to simulate the random stochastic analysis. During the present analysis, the upper bound elastic modulus C.O.V. is constant at 15% with a correlation distance factor of .50. Using the different starting values, s_0 , to initiate the random number sequences listed in Table 3.2, three pseudo-random versions of the stochastic analysis are computed. In the following discussion, the pseudo-random sample numbers 1, 2 and 3

correspond to results obtained with starting values 1000, 123457 and 500000, respectively. The mean displacements and stresses of Figures 4.8, 4.23 and 4.33 are applied to the pseudo-random variances to determine the coefficients of variation.

In Figures 4.41 and 4.42, the pseudo-random standard deviations and coefficients of variation for displacements beneath the tank are compared to the upper bound analysis. The pseudo-random curves exhibit little deviation between them. These curves are shown to have a 50% reduction from the upper bound values. This is attributed to the statistical probability that the sequence of random numbers varying between zero and unity has an average of 0.5.

The statistical parameter curves for vertical stress are presented in Figures 4.43 and 4.44 for both load conditions. Similarly, the results for the shear stress are indicated in Figures 4.45 and 4.46. Unlike the vertical displacement results, these curves have erratic fluctuations throughout indicating the increased influence of randomness in the spread of results. Typically, the pseudo-random results range between 20% to 80% reduction from the upper bound levels. This suggests that due to the nature of Eq. (3.32), the combination of random effects in the nodal

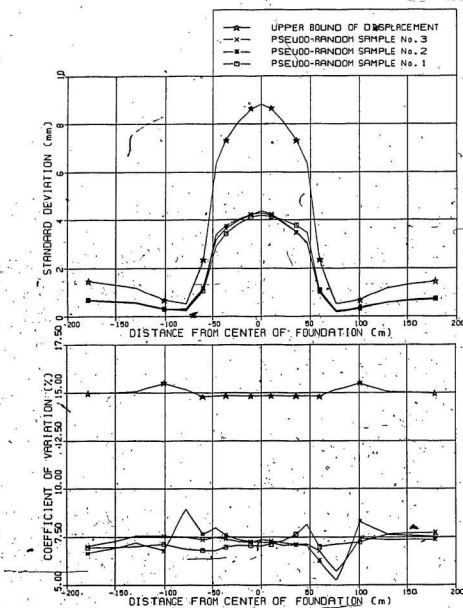


FIGURE 4.41. STATISTICAL PARAMETERS FOR VERTICAL
DISPLACEMENT DUE TO GRAVITY LOAD

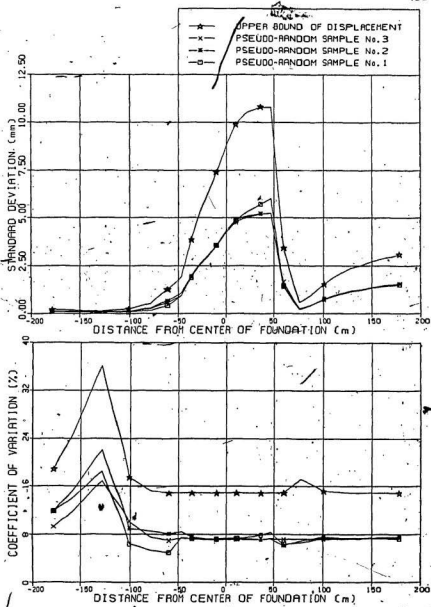


FIGURE 4.42 STATISTICAL PARAMETERS FOR VERTICAL
DISPLACEMENT DUE TO GRAVITY & WAVE LOADS

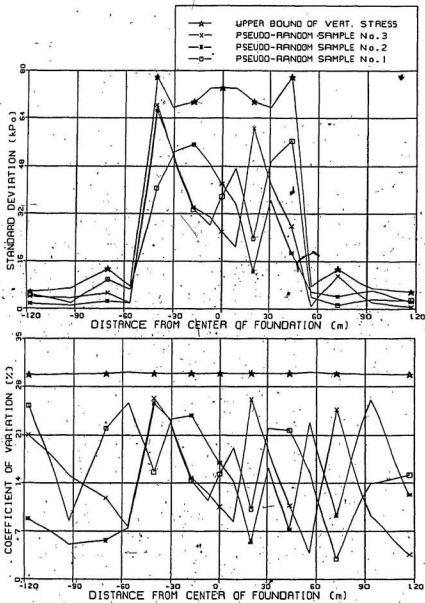


FIGURE 4.43 STATISTICAL PARAMETERS FOR VERTICAL STRESS DUE TO GRAVITY LOAD

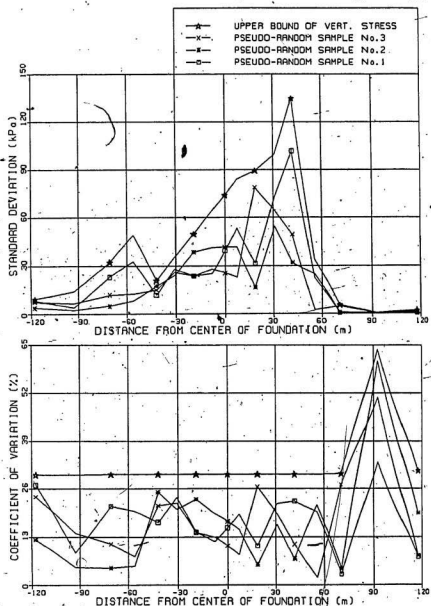


FIGURE 4.44 STATISTICAL PARAMETERS FOR VERTICAL STRESS DUE TO GRAVITY & WAVE LOADS

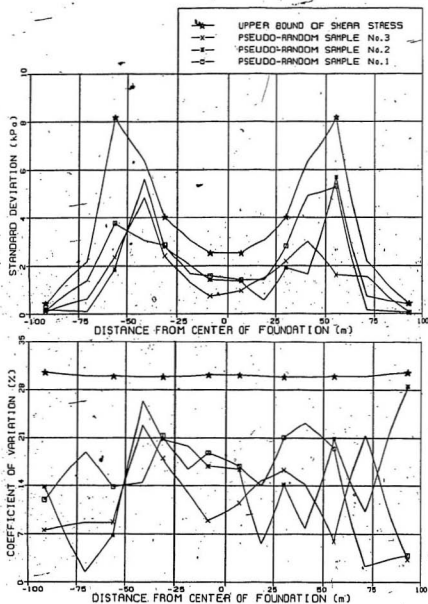


FIGURE 4.45 STATISTICAL PARAMETERS FOR SHEAR STRESS DUE TO GRAVITY LOAD

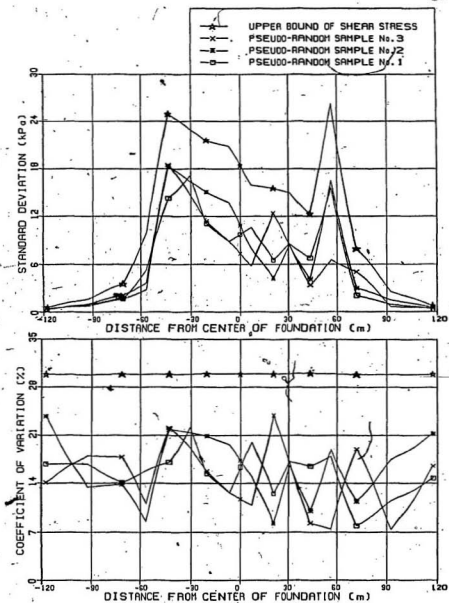


FIGURE 4.46 STATISTICAL PARAMETERS FOR SHEAR STRESS DUE TO GRAVITY & WAVE LOADS

displacements and element stresses will provide more significant variation.

As observed in the results from Figures 4.41 to 4.46 inclusive, the upper bound solutions provide a worst case scenario of the calculated uncertainty in settlements and stresses arising from material uncertainty. The pseudo-random results present a more realistic situation for a given level of soil uncertainty.

4.4 Piecewise Linear Elastic Analysis

To incorporate the nonlinear constitutive elastic modulus relationship in the stochastic analysis, the program NONLIN.FTN is used. Discussions on the logistics and mechanics of the program are presented in Sections 3.3 and 3.5. The present analysis will highlight a few of the principle features relevant to the soil-foundation interaction results of the Ekofisk Tank problem.

As with the linear elastic model, two load cases are examined: the gravity load case of the tank including its contents and the quasistatic wave force of the November 1973 storm. For the piecewise linear process the two types of forces, gravitational and wave have to be treated separately. This is achieved by subtracting the gravity load component from the combined nodal forces given in Figure 4.6. Table 4.3 reflects this calculation, indicating the forces used in the piecewise linear analysis. Using eight load steps for the load application rate, four 25% increments of the gravity load followed by four 25% increments of the wave load are applied to the finite element model.

In the version of NONLIN.FTN listed in Appendix III, the elastic modulus has a routine check to ensure the modulus never falls below the minimum of 20% of its initial

Table 4.3 Nodal Forces for Piecewise Linear Analysis

NODAL FORCE*	GRAVITY LOAD (MN)	WAVE LOAD (MN)
H ₁	0.00	0.5688
H ₂	0.00	0.5688
V ₁	1.453	-1.4048
V ₂	2.906	-2.2479
V ₃	2.906	-1.4987
V ₄	2.906	-0.7495
V ₅	2.906	0.0
V ₆	2.906	0.7490
V ₇	2.906	1.4987
V ₈	2.906	2.2479
V ₉	1.453	1.4048

*Notation used is the same as Figure 4.6

modulus value. (In subroutine NLIN, this term is denoted by EMIN). Through the iterative procedure of the piecewise linear analysis, the initial moduli values of Table 4.1 are reduced according to the shear strain level in the elements. The EMIN terms provide a superficial method of accounting for plastic deformation in the soil continuum and provides numerical stability to the finite element process. The elements that have attained strain levels equivalent to EMIN values for the total gravity load and the total gravity and wave loads are presented in Figures 4.47 and 4.48, respectively. For Figure 4.47, it is observed that the plastically deforming elements occur initially in the two totally clay layers between levels 24 m to 40 m and 80 m to 100 m. This is attributed to the higher Poisson's ratio of 0.49 for

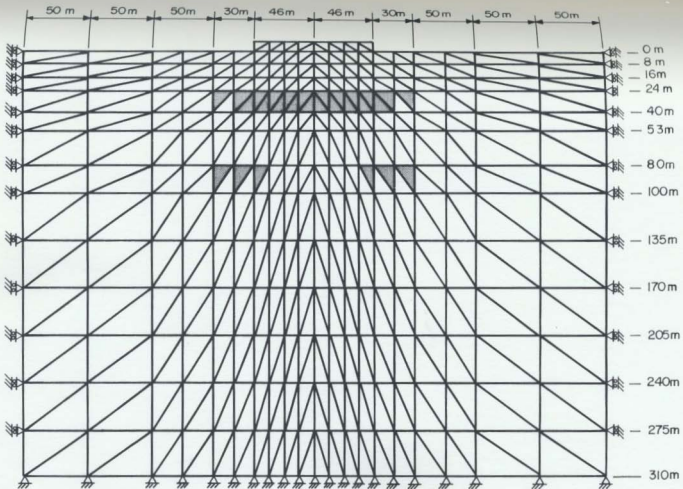


FIGURE 4.47 ELEMENTS ATTAINING EMIN MODULI VALUES
FOR 100% GRAVITY LOADS

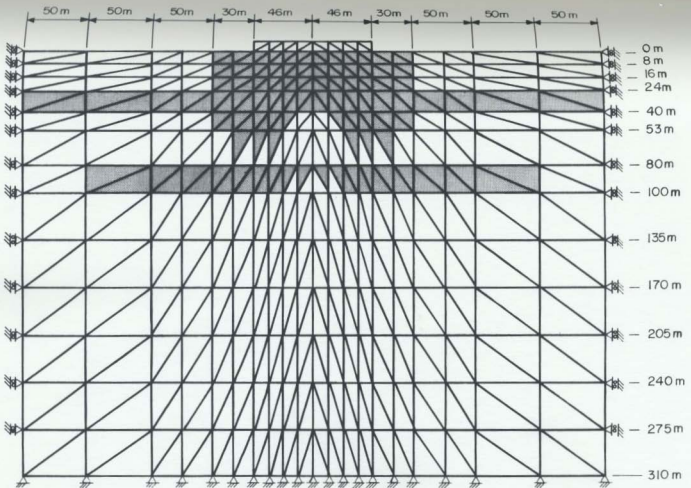


FIGURE 4.48 ELEMENTS ATTAINING EMIN MODULI VALUES
FOR 100% GRAVITY AND WAVE LOADS

these two layers. As the combined load is applied, a wedge shape of plastic deformation spreading beneath the foundation is indicated. This is a result of the higher strain levels experienced in these locations.

In Section 4.3, it has been observed that at a correlation distance above 4600 m, no appreciable change occurs in the variance of the results. This condition of a highly correlated soil continuum over such a range is very unlikely in nature, especially in a subsea environment. A more realistic range for the correlation distance is from 30 m to 100 m range [30]. Using a correlation distance of 46 m (i.e. CDF = 0.5) and a modulus C.O.V. of 15% in material uncertainty, the nonlinear stochastic analysis is computed. For comparison with the linear elastic model, the results using the same parameters are used.

In the following sections, the vertical displacement, vertical stress and shear stress along the seabed surface in the vicinity of the platform foundation are examined. Sensitivity of the stochastic procedure to the constitutive models, linear and piecewise linear, is expressed through graphical analysis.

4.4.1 Vertical Displacement Results

The vertical nodal displacements along the seabed surface are presented in Figures 4.49 and 4.50 for the piecewise linear model. Using the load increment approach, a realistic load-settlement relationship is maintained. This procedure reflects the gradual increase in self-weight during ballasting operations and the accumulative effect of smaller wave forces prior to the November 1973 storm waves. This factor combined with the inclusion of soil nonlinearity has led to closer agreement between field measurements and finite element analysis. Compared to the linear elastic analysis, the magnitude of the settlements are significantly higher in the nonlinear soil model.

In Figure 4.49, the nonlinear properties are apparent. For equal load increments, the amount of displacement corresponding to the load step increases. To illustrate the effect, the settlement at the center of the foundation is observed to increase by 22.5 mm, 29.5 mm, 35.5 mm and 43.0 mm, respectively for each 25% load step. Similarly, nonlinear effects are evident in Figure 4.50 for the wave load increments. At 25% wave load, the displacement curve still exhibits the symmetrical shape characteristic of gravity loading. This suggests the effect of the total gravity load suppresses the influence of the first wave

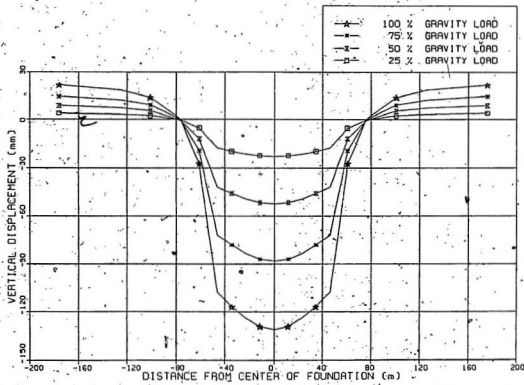


FIGURE 449. MEAN VERTICAL DISPLACEMENT FOR GRAVITY LOAD.

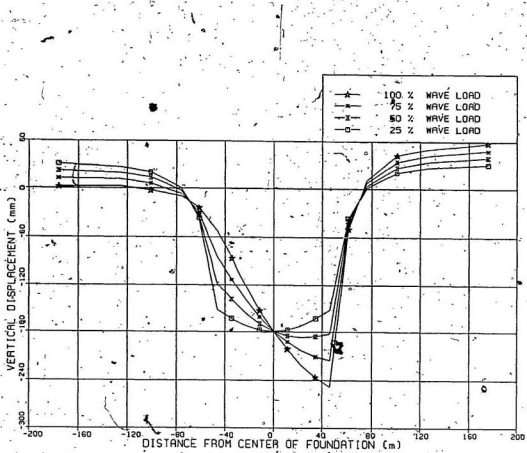


FIGURE 4.50 MEAN VERTICAL DISPLACEMENT FOR GRAVITY & WAVE
(NOTE THAT RESULTS INCLUDE 100% GRAVITY LOAD)

increment. Above this level of loading, the wave effects become prominent.

For the total gravity load case, Clausen et al. [89] had measured an average settlement of 140 mm. Maximum tank settlement predicted by the 100% gravity load in Figure 4.49 is 130 mm and the average is approximately 125 mm. The 10 mm difference between the predicted and measured values is partially attributed to the fact that the 140 mm field value includes settlement caused by repeated wave loadings on the tank and consolidation of the clay layers during the two month installation period.

After the storm wave loading, the total settlement is reported at 220 mm [89]. Figure 4.50 indicates an average settlement of 180 mm with a maximum displacement of 250 mm at the edge. The 40 mm difference between the actual and the nonlinear predicted settlements may be partially explained by the consolidation of the clay layers during the five month period between installation and storm. The finite element procedure used in this study does not account for soil consolidation.

A comparison of the piecewise linear results of the stochastic analysis to the corresponding linear curves is made for the total gravity load in Figure 4.51. The

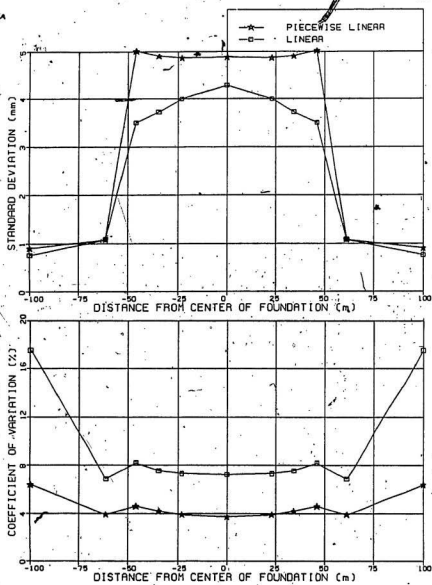


FIGURE 4.51 STATISTICAL PARAMETERS FOR VERTICAL DISPLACEMENT DUE TO 100% GRAVITY LOAD

standard deviation of the vertical displacement is observed to be 20 to 40% higher for the piecewise linear analysis results. The coefficient of variation for the displacement is 50% lower than the linear analysis results. A couple of factors lead to these results. Use of a nonlinear stress-strain relationship has accounted for a twofold increase in settlements as seen in Figures 4.8 and 4.49. With these larger displacements, the standard deviations tend to be greater. The net effect of a slight increase in standard deviation over a substantially larger mean displacement is to reduce the coefficient of variation.

The combined gravity and wave results are presented in Figure 4.52. As before, the standard deviation is larger for the piecewise linear analysis and the coefficient of variation is larger for the linear analysis. The symmetrical distribution of the standard deviation about the foundation centerline is unexpected.

In Figure 4.53, the 95% confidence intervals for the vertical displacement are presented. With the increase in standard deviations, the bandwidths for the piecewise linear analysis have increased. For the 100% gravity load, the maximum bandwidth has increased to 20 mm from 17 mm for the linear case. For the 100% gravity and wave loads, the maximum bandwidth has increased to 32 mm from 24 mm. These

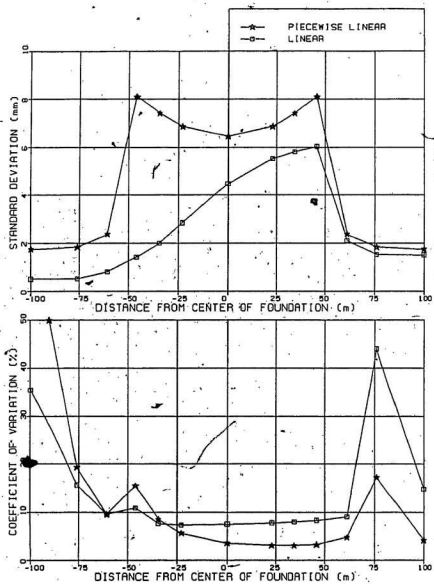


FIGURE 4.52 STATISTICAL PARAMETERS FOR VERTICAL
DISPLACEMENT DUE TO 100% GRAVITY & WAVE LOADS.

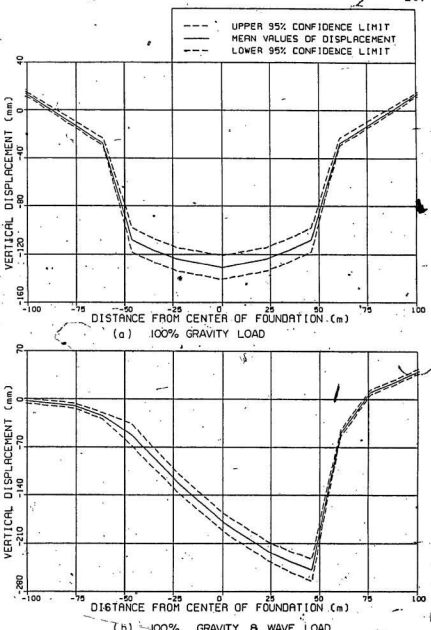


FIGURE 4.53 95% CONFIDENCE INTERVALS FOR VERTICAL DISPLACEMENT

95% confidence limits indicate that the range of possible values deviate from the mean displacement by less than 110t.

4.4.2 Vertical Stress Distributions

The mean vertical stress distributions shown in Figures 4.54 and 4.55 follow the same basic shape as the linear elastic results presented in Section 4.3.3. The highest vertical stresses occur directly beneath the tank foundation. The piecewise linear results have a slight increase in magnitude over the linear values. In both Figures 4.54 and 4.55, equal load increments induce essentially equal stress increases, suggesting the model's insensitivity to changes in constitutive relationships. For the gravity load, the vertical stress is maximum at -290 kPa along the edges reducing to -240 kPa at the center. This corresponds well with Lee and Focht's [100] calculation of -267 kPa for average contact bearing pressure. For the combined gravity and wave loads, the curves indicate the pressure distribution of -220 kPa to -510 kPa directly beneath the platform. The maximum agrees with the -513 kPa predicted by simple footing bearing pressure formulae.

In Figures 4.56 and 4.57, the standard deviation and coefficient of variation for vertical stress are presented for both load conditions. The linear curves are typically

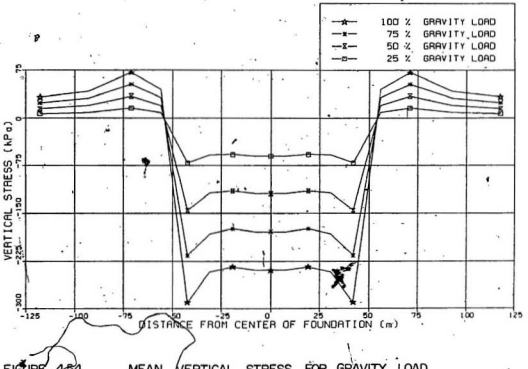


FIGURE 4-54

MEAN VERTICAL STRESS FOR GRAVITY LOAD

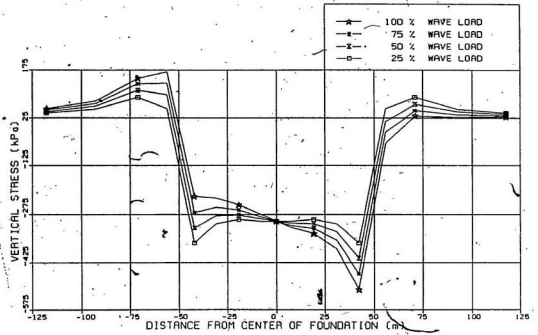


FIGURE 4.55 MEAN VERTICAL STRESS FOR GRAVITY & WAVE LOADS

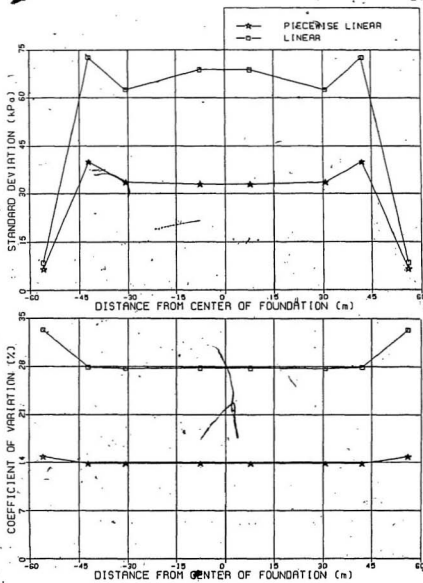


FIGURE 4.56. STATISTICAL PARAMETERS FOR VERTICAL STRESS DUE TO 100% GRAVITY LOAD

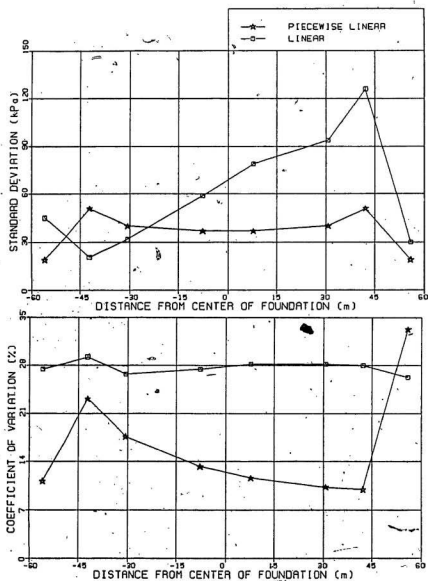


FIGURE 4.57 STATISTICAL PARAMETERS FOR VERTICAL STRESS DUE TO 100% GRAVITY & WAVE LOADS

greater than the piecewise linear results. This differs from the previous displacement graphs where the standard deviation curves for nonlinear analysis are larger. In Figure 4.56, the standard deviation for the linear analysis is 65 kPa but reduces to 33 kPa for piecewise linear. Similarly, there is a 50% reduction in the coefficient of variation, falling from 28% to 14%. The coefficient of variation values for the vertical stress are much greater than the corresponding 7% and 4% values determined for the vertical displacement (i.e. Figures 4.51 and 4.52). The results for the combined gravity and wave loads (Figure 4.57) exhibit more variation in the statistical parameters due to the unsymmetrical loading.

The 95% confidence limits are presented in Figure 4.58. The bandwidth for the gravity load is 130 kPa on average compared with 260 kPa for the linear results in Section 4.3.3.2. The combined loading bandwidth is approximately 150 kPa throughout the tank's breadth. This value compares with the increasing bandwidth of 80 kPa to 500 kPa from left to right for the linear analysis (Figure 4.28). Generally, these lower bandwidths for the piecewise linear procedure reflect the reduction in standard deviation and consequently provide improved predictability for the stress values.

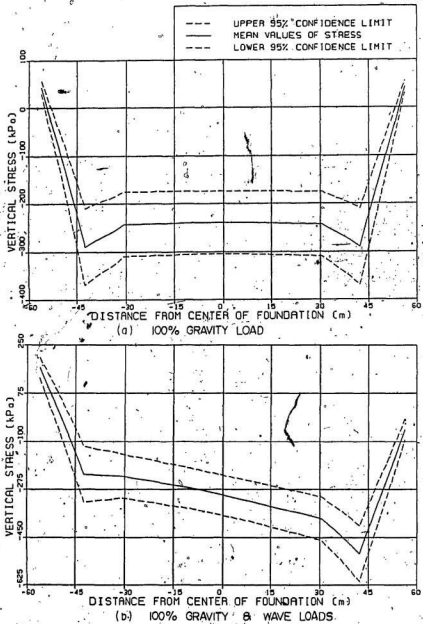


FIGURE 4.58 95% CONFIDENCE INTERVALS FOR VERTICAL STRESS

4.4.3 Shear Stress Distributions

The mean shear stress distributions for the piecewise linear analysis are shown in Figures 4.59 and 5.60. The shear stress is insensitive to changes in the constitutive relationship as shown by the equal stress changes with equal load increments. For the gravity load, the shear stress of 27 kPa is maximum at the platform edges, then stabilizes to 24 kPa beneath the tank. By comparison, the linear results in Figure 4.33 indicate an edge shear stress of 27 kPa with the interior reducing to 10 kPa. For the combined gravity and wave loads, the shear stresses are largest in the boundary layers next to the foundation edge, reaching 73 kPa and 54 kPa. In the region beneath the foundation, the shear stress averages 30 kPa. These values are lower than the shear stresses predicted by the linear model for the combined loading (Figure 4.33).

The standard deviation and coefficient of variation for shear stress are presented graphically for the linear and the piecewise linear analyses in Figures 4.61 and 4.62. As with vertical stress results, typically the linear curves are greater than the piecewise linear values.

The 95% confidence limits are presented in Figure 4.63. The bandwidth for the gravity load ranges from 6 to 15 kPa.

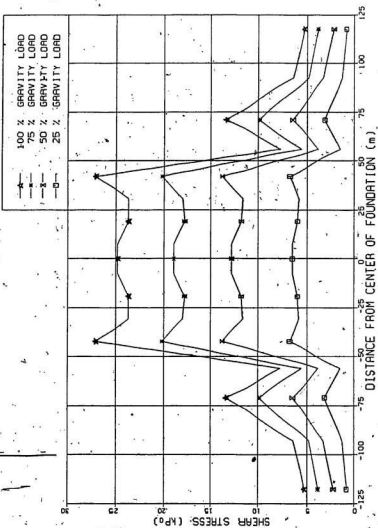


FIGURE 4.59 MEAN SHEAR STRESS FOR GRAVITY LOAD

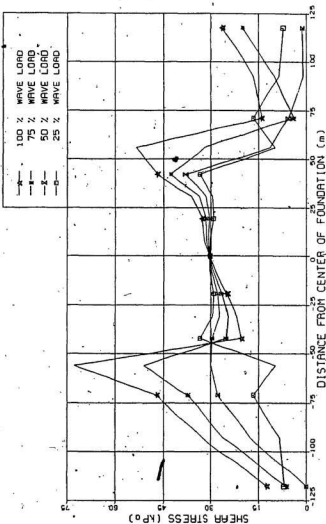


FIGURE 4.60 MEAN SHEAR STRESS FOR GRAVITY & WAVE LOADS *

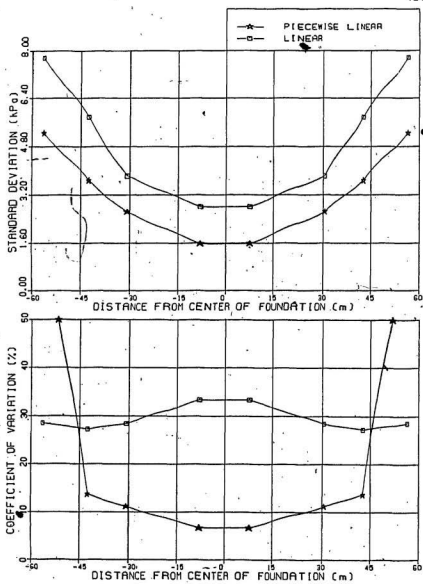


FIGURE 4.61 STATISTICAL PARAMETERS FOR SHEAR STRESS DUE TO 100% GRAVITY LOAD

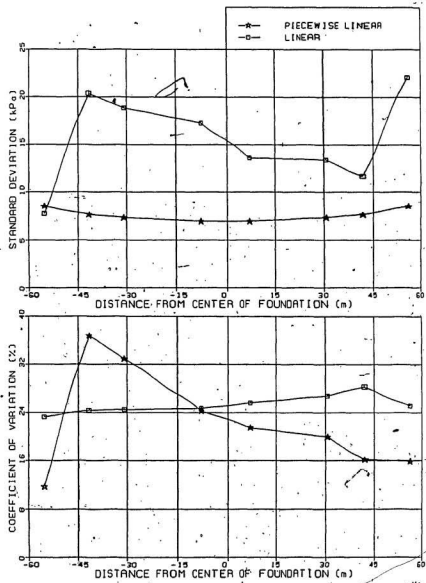


FIGURE 4.62 STATISTICAL PARAMETERS FOR SHEAR STRESS DUE TO 100% GRAVITY - 8 WAVE LOADS

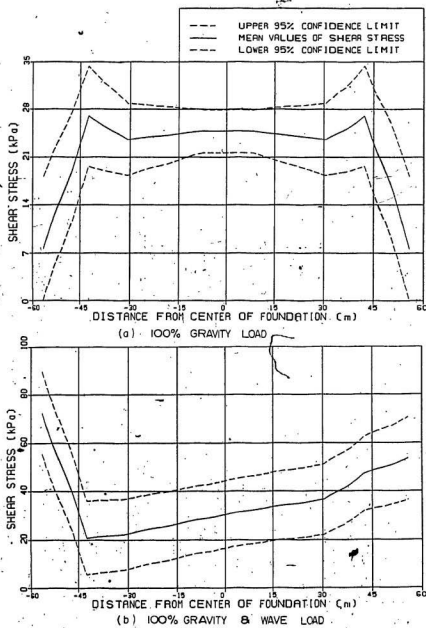


FIGURE 4.63 95% CONFIDENCE INTERVALS FOR SHEAR STRESS

compared with 11 to 23 kPa for linear analysis of Section 4.3.3.3. The combined load bandwidth for piecewise linear analysis is typically 28 kPa beneath the tank foundation. This value is in contrast to the 45 to 80 kPa range for the linear analysis (Figure 4.40).

CHAPTER 5

STOCHASTIC FINITE ELEMENT ANALYSIS OF SOIL-FOUNDATION
INTERACTION FOR A CAISSON RETAINED ISLAND

5.1 Introduction

To further demonstrate the versatility of the stochastic finite element procedure to geotechnical and structural problems another type of gravity structure is examined. Recent exploration and development of offshore energy and mineral resources in the Beaufort Sea has necessitated a fixed year-round drilling and production platform. In the harsh Arctic environment, severe and enduring ice forces are the norm. For shallow waters one viable solution has been an artificial island constructed of compacted sand berm with protective riprap. But for deeper waters this has not been economical. Thus, the concept of a caisson retained island has been examined and found feasible for water depths ranging from 15 to 40 m [7, 8, 11].

In general, caisson retained islands are capable of remaining in service year round and withstanding the on-site ice forces. These structures consists of three basic components: an outer caisson structure made of prestressed concrete or high tension steel, a hydraulically placed sand

filled core, and a carefully compacted sand berm. The outer caisson has three essential functions: (i) It confines the sand filled core to within the caisson thereby obtaining the required height using less material; (ii) It serves as a protective armour, deflecting and restraining ice from eroding the sand core; and (iii) It provides a firm support for the drilling and production platform. The caisson concept is more economical largely due to its ability to be removed and relocated after completion of exploratory drilling operations or the depletion of the field. The inner sand core provides the large mass required to resist the lateral ice forces. The sand material serves as a medium through which the lateral shear forces are transmitted by friction to the berm and eventually to the underlying seabed material. The sand berm is an economical method of obtaining a maximum additional height of 15 m. It provides flexibility in the design to make the caisson structure suit a number of varying water depths.

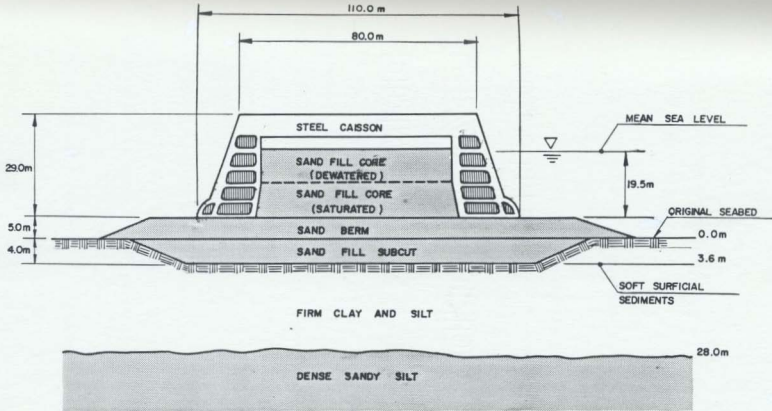
The novelty of caisson retained construction has meant increased uncertainties inherent with the structural and foundation design. Uncertainties arise from several sources: (i) unpredictable wave, wind, ice and pack ice loads; (ii) lack of understanding and experience of the physical response mechanisms of these structural systems, and (iii) variation of actual material properties from the

design values. This has necessitated more conservative foundation designs. The designer must identify the significant sources of uncertainty and properly assess the effect on structural response. The stochastic finite element is a quantitative scientific approach to measuring these effects. To illustrate its application, the Mobile Arctic Caisson (M.A.C.) is examined.

5.2 Mobile Arctic Caisson Description

The Mobile Arctic Caisson is a hybrid soil-steel structure designed and constructed for Gulf Canada Resources during the early 1980's [8, 102]. The steel caisson, called Molikpaq, is basically an octagonal annulus in plan with a simply supported operations deck. The steel caisson has twelve ballasting compartments which permit it to be floated to location, then installed on a previously placed underwater berm by flooding the compartments with seawater. Freezing is avoided in the ballast tanks and the sand core by using insulation and heating units.

A schematic cross-section of the M.A.C. is presented in Figure 5.1. This schematic is based on the 24.5 m water depth at the Tarsiut P-45 wellsite, 110 km northwest of Tuktoyaktuk, N.W.T. The caisson is 29 m above the berm with the deck and base widths approximately 73 m and 110 m, respectively. The caisson base rests on a 5 m sand berm, 19.5 m below mean sea level. At the top of the berm, the width is roughly 170 m with side slopes of one to three. In the bearing regions directly beneath the caisson the top 3.6 m of soil had consisted of soft clays with shear strength less than 175 kPa. These weak surficial sediments had been removed in a 4 m subcut into the original seabed surface. The sand fill core is dewatered to approximately 10 m below



M.A.C. SCHEMATIC CROSS - SECTION

FIGURE 5.1

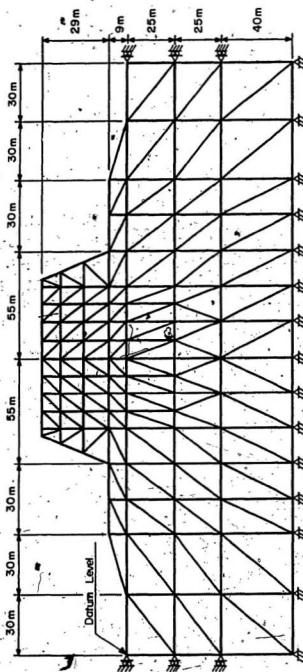
sea level to ensure greater stability by increasing the core's effective mass.

5.2.1 Finite Element Representation

The M.A.C. and soil continuum have been discretized into triangular elements as shown in Figure 5.2. The model consists of 116 nodes and 186 elements for the plane strain finite element analysis. For best results, the analysis is representative of an interior section through the structure.

The overall dimensions of the model have been made to correspond with the cross-section of Figure 5.1. As recommended by researchers [69, 85], the horizontal dimension of the model is approximately four times the core width of 73 m. The overall vertical dimension is less than the suggested three to four width range. This is due to insufficient information on the in-situ soil strata and the possibility of encountering frozen soil at depth beneath the seabed surface in the Beaufort [103]. The soil below the 90 m level will not greatly influence the results.

Boundary conditions have been selected to best simulate the soil behaviour. At the lowest horizontal boundary, the nodes are fixed both horizontally and vertically to represent the reduction in nodal displacements at this level.



FINITE ELEMENT MESH FOR TWO-DIMENSIONAL MODEL

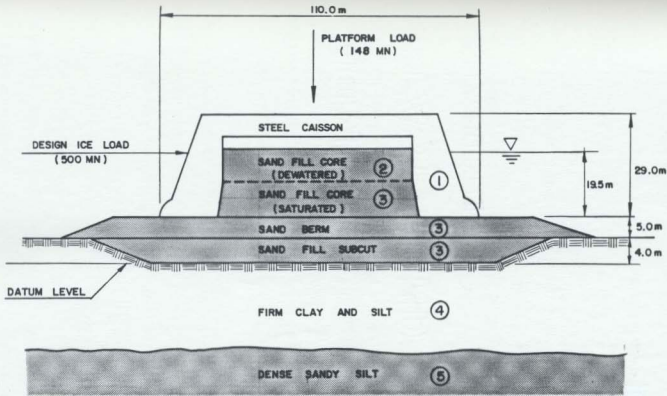
FIGURE 5.2

Vertical rollers are used at the two vertical edges of the mesh to indicate the heaving or sinking motion of the soil surface due to loadings on the caisson structure. Lateral resistance provided by neighbouring soils is considered sufficient to restrain any horizontal movement.

Selection of internal dimensions of the mesh are determined by the combination of material configuration and element aspect ratios. The combination of structural shape and material type (denoted by circled numbers in Figure 5.3) determines the basic element discretization. For highly stressed zones, a finer mesh of elements will provide better results. Once this criterion has been satisfied, the mesh is subjected to an aspect ratio test whereby the ratios are to be no greater than six. Ideally, the aspect ratio should be in the range of one to two. In Figure 5.2, the majority of elements fall within these limits, with the maximum aspect ratio of 3.3 occurring in the berm layer edge elements.

5.2.2 Mean Material Properties

The expected properties of the Mobile Arctic Caisson system have to be determined to implement the finite element procedure. The mesh configuration shown in Figure 5.2 is subdivided into five material types as suggested by Figure



LOADINGS ON MOBILE ARCTIC CAISSON

FIGURE 5.3

5.3. The required material properties of submerged density, elastic modulus and Poisson's ratio are indicated in Table 5.1 for the Tarsiut P-45 wellsite.

The weight densities for the material types are representative of the gravitation forces resulting from material weight applied to the original seabed. For this reason, the weight density for in-situ soils are zero. The net submerged weight of the steel caisson plus ballast above neutral buoyancy combine to give a net weight of 673 MN. With the overall caisson volume being approximately 150,000 m³, a load density of 4.5 kN/m³ is obtained. This low value reflects the hollow cellular structure of the caissons. The density of the dewatered sand is 20 kN/m³ while the saturated sand is reduced to 10 kN/m³ due to buoyancy effects.

For the steel caisson, the standard textbook values of 200,000 MPa for elastic modulus and 0.33 for Poisson's ratio are selected. The influence of the hollow steel caisson is investigated by reducing the modulus by a factor of one tenth. Less than 2% difference in nodal displacements is observed. Kent et al. [103] have proposed drained elastic moduli for typical sand fill core materials. Sand fills in the stress range of 300 to 350 kPa have drained moduli of 40 MPa. For quasi-static analysis, the elastic modulus remains essentially equal for dewatered and saturated conditions,

125 MPa is selected for the dense sandy silt. Poisson's ratios for undrained conditions are 0.45 for clay and 0.40 for silt.

5.2.3 Load Cases for Analysis

To illustrate the application of the stochastic finite element model, the M.A.C. is examined under two practical load conditions, operating (gravity) loads and combined ice and gravity loads [11, 104, 105, 106, 107]. The presence of a constructed sand berm with the M.A.C. structure and densified core has added substantial gravity loads to the founding seabed soils. The M.A.C. has an equivalent submerged weight of 673 MN for the combined weight of emission and ballast water above neutral buoyancy. From drilling operations and equipment on the deck, a platform live load of 148 MN is expected. In addition to these loads, the submerged weight of the sand fill core and berm materials have a loading effect on the original seabed material.

Jefferies et al. [11] have suggested values for the extreme environmental horizontal loadings on Molikpaq. For a 4% probability of exceedance, maximum loads of 110 MN and 140 MN have been predicted for wave and earthquake lateral forces, respectively, at the Tarsitut P-45 site. But the

Table 5.1 Mean Material Properties at Tarsiut P-45 Site

Material*	Description	Weight** Density (kN/m ³)	Elastic Modulus (MPa)	Poisson's Ratio
1	Steel Caisson	4.5	200,000	0.33
2	Sand (Dewatered)	20.0	40	0.25
3	Sand (Saturated)	10.0	40	0.40
4	Firm Silty Clay (In-situ 0-25 m)	0.0	100	0.45
5	Dense Sandy Silt (In-situ 25-90 m)	0.0	125	0.40

* For material number, refer to Figure 5.3.

** Weight density denotes loadings in addition to seabed self-weight, excluding external forces such as platform and ice loadings.

References: Stewart et al. [102], Kent et al. [103], and Bruce and Harrington [104].

with the physical change being indicated through the Poisson's ratio. Based on recommended values by Selvadurai [105], Poisson's ratio is taken as 0.25 for dewatered sand and 0.40 for saturated sand.

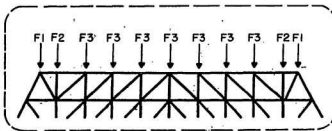
For the in-situ materials, the firm silty clay has an undrained shear strength of 100 kPa (Rogers et al. [106]). For stiff clays, the elastic modulus is proportional to the undrained shear strength [105]. Using the suggested factor of 1000, the elastic modulus is estimated at 100 MPa for clay. Due to unavailable information, an elastic modulus of

critical environmental condition is that of a 500 MN horizontal ice load, expected once every 25 years. In physical terms, this situation corresponds to a 1.2 km diameter multi-year ice floe which averages 6.1 m in thickness with pressure ridges of 12.2 m thick travelling at 1.85 km/hr. Although the earthquake, wave and current loads are significant external loads on the caisson system, only the combined ice and gravity loads are examined as the second loading condition. Actual field data on lateral ice forces indicate that M.A.C. has been subjected to only 45% of the 500 MN value [106].

For the gravity load case, sources that introduce new loads on the original seabed are considered. This requires the inclusion of platform loads, caisson self-weight, and weight of sand fill core and berm in the analysis. These loads are applied to the finite element mesh in the most representative manner. The actual nodal loads are based on a one meter (plane strain) slice through the base of the structure. For materials beneath the water level, submerged weights have to be used. As outlined in subroutine LOAD (Appendix IV), the rate of loading per unit area (based on a slice of one meter) is calculated for each material type. The load densities presented in Table 5.1 are used for this purpose. The weight for each element is determined and distributed equally as a vertical force at its three nodes.

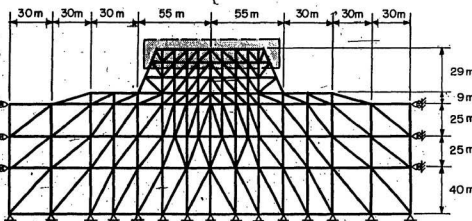
To include the external platform load of 148 MN, the force is distributed over the 6400 m² surface. The nodal forces are in proportion to the tributary load area. Figure 5.4 indicates the nodal forces used in the analysis.

To represent the design ice force of 500 MN, the distribution of the lateral force along the caisson's side has to be divided among the three nodes of the mesh. The ice force on the one meter strip is obtained by dividing the 500 MN by the structure's width at water level. The force is estimated at 5.65 MN/m. Considering the likelihood of ice riding up on the sides, 20% of the force is at the uppermost node. The remainder is proportioned such that the moments generated by the nodal forces about the base balance the moment generated by the ice force acting at water level. The resulting nodal forces are indicated in Figure 5.5.



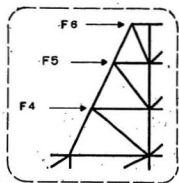
F_1	40.5 kN
F_2	146.1 kN
F_3	211.2 kN

NODAL FORCES



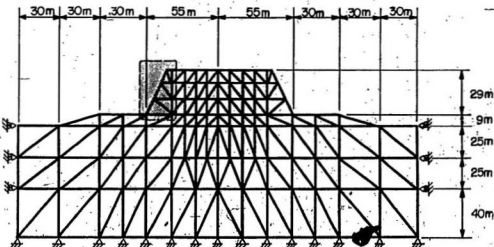
NODAL FORCES REPRESENTING
PLATFORM LIVE LOAD

FIGURE 5.4



F4	861 kN
F5	3659 kN
F6	1130 kN

NODAL FORCES



NODAL FORCES REPRESENTING
LATERAL ICE FORCE

FIGURE 5.5

5.3 Linear Elastic Analysis

Using a linear elastic constitutive relationship for the elastic modulus, the stochastic finite element procedure is applied to the Mobile Arctic Caisson. Using the program CAISON.FTN (Appendix III), the soil-foundation interaction is examined for the gravity load and the combined gravity and ice load cases. Vertical displacement, vertical stress and horizontal stress along the datum level (see Figure 5.2) are examined. The datum level represents the interface between the original seabed material and the sand fill berm.

The stochastic nature of the materials is simulated by the correlation function as defined by Eq. (3.17). The correlation function describes the likelihood of similar material properties occurring as a function of r_{ij} , the distance between element centroids. The rate of exponential decay of the correlation function is determined by the correlation distance, L . The correlation distance is simply the product of foundation width (e.g. 110 m) and the correlation distance factor, CDF. Figure 5.6 shows the correlation function for various correlation distances corresponding to CDF's of 0.1, 0.5, 1, 5 and 50. For a correlation distance of 11 m, elements separated by 50 m or more are perfectly uncorrelated. This means the uncertainty in material properties will not be influenced by elements

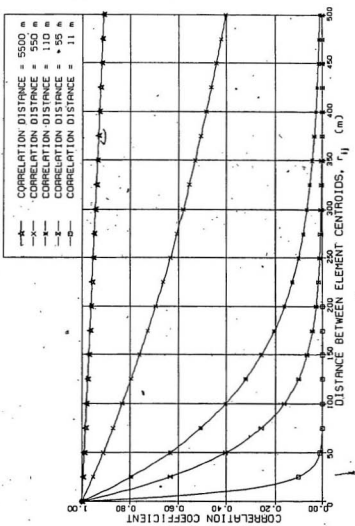


FIGURE 5.6 CORRELATION COEFFICIENT FUNCTION FOR M.A.C.

beyond a 50 m radius. According to Baecher et al. [30], offshore soil properties typically have correlation distances in the range of 50 to 250 m. Based on this information, a CDF of 1 would best simulate field conditions.

To establish the sensitivity of the stochastic procedure to correlation distance factor, several versions of the analysis are compared. For this parametric analysis, the coefficient of variation for the elastic modulus is fixed at 15%.

5.3.1 Nodal Displacement Analysis

The nodal displacements as obtained from the finite element analysis are considered as mean displacements for the stochastic analysis. Mean vertical and horizontal displacements at datum level are presented in Figure 5.7 for both load conditions. The M.A.C. is located between -55 m and +55 m with zero representing the center of the planar section. The results indicate symmetrical settlements for the gravity load. Maximum nodal displacements occur directly beneath the structure. For vertical settlement, the results indicate little difference between the load conditions, with the average caisson settlement being 110 mm. Rogers et al. [106] have measured a total settlement of 185 mm after nine months. This includes consolidation

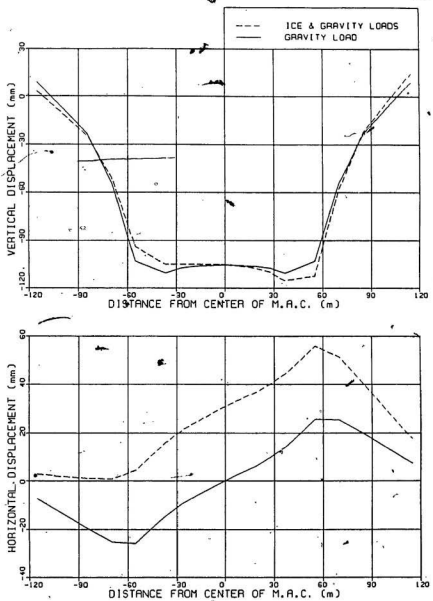
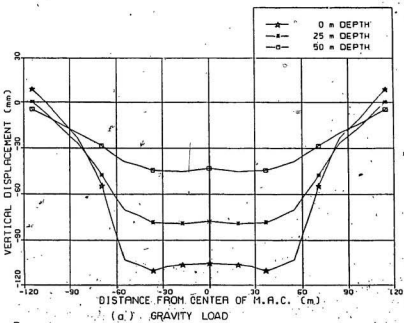


FIGURE 5:7 MEAN VERTICAL & HORIZONTAL DISPLACEMENTS AT DATUM LEVEL

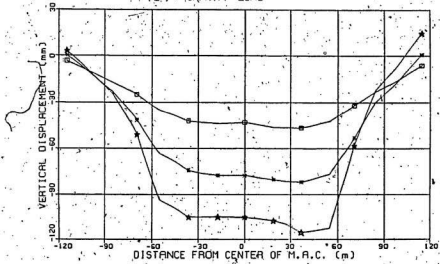
settlement of the clay layers whereas the present analysis estimates short term settlements only. In Figure 5.7, horizontal displacement is measured positive to the right of center. The net effect of the ice load is to cause a 30 mm horizontal movement of the structure. This value is within the 100 mm maximum response range of the inclinometers used in interpreting horizontal motion [107].

In Figure 5.8, the vertical displacement profiles at different depths are compared. The depths considered are 0 m, 25 m, and 50 m with the zero denoting the seabed datum. The results are plotted for both load conditions. The settlements are as anticipated with 25% occurring in the upper 25 m and 35% occurring between the 25 m and 50 m levels. It is observed that the local distortions become less pronounced as the depth increases, indicating the redistribution of stresses in the soil.

Using computer solutions for Eq. (3.15), vertical settlement variances are determined based on a 15% elastic modulus C.O.V. The standard deviation and coefficient of variation curves are plotted in Figures 5.9 and 5.10 for both load conditions. Comparison of the two figures show little difference with the exception of boundary effects in the finite element analysis. Within the zone directly beneath the M.A.C., the curves are fairly constant. By



(a) GRAVITY LOAD



(b) GRAVITY & ICE LOADS

FIGURE 5.8 VERTICAL DISPLACEMENTS AT VARIOUS DEPTHS

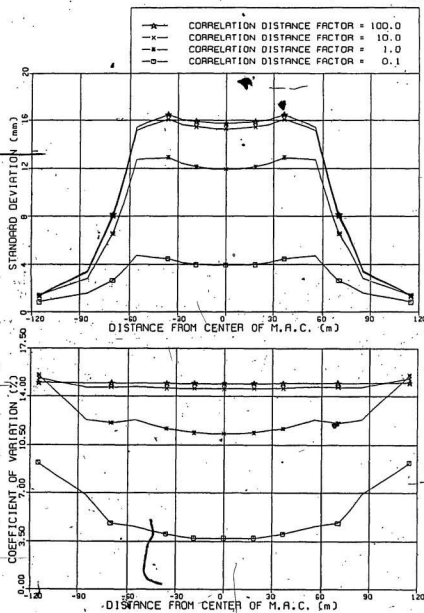


FIGURE 5.9 STATISTICAL PARAMETER FOR VERTICAL DISPLACEMENT DUE TO GRAVITY LOAD

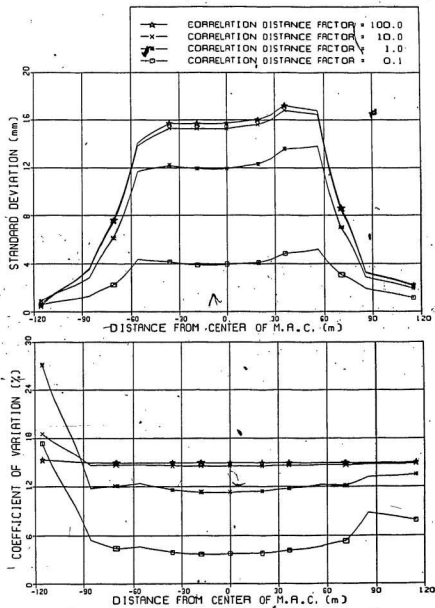


FIGURE 5.10 STATISTICAL PARAMETERS FOR VERTICAL DISPLACEMENT DUE TO ICE & GRAVITY LOADS

increasing the correlation distance factor, it is observed that the curves approach a maximum C.O.V. equal to the assumed modulus C.O.V. This represents a highly correlated continuum. For an uncorrelated continuum, the resulting C.O.V. becomes much less, approaching zero as indicated by a CDF of 0.1 or smaller. These results are anticipated if the exponential decay correlation coefficient function of Eq. (3.17) is closely examined.

Using the standard deviation curve for a CDF of 1.0 in Figure 5.10, the 95% confidence limits are computed. Assuming that the uncertainty follows a normal distribution, upper and lower limits are determined by adding and subtracting, respectively, two standard deviations from the mean. Figure 5.11 shows the 95% confidence interval for the combined ice and gravity loads. This reveals the likely boundaries within which the vertical displacements will coincide. The bandwidth is widest directly beneath the structure, reaching a maximum of 55 mm at +55 m.

5.3.2 Vertical Stress Distribution

The mean vertical stresses for the M.A.C. are obtained from the plane strain finite element results. These stresses are presented in Figure 5.12 for the elements at the datum level. The stress values are best representative

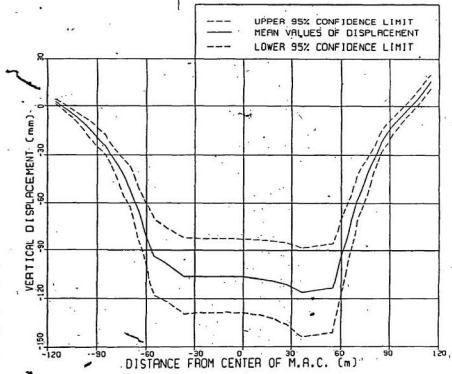


FIGURE 5.11 95% CONFIDENCE INTERVAL FOR VERTICAL
DISPLACEMENT DUE TO ICE & GRAVITY LOADS

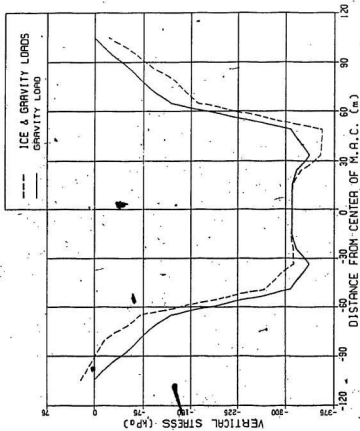


FIGURE 5.12 MEAN VERTICAL STRESS AT DATUM LEVEL

of the triangular elements' centroids, 8.33 m below datum. The results indicate maximum vertical stress occurs directly beneath the caissons at -325 kPa, then reduces to -310 kPa at the sand core interior. The combined load shows the ice effect at the caisson by decreasing the stress to -310 kPa on the ice-impacted side and increasing the stress to -350 kPa on the opposite side. This signifies the frame action of the steel caisson and deck in transferring the lateral force and resulting overturning moment to the seabed. Rogers et al. [106] have reported a vertical stress of -280 kPa to represent the total load increase on the subcut material. This indicates less than a 10% difference in the average stress predicted by the finite element analysis. The difference may be partially attributed to differences in platform load and sand fill densities.

In Figure 5.13, the vertical stress distributions at 8 m, 33 m, and 63 m depth below the datum level are compared. The vertical stress is greatest at the caisson and soil interface (i.e. 8 m depth) reaching a magnitude of -350 kPa. Between the 8 m and 33 m depths, the stress is reduced by 25 kPa. At the 63 m depth, the vertical stress profile is tending towards a uniform value of approximately -150 kPa.

Using Eq. (3.34), the variances for the vertical stresses are estimated. In Figure 5.14, the standard

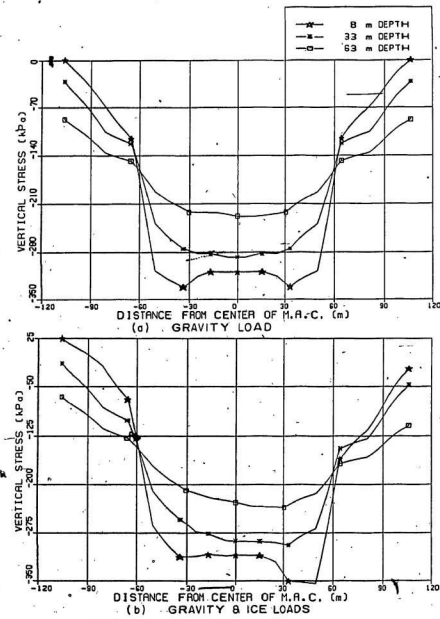


FIGURE 5.13 VERTICAL STRESS AT VARIOUS DEPTHS

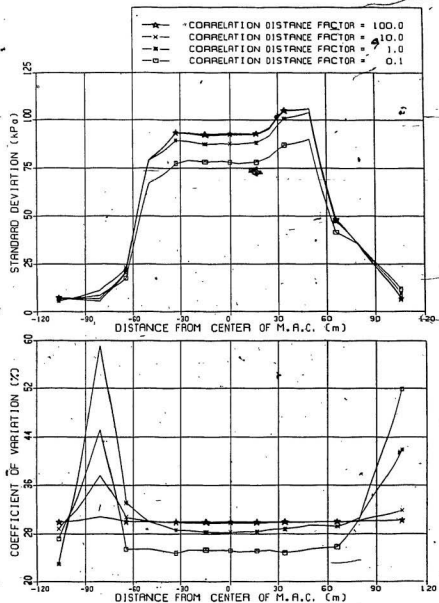


FIGURE 5.14 STATISTICAL PARAMETERS FOR VERTICAL STRESS
DUE TO ICE & GRAVITY LOADS

deviation curves for the combined ice and gravity loads follow the basic shape of the mean vertical stress curve (Figure 5.12). This is an indication that the stress magnitude influences the standard deviation value. The previously mentioned trends for displacement apply here as well. The curves for standard deviation and coefficient of variation approach a maximum as the CDF increases. For a CDF equal to 10 or greater, the vertical stress C.O.V. attains a 30% value, twice the elastic modulus C.O.V. of 15%. This suggests that element stresses are more sensitive to material strength uncertainty than nodal displacements. This conclusion is verified through examination of Eq. (3.32), where the first term represents uncertainty from element stress and the second term, uncertainty from all the nodal displacements in the finite element mesh. For a highly correlated continuum, each of the two terms approach a particular value such that the resulting contribution to the coefficient of variation is equivalent to the modulus C.O.V.

With the standard deviations for vertical stresses being a greater percentage of the mean values as compared to the displacement results, the confidence intervals will exhibit increased uncertainty. Using the CDF of 1.0, a wide range of possible stresses are indicated in Figure 5.15. The bandwidth averages -350 kPa below the M.A.C., reaching a

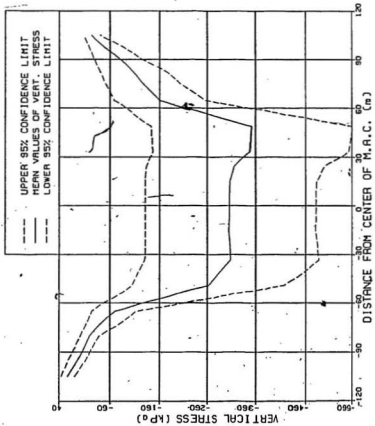


FIGURE 5.15 95% CONFIDENCE INTERVAL FOR VERTICAL STRESS
DUE TO ICE & GRAVITY LOADS.

maximum of -416 kPa at +50 m. These large stress variations indicate the importance of quantifying uncertainty in design work.

5.3.3 Horizontal Stress Distribution

The horizontal stress distribution at the datum level is presented in Figure 5.16. The gravity load results are symmetrical about the center of the M.A.C. structure. The stress is maximum at -210 kPa at 0 m remaining constant through the sand core. Under the steel caissons (between 35 to 55 m), the stress reduces to -150 kPa. Beyond the caisson, the horizontal stress decreases until the load effect is negligible. For the combined ice and gravity case, the 500 MN lateral ice force slightly alters the horizontal stress pattern. On the ice-impacted side of the caisson, the horizontal stress is actually smaller than the previous case. To the left of center, the stress gradually decreases from -210 kPa to -100 kPa at the caisson's outside edge. The overturning moment caused by the ice force generates an uplifting effect to the left of center, thereby reducing the horizontal stress. By the same token, the stress is increased to the right, reaching a maximum of -225 kPa. This stress increase is attributed to the caisson digging into the seabed as the ice contacts the structure.

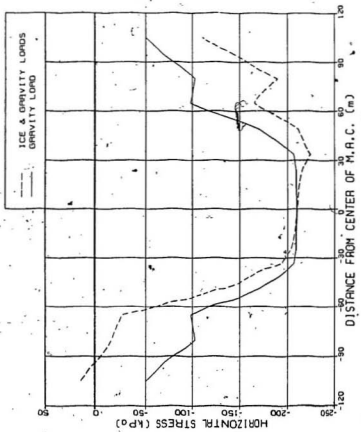


FIGURE 5.16 MEAN HORIZONTAL STRESS AT DATUM LEVEL

The standard deviation and coefficient of variation for horizontal stresses are computed in the same manner as the vertical stresses, using Eq. (3.34) and the mean stresses. The analysis is based on the stochastic results of 15^t modulus C.O.V. In Figure 5.17, the statistical parameters are presented for the gravity load. The standard deviation curves are closely spaced, indicating the insensitivity of the stochastic analysis to changes in correlation distance factors. The vertical stresses and displacements displayed a wider range of standard deviations as the CDF increased from 0.1 to 100. The combined ice and gravity results in Figure 5.18 indicate the same pattern, suggesting that the differing load conditions do not strongly influence the stochastic analysis. This is true in the highly stressed zones below the caisson and the sand fill berm. The coefficients of variation are fairly constant within the confines of the M.A.C. but tend to become erratic at the boundaries. This is explained as low stress values have an inflating effect on coefficient of variation computations. Small changes in the standard deviation are exaggerated many times when divided by small horizontal stress values. In the regions beneath the M.A.C., the horizontal stress C.O.V. approaches a magnitude of twice the modulus C.O.V. This result is similar to the vertical stress analysis.

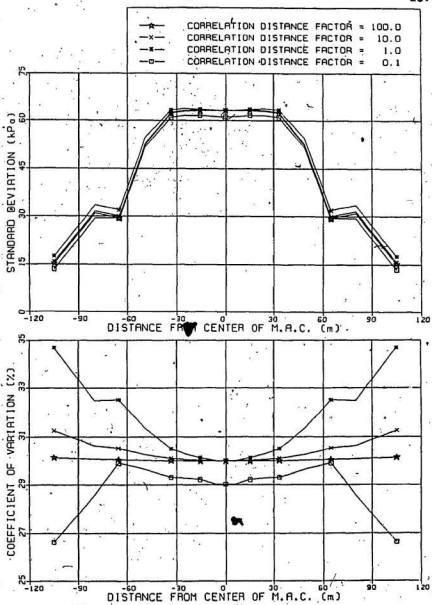


FIGURE 5.17 STATISTICAL PARAMETERS FOR HORIZONTAL STRESS DUE TO GRAVITY LOAD

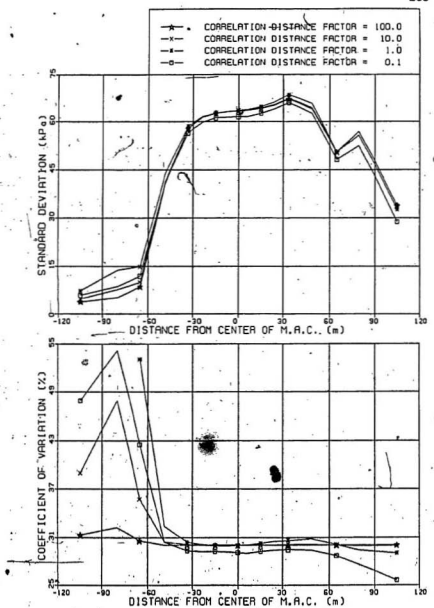


FIGURE 5.18 STATISTICAL PARAMETERS FOR HORIZONTAL STRESS DUE TO ICE & GRAVITY LOADS

In Figure 5.19, the 95% confidence interval for the horizontal stress is presented for the CDF of 1.0. Below the M.A.C., the bandwidth averages -250 kPa, varying from -175 kPa at -50 m to -275 kPa at +35 m. As compared to Figure 5.15, this bandwidth is 100 kPa smaller on average than the vertical stress bandwidth.

5.3.4 Random Stochastic Analysis

The previous stochastic analysis has assumed the soil continuum to have a fixed modulus C.O.V. of 15% for all elements. This procedure maximizes the material property uncertainty, thereby establishing the upper bound of the stress and displacement variation. In a purely stochastic analysis, the elastic modulus in the field varies randomly about an assumed constant mean. As outlined in Section 3.4, a pseudo-random number generator is used to create a sequence of thirty-two random numbers between zero and unity. Using Eq. (3.47), a random variation of elastic moduli standard deviations are generated for the finite element mesh.

For the M.A.C. problem, the computer program RAND.FTN of Appendix III is used to simulate the random stochastic analysis. For demonstration of the procedure, the maximum anticipated modulus C.O.V. is 15% and the CDF is set at 1.

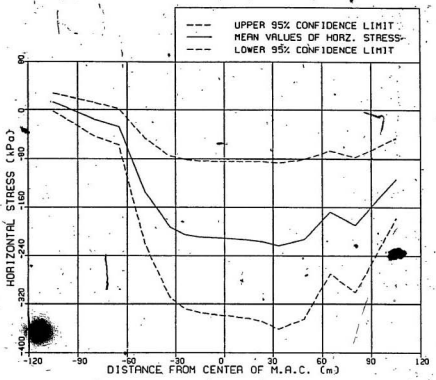


FIGURE 5.19 95% CONFIDENCE INTERVAL FOR HORIZONTAL STRESS DUE TO ICE & GRAVITY LOADS

Using different starting values, S_0 , to initiate the random number sequences (Table 3.2), three pseudo-random versions are investigated. Pseudo-random sample numbers 1, 2 and 3 correspond to S_0 values of 1000, 123457 and 500000, respectively. The mean displacements and stresses of Figures 5.7, 5.12 and 5.16 are applied to the pseudo-random standard deviations to obtain the coefficients of variation. For the pseudo-random analysis, only the combined ice and gravity load is examined.

In Figure 5.20, the standard deviation and coefficient of variation distributions at datum level are presented for the vertical displacement. The pseudo-random curves show relatively small variations between the three samples. Typically the variations are about 1.5 mm in the standard deviation and 1% in the coefficient of variation. Collectively, these curves are approximately 50% of the upper bound distribution. This is attributed to the statistical probability that the sequence of random numbers varying between zero and unity has an average of 0.5. With the expected material uncertainty of 15%, the upper bound curve represents the worst case scenario. As indicated by the random stochastic analysis, the actual degree of expected uncertainty in displacements will be much less.

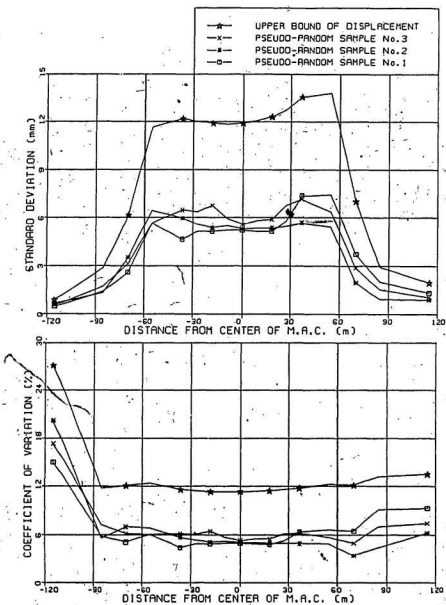


FIGURE 5.20 STATISTICAL PARAMETERS FOR VERTICAL
DISPLACEMENT DUE TO ICE & GRAVITY LOADS

In Figures 5.21 and 5.22, the statistical parameters are shown for vertical and horizontal stresses, respectively. These results have erratic fluctuations throughout, indicating the increased influence of randomness in the spread of results. The randomness in the statistical parameters for stress are affected by the element stress uncertainty and then compounded by the randomness of the displacement. After examining Eq. (3.32), the combination of random effects in the displacements and stresses will provide more significant variation. The pseudo-random stress results range between 20% to 80% reduction from the upper bound levels. At some point locations the random results attain values close to the upper bound. For large scale analysis, these localized anomalies can be considered redistributed among neighbouring elements. Figures 5.21 and 5.22 indicate that the random stochastic analysis affects vertical and horizontal stress in the same manner.

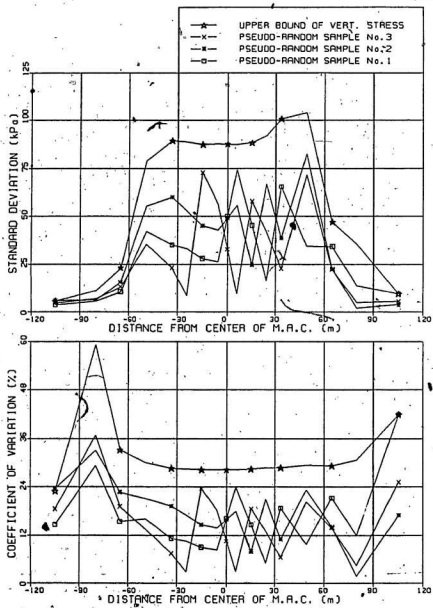


FIGURE 5.21 STATISTICAL PARAMETERS FOR VERTICAL STRESS
DUE TO ICE- & GRAVITY LOADS

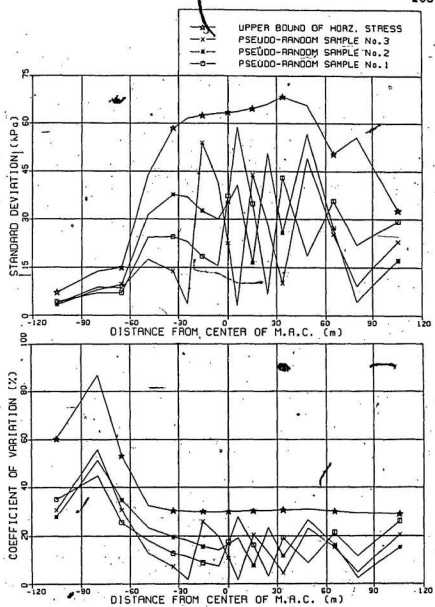


FIGURE 5.22 STATISTICAL PARAMETERS FOR HORIZONTAL
STRESS DUE TO ICE & GRAVITY LOADS

CHAPTER 6

CONCLUSIONS AND RECOMMENDATIONS

6.1 Conclusions

A stochastic finite element procedure is developed to estimate the influence of elastic modulus uncertainty on the short term settlements and stresses of foundations. The procedure is based on a plane strain triangular finite element model that incorporates the elastic modulus variation by considering a two term Taylor series expansion of the equilibrium equations. Two soil models are examined; (i) an elastic, single phase, layered soil and (ii) a piecewise linear elastic, single phase, layered soil representing the nonlinear soil behaviour. Using FORTRAN computer programming, a parametric analysis is carried out to establish the sensitivity of the stochastic finite element procedure to correlation distance, modulus coefficient of variation (C.O.V.), and soil models.

Two ocean structure cases are examined to verify the procedure, namely, (i) the Ekofisk Tank, an offshore gravity platform and (ii) the Mobile Arctic Caisson (M.A.C.), a caisson retained island. In both cases, numerical results have compared very well with those published in literature.

for the prototype structures, differing by less than 10% for most conditions. Parametric studies of both problems have similar results. The general conclusions are summarized as follows:

- (i) For the elastic soil model, the sensitivity of the standard deviations of displacement and stress to changes in modulus C.O.V. is a linear relationship.
- (ii) The effect of modulus uncertainty is more pronounced in the uncertainty of stresses than the uncertainty of displacements.
- (iii) As the correlation distance factor becomes large (greater than 10), the variation of displacements or stresses attributed to local material uncertainty is smaller. Under this condition the soil continuum is highly correlated.
- (iv) For large correlation distance factors, the displacement C.O.V. approaches a value equal to the assumed modulus C.O.V. Similarly, the stress C.O.V. (e.g., vertical, horizontal and shear) approaches a value equal to twice the assumed modulus C.O.V.

- (v) With smaller correlation distances, the coefficients of variation for displacements and stresses are decreased.
- (vi) The level of uncertainty in results are insensitive to the varying load conditions. Approximately the same C.O.V.'s are observed for the highly stressed zones, regardless of the loading, whether it is totally gravitational or combined with lateral forces.
- (vii) The random stochastic analysis yields an approximate 50% reduction in the displacement C.O.V. from the upper bound values. For stress, the results are more erratic ranging from 20% to 80% reduction from the upper bound values.
- (viii) The piecewise linear soil model provides closer agreement with the published data for prototype structures and yields lower coefficients of variation for displacements and stresses than the elastic model.

6.2 Contributions

- (i) A parametric analysis of the linear elastic stochastic finite element procedure is carried out and the procedure verified using two problem applications.
- (ii) A random stochastic model is incorporated into the elastic finite element program.
- (iii) A piecewise linear procedure with shear strain dependent modulus for soil is investigated in conjunction with the stochastic finite element analysis.

6.3 Recommendations for Future Research

The following recommendations are made as possible avenues of research to extend the present work:

- (i) apply the stochastic procedure to other finite element models such as linear strain triangles, linear strain rectangles, and 8-noded/16-noded bricks,

- (ii) interpret stochastic analysis in terms of principal stresses,
- (iii) include higher order terms in Taylor series expansion of equilibrium equations to permit investigation of higher modulus C.O.V.,
- (iv) study different correlation functions to correspond with field data,
- (v) incorporate a two phase soil model (i.e. solid and fluid phases) to determine the pore pressures and "soil skeleton" stresses,
- (vi) improve on the nonlinear modeling of soil properties,
- (vii) provide a better random number generator in computer programs, and
- (viii) develop a correlation function for adding covariances for each load step in the piecewise linear analysis.

CHAPTER 7

REFERENCES

- [1] Eide, O., and Andersen, K.H., "Foundation Engineering for Gravity Structures in the Northern North Sea", Norges Geotekniske Institutt (Norwegian Geotechnical Institute), Publication No.154, 1984, pp. 1-48.
- [2] Dawson, T.H., Offshore Structural Design, Prentice-Hall, Inc., Englewood Cliffs, N.J., 1983, pp. 3-25.
- [3] Bech, H. and Haugsgen, P.B., "Saga's Hybrid Gravity Platform Design for Deep Water", Ocean Industry, Vol. 19, No. 6, 1984, pp. 51-53.
- [4] Høeg, K., "Geotechnical Issues in Offshore Engineering", Norges Geotekniske Institutt (Norwegian Geotechnical Institute), Publication No. 144, 1983, pp. 1-21.
- [5] Graff, W.J., Introduction to Offshore Structures: Design, Fabrication, Installation, Gulf Publishing Company, Houston, Texas, U.S.A., 1981.
- [6] Graff, W.J. and Chen, W.F., "Bottom-Supported Concrete Platforms: Overview", Journal of the Structural Division, ASCE, Vol. 107, No. ST6, June, 1981, pp. 1059-1081.
- [7] "Environmental Impact Statement for Hydrocarbon Development in the Beaufort Sea" - MacKenzie Delta Region Volume 2: Development Systems 1982 Chapters 2, 3 and 4 (Prepared by Dome Petroleum Limited, Esso Resources Canada Limited—and Gulf Canada Resources Inc.)
- [8] Hnatiuk, J., and Felzen, E.E., "Molikpag: An Integrated Mobile Arctic Drilling Caisson", Proceedings, Offshore Technology Conference, Houston, 1985, Paper No. OTC 4940, pp. 373-381.
- [9] Brophy, P., "Arctic Experience: A Visit to CANMAR's Beaufort Operation", Canadian Shipping and Marine Engineering, Vol. 55, No. 2, November 1983, pp. 10-16.
- [10] Mancini, C.V., Dowse, B.E.W. and Chevallier, J., "Caisson Retained Island for Canadian Beaufort Sea—Geotechnical Design and Construction Considerations",

- Proceedings, Offshore Technology Conference, Houston, 1983, Paper No. OTC 4581, pp. 17-22.
- [11] Jefferies, M.G., Stewart, H.R., Thomson, R.A.A. and Rogers, B.T., "Molikpaq Deployment at Tarsius P-45", Civil Engineering in the Arctic Offshore (Proceedings of the ASCE Specialty Conference Arctic '85), San Francisco, CA, 1985, pp. 1-27.
 - [12] Young, A.G., Kraft, L.M. and Focht, J.A., "Geotechnical Considerations in Foundation Design of Offshore Gravity Structures", Proceedings, Offshore Technology Conference, Houston, 1975, Paper No. OTC 2371, pp. 367-386.
 - [13] Eide, O., "Marine Soil Mechanics: Applications to North Sea Offshore Structures", Proceedings, Offshore North Sea Conference, Stavanger, Norway, (Reprint: Norges Geotekniske Institutt, Publication No. 103, 1974, pp. 1-20).
 - [14] Terzaghi, K., Theoretical Soil Mechanics, John Wiley and Sons, Inc., New York, 1943.
 - [15] Terzaghi, K. and Peck, R.B., Soil Mechanics in Engineering Practice (Second Edition), John Wiley and Sons, Inc., New York, 1967, Chapter 5.
 - [16] Meyerhof, G.G., "Some Recent Research on the Bearing Capacity of Foundations", Canadian Geotechnical Journal, Vol. 1, No. 1, September 1963, pp. 16-26.
 - [17] Vesic, A.S., "Bearing Capacity of Shallow Foundations", Handbook of Foundation Engineering (Chapter 3), Winterhorn, H.F. and Fang, H., Editors, New York, Van Nostrand.
 - [18] Hansen, J.B., "A Revised and Extended Formula for Bearing Capacity", Danish Geotechnical Institute, Copenhagen, Bulletin No. 28, 1970, pp. 5-11.
 - [19] Bjerrum, L., "Geotechnical Problems Involved in Foundations of Structures in the North Sea", Geotechnique, Vol. 23, No. 3, 1973, pp. 319-358.
 - [20] Meyerhof, G.G., "Ultimate Bearing Capacity of Footings on Sand Layer Overlying Clay", Canadian Geotechnical Journal, Vol. 11, No. 2, 1974, pp. 223-229.
 - [21] Reddy, A.S. and Srinivasan, R.J., "Bearing Capacity of Footings on Layered Clays", Journal of Soil Mechanics

- and Foundations Division, ASCE, Vol. 93, No. SMI, 1967, pp. 83-99.
- [22] Brown, J.D. and Meyerhof, G.G., "Experimental Study of Bearing Capacity in Layered Clays", Proceedings, Seventh International Conference on Soil Mechanics and Foundation Engineering, Mexico City, Vol. II, 1969, pp. 45-51.
- [23] Mitchell, R.J., Sangrey, D.A. and Webb, G.S., "Foundations in the Crust of Sensitive Clay Deposits", Proceedings, Performance of Earth-Supported Structures, ASCE Specialty Conference, Lafayette, Ind., Vol. 1, Part 2, 1972, pp. 1051-1072.
- [24] Vesic, A.S., "Analysis of Ultimate Loads of Shallow Foundations", Journal of Soil Mechanics and Foundations Division, ASCE, Vol. 99, No. SMI, January 1973, pp. 45-73.
- [25] Janbu, N., Grande, L. and Eggereide, K., "Effective Stress Stability Analysis for Gravity Structures", Proceedings, International Conference on Behaviour of Offshore Structures, BOSS '76, Vol. 1, pp. 449-466.
- [26] Murff, J.D. and Miller, T.W., "Stability of Offshore Gravity Structure Foundations by the Upper Bound Method", Proceedings, Offshore Technology Conference, Houston, 1977, Paper No. OTC 2896, pp. 147-154.
- [27] Lauritzen, R. and Schjetne, K., "Stability Calculations for Offshore Gravity Structures", Proceedings, Offshore Technology Conference, Houston, 1976, Paper No. OTC 2431, pp. 75-82.
- [28] Saxena, S.K., Kilkenny, W.M. and Fischer, J.A., "Bearing Capacity of Offshore Gravity Structures", Proceedings on Civil Engineering in the Oceans III, University of Delaware, Newmark, June 1975, pp. 450-469.
- [29] Poulos, H.G. and Davis, E.H., Elastic Solutions for Soil and Rock Mechanics, John Wiley and Sons, Inc., New York, 1974.
- [30] Baecher, G.B., Chan, M., Ingra, T.S., Lee, T. and Nucci, L.R., "Geotechnical Reliability of Offshore Gravity Platforms", Massachusetts Institute of Technology, Cambridge, Report No. MITSG80-20, December 1980.

- [31] Prévost, J.H., Cuny, B., Hughes, T.J.R. and Scott, R.F., "Offshore Gravity Structures", Journal of Geotechnical Engineering Division, ASCE, Vol. 107, No. GT2, February 1981, pp. 143-165.
- [32] Prévost, J.H., Cuny, B. and Scott, R.F., "Offshore Gravity Structures: Centrifugal Modeling", Journal of Geotechnical Engineering Division, ASCE, Vol. 107, No. GT2, February 1981, pp. 125-141.
- [33] Rowe, P.W. and Craig, W.H., "Application of Models to the Prediction of Offshore Gravity Platform Foundation Performance", Offshore Site Investigation, Ardus, D.A. (editor), Graham and Trotman Ltd., 1980, pp. 269-281.
- [34] Andersen, K.H., Selnes, P.B., Rowe, P.W. and Craig, W.H., "Prediction and Observation of a Model Gravity Platform on Drammen Clay", Proceedings, Second International Conference on the Behaviour of Offshore Structures, BOSS '79, Vol. 1, pp. 427-446.
- [35] Zienkiewicz, O.C., Norris, V.A., Winnicki, L.A., Naylor, D.J. and Lewis, R.W., "A Unified Approach to the Soil Mechanics Problems of Offshore Foundations", Numerical Methods in Offshore Engineering, Zienkiewicz, O.C., Lewis, R.W. and Stagg, K.G. (editors), John Wiley and Sons, 1978, Chapter 12, pp. 361-411.
- [36] Andersen, K.H., Hansteen, O.E., Høeg, K. and Prévost, J.H., "Soil Deformations due to Cyclic Loads on Offshore Structures", Numerical Methods in Offshore Engineering, Zienkiewicz, O.C., Lewis, R.W. and Stagg, K.G. (editors), John Wiley and Sons, 1978, Chapter 13, pp. 413-452.
- [37] Broughton, P., "Offshore Gravity Based Oil Production Platform Interaction with the Sea Bed", Proceedings, Offshore Technology Conference, Houston, 1975, Paper No. OTC 2372, pp. 387-398.
- [38] Vaughan, P.R., Davachi, M.M., El Ghamrawy, M.K., Hamza, M.M. and Hight, D.W., "Stability Analysis of Large Gravity Structures", Proceedings, International Conference on the Behaviour of Offshore Structures, BOSS '76, Vol. 1, pp. 467-487.
- [39] Prévost, J.H., Hughes, T.J.R. and Cohen, M.F., "Analysis of Gravity Offshore Structure Foundations", Journal of Petroleum Technology, Vol. 32, No. 2, February 1980, pp. 199-209.

- [40] Whitman, R.V., "Soil-Platform Interaction", Proceedings, International Conference on the Behaviour of Offshore Structures, BOSS '76, Vol. 1, pp. 817-829.
- [41] Crouch, S.L. and Starfield, A.M., Boundary Element Methods in Solid Mechanics (with applications in rock mechanics and geological engineering), George Allen and Unwin (Publishers) Ltd., London, 1983, Chapters 3 and 8.
- [42] Hobbs, R., George, P.J. and Mustoe, G.G.W., "Some Applications of Numerical Methods to the Design of Offshore Gravity Structure Foundations", Numerical Methods in Offshore Engineering, Zienkiewicz, O.C., Lewis, R.W. and Stagg, K.G. (editors), John Wiley and Sons, 1978, Chapter 14, pp. 453-482.
- [43] Samuels, J.C. and Eringen, A.C., "On Stochastic Linear Systems", Journal of Mathematics and Physics, Vol. 38, 1959, pp. 83-103.
- [44] Collins, J.D. and Thomson, W.T., "The Eigenvalue Problem for Structural Systems with Statistical Properties", AIAA Journal, Vol. 7, No. 4, April 1969, pp. 642-648.
- [45] Chen, P.C. and Soroka, W.W., "Impulse Response of a Dynamic System with Statistical Properties", Journal of Sound and Vibration, Vol. 31, No. 3, December 1973, pp. 309-314.
- [46] Chen, P.C. and Soroka, W.W., "Multi-Degree Dynamic Response of a System with Statistical Properties", Journal of Sound and Vibration, Vol. 37, No. 4, December 1974, pp. 547-556.
- [47] Christian, J.T., "Probabilistic Soil Dynamics: State-of-the-Art", Journal of the Geotechnical Engineering Division, ASCE, Vol. 106, No. GT4, April 1980, pp. 385-397.
- [48] Lumb, P., "The Variability of Natural Soils", Canadian Geotechnical Journal, Vol. 3, No. 2, May 1966, pp. 74-97.
- [49] Cornell, C.A., "First-Order Uncertainty Analysis of Soil Deformation and Stability", Proceedings of the First International Conference on Applications of Statistics and Probability to Soil and Structural Engineering, Lumb, P. (editor), Hong Kong University Press, 1972, pp. 129-144.

- [50] Vanmarcke, E.H., "Probabilistic Modeling of Soil Profiles", Journal of the Geotechnical Engineering Division, ASCE, Vol. 103, GT11, November 1977, pp. 1227-1246.
- [51] Tang, W.H., "A Bayesian Evaluation of Information for Foundation Engineering Design", Proceedings of the First International Conference on Applications of Statistics and Probability to Soil and Structural Engineering, Lumb, P. (editor), Hong Kong University Press, 1972, pp. 173-185.
- [52] Meyerhof, G.G., "Concepts of Safety in Foundation Engineering Ashore and Offshore", Proceedings, First International Conference on Behaviour of Offshore Structures, BOSS '76, Vol. 1, pp. 900-912.
- [53] Lumb, P., "Precision and Accuracy of Soil Tests", Proceedings of the First International Conference on Applications of Statistics and Probability to Soil and Structural Engineering, Lumb, P. (editor), Hong Kong University Press, 1972, pp. 329-345.
- [54] Morse, R.K., "The Importance of Proper Soil Units for Statistical Analysis", Proceedings of the First International Conference on Applications of Statistics and Probability to Soil and Structural Engineering, Lumb, P. (editor), Hong Kong University Press, 1972, pp. 347-355.
- [55] Schultze, E., "Frequency Distributions and Correlations of Soil Properties", Proceedings of the First International Conference on Applications of Statistics and Probability to Soil and Structural Engineering, Lumb, P. (editor), Hong Kong University Press, 1972, pp. 371-387.
- [56] Singh, A., "How Reliable is the Factor of Safety in Foundation Engineering", Proceedings of the First International Conference on Applications of Statistics and Probability to Soil and Structural Engineering, Lumb, P. (editor), Hong Kong University Press, 1972.
- [57] Schultze, E., "The General Significance of Statistics for the Civil Engineer", Proceedings, Second International Conference on Applications of Statistics and Probability in Soil and Structural Engineering, Aachen, Germany, 1975.
- [58] Kraft, L.M. and Murff, J.D., "A Probabilistic Investigation of Foundation Design for Offshore Gravity

- Structures", Proceedings Offshore Technology Conference, Houston, 1975, Paper No. OTC 2370, pp. 361-365.
- [59] Tang, W.H., Michols, K.A. and Kjekstad, O., "Probabilistic Stability Analysis of Gravity Platforms", Norges Geotekniske Institutt (Norwegian Geotechnical Institute), Publication No. 152, 1984, pp. 1-7.
- [60] Høeg, K. and Tang, W.H., "Probabilistic Considerations in the Foundation Engineering for Offshore Structures", Norges Geotekniske Institutt (Norwegian Geotechnical Institute), Publication No. 120, 1978, pp. 41-69.
- [61] Reséndiz, D. and Herrera, I., "A Probabilistic Formulation of Settlement-Controlled Design", Proceedings of the Seventh International Conference on Soil Mechanics and Foundation Engineering, Vol. 2, Mexico, 1969, pp. 217-225.
- [62] Hilldale, C., "A Probabilistic Approach to Estimation of Differential Settlement of Footings on Sand", Thesis presented to the M.I.T. at Cambridge, Massachusetts, 1971.
- [63] Diaz, J. and Vanmarcke, E.H., "Settlement Prediction A Probabilistic Approach", Research Report R73-40, Massachusetts Institute of Technology, Cambridge, 1973.
- [64] Dendrou, B.A. and Houstis, E.N., "Uncertainty Finite Element Dynamic Analysis", Applied Mathematical Modelling, Vol. 3, April 1979, pp. 143-150.
- [65] Dendrou, B.A. and Houstis, E.N., "An Inference-Finite Element Model for Field Problems", Applied Mathematical Modelling, Vol. 2, June 1978, pp. 109-114.
- [66] Su, Y.L., Wang, Y.L. and Stefanko, R., "Finite Element Analysis of Underground Stresses Utilizing Stochastically Simulated Material Properties", Proceedings of the Seventh United States Symposium on Rock Mechanics, Berkley, California, 1969, Chapter 15, pp. 253-266.
- [67] Cambou, B., "Application of First Order Uncertainty Analysis in the Finite Elements Method in Linear Elasticity", Proceedings Second International Conference on Application of Statistics and Probability in Soil and Structural Engineering, Aachen, Germany, 1975, pp. 67-80.

- [68] Kraft, L.M. and Yeung, J.Y., "Deformation of Statistically Heterogeneous Earth Structures", Geotechnical Engineering, Volume V, No. 1, pp. 39-52.
- [69] Baecher, G.B. and Ingra, T.S., "Stochastic FEM in Settlement Predictions", Journal of the Geotechnical Engineering Division, ASCE, Vol. 107, No. GT4, April 1981, pp. 449-463.
- [70] Munaswamy, K. and Arockiasamy, M., "Stochastic Finite Element Analysis of Gravity Platform Foundation", Proceedings, ASCE Conference Arctic '85, San Francisco, March 1985, pp. 1049-1062.
- [71] Hoddinott, T., Arockiasamy, M., Munaswamy, K. and Swamidas, A.S.J., "Analysis of Gravity Platform Foundations Using F.E.M. with Stochastic Materials", Proceedings, OMAE Specialty Symposium, New Orleans, February 1986.
- [72] Hoddinott, T., Swamidas, A.S.J., Munaswamy, K. and Arockiasamy, M., "F.E.M. Analysis of Mobile Arctic Caisson Island with Stochastic Material Properties", Proceedings, Fourth International Cold Regions Specialty Conference, ASCE, Anchorage, February 1986, pp. 546-557.
- [73] Vanmarcke, E., Random Fields: Analysis and Synthesis, The Massachusetts Institute of Technology Press, Cambridge, 1983, Chapter 2, pp. 20-77.
- [74] Dwass, M., Probability and Statistics, W.A. Benjamin, Inc., New York, 1970, pp. 317-320.
- [75] Christian, J.T. and Desai, C.S., "Constitutive Laws for Geologic Media", Numerical Methods in Geotechnical Engineering, Desai, C.S. and Christian, J.T. (editors), McGraw-Hill, Inc., New York, 1977, Chapter 2, pp. 65-115.
- [76] Duncan, J.M. and Chang, C.Y., "Non-linear Analysis of Stress and Strain in Soils", Journal of Soil Mechanics and Foundations Division, ASCE, Vol. 96, No. SM5, September 1970, pp. 1629-1653.
- [77] Chang, C.Y. and Duncan, J.M., "Analysis of Soil Movement around a Deep Excavation", Journal of Soil Mechanics and Foundations Division, ASCE, Vol. 96, No. SM5, September 1970, pp. 1655-1681.
- [78] Kondner, R.L., "Hyperbolic Stress-Strain Response: Cohesive Soils", Journal of Soil Mechanics and

- Foundations Division, ASCE, Vol. 89, No. SMI, January 1963, pp. 115-143.
- [79] Hardin, B.O. and Black, W.L., "Closure to Vibration Modulus of Normally Consolidated Clays", Journal of Soil Mechanics and Foundations Division, ASCE, Vol. 95, No. SM6, November 1969, pp. 1531-1537.
- [80] Hardin, B.O. and Drnevich, P., "Shear Modulus and Damping in Soils: Design Equations and Curves", Journal of Soil Mechanics and Foundations Division, ASCE, Vol. 98, No. SM7, July 1972, pp. 667-692.
- [81] Seed, H.B. and Idriss, I.M., "Influence of Soil Conditions on Ground Motions During Earthquakes", Journal of Soil Mechanics and Foundations Division, ASCE, Vol. 95, No. SMI, January 1969, pp. 99-137.
- [82] Idriss, I.M., Dezfulian, H. and Seed, H.B., "Computer Programs for Evaluating the Seismic Response of Soil Deposits with Non-linear Characteristics using Equivalent Linear Procedures", Department of Civil Engineering, University of California, Berkeley, April 1969.
- [83] Seed, H.B. and Idriss, I.M., "Soil Moduli and Damping Factors for Dynamic Response Analyses", Earthquake Engineering Research Center (EERC), Report Number 70-10, December 1970, University of California, Berkeley.
- [84] Lysmer, J., Uda, T., Seed, H.B. and Hwang, R., "LUSH: A Computer Program for Complex Response Analysis of Soil-Structure Systems", Earthquake Engineering Research Center (EERC), Report Number 74-4, April 1974, University of California, Berkeley.
- [85] Cook, Robert D., Concepts and Applications of Finite Element Analysis (Second Edition), John Wiley and Sons, Inc., 1981, Chapter 13, pp. 367-374.
- [86] Lewis, P.A.W., Goodman, A.S. and Miller, J.M., "A Pseudo-Random Number Generator for the System/360", IBM Systems Journal, Vol. 8, No. 2, 1969, pp. 136-146.
- [87] Meissner, L.P. and Organick, E.I., Fortran 77: Featuring Structured Programming, Addison-Wesley Publishing Company, April 1982, pp. 66, 67, 334-340.
- [88] Russell, W.E. and Muggeridge, D.B., (Editors), Proceedings of the Symposium Production and Transportation Systems for the Hibernia Discovery, St. John's, Newfoundland, February 1981, Preface, pp. iii-iv.

- [89] Clausen, C.J.F., DiBiagio, E., Andersen, K.H. and Duncan, J.M., "Observed Behaviour of the Ekofisk Oil Storage-Tank Foundation", Journal of Petroleum Technology, Vol. 28, No. 3, March 1976, pp. 329-336.
- [90] Gerwick, B.C. and Hognestad, E., "Concrete Oil Storage Tank Placed on North Sea Floor", Civil Engineering ASCE, Vol. 43, No. 8, 1973, pp. 81-85.
- [91] Jarlan, G.E., "A Prestressed Concrete Fixed Drilling and Production Platform for the Hibernia Oil Field Development", Proceedings of the Symposium Production and Transportation Systems for the Hibernia Discovery, February 1981, pp. 18-26.
- [92] Schjetne, K., Andersen, K.H., Lauritszen, R. and Hansteen, O.E., "Foundation Engineering for Offshore Gravity Structures", Marine Geotechnology, Vol. 3, No. 4, 1979, pp. 1-15.
- [93] Wang, C. and Salmon, C.G., Reinforced Concrete Design (third edition), Harper and Row, Publishers, Inc., New York, 1979, pp. 13-14.
- [94] Canadian Portland Cement Association, "Design and Control of Concrete Mixtures", (metric edition), PCA Engineering Bulletin, 1979.
- [95] Kjekstad, O. and Lunne, T., "Soil Parameters Used for Design of Gravity Platforms in the North Sea", Proceedings of the Second International Conference on the Behaviour of Offshore Structures, Vol. 1, London, 1979, pp. 175-192.
- [96] Bowles, J.E., Foundation Analysis and Design, (second edition), McGraw-Hill, New York, pp. 750.
- [97] Sowers, G.B. and Sowers, G.P., Introductory Soil Mechanics and Foundations (third edition), MacMillan Publishing Co., Inc., New York, 1970, pp. 403.
- [98] LeTirant, P., Seabed Reconnaissance and Offshore Soil Mechanics for the Installation of Petroleum Structures, Institut Francais de Petrole Publications, Paris, 1979, pp. 353-355.
- [99] Pfaffenberger, R.C. and Patterson, J.H., Statistical Methods for Business and Economics, Richard D. Irwin, Ltd., Illinois, U.S.A., 1977, pp. 180-204.

- [100] Lee, K.L. and Focht, J.A., "Liquefaction Potential at Ekofisk Tank in North Sea", Journal of the Geotechnical Engineering Division, ASCE, Vol. 101, No. GT1, January 1975, pp. 1-18.
- [101] Timoshenko, S.P. and Goodier, J.N., Theory of Elasticity, McGraw-Hill, 1933, pp. 85-96.
- [102] Stewart, H.R., Jefferies, M.G. and Goldby, H.M., "Berm Construction for the Gulf Canada Mobile Arctic Caisson", Proceedings, Offshore Technology Conference, Houston, 1983, Paper No. OTC 4552, pp. 339-346.
- [103] Kent, D.D., Graham, B.W. and Sangster, R.H.B., "Geotechnical Design of a Caisson Retained Island for Exploration Drilling in the Beaufort Sea", Proceedings of the First Canadian Conference on Marine Geotechnical Engineering, Calgary, Alberta, April 1979, pp. 429-437.
- [104] Bruce, J.C. and Harrington, A.G., "Design Aspects of a Mobile Arctic Caisson", Proceedings, Offshore Technology Conference, Houston, 1982, Paper No. OTC 4333, pp. 405-416.
- [105] Selvadurai, A.P.S., Elastic Analysis of Soil-Foundation Interaction, Developments in Geotechnical Engineering, Vol. 17, Elsevier Scientific Publishing Company, New York, 1979, pp. 407-437.
- [106] Rogers, B.T., Hardy, M.D., Neth, V.W. and Metge, M., "Performance Monitoring of the Molikpaq While Deployed at Tarsitut P-45", Proceedings, Third Canadian Conference on Marine Geotechnical Engineering, St. John's, Newfoundland, June 1986, Vol. 1, pp. 363-383.
- [107] McCreath, D.R., Hodge, W.E. and Harrington, A.G., "Geotechnical Design Considerations for the Gulf Oil Mobile Arctic Caisson, Beaufort Sea", Proceedings, Second Canadian Conference on Marine Geotechnical Engineering, Halifax, Nova Scotia, June 1982, pp. 1-11.
- [108] Fogiel, M. (Director), Handbook of Mathematical Formulas for Mathematicians, Scientists, Engineers, Research and Education Association, New York, 1983, pp. 307-308.
- [109] Rao, S.S., The Finite Element Method in Engineering, Pergamon Press, 1982, pp. 49.

- [110] Przemieniecki, J.S., Theory of Matrix Structural Analysis, McGraw-Hill, 1968, pp. 18-19, 83-85.
- [111] Popov, E.P., Mechanics of Materials (Second Edition), Prentice-Hall, Inc., 1978, pp. 47, 240-243, 263.
- [112] Segerlind, L.J., Applied Finite Element Analysis, John Wiley & Sons, 1976, pp. 377-379.

APPENDIX I

Taylor Series Approximation of
Nodal Displacements

The Taylor series for functions of one variable is presented in many mathematical books [108]. Let "f" be a function that is continuous together with its first "n" derivatives on an integral containing "a" and "x". Then the value of the function at "x" is given by:

$$f(x) = f(a) + f'(a)(x-a) + \frac{f''(a)(x-a)^2}{2!} + \dots + \frac{f^{(n-1)}(a)(x-a)^{n-1}}{(n-1)!} + R_n \quad (I.1)$$

where R_n is the remainder after " n " terms.

For the approximation of nodal displacements by a Taylor series expansion, the following parameter associations are made:

$x = E$, elastic modulus variable

$a = \bar{E}$, mean elastic modulus variable

$f(x) = (U)$, nodal displacement vector

$f(a) = (\bar{U})$, mean nodal displacement vector

$f'(a) = \frac{\partial(U)}{\partial E_i}$, first derivative of displacements w.r.t. element moduli

$f''(a) = \frac{\partial^2(U)}{\partial E_i^2}$, second derivative of displacements, w.r.t. element moduli

$(x-a) = (E_i - \bar{E}_i)$, difference of modulus and mean modulus.

etc.

Substituting into Eq. (I.1), the expression becomes:

$$(U) = (\bar{U}) + \sum_{i=1}^N \frac{\partial(U)}{\partial E_i} (E_i - \bar{E}_i) + \frac{1}{2!} \sum_{i=1}^N \frac{\partial^2(U)}{\partial E_i^2} (E_i - \bar{E}_i)^2 + \dots \quad (I.2)$$

APPENDIX II

Taylor Series Approximation of
Element Stresses

The Taylor series for functions of two variables, $f(x, y)$, is as follows [108]:

$$\begin{aligned}
 f(x, y) = & f(a, b) + (x-a)f_x(a, b) + (y-b)f_y(a, b) \\
 & + \frac{1}{2}((x-a)^2f_{xx}(a, b) + 2(x-a)(y-b)f_{xy}(a, b) \\
 & + (y-b)^2f_{yy}(a, b)) + \dots \quad (\text{II.1})
 \end{aligned}$$

where $f_x(a, b)$, $f_y(a, b)$, $f_{xx}(a, b)$, $f_{yy}(a, b)$, etc. denote partial derivatives with respect to variables x and y evaluated at $x = a$ and $y = b$.

For linearized Taylor series, all second order and higher partial derivatives are neglected. For approximating element stresses of element i by the linearized Taylor series, these parameter associations are assumed:

- $x = E_i$, elastic modulus variable
- $y = (U)_i$, nodal displacement variable vector
- $a = \bar{E}_i$, mean elastic modulus
- $b = \bar{(U)}_i$, mean nodal displacements
(i.e. six nodal displacements for element i with triangular plane strain formulation.)

$$f(x,y) = (S)_i,$$

element stress vector as a function of two random variables, E_i and U_i

$$f(a,b) = (\bar{S})_i,$$

mean element stress vector evaluated at variable means \bar{E}_i and \bar{U}_i

$$f_x(a,b) = \frac{\partial(S)_i}{\partial E_i},$$

first order partial derivative of $(S)_i$ w.r.t. element modulus, E_i

$$f_y(a,b) = \frac{\partial(S)_i}{\partial(U)_i}$$

first order partial derivative of $(S)_i$ w.r.t. nodal displacements, U_i

$$(x-a) = (E_i - \bar{E}_i), \text{ difference of modulus and mean modulus}$$

$$(y-b) = ((U)_i - (\bar{U})_i), \text{ difference of node displacement and mean node displacement}$$

Substituting into Eq. (II.1), the matrix for linearized Taylor series of element stresses becomes:

$$(S)_i = (\bar{S})_i + \frac{\partial(S)_i}{\partial E_i} (E_i - \bar{E}_i) + \frac{\partial(S)_i}{\partial(U)_i} ((U)_i - (\bar{U})_i)$$

(II.2)

APPENDIX III

Main Programs for Stochastic Finite
Element Analysis

The problem applications were analyzed using computer programs developed in FORTRAN language. The main frame VAX 11/780 digital computer at Memorial University of Newfoundland was utilized for the compiling and running of programs. All main programs used for the stochastic finite element analysis are listed below with all subroutines provided in Appendix IV. All programs are self-sufficient and can be executed with the corresponding input data files.

- (1) CAISON.FTN: Analysis of Mobile Arctic Caisson structure and seabed using linear elastic finite element with stochastic material properties
- (2) ELASTC.FTN: Analysis of gravity platform foundation and seabed using linear elastic finite element with stochastic material properties
- (3) ELRAN.D.FTN: Analysis of gravity platform foundation and seabed using linear elastic finite element with random stochastic material properties
- (4) NONLIN.FTN: Analysis of gravity platform foundation and seabed using piecewise linear approximation

soil stress-strain behaviour in elastic finite element with stochastic material properties

- (5) RAND.FTN: Analysis of Mobile Arctic Caisson structure and seabed using linear elastic finite element with random stochastic material properties

```

C*****
C*
C* MAIN PROGRAM CAISON.FTN: MAIN BODY OF THE PROGRAM FOR
C* ANALYSIS OF LINEAR ELASTIC FINITE ELEMENT WITH
C* STOCHASTIC MATERIAL PROPERTIES
C*
C*****
C*
C* THIS PROGRAM (WRITTEN IN THE FORTRAN LANGUAGE) ANALYZES
C* THE SOIL-STRUCTURE INTERACTION OF A MOBILE ARCTIC CAIS-
C* SON RETAINED ISLAND (M.A.C.) AND THE IN-SITU FOUNDATION
C* MATERIAL. A PLANE STRAIN FINITE ELEMENT MODEL IS DEVEL-
C* OPED WITH LINEAR ELASTIC MATERIAL PROPERTIES. MATERIALS
C* ARE TREATED AS STOCHASTIC WITH REFERENCE TO DISTANCE
C* BETWEEN ELEMENT CENTROIDS. THIS PROGRAM EXAMINES THE
C* UNCERTAINTY IN MATERIAL STRENGTH AND THE CORRELATION OF
C* THE MATERIAL PROPERTIES WITH RESPECT TO DISTANCE. ESTI-
C* MATES OF NORMAL AND SHEAR STRESSES OF SELECTED NODES
C* AND ELEMENTS ARE GIVEN. THE PROCEDURE APPROXIMATES THE
C* DISPLACEMENT AND STRESS FUNCTIONS AS THE FIRST TWO
C* TERMS OF A TAYLOR SERIES EXPANSION.
C*
C*****
C*
C* NUMMAT = NUMBER OF LAYERS IN F.E.M. MODEL
C* NUMNP = TOTAL NUMBER OF NODES
C* NUMEL = TOTAL NUMBER OF ELEMENTS
C* X,Y = X & Y COORDINATES FOR NODES (m)
C* ID(I,J) = BOUNDARY CONSTRAINTS FOR NODAL DEGREES OF
C* FREEDOM (D.F.): 0 = FREE
C* 1 = FIXED
C* NC(N,LL) = MEMBER INCIDENCES FOR 'N' WHERE 'LL' EQUALS
C* 1,2 & 3
C* NC(N,4) = LAYER NUMBER FOR ELEMENT 'N'
C* NC(N,5) = MATERIAL CLASSIFICATION FOR ELEMENT 'N':
C* STEEL CAISSON = 1
C* BERM (DEWATERED) = 2
C* BERM (SATURATED) = 3
C* SAND (IN-SITU) = 4
C* NE(I,J) = NUMBER SIGNIFYING A PARTICULAR D.F. AT NODE
C* 'I': J = 1, X-DIRECTION D.F.
C* J = 2, Y-DIRECTION D.F.
C* NF = TOTAL NUMBER OF D.F.
C* EM(I) = MEAN ELASTIC MODULUS OF MATERIAL LAYER 'I'
C* (MPa)
C* PNU(I) = MEAN POISSON'S RATIO OF MATERIAL LAYER 'I'
C* DENS(I) = RATE OF GRAVITY LOADING PER UNIT AREA OF 2-B
C* MODEL FOR LAYER 'I' (MN/m2)
C* JJ = TOTAL NUMBER OF NODES UNDER EXTERNAL LOADS
C* FRI,FR2 = FACTORS TO DETERMINE PORTIONS OF TOTAL LOAD
C* APPLIED: FRI FOR AREA LOADINGS
C* FR2 FOR NODAL LOADINGS
C*****

```

```

***** C*****
C*
C* NN(I)      = NODE NUMBER FOR LOCATION OF EXTERNAL LOADS   *
C* FX(I)       = HORIZONTAL FORCE VECTOR (MN)                   *
C* FY(I)       = VERTICAL FORCE VECTOR (MN)                   *
C* COV        = COEFFICIENT OF VARIATION (C.O.V.) OF MATER-   *
C*            IAL PROPERTIES AS EXPRESSED THROUGH A FIXED      *
C*             PERCENTAGE OF THE ELEMENT MODULI                 *
C* NW          = INTEGER FOR DETERMINING CORRELATION           *
C*             DISTANCE FACTOR                                *
C* NEP         = NUMBER OF NODES CONSIDERED FOR STOCHASTIC    *
C*             DISPLACEMENT ANALYSIS                         *
C* IV(I)        = NODE NUMBERS FOR NODES CONSIDERED FOR STO-   *
C*                 CHASTIC DISPLACEMENT ANALYSIS             *
C* NES         = NUMBER OF ELEMENTS CONSIDERED FOR STOCHASTIC *
C*                 STRESS ANALYSIS                          *
C* IVV(I)      = ELEMENT NUMBERS FOR ELEMENTS CONSIDERED FOR *
C*                 STOCHASTIC STRESS ANALYSIS                *
C* ST(I,J)     = GLOBAL STIFFNESS MATRIX                     *
C*
***** C*****

```

```

DIMENSION ST(538,32), PLOAD(538), X(303), Y(303),
1 ID(315,2), NC(536,4), EM(14), NE(303,2), D(3,3), SK(6,6),
2 XX(3), YY(3), SIGN(3,536), STI(538,32), DFU(538,536)
DIMENSION PNU(14), DENS(14), FX(18), FY(18), VVAR(35,35)
1 , E(536), NN(18), IV(35), U(303,2), IVV(47)
EQUIVALENCE (ST,STI)
K=0
READ(1,*) NUMNP,NUMEL
READ(1,*)(X(I),Y(I),ID(I,1),ID(I,2),I=1,NUMNP)
READ(1,*)(NC(J,1),NC(J,2),NC(J,3),NC(J,4),NC(J,5),
1 J=1,NUMEL)
DO 10 I=1,NUMNP
DO 10 J=1,2
NE(I,J)=0
IF (ID(I,J)) 10,20,10
20 K=K+1
NE(I,J)=K
CONTINUE
WRITE(6,1000) NUMNP,NUMEL
WRITE(6,1030)
WRITE(6,1040) (I,X(I),Y(I),ID(I,1),ID(I,2),
1 I=1,NUMNP)
HF=K
READ(1,*) NUMMAT
READ(1,*)(EM(I),I=1,NUMMAT)
READ(1,*)(PNU(I),I=1,NUMMAT)
READ(1,*)(DENS(I),I=1,NUMMAT)
WRITE(6,1005) NUMMAT
WRITE(6,*)(PNU(I),I=1,NUMMAT)
WRITE(6,1015) NUMMAT
WRITE(6,*)(EM(I),I=1,NUMMAT)
WRITE(6,1035) NUMMAT

```

```

      WRITE(6,*) (DENS(I),I=1,NUMMAT)
      WRITE(6,1045)
      READ(1,*) JJ,FRI1,FR2
      DO 200 II=1,JJ
      READ(1,*) NN(II),FX(II),FY(II)
      WRITE(6,*) NN(II),FX(II),FY(II)
200   CONTINUE
      WRITE(6,1025)
      DO 50 N=1,NUMEL
      WRITE(6,*) N,(NC(N,J),J=1,4)
50    CONTINUE
      READ(1,*) CDM,NW
      READ(1,*) NEP,(IV(I),I=1,NEP)
      READ(1,*) NES,(IVV(I),I=1,NES)
      MB=0
      DO 5 I=1,NF
      DO 5 J=1,32
5     ST(I,J)=0.0
      DO 100 N=1,NUMEL
      DO 150 LL=1,3
      XX(LL)=X(NC(N,LL))
      YY(LL)=Y(NC(N,LL))
150   CONTINUE
      MT=NC(N,4)
      PR=PNU(MT)
      EEX=EM(MT)
      E(N)=EEX
      CALL DMAT(PR,D)
      CALL ELST(SK,XX,YY,EEX,D)
      CALL ASMB(ST,SK,N,NC,NE,MB)
100   CONTINUE
      CALL SYMBOL(1,ST,PLOAD,NF,MB,538)
      WRITE(6,1070) MB
      CALL LOAD(NE,PLOAD,NUMEL,X,Y,NC,DENS,JJ,NN,FX,FY,
1     FRI,FR2)
      CALL SYMBOL(2,ST,PLOAD,NF,MB,538)
      CALL RDIS(PLOAD,D,SIGN,NUMEL,NUMNP,NE,NC,X,Y,EM,PNU,
1     E,U)
      CALL DUWH(D,DFU,STI,PLOAD,X,Y,PNU,NE,NC,NUMEL,NF,MB)
      CALL DCOV2(E,PNU,DFU,PLOAD,NUMEL,X,Y,NUMNP,NC,NE,NEP
1     ,IV,NES,IVV,COV,NW,U,SIGN)
1000  FORMAT(//', NO. OF NODAL POINTS ',I3,' NO. OF ELEM
1     ENTS ',I3 '/')
1005  FORMAT(//',3X,'POISSONS RATIO (MATERIAL 1 TO',I3,')
1     ,/')
1015  FORMAT(//',3X,'MODULUS OF ELASTICITY (MATERIAL 1 TO'
1     ,I3,')
1025  FORMAT(//',4X,' ELEM. NO.           MEMBER INCIDENCES
1     (I,J,K)           MATERIAL NO. ',/)
1030  FORMAT(//2(2X,'NODE',6X,'CO-ORDINATES',5X,'BD.
1     CONSTRTS.'))/2(3X,'NO.',10X,'X',5X,'Y',9X,'X',5X,'Y'
2     ,3X)/1X,2(1X,6(1H*),5X,14(1H*),3X,15(1H*))/)
1035  FORMAT(//',3X,'SUBMERGED WEIGHT (MATERIAL 1 TO',I3,
1     ),'/)

```

```
1040 FORMAT(2(3X,13,6X,2(F6.1,1X),6X,1X,5X,11+3X))  
1045 FORMAT(///,6X,'NODE NO. X-LOAD Y-LOAD',/)  
1070 FORMAT(///,' BANDWIDTH = ',13,/)  
STOP  
END.
```

```

C*****
C*
C* MAIN PROGRAM ELASTC.FTN: MAIN BODY OF THE PROGRAM FOR *
C* ANALYSIS OF LINEAR ELASTIC FINITE ELEMENT WITH *
C* STOCHASTIC MATERIAL PROPERTIES
C*
C*****
C*
C* THIS PROGRAM (WRITTEN IN THE FORTRAN LANGUAGE) ANALYZES *
C* AN OFFSHORE TANK FOUNDATION AND SOIL INTERACTION USING *
C* A PLANE STRAIN FINITE ELEMENT MODEL. THE ANALYSIS USES *
C* A LINEAR ELASTIC SOIL MODEL WITH STOCHASTIC MATERIAL *
C* PROPERTIES. THE STOCHASTIC ANALYSIS IS WITH REFERENCE *
C* TO DISTANCE BETWEEN ELEMENT CENTROIDS. THIS PROGRAM EX- *
C* AMINES THE UNCERTAINTY IN SOIL STRENGTH AND THE CORRE- *
C* LATION OF THE SOIL PROPERTIES WITH RESPECT TO DISTANCE. *
C* ESTIMATES OF THE COVARIANCE OF DISPLACEMENTS AND VAR- *
C* IANCES OF NORMAL AND SHEAR STRESSES OF SELECTED NODES *
C* AND ELEMENTS ARE GIVEN. THE PROCEDURE APPROXIMATES THE *
C* DISPLACEMENT AND STRESS FUNCTIONS AS THE FIRST TWO *
C* TERMS OF A TAYLOR SERIES EXPANSION.
C*
C*****
C*
C* NUMMAT = NUMBER OF LAYERS IN F.E.M. MODEL
C* NE(I,J) = NUMBER SIGNIFYING A PARTICULAR DEGREE OF:
C*           FREEDOM (D.F.) AT NODE 'I':
C*           J = 1, X-DIRECTION D.F.
C*           J = 2, Y-DIRECTION D.F.
C*
C* NUMNP = TOTAL NUMBER OF NODES
C* NUMEL = TOTAL NUMBER OF ELEMENTS
C* NF = TOTAL NUMBER OF D.F.
C* ID(I,1) = HORIZONTAL BOUNDARY CONSTRAINT FOR NODE 'I':
C*           ID = 0, FREE
C*           ID = 1, FIXED
C* ID(I,2) = VERTICAL BOUNDARY CONSTRAINT FOR NODE 'I':
C*           ID = 0, FREE
C*           ID = 1, FIXED
C* EM(I) = MEAN ELASTIC MODULUS OF MATERIAL LAYER 'I'
C*          (MPa)
C* PNU(I) = MEAN POISSON'S RATIO OF MATERIAL LAYER 'I'
C* DENS(I) = RATE OF GRAVITY LOADING PER UNIT AREA OF 2-D
C*           MODEL FOR LAYER 'I' (MN/sq.m)
C* JJ = TOTAL NUMBER OF NODES UNDER EXTERNAL LOADS
C* FR1,FR2 = FACTORS TO DETERMINE PORTIONS OF TOTAL LOAD
C*           APPLIED: FR1-FOR AREA LOADINGS
C*           FR2-FOR NODAL LOADINGS
C* NN(II) = NODE NUMBER FOR LOCATION OF EXTERNAL LOADS
C* FX(II) = HORIZONTAL FORCE VECTOR (MN)
C* FY(II) = VERTICAL FORCE VECTOR (MN)
C*
C*****

```

```

*****
C*
C* COV   - COEFFICIENT OF VARIATION (C.O.V.) OF MATERIAL PROPERTIES AS EXPRESSED THROUGH A FIXED
C*       PERCENTAGE OF THE ELEMENT MODULI
C* NW    - INTEGER FOR DETERMINING CORRELATION DISTANCE FACTOR
C* NNP   - NUMBER OF NODES CONSIDERED FOR STOCHASTIC DISPLACEMENT ANALYSIS
C* IV(I) - NODE NUMBERS FOR NODES CONSIDERED FOR STOCHASTIC DISPLACEMENT ANALYSIS
C* NES   - NUMBER OF ELEMENTS CONSIDERED FOR STOCHASTIC STRESS ANALYSIS
C*       IVV(I) - ELEMENT NUMBERS FOR ELEMENTS CONSIDERED FOR STOCHASTIC STRESS ANALYSIS
C* NC(N,LL) - MEMBER INCIDENCES FOR 'N' WHERE 'LL' EQUALS 1, 2 & 3
C* NC(N,4)  - LAYER NUMBER FOR ELEMENT 'N'
C* ST(I,J)  - GLOBAL STIFFNESS MATRIX
C* X,Y    - X & Y COORDINATES FOR NODES (m)
C*
*****

```

```

DIMENSION ST(538,32),PLOAD(538),X(303),Y(303),
1  NC(536,5),EM(14),NE(303,2),D(3,3),SK(6,6),XX(3),
2  ID(315,2),YY(3)
DIMENSION SIGM(3,536),STI(538,32),DFU(538,536),
1  PNU(14),DENS(14),FX(18),FY(18),VVAR(35,35)
DIMENSION E(536),NN(18),IV(35),U(303,2),IVV(47)
EQUIVALENCE (ST,STI)
K=0
READ (1,*) NUMMAT
CALL GGEN(X,Y,ID,NC,NUMNP,NUMEL)
DO 10 I=1,NUMNP
DO 10 J=1,2
NE(I,J)=0
IF (ID(I,J)) 10,20,10
20 K=K+1
NE(I,J)=K
CONTINUE
WRITE(6,1000) NUMNE,NUMEL,NUMMAT
WRITE(6,1030)
WRITE(6,1040) (I,X(I),Y(I),ID(I,1),ID(I,2),I=1,
1  NUMNP)
NF=K
READ(1,*) (EM(I),I=1,NUMMAT)
READ(1,*)(PNU(I),I=1,NUMMAT)
READ(1,*)(DENS(I),I=1,NUMMAT)
WRITE(6,1005) NUMMAT
WRITE(6,*)(PNU(I),I=1,NUMMAT)
WRITE(6,1015) NUMMAT
WRITE(6,*)(EM(I),I=1,NUMMAT)
WRITE(6,1035) NUMMAT
WRITE(6,*)(DENS(I),I=1,NUMMAT)

```

```

      WRITE(6,1045)
      READ(1,*) JJ,FR1,FR2
      DO 200 II=1,3J
      READ(1,*) NN(II),FX(II),FY(II)
      WRITE(6,*) NN(II),FX(II),FY(II)
200   CONTINUE
      WRITE(6,1025)
      DO 50 N=1,NUMEL
      WRITE(6,*) N,(NC(N,J),J=1,5)
50    CONTINUE
      READ(1,*) COV,NW
      READ(1,*) NEP,(IV(I),I=1,NEP)
      READ(1,*) NES,(IVV(I),I=1,NES)
      MB=0
C***** INITIATE GLOBAL STIFFNESS MATRIX TO ZERO *****
      DO 5 I=1,NF
      DO 5 J=1,32
5     ST(I,J)=0.0
      DO 100 N=1,NUMEL
      DO 150 LL=1,3
      XX(LL)=X(NC(N,LL))
      YY(LL)=Y(NC(N,LL))
100   CONTINUE
      HT=NC(N,4)
      PR=PNU(HT)
      EEX=EH(HT)
      E(N)=EEX
      CALL DHAT(PR,D)
      CALL ELST(SK,XX,YY,EEX,D)
      CALL ASMB(ST,SK,N,NC,NE,MB)
150   CONTINUE
      CALL SYMBOL(1,ST,PLOAD,NF,MB,538)
      WRITE(6,1070) MB
      CALL LOAD(NE,PLOAD,NUMEL,X,Y,NC,DENS,JJ,NN,FX,FY,
1     FR1,FR2)
      CALL SYMBOL(2,ST,PLOAD,NF,MB,538)
      CALL RDIS(PLOAD,D,SIGN,NUMEL,NUMNP,NE,NC,X,Y,EH,PNU,
1     E,U)
      CALL DDM(D,DFU,STL,PLOAD,X,Y,PNU,NE,NC,NUMEL,NF,MB)
      CALL DCOV1(E,PNU,DFU,PLOAD,NUMEL,X,Y,NUMNP,NC,NE,NEP
1     ,IV,NES,IVV,COV,NW,U,SIGN)
1000  FORMAT(//,' NO. OF NODAL POINTS = ',I3)
1     ' NO. OF ELEMENTS = ',I3/
2     ' NO. OF LAYERS (SOIL/FOUNDATION) = ',I3)
1005  FORMAT(//,3X,'POISONS RATIO (LAYERS 1 TO ',I3,')',/)
1015  FORMAT(//,3X,'MODULUS OF ELASTICITY (LAYERS 1 TO ',
1     I3,')',/)
1025  FORMAT(//,4X,' ELEM. NO. MEMBER INCIDENCES
1     (I,J,K), LAYER NO. SOIL CLASS',/)
1030  FORMAT(//2(2X,'NODE',6X,'CO-ORDINATES',5X,
1     'BD. CONSTRTS.')/2(3X,'NO.',10X,'X',5X,'Y',9X,'X',5X
2     , 'Y',3X)/1X,2(1X,4(1H*),5X,14(1H*),3X,15(1H*))//)
1035  FORMAT(//,3X,'SUBMERGED SOIL DENSITY (LAYERS 1 TO ',
1     I3,')',/)

```

```
1040      FORMAT(2(3X,I3,6X,2(F6.2,1X),X,11,5X,11,3X))  
1045      FORMAT(////,6I,'NODE NO. X-LOAD Y-LOAD',/)-  
1070      FORMAT(////,' BANDWIDTH ',I3,/)  
        STOP  
        END
```

```

C*****MAIN PROGRAM ERLAND.FTN: MAIN BODY OF THE PROGRAM FOR
C*      ANALYSIS OF LINEAR ELASTIC FINITE ELEMENT WITH
C*      STOCHASTIC MATERIAL PROPERTIES
C*
C*****THIS PROGRAM (WRITTEN IN THE FORTRAN LANGUAGE) ANALYZES
C*      AN OFFSHORE TANK FOUNDATION AND SOIL INTERACTION USING
C*      A PLANE STRAIN FINITE ELEMENT MODEL. THE ANALYSIS USES
C*      A LINEAR ELASTIC SOIL MODEL WITH STOCHASTIC MATERIAL
C*      PROPERTIES. THE STOCHASTIC ANALYSIS IS WITH REFERENCE
C*      TO DISTANCE BETWEEN ELEMENT CENTROIDS. THIS PROGRAM EX-
C*      AMINES THE UNCERTAINTY IN SOIL STRENGTH AND THE CORRE-
C*      LATION OF THE SOIL PROPERTIES WITH RESPECT TO DISTANCE.
C*      ESTIMATES OF THE COVARIANCE OF DISPLACEMENTS AND VAR-
C*      IANCES OF NORMAL AND SHEAR STRESSES OF SELECTED NODES
C*      AND ELEMENTS ARE GIVEN. THE PROCEDURE APPROXIMATES THE
C*      DISPLACEMENT AND STRESS FUNCTIONS AS THE FIRST TWO
C*      TERMS OF A TAYLOR SERIES EXPANSION. THIS PROGRAM WILL
C*      GENERATE A RANDOM STOCHASTIC ANALYSIS OF DISPLACEMENTS
C*      AND STRESSES.
C*
C*****RR(I)      - OUTPUT VECTOR OF PSEUDO-RANDOM UNIFORM
C*      DEVIATES WITH VALUES BETWEEN ZERO & ONE FOR
C*      EACH ELEMENT 'I'.
C*      NUMMAT      - NUMBER OF LAYERS IN F.E.M. MODEL
C*      NE(I,J)      - NUMBER SIGNIFYING A PARTICULAR DEGREE OF
C*      FREEDOM (D.F.) AT NODE 'I';
C*          J = 1, X-DIRECTION D.F.
C*          J = 2, Y-DIRECTION D.F.
C*      NUMNP       - TOTAL NUMBER OF NODES
C*      NUMEL       - TOTAL NUMBER OF ELEMENTS
C*      NF          - TOTAL NUMBER OF D.F.
C*      ID(I,1)     - HORIZONTAL BOUNDARY CONSTRAINT FOR NODE 'I':
C*          ID = 0, FREE
C*          ID = 1, FIXED
C*      ID(I,2)     - VERTICAL BOUNDARY CONSTRAINT FOR NODE 'I':
C*          ID = 0, FREE
C*          ID = 1, FIXED
C*      EM(I)       - MEAN ELASTIC MODULUS OF MATERIAL LAYER 'I'
C*          (MPa)
C*      PNU(I)      - MEAN POISSON'S RATIO OF MATERIAL LAYER 'I'
C*      DENS(I)     - RATE OF GRAVITY LOADING PER UNIT AREA OF 2-D
C*          MODEL FOR LAYER 'I' (MN/sq.m)
C*      JJ          - TOTAL NUMBER OF NODES UNDER EXTERNAL LOADS
C*      FR1,FR2    - FACTORS TO DETERMINE PORTIONS OF TOTAL LOAD
C*          APPLIED: FR1 FOR AREA LOADINGS
C*          FR2 FOR NODAL LOADINGS
C*
C*****

```

```
*****
C*
C* NN(II) = NODE NUMBER FOR LOCATION OF EXTERNAL LOADS *
C* FX(II) = HORIZONTAL FORCE VECTOR (MN) *
C* FY(II) = VERTICAL FORCE VECTOR (MN) *
C* COV = COEFFICIENT OF VARIATION (C.O.V.) OF MATER- *
C* IAL PROPERTIES AS EXPRESSED THROUGH A FIXED *
C* PERCENTAGE OF THE ELEMENT MODULI *
C* NW = INTEGER FOR DETERMINING CORRELATION *
C* DISTANCE FACTOR *
C* NEP = NUMBER OF NODES CONSIDERED FOR STOCHASTIC *
C* DISPLACEMENT ANALYSIS *
C* IV(I) = NODE NUMBERS FOR NODES CONSIDERED FOR STO- *
C* CHASTIC DISPLACEMENT ANALYSIS *
C* NES = NUMBER OF ELEMENTS CONSIDERED FOR STOCHASTIC *
C* STRESS ANALYSIS *
C* IVV(I) = ELEMENT NUMBERS FOR ELEMENTS CONSIDERED FOR *
C* STOCHASTIC STRESS ANALYSIS *
C* NC(N,LL) = MEMBER INCIDENCES FOR 'N' WHERE 'LL' EQUALS *
C* 1, 2 & 3 *
C* NC(N,4) = LAYER NUMBER FOR ELEMENT 'N' *
C* ST(I,J) = GLOBAL STIFFNESS MATRIX *
C* X,Y = X & Y COORDINATES FOR NODES (m) *
C*
*****
```

```
DIMENSION ST(538,32),PLOAD(538),X(303),Y(303),
1 NC(536,5),EM(14),NE(303,2),D(3,3),SK(6,6),XX(3),
2 LD(315,2),YY(3)
DIMENSION SIGM(3,536),STI(538,32),DFU(538,536),
1 PNU(14),DENS(14),FX(18),FY(18),VVAR(35,35)
DIMENSION E(536),NN(18),IV(35),U(303,2),IVV(47)
EQUIVALENCE (ST,STI)
REAL RR(536)
K=0
READ (1,*) NUMMAT
CALL GGEN(X,Y,LD,NC,NUMNP,NUMEL)
DO 10 I=1,NUMNP
DO 10 J=1,2
NE(I,J)=0
10 IF (LD(I,J)) 10,20,10
K=K+1
NE(I,J)=K
CONTINUE
WRITE(6,1000) NUMNP,NUMEL,NUMMAT
WRITE(6,1030)
1 WRITE(6,1040) (I,X(I),Y(I),ID(I,1),ID(I,2),I=1,
NUMNP)
NF=K
READ(1,*) (EM(I),I=1,NUMMAT)
READ(1,*)(PNU(I),I=1,NUMMAT)
READ(1,*)(DENS(I),I=1,NUMMAT)
WRITE(6,1005) NUMMAT
WRITE(6,*)(PNU(I),I=1,NUMMAT)
```

```

      WRITE(6,1015) NUMMAT
      WRITE(6,*)(EM(I),I=1,NUMMAT)
      WRITE(6,1035) NUMMAT
      WRITE(6,*)(DENS(I),I=1,NUMMAT)
      WRITE(6,1045)
      READ(1,*) JJ,FR1,FR2
      DO 200 II=1,JJ
      READ(1,*) NN(II),FX(II),FY(II)
      WRITE(6,*) NN(II),FX(II),FY(II)
200   CONTINUE
      WRITE(6,1025)
      DO 50 N=1,NUMEL
      WRITE(6,*)N,(NC(N,J),J=1,5)
50    CONTINUE
      READ(1,*) COV,NW
      READ(1,*) NEP,(IV(I),I=1,NEP)
      READ(1,*) NES,(IVV(I),I=1,NES)
      MB=0
C***** INITIALIZE GLOBAL STIFFNESS MATRIX TO ZERO *****
      DO 5   I=1,NF
      DO 5   J=1,32
5     ST(I,J)=0.0
      DO 100 N=1,NUMEL
      DO 150 LL=1,3
      XX(LL)=X(NC(N,LL))
      YY(LL)=Y(NC(N,LL))
150   CONTINUE
      MT=NC(N,4)
      PR=PNU(MT)
      EEX=EM(MT)
      E(N)=EEX
      CALL DMAT(PR,D)
      CALL ELST(SK,XX,YY,EEX,D)
      CALL ASHB(ST,SK,N,NC,NE,MB)
100   CONTINUE
      CALL SYMBOL(1,ST,PLOAD,NF,MB,538)
      WRITE(6,1070) MB
      CALL LOAD(NE,PLOAD,NUMEL,X,Y,NC,DENS,JJ,NN,FX,FY,
1     ,FR1,FR2)
      CALL SYMBOL(2,ST,PLOAD,NF,MB,538)
      CALL RDLS(PLOAD,D,SIGM,NUMEL,NUMNP,NE,NC,X,Y,EM,PNU,
1     ,E,U)
      CALL DUWH(D,DFU,ST,PLOAD,X,Y,PNU,NE,NC,NUMEL,NF,MB)
      CALL DCOV4(E,PNU,DFU,PLOAD,NUMEL,X,Y,NUMNP,NC,NE,NEP
1     ,IV,NES,IVV,COV,NW,U,SIGM)
1000  FORMAT(//,' NO. OF NODAL POINTS ',I3/
1     , ' NO. OF ELEMENTS ',I3/
2     , ' NO. OF LAYERS (SOIL/FOUNDATION) ',I3)
1005  FORMAT(//,3X,'POISONS RATIO (LAYERS 1 TO ',I3,')',/)
1015  FORMAT(//,3X,'MODULUS OF ELASTICITY (LAYERS 1 TO '
1     ,I3,')',/)
1025  FORMAT(//,4X,' ELEM. NO. MEMBER INCIDENCES
1     ,(I,J,K), ' LAYER NO. SOIL CLASS',/)


```

```
1030 FORMAT(//2(2X,'NODE',6X,'CO-ORDINATES',5X,  
1 'BD. CONSTRTS.')/2(3X,'NO.',10X,'X',5X,'Y',9X,'X',5X  
2 , 'Y',3X)/1X,2(1X,4(1H*),5X,14(1H*),3X,15(1H*))7//)  
1035 FORMAT(///,3X,'SUBMERGED SOIL DENSITY (LAYERS 1 TO',  
1 13,':')/  
1040 FORMAT(2(3X,13,6X,2(F6.2,1X),6X,11,5X,11,3X))  
1045 FORMAT(////,6X,'NODE NO. X-LOAD Y-LOAD',/)  
1070 FORMAT(////,' BANDWIDTH -',13,/) STOP  
END
```

C*****
C*
C* MAIN PROGRAM NONLIN.FTN: MAIN BODY OF THE PROGRAM FOR *
C* ANALYSIS OR PIECEWISE LINEAR ELASTIC FINITE ELEMENT *
C* WITH STOCHASTIC MATERIAL PROPERTIES
C*
C*****
C*
C* THIS MAIN PROGRAM (WRITTEN IN THE FORTRAN LANGUAGE) AN- *
C* ALYZES AN OFFSHORE TANK FOUNDATION AND SOIL INTERACTION *
C* USING A PLANE STRAIN FINITE ELEMENT MODEL. THE ANALYSIS *
C* USES A NONLINEAR ELASTIC SOIL MODEL, WHEREBY PIECEWISE *
C* LINEAR APPROXIMATIONS OF ELASTIC MODULI FOR BOTH SAND & *
C* CLAY SOILS ARE IMPLEMENTED. THE F.E.M. MODEL INCLUDES A *
C* STOCHASTIC MATERIAL PROPERTIES, WHEREIN THE STOCHASTIC *
C* ANALYSIS IS WITH REFERENCE TO DISTANCE BETWEEN ELEMENT *
C* CENTROIDS. THIS PROGRAM EXAMINES UNCERTAINTY IN SOIL *
C* STRENGTH AND CORRELATION OF SOIL PROPERTIES WITH RE- *
C* SPECT TO DISTANCE. ESTIMATES OF THE COVARIANCE OF DIS- *
C* PLACEMENTS AND VARIANCES OF NORMAL AND SHEAR STRESSES *
C* OF SELECTED NODES AND ELEMENTS ARE GIVEN. THE PROCEDURE *
C* APPROXIMATES THE DISPLACEMENT AND STRESS FUNCTIONS AS *
C* THE FIRST TWO TERMS OF A TAYLOR SERIES EXPANSION. THE *
C* LOAD IS SPLIT INTO SEVERAL EQUAL LOADING STAGES. FOR *
C* EACH LOAD STAGE, THE ANALYSIS HAS TO REPEAT THROUGH A *
C* NUMBER OF ITERATIONS UNTIL THE ELASTIC MODULI FOR THE *
C* ELEMENTS HAVE CONVERGED TO VALUES OF LESS THAN 5.0 PER- *
C* CENT DIFFERENCE. ONCE THE CONVERGED MODULI ARE OBTAINED, *
C* THE STOCHASTIC ANALYSIS IS APPLIED. FOR EACH LOAD STAGE, *
C* THIS IS REPEATED UNTIL THE TOTAL LOAD IS APPLIED. TO *
C* DETERMINE THE NET EFFECT ON THE COVARIANCE OF DISPLA- *
C* MENTS AND VARIANCE OF STRESSES, THE RESULTS OF EACH *
C* LOAD STAGE ARE ADDED TOGETHER ASSUMING STATISTICAL IN- *
C* DEPENDENCE BETWEEN LOAD STAGES.
C*
C* THE LATTER SECTIONS DETERMINE THE COEFFICIENT OF VARIA- *
C* CION OF VERTICAL DISPLACEMENTS AND STRESSES (HORIZONTAL, *
C* VERTICAL & SHEAR) BY CALCULATING THE RATIO OF STANDARD *
C* DEVIATION (SQUARE ROOT OF VARIANCE) TO MEAN VERTICAL *
C* DISPLACEMENT OR STRESS (USING MEAN ELASTIC MODULI).
C*
C*****
C*
C* NUMMAT = NUMBER OF LAYERS IN F.E.M. MODEL
C* NE(I,J) = NUMBER SIGNIFYING A PARTICULAR DEGREE OF *
C* FREEDOM (D.F.) AT NODE 'I':
C* J = 1, X-DIRECTION D.F.
C* J = 2, Y-DIRECTION D.F.
C*
C* NUMNP = TOTAL NUMBER OF NODES
C* NUMEL = TOTAL NUMBER OF ELEMENTS
C* X,Y = X & Y COORDINATES FOR NODES (m)
C*

```

*****
C*
C* ID(I,1)      - HORIZONTAL BOUNDARY CONSTRAINTS FOR NODAL   *
C*                   D.F.:          ID = 0, FREE           *
C*                               ID = 1, FIXED        *
C*
C* ID(I,2)      - VERTICAL BOUNDARY CONSTRAINTS FOR NODAL   *
C*                   D.F.:          ID = 0, FREE           *
C*                               ID = 1, FIXED        *
C*
C* NF           - TOTAL NUMBER OF D.F.                      *
C* EM(I)         - MEAN ELASTIC MODULUS OF MATERIAL LAYER 'I'   *
C*                   (MPa)                         *
C* PNU(I)        - MEAN POISSON'S RATIO OF MATERIAL LAYER 'I'   *
C* DENS(I)       - RATE OF GRAVITY. LOADING PER UNIT AREA OF   *
C*                   2-D MODEL FOR LAYER 'I' (MN/sq.m)    *
C* JJ            - TOTAL NUMBER OF NODES UNDER EXTERNAL LOADS   *
C* FR1,FR2      - FACTORS TO DETERMINE PORTIONS OF TOTAL   *
C*                   LOAD APPLIED:     FR1 FOR AREA LOADINGS   *
C*                               FR2 FOR NODAL LOADINGS   *
C*
C* NN(II)        - NODE NUMBER FOR LOCATION OF EXTERNAL LOADS   *
C* FX(II)        - HORIZONTAL FORCE VECTOR DUE TO WAVE (MN)   *
C* FY(II)        - VERTICAL FORCE VECTOR DUE TO WAVE (MN)   *
C* FXG(II)       - HORIZONTAL FORCE VECTOR DUE TO GRAVITY (MN)  *
C* FYG(II)       - VERTICAL FORCE VECTOR DUE TO GRAVITY (MN)  *
C* NC(N,J)       - MEMBER INCIDENCES FOR 'N' WHERE 'J' EQUALS   *
C*                   1, Z, & 3
C* NC(N,4)       - LAYER NUMBER FOR ELEMENT 'N'
C* NC(N,5)       - MATERIAL CLASSIFICATION: CONCRETE = 0
C*                   SAND = 1
C*                   CLAY = 2
C*
C* COV          - COEFFICIENT OF VARIATION (C.O.V.) OF MAT-   *
C*                   ERIAL PROPERTIES EXPRESSED AS A FIXED   *
C*                   PERCENTAGE OF THE ELEMENT MODULI   *
C*
C* NW            - INTEGER FOR DETERMINING CORRELATION   *
C*                   DISTANCE FACTOR
C*
C* NEP          - NUMBER OF NODES CONSIDERED FOR STOCHASTIC   *
C*                   DISPLACEMENT ANALYSIS
C*
C* IV(I)         - NODE NUMBERS FOR NODES CONSIDERED FOR   *
C*                   STOCHASTIC DISPLACEMENT ANALYSIS
C*
C* NES          - NUMBER OF ELEMENTS CONSIDERED FOR   *
C*                   STOCHASTIC STRESS ANALYSIS
C*
C* Ivv(I)        - ELEMENT NUMBERS FOR ELEMENTS CONSIDERED   *
C*                   FOR STOCHASTIC STRESS ANALYSIS
C*
C* NL            - ITERATION NUMBER FOR PIECEWISE LINEAR   *
C*                   ANALYSIS
C*
C* L(I)          - VECTOR TO DETERMINE WHEN MODULUS OF   *
C*                   ELEMENT 'I' HAS CONVERGED DURING EACH   *
C*                   LOADING STAGE:      L = 0, UNCONVERGED   *
C*                               L = 1, CONVERGED
C*
C* ST(I,J)        - GLOBAL STIFFNESS MATRIX
C* PLOAD(K)      - NODAL DISPLACEMENT VECTOR FOR LOAD STEP (m)
C* TLOAD(K)      - TOTAL NODAL DISPLACEMENT VECTOR (m)
C*
*****

```

```

C*****
C* SIGN(1,MM) = HORIZONTAL STRESS (MPa) FOR LOAD STEP
C* SIGN(2,MM) = VERTICAL STRESS (MPa) FOR LOAD STEP
C* SIGN(3,MM) = SHEAR STRESS (MPa) FOR LOAD STEP
C* TPS1(MM) = TOTAL HORIZONTAL STRESS (MPa)
C* TPS2(MM) = TOTAL VERTICAL STRESS (MPa)
C* SHEAR(MM) = TOTAL SHEAR STRESS (MPa)
C* VVAR(I,J) = COVARIANCE OF DISPLACEMENT MATRIX FOR LOAD
C* STEP
C* TVVAR(I,J) = TOTAL COVARIANCE OF DISPLACEMENT MATRIX
C* VARS(I,J) = VARIANCE OF STRESS MATRIX FOR LOAD STEP
C* TVARS(I,J) = TOTAL VARIANCE OF STRESS MATRIX
C* QCov = C.O.V. OF VERTICAL DISPLACEMENT
C* = RATIO OF STANDARD DEVIATION TO MEAN TOTAL
C* DISPLACEMENT
C* RCOV = C.O.V. OF STRESS
C* = RATIO OF STANDARD DEVIATION TO MEAN TOTAL
C* STRESS
C*
C*****

```

```

1 DIMENSION ST(538,32),PLOAD(538),X(303),Y(303),
2 ID(315,2),NC(536,5),EM(14),NE(303,2),D(3,3),SK(6,6)
2 ,XX(3),YY(3),SIGM(3,536),STI(538,32),DFU(538,536),
3 TVARS(47,3),PNUM(14),DENS(14),FX(18),FY(18)
4 DIMENSION PSL(536),PS2(536),GAMMA(536),TVVAR(47,47);
4 VVAR(47,47),VARS(47,3),FXG(18),FYG(18),EE(536),NN(18)
4 ,L(536),RATIO(536),EPS1(536),EPS2(536),EE(536),
4 GAH(536),STRAIN(536),TLOAD(538),IV(47),U(303,2)
4 DIMENSION TPS1(536),TPS2(536),SHEAR(536),IVV(47)
4 EQUIVALENCE (ST,ST1)
4 K=0
4 LH=0
4 READ (1,*) NUMMAT
4 CALL GGEN(X,Y,ID,NC,NUMNP,NUMEL)
4 DO 10 L=1,NUMNP
4 DO 10 J=1,2
4 NE(I,J)=0
4 IF (ID(I,J)) 10,20,10
4
20 K=K+1
4 NE(I,J)=K
4 CONTINUE
4 WRITE(6,1000) NUMNP,NUMEL,NUMMAT
4 WRITE(6,1030)
4 WRITE(6,1040) (I,X(I),Y(I),ID(I,1),ID(I,2),I=1,
1 NUMNP)
4 NF=K
C***** INPUT MEAN MATERIAL PROPERTIES *****
4 READ(1,*) (EM(I),I=1,NUMMAT)
4 READ(1,*)(PNU(I),I=1,NUMMAT)
C***** INPUT AREA LOADINGS *****
4 READ(1,*)(DENS(I),I=1,NUMMAT)
4 WRITE(6,1005) NUMMAT

```

```

      WRITE(6,*)(PNU(I),I=1,NUMMAT)
      WRITE(6,1015) NUMMAT
      WRITE(6,*)(EM(I),I=1,NUMMAT)
      WRITE(6,1035) NUMMAT
      WRITE(6,*)(DENS(I),I=1,NUMMAT)
      WRITE(6,1045)

C***** INPUT NODAL LOADINGS (EXTERNAL) *****
      READ(1,*) JJ,PR1,FR2
      DO 200 II=1,JJ
      READ(1,*) NN(II),FX(II),FY(II),FXG(II),FYG(II)
      WRITE(6,*)(NN(II),FX(II),FY(II),FXG(II),FYG(II))

200    CONTINUE
      WRITE(6,1025)
      DO 50 N=1,NUMEL
      WRITE(6,*)(NC(N,J),J=1,5)
50     CONTINUE

C***** INPUT INFORMATION FOR STOCHASTIC ANALYSIS *****
      READ(1,*) COV,NW
      READ(1,*) NEP,(IV(I),I=1,NEP)
      READ(1,*) NES,(IVV(I),I=1,NES)

C***** INITIALIZE VARIABLES TO ZERO *****
      MB=0
      DO 75 I=1,NUMEL
      STRAIN(I)=0.0
      TPS1(I)=0.0
      TPS2(I)=0.0
      L(I)=0
      CONTINUE
      DO 80 I=1,NUMNP
      DO 80 J=1,2
      K=NE(I,J)
      TLOAD(K)=0.0
      DO 85 I=1,NEP
      DO 85 J=1,NEP
85     TVVAR(I,J)=0.0
      DO 90 I=1,NES
      DO 90 J=1,3
90     TVARS(I,J)=0.0

C***** START OF ITERATION STAGE *****
      DO 500 NI=1,32
      WRITE(6,1500) NI

C***** STIFFNESS MATRIX MUST BE RESET TO ZERO *****
C     FOR EACH ITERATION
      DO 5   I=1,NF
      DO 5   J=1,32
5       ST(I,J)=0.0
      DO 100  N=1,NUMEL
      DO 150  LL=1,3
      XX(LL)=X(NC(N,LL))
      YY(LL)=Y(NC(N,LL))

150    CONTINUE
      MT=NC(N,4)
      PR=PNU(MT)
      IF (NI.NE.1) GOTO 250

```

```

EEX-EM(MT)
GOTO 300
250 EEX-E(N)
300 CONTINUE
CALL DMAT(PR,D)
CALL ELST(SK,XX,YY,EEX,D)
CALL ASMB(ST,SK,N,NC,NE,MB)
CONTINUE
CALL SYMBOL(1,ST,PLOAD,NF,MB,538)
WRITE(6,1070) MB
CALL LOADD(NE,PLOAD,NUMEL,X,Y,NC,DENS,NI,JJ,NN,FX,FY
1 ,FRI,FR2,FXG,FYG)
CALL SYMBOL(2,ST,PLOAD,NF,MB,538)
CALL RRDIS(PLOAD,D,SIGM,NUMEL,NUMNP,NE,NC,X,Y,EM,PNU
1 ,PS1,PS2,NI,E)
C***** FOR LAST ITERATION OMIT 'NLIN' SUBROUTINE *****
IF(NI.EQ.32) GOTO 400
CALL NLIN(PS1,PS2,NUMEL,EM,PNU,E,NC,NI,L,RATIO,EE,
1 GAM,STRAIN,LL)
400 CONTINUE
C***** ESTABLISHING ITERATION NUMBERS FOR ADVANCING *****
C TO NEXT LOAD STAGE
IF (NI.EQ.6) GOTO 450
IF (NI.EQ.10) GOTO 450
IF (NI.EQ.14) GOTO 450
IF (NI.EQ.18) GOTO 450
IF (NI.EQ.21) GOTO 450
IF (NI.EQ.25) GOTO 450
IF (NI.EQ.28) GOTO 450
IF (NI.EQ.32) GOTO 450
GOTO 500
450 CONTINUE
LL=0
DO 130 I=1,NUMNP
DO 130 J=1,2
K=NE(I,J)
C***** ACCUMULATION OF NODAL DISPLACEMENTS FOR EACH *****
C LOAD STAGE
130 TLOAD(K)=TLOAD(K)+PLOAD(K)
DO 135 I=1,NUMNP
IF(NE(I,1)) 165,160,165
160 U(I,1)=0.0
GOTO 170
165 U(I,1)=TLOAD(NE(I,1))
170 IF(NE(I,2)) 180,175,180
175 U(I,2)=0.0
GOTO 135
180 U(I,2)=TLOAD(NE(I,2))
CONTINUE.
WRITE(6,1200)
WRITE(6,1300) (I,U(I,1),U(I,2),I=1,NUMNP)
WRITE(6,1400)

```

```

***** ACCUMULATION OF ELEMENT STRESSES FOR EACH *****
C LOAD STAGE
DO 140 MM=1,NUMEL
TPS1(MM)=TPS1(MM)+SIGN(1,MM)
TPS2(MM)=TPS2(MM)+SIGN(2,MM)
SHEAR(MM)=(TPS1(MM)-TPS2(MM))*0.5
WRITE(6,*) MM,TPS1(MM),TPS2(MM),SHEAR(MM)
140 L(MM)=0
***** SUBROUTINES FOR STOCHASTIC ANALYSIS *****
CALL DUWM(D,DFU,STI,PLOAD,X,Y,PNU,NE,NC,NUMEL,NF,NB)
CALL DCOVE(E,PNU,DFU,PLOAD,NUMEL,X,Y,NUMNP,NC,NE,NEP
1 ,IV,NES,IVV,COV,NW,VVAR,VARS,NI)
WRITE(6,1600)
DO 460 I=1,NEP
DO 460 J=1,NEP
***** ACCUMULATION OF COVARIANCES OF DISPLACEMENT *****
C FOR EACH LOAD STAGE
460 TVVAR(I,J)=TVVAR(I,J)+VVAR(I,J)
DO 470 I=1,NEP
470 WRITE(6,1700) IV(I),(TVVAR(I,J),J=1,NEP)
***** CALCULATE C.O.V. OF VERTICAL DISPLACEMENT *****
C
WRITE(6,1840)
DO 600 I=1,NES
JJ=IV(I)
DISP=U(JJ,2)*1000.0
***** TVVAR(I,I)= VARIANCE FOR VERT. DISP. AT NODE *****
C
STAND=(SQRT(TVVAR(I,I)))*1000.0
QCOV=ABS(STAND/DISP)
WRITE(6,*) JJ,DISP,STAND,QCOV
600 CONTINUE
WRITE(6,*) ' VARIANCES OF TOTAL STRESSES'
WRITE(6,1800)
DO 480 I=1,NES
DO 480 J=1,3
***** ACCUMULATION OF VARIANCES OF STRESSES FOR EACH *****
C LOAD STAGE
480 TVARS(I,J)=TVARS(I,J)+VARS(I,J)
DO 490 I=1,NES
490 WRITE(6,*) IVV(I),TVARS(I,1),TVARS(I,2),TVARS(I,3)
***** CALCULATE C.O.V. OF HORIZONTAL STRESS *****
C
WRITE(6,1810)
DO 700 I=1,NES
JJ=IVV(I)
STRESS=TPS1(JJ)*1000.0
STND=(SQRT(TVARS(I,1)))*1000.0
RCOV=ABS(STND/STRESS)
WRITE(6,*) JJ,STRESS,STND,RCOV
700 CONTINUE
***** CALCULATES C.O.V. OF VERTICAL STRESS *****
C
WRITE(6,1820)
DO 800 I=1,NES
JJ=IVV(I)
STRESS=TPS2(JJ)*1000.0
STND=(SQRT(TVARS(I,2)))*1000.0

```

```

RCOV=ABS(STND/STRESS)
WRITE(6,*) JJ,STRESS,STND,RCOV
800
CONTINUE
C***** CALCULATES C.O.V. OF SHEAR STRESS *****
WRITE(6,1830)
DO 900 I=1,NES
JJ=IVV(I)
STRESS=SHEAR(JJ)*1000.0
STND=(SQRT(TVARS(I,3)))*1000.0
RCOV=ABS(STND/STRESS)
WRITE(6,*) JJ,STRESS,STND,RCOV
900
CONTINUE
500
CONTINUE
1000 FORMAT(///' NO. OF NODAL POINTS =',I3/ ' NO. OF
1 ELEMENTS =',I3/ ' NO. OF LAYERS (SOIL/FOUNDATION) ='
2 ,I3)
1005 FORMAT(///,3X,'POISONS RATIO (LAYERS 1 TO',I3,')',/)
1015 FORMAT(///,3X,'MODULUS OF ELASTICITY (LAYERS 1 TO',
1 I3,')',/)
1025 FORMAT(///,4X,' ELEM. NO. MEMBER INCIDENCES
1 (I,J,K) LAYER NO. SOIL CLASS',/)
1030 FORMAT(/2(2X,'NODE',6X,'CO-ORDINATES',5X,
1 'BD. CONSTR.')/2(3X,'NO.',10X,'X',5X,'Y',9X,'X',5X
2 , 'Y',3X)/1X,2(1X,4(1H*),5X,14(1H*),3X,15(1H*))/)
1035 FORMAT(///,3X,'SUBMERGED SOIL DENSITY (LAYERS 1 TO
1 ,I3,')',/)
1040 FORMAT(2(3X,I3,6X,2(F6.2,1X),6X,I1,5X,I1,3X))
1045 FORMAT(///,4X,'NODE NO.',4X,'X-LOAD',9X,'Y-LOAD',9X
1 , 'X-LOAD',9X,'Y-LOAD',/,19X,(WAVE FORCES)',16X,
2 ,(GRAVITY FORCES)',/)
1070 FORMAT(///, ' BANDWIDTH =',I3,/ )
1200 FORMAT('1'/2(6X'NODE NO.',4X,'X-DISPL',6X,'Y-DISPL')
1 /2X,2(4X,10(1H*),2X,9(1H*),4X,9(1H*))/)
1300 FORMAT(2X,2(7X,I3,7X,E9.3,4X,E9.3))
1400 FORMAT(///, ' ELEM.NO SIGMA-X SIGMA-Y
1 -- SHEAR STRESS',/)
1500 FORMAT(/, ' ITERATION NUMBER .',I3,/ )
1600 FORMAT(///, ' MATRIX OF TOTAL DISPLACEMENT
1 COVARIANCES',/)
1700 FORMAT(1X,I3,11E11.3/4X,11E11.3/4X,11E11.3/4X,
1 11E11.3)
1800 FORMAT(3X,' ELEM. NO.',5X,'SIGMA-X',8X,'SIGMA-Y',
1 7X,'SIGMA-XY')
1810 FORMAT(///, ' ELEM. NO. HORZ-STRESS(kPa) STD(kPa)
1 C.O.V. ',/)
1820 FORMAT(///, ' ELEM. NO. VERT-STRESS(kPa) STD(kPa)
1 C.O.V. ',/)
1830 FORMAT(///, ' ELEM. NO. SHEAR STRESS(kPa) STD(kPa)
1 C.O.V. ',/)
1840 FORMAT(///, ' NODE NO. VERT.DISP.(mm) STD(kPa)
1 C.O.V. ',/)
STOP
END

```

```

C*****
C*
C*      MAIN PROGRAM RAND.FTN: MAIN BODY OF THE PROGRAM FOR
C*          ANALYSIS OF LINEAR ELASTIC FINITE ELEMENT WITH
C*          STOCHASTIC MATERIAL PROPERTIES
C*
C*****
C*
C* THIS PROGRAM (WRITTEN IN THE FORTRAN LANGUAGE) ANALYZES
C* THE SOIL-STRUCTURE INTERACTION OF A(MOBILE ARCTIC CAIS-
C* SON RETAINED ISLAND (M.A.C.) AND THE IN-SITU FOUNDATION
C* MATERIAL. A PLANE STRAIN FINITE ELEMENT MODEL IS DEVEL-
C* OPED WITH LINEAR ELASTIC MATERIAL PROPERTIES. MATERIALS
C* ARE TREATED AS STOCHASTIC WITH REFERENCE TO DISTANCE
C* BETWEEN ELEMENT CENTROIDS. THIS PROGRAM EXAMINES THE
C* UNCERTAINTY IN MATERIAL STRENGTH AND THE CORRELATION OF
C* THE MATERIAL PROPERTIES WITH RESPECT TO DISTANCE. ESTI-
C* MATES OF NORMAL AND SHEAR STRESSES OF SELECTED NODES
C* AND ELEMENTS ARE GIVEN. THE PROCEDURE APPROXIMATES THE
C* DISPLACEMENT AND STRESS FUNCTIONS AS THE FIRST TWO
C* TERMS OF A TAYLOR SERIES EXPANSION. THIS PROGRAM WILL
C* GENERATE A RANDOM STOCHASTIC ANALYSIS OF DISPLACEMENTS
C* AND STRESSES.
C*
C*****
C*
C* RR(I)      = OUTPUT VECTOR OF PSEUDO-RANDOM UNIFORM
C*              DEVIATES WITH VALUES BETWEEN ZERO & ONE FOR
C*              EACH ELEMENT 'I'
C* NUMMAT     = NUMBER OF LAYERS IN F.E.M. MODEL
C* NUMNP      = TOTAL NUMBER OF NODES
C* NUMEL      = TOTAL NUMBER OF ELEMENTS
C* X,Y        = X & Y COORDINATES FOR NODES (m)
C* ID(I,J)    = BOUNDARY CONSTRAINTS FOR NODAL DEGREES OF
C*              FREEDOM (D.F.):
C*                      0 - FREE
C*                      1 - FIXED
C* NC(N,LL)   = MEMBER INCIDENCES FOR 'N' WHERE 'LL' EQUALS
C*              1,2 & 3
C* NC(N,4)    = LAYER NUMBER FOR ELEMENT 'N'
C* NC(N,5)    = MATERIAL CLASSIFICATION FOR ELEMENT 'N':
C*                      STEEL CAISSON - 1
C*                      BERM (DEWATERED) - 2
C*                      BERM (SATURATED) - 3
C*                      SAND (IN-SITU) - 4
C* NE(I,J)    = NUMBER SIGNIFYING A PARTICULAR D.F. AT NODE
C*              'I':
C*                      J = 1, X-DIRECTION D.F.
C*                      J = 2, Y-DIRECTION D.F.
C* NF         = TOTAL NUMBER OF D.F.
C* EM(i)      = MEAN ELASTIC MODULUS OF MATERIAL LAYER 'i'
C*             (MPa)
C* PHU(i)     = MEAN POISSON'S RATIO OF MATERIAL LAYER 'i'
C*
C*****

```

```

***** C*****
C* DENS(I) = RATE OF GRAVITY LOADING PER UNIT AREA OF 2-D *
C* JJ = TOTAL NUMBER OF NODES UNDER EXTERNAL LOADS *
C* FR1,FR2 = FACTORS TO DETERMINE PORTIONS OF TOTAL LOAD *
C* APPLIED: FR1 FOR AREA LOADINGS *
C* FR2 FOR NODAL LOADINGS *
C* NN(II) = NODE NUMBER FOR LOCATION OF EXTERNAL LOADS *
C* FX(II) = HORIZONTAL FORCE VECTOR (MN) *
C* FY(II) = VERTICAL FORCE VECTOR (MN) *
C* COV = COEFFICIENT OF VARIATION (C.O.V.) OF MATERIAL *
C* PROPERTIES AS EXPRESSED THROUGH A FIXED *
C* PERCENTAGE OF THE ELEMENT MODULI *
C* NW = INTEGER FOR DETERMINING CORRELATION *
C* DISTANCE FACTOR *
C* NEP = NUMBER OF NODES CONSIDERED FOR STOCHASTIC *
C* DISPLACEMENT ANALYSIS *
C* IV(I) = NODE NUMBERS FOR NODES CONSIDERED FOR STO- *
C* CHASTIC DISPLACEMENT ANALYSIS *
C* NES = NUMBER OF ELEMENTS CONSIDERED FOR STOCHASTIC *
C* STRESS ANALYSIS *
C* Ivv(I) = ELEMENT NUMBERS FOR ELEMENTS CONSIDERED FOR *
C* STOCHASTIC STRESS ANALYSIS *
C* ST(I,J) = GLOBAL STIFFNESS MATRIX *
C*
*****
```

```

DIMENSION ST(53,32),PLOAD(538),X(303),Y(303),
1 ID(315,2),NC(536,4),EM(14),NE(303,2),D(3,3),SK(6,6),
2 XX(3),YY(3),SIGM(3,536),STI(538,32),DFU(538,536)
DIMENSION PNUC(14),DENS(14),FX(18),FY(18),VVAR(35,35)
1 ,E(536),NN(10),IV(35),U(303,2),IVV(47)
EQUIVALENCE (ST,STI)
REAL RR(536)
K=0
READ(1,*) NUMNP,NUMEL
READ(1,*)(X(I),Y(I),ID(I,1),ID(I,2),I=1,NUMNP)
READ(1,*)(NC(J,1),NC(J,2),NC(J,3),NC(J,4),NC(J,5),
1 J=1,NUMEL)
DO 10 I=1,NUMNP
DO 10 J=1,2
NE(I,J)=0
IF (ID(I,J)) 10,20,10
20 K=K+1
NE(I,J)=K
CONTINUE
WRITE(6,1000) NUMNP,NUMEL
WRITE(6,1030)
WRITE(6,1040) (I,X(I),Y(I),ID(I,1),ID(I,2),
1 I=1,NUMNP)
NF=K
READ(1,*) NUMMAT
READ(1,*)(EM(I),I=1,NUMMAT)
```

```

      READ(1,*)(PNU(I),I=1,NUMMAT)
      READ(1,*) (DENS(I),I=1,NUMMAT)
      WRITE(6,1005) NUMMAT
      WRITE(6,*)(PNU(I),I=1,NUMMAT)
      WRITE(6,1015) NUMMAT
      WRITE(6,*)(EM(I),I=1,NUMMAT)
      WRITE(6,1035) NUMMAT
      WRITE(6,*)(DENS(I),I=1,NUMMAT)
      WRITE(6,1045)
      READ(1,*) JJ,FR1,FR2
      DQ 200 II=1,JJ
      READ(1,*) NN(II),FX(II),FY(II)
      WRITE(6,*) NN(II),EX(II),FY(II)
200   CONTINUE
      WRITE(6,1025)
      DO 50 N=1,NUMEL
      WRITE(6,*)N,(NC(N,J),J=1,4)
50    CONTINUE
      READ(1,*) COV,NW
      READ(1,*) NEP,(IV(I),I=1,NEP)
      READ(1,*) NES,(IVV(I),I=1,NES)
      MB=0
      DO 5 I=1,NF
      DO 5 J=1,32
5     ST(I,J)=0.0
      DO 100 N=1,NUMEL
      DO 150 LL=1,3
      XX(LL)=X(NC(N,LL))
      YY(LL)=Y(NC(N,LL))
150   CONTINUE
      HT=NC(N,4)
      PR=PNU(HT)
      EEX=EM(HT)
      E(N)=EEX
      CALL DMAT(PR,D)
      CALL ELST(SK,XX,YY,EEX,D)
      CALL ASMB(ST,SK,N,NC,NE,MB);
100   CONTINUE
      CALL SYMBOL(1,ST,PLOAD,NF,MB,538)
      WRITE(6,1070) MB
      CALL LOAD(NE,PLOAD,NUMEL,X,Y,NC,DENS,JJ,NN,FX,FY,
1     FR1,FR2)
      CALL SYMBOL(2,ST,PLOAD,NF,MB,538)
      CALL RDIS(PLOAD,D,SIGH,NUMEL,NUMNP,NE,NC,X,Y,EM,PNU,
1     E,U)
      CALL DUWM(D,DFU,STI,PLOAD,X,Y,PNU,NE,NC,NUMEL,NF,MB)
      CALL DCOV3(E,PNU,DFU,PLOAD,NUMEL,X,Y,NUMNP,NC,NE,NEP
1     ,IV,NES,IVV,COV,NW,U,SIGH)
1000  FORMAT(///' NO. OF NODAL POINTS =',I3/' NO. OF ELEM
1     ENTS =',I3/')
1005  FORMAT(///,3X,'POISSONS RATIO (MATERIAL 1 TO',I3,')
1     ,/')
1015  FORMAT(///,3X,'MODULUS OF ELASTICITY (MATERIAL 1 TO'
1     ,I3,')',/)


```

```
1025 FORMAT(//,4X,' ELEM. NO.      MEMBER INCIDENCES  
1     (I,J,K)      MATERIAL NO. ',/)  
1030 FORMAT(//2(2X,'NODE',6X,'CO-ORDINATES',5X,'BD.  
1     CONSTRTS.')/2(3X,'NO.',10X,'X',5X,'Y',9X,'X',5X,'Y'  
2     ,3X)/IX,2(1X,4(1H*),5X,14(1H*),3X,15(1H*))/)  
1035 FORMAT('///,3X,'SUBMERGED WEIGHT (MATERIAL 1 TO',13,  
1     ),/)  
1040 FORMAT(2(3X,13,6X,2(F6.1,1X),6X,11,5X,11,3X))  
1045 FORMAT(////,6X,'NODE NO.   X-LOAD          Y-LOAD',/)  
1070 FORMAT(////,' BANDWIDTH -',13,/) )  
      STOP  
      END
```

APPENDIX IV

Subroutines for Stochastic Finite Element Analysis

The subroutines listed below supplement the main programs presented in Appendix III. The subroutines simulate the theory developed in Chapter 3.

- (1) ASMB : Assembles global stiffness matrix
- (2) BDEFIN : Generates B-matrix (interpolation matrix for triangular elements)
- (3) CTRD : Calculates centroid of each discrete element
- (4) CTRDD : Calculates centroid of each discrete element for main program NONLIN.FTN
- (5) DCOV1 : Determines displacement covariances for main program ELASTC.FTN
- (6) DCOV2 : Determines displacement covariances for main program CAISON.FTN
- (7) DCOV3 : Determines displacement covariances for main program RAND.FTN
- (8) DCOV4 : Determines displacement covariances for main program ELRAND.FTN
- (9) DCOVE : Determines displacement covariances for main program NONLIN.FTN

- (10) DMAT : Generates elastic constituent matrix of material properties
- (11) DUWM : Differentiates displacement w.r.t. elastic modulus to obtain coefficients used in calculating the covariances of node displacements.
- (12) ELST : Assembles local stiffness matrix for individual element.
- (13) GGEN : Generation of nodes and elements for gravity platform foundation and soil interaction problem (triangular plane strain formulation)
- (14) GGUBS : Pseudo-random number generator between zero and one
- (15) LOAD : Generates load vectors
- (16) LOADD : Generates load vectors for main program NONLIN.FTN
- (17) MAT : Determines $(H)_{ij}$ values for selected elements
- (18) NLIN : Selects piecewise linear elastic modulus based on shear modulus and principal strains for each element
- (19) RDIS : Generates displacement vector and stresses for each element
- (20) RRDIS : Generates displacement vector and stresses for each element for main program NONLIN.FTN
- (21) SCOVE : Determines variances of stresses
- (22) SCOVEN : Determines variances of stresses for main program NONLIN.FTN

(23) SYMBOL: Decomposes and back-substitution of degrees of freedom

C*****
C*
C* SUBROUTINE ASMB: ASSEMBLES THE GLOBAL STIFFNESS MATRIX *
C*
C*
C* COMMENTS: THIS SUBROUTINE ASSEMBLES GLOBAL STIFFNESS *
C* MATRIX IN A CONDENSED STORAGE SPACE. GLOBAL STIFFNESS *
C* MATRIX IS A SYMMETRIC BANDED MATRIX OF ORDER 'NF' - *
C* TOTAL NUMBER OF FREEDOM. DUE TO ITS BANDED NATURE, *
C* THERE IS A MAXIMUM BANDWIDTH ABOUT THE MAIN DIAGONAL *
C* WHEREBY ALL VALUES OUTSIDE IT ARE ZERO. BECAUSE OF *
C* SYMMETRY OF THIS MATRIX ONLY HALF OF THE VALUES ABOUT *
C* THE MAIN DIAGONAL NEED BE STORED. THUS THE GLOBAL *
C* STIFFNESS MATRIX IS REDUCED TO A STORAGE SPACE OF 'NF' *
C* BY 'MB' WHERE 'MB' = SEMI-BANDWIDTH. THIS PROCEDURE *
C* IS DISCUSSED IN FURTHER DETAIL BY S. S. RAO IN "THE *
C* FINITE ELEMENT METHOD IN ENGINEERING", PERGAMON *
C* PRESS (1982), PAGE 49.
C*
C*
C* N. = ELEMENT NUMBER
C* NE(N, I) = MEMBER INCIDENCES WHERE 'I' HAS VALUES OF 1, 2 *
C* & 3 INDICATING THE THREE NODES OF THE TRIANG- *
C* UALAR ELEMENT
C* IE(J, 1) = NUMBER SIGNIFYING A PARTICULAR DEGREE OF *
C* FREEDOM IN THE X-DIRECTION AT NODE 'J'
C* IE(J, 2) = NUMBER SIGNIFYING A PARTICULAR DEGREE OF *
C* FREEDOM IN THE Y-DIRECTION AT NODE 'J'
C* ND(*) = VECTOR OF SIZE 6 INDICATING THE DEGREES OF *
C* FREEDOM FOR THE ELEMENT
C* MB = SEMI-BANDWIDTH
C* SK(I, J) = LOCAL STIFFNESS MATRIX
C* ST(I, J) = GLOBAL STIFFNESS MATRIX STORED IN MINIMUM- *
C* SPACE
C*
C*****

```
SUBROUTINE ASHB(ST,SK,N,NE,IE,MB)
DIMENSION ST(538,32),SK(6,6),NE(536,5),IE(303,2),
1 ND(6)
K=1
DO 10 I=1,3
J=NE(N,I)
ND(K)=IE(J,1)
ND(K+1)=IE(J,2)
K=K+2
10 CONTINUE
DO 100 I=1,6
K=ND(I)
IF (K.LE.0) GOTO 100
DO 100 J=1,6
L=ND(J)
```

```
IF (L.LE.0) GOTO 100
LL=L-K+1
IF(LL.LE.0)GO TO 100
C***** SELECTING SEMI-BANDWIDTH *****
IF(MB.LE.LL)MB=LL
ST(K,LL)=ST(K,LL)+SK(I,J)
100   CONTINUE
      RETURN
      END
```

```

***** C***** SUBROUTINE BDEFIN: GENERATION OF THE B-MATRIX: THE
***** C***** INTERPOLATION MATRIX FOR TRIANGULAR ELEMENTS
***** C***** C***** COMMENTS: THIS SUBROUTINE GENERATES THE LOCAL STRAIN
***** C***** DISPLACEMENT MATRIX (B-MATRIX) FOR A TRIANGULAR PLANE
***** C***** STRAIN ELEMENT. THIS PROCEDURE MAY BE FOUND IN BASIC
***** C***** MATRIX STRUCTURAL ANALYSIS BOOKS OR ELEMENTARY FINITE
***** C***** ELEMENT TEXTS. ONE SUCH REFERENCE IS J. S. PRZEMIENIE
***** C***** CKI'S "THEORY OF MATRIX STRUCTURAL ANALYSIS",
***** C***** McGRAW-HILL BOOK COMPANY (1968), PAGES 83-84. PLEASE
***** C***** NOTE THAT THIS SUBROUTINE DERIVES THE B-MATRIX FOR A
***** C***** COORDINATE SYSTEM WHERE THE Y-AXIS IS POSITIVE IN THE
***** C***** DIRECTION OF GRAVITY.
***** C***** C***** B(I,J) = LOCAL STRAIN DISPLACEMENT MATRIX
***** C***** X, Y = CARTESIAN COORDINATES FOR NODES OF TRIANGULAR
***** C***** ELEMENT (X-AXIS IS POSITIVE TO THE RIGHT AND
***** C***** Y-AXIS IS POSITIVE DOWNWARDS).
***** C***** A = DETERMINANT OF SYSTEM OF ELEMENT'S INTERPOLAT-
***** C***** ING POLYNOMIALS
***** C***** - TWICE THE AREA OF THE TRIANGULAR ELEMENT
***** C*****

```

```

10      SUBROUTINE BDEFIN(B,X,Y,A)
      DIMENSION B(3,6),X(3),Y(3)
      DO 10   I=1,3
      DO 10   J=1,6
      B(I,J)=0.0
      X32=X(3)-X(2)
      X31=X(3)-X(1)
      X21=X(2)-X(1)
      Y32=Y(3)-Y(2)
      Y31=Y(3)-Y(1)
      Y21=Y(2)-Y(1)
      A= X(2)*Y(3)-X(3)*Y(2)-(X(1)*Y(3)-X(3)*Y(1))+(X(1)*
1      Y(2)-X(2)*Y(1))
      B(1,1)=-Y32
      B(1,3)=Y31
      B(1,5)=-Y21
      B(2,2)=X32
      B(2,4)=-X31
      B(2,6)=-X21
      B(3,1)=X32
      B(3,2)=-Y32
      B(3,3)=-X31

```

B(3,4)=Y31
B(3,5)=X21-
B(3,6)--Y21
RETURN
END

```

C*****
C*
C* SUBROUTINE CTRD: CALCULATES CENTROID OF EACH DISCRETE
C* ELEMENT FOR PROBABILISTIC ANALYSIS
C*
C*****
C*
C* NL      - ELEMENT NUMBER
C* NC(NL,L) - MEMBER INCIDENCES WHERE 'L' HAS VALUES OF 1,
C*              2 & 3- INDICATING THREE NODES OF TRIANGULAR
C* ELEMENT
C* XX(L)   - X-COORDINATE FOR NODE 'L'
C* YY(L)   - Y-COORDINATE FOR NODE 'L'
C* XM     - MEAN OF X-COORDINATE VALUES
C* XY     - MEAN OF Y-COORDINATE VALUES
C* CRT(NL) - X-COORDINATE OF CENTROID FOR ELEMENT 'NL'
C* CRT(NL) - Y-COORDINATE OF CENTROID FOR ELEMENT 'NL'
C*
C*****

```

```

SUBROUTINE CTRD(X,Y,NC,CTX,CTY,NUMNP,NUMEL),
DIMENSION X(303),Y(303),NC(536,5),XX(3),YY(3),
1  CTX(536),CTY(536)
DO 50  NL=1,NUMEL
  CTX(NL)=0.0
  CTY(NL)=0.0
50  CONTINUE
DO 100  NL=1,NUMEL
  DO 150  L=1,3
    XX(L)=X(NC(NL,L))
    YY(L)=Y(NC(NL,L))
150  CONTINUE
  X1=XX(1)
  X2=XX(2)
  X3=XX(3)
  Y1=YY(1)
  Y2=YY(2)
  Y3=YY(3)
  XM=(X1+X2+X3)/3.0
  YM=(Y1+Y2+Y3)/3.0
  CTX(NL)=XM
  CTY(NL)=YM
100  CONTINUE
  WRITE(6,1025)
  DO 200  I=1,NUMEL
    WRITE(6,1000) I,CTX(I),CTY(I)
200  CONTINUE
300  CONTINUE
1000  FORMAT(5X,I3,6X,F8.3,3X,F8.3)
1025  FORMAT(//,' ELEMENT NO.      X & Y CENTROIDS',/)
  RETURN
END

```

```

C*****
C*
C* SUBROUTINE CTRDD: CALCULATES CENTROID OF EACH DISCRETE
C* ELEMENT FOR PROBABILISTIC ANALYSIS
C*
C*****
C*
C* NL      = ELEMENT NUMBER
C* NC(NL,L) = MEMBER INCIDENCES WHERE 'L' HAS VALUES OF 1,
C*             2 & 3 INDICATING THREE NODES OF TRIANGULAR
C*             ELEMENT
C* XX(L)   = X-COORDINATE FOR NODE 'L'
C* YY(L)   = Y-COORDINATE FOR NODE 'L'
C* XM     = MEAN OF X-COORDINATE VALUES
C* XY     = MEAN OF Y-COORDINATE VALUES
C* CRT(NL) = X-COORDINATE OF CENTROID FOR ELEMENT 'NL'
C* CRT(NL) = Y-COORDINATE OF CENTROID FOR ELEMENT 'NL'
C* NI      = ITERATION NUMBER FOR PIECEWISE LINEAR
C*           ANALYSES
C*
C*****
C*          SUBROUTINE CTRDD(X,Y,NC,CTX,CTY,NUMNP,NUMEL,NI)
C*          DIMENSION X(303),Y(303),NC(536,5),XX(3),YY(3),
C*          1 CTX(536),CTY(536)
C*          DO 50 NL=1,NUMEL
C*              CTX(NL)=0.0
C*              CTY(NL)=0.0
C* 50        CONTINUE
C*          DO 100 NL=1,NUMEL
C*              DO 150 L=1,3
C*                  XX(L)=X(NC(NL,L))
C*                  YY(L)=Y(NC(NL,L))
C* 150       CONTINUE
C*          X1=XX(1)
C*          X2=XX(2)
C*          X3=XX(3)
C*          Y1=YY(1)
C*          Y2=YY(2)
C*          Y3=YY(3)
C*          XM=(X1+X2+X3)/3.0
C*          YM=(Y1+Y2+Y3)/3.0
C*          CTX(NL)=XM
C*          CTY(NL)=YM
C* 100       CONTINUE
C***** PRINT CENTROID LOCATIONS ONCE (WHEN NI = 6) *****
C*          IF (NI.EQ.6) GOTO 250
C*          GOTO 300

```

```
250    WRITE(6,1025)
      DO 200 I=1,NUMEL
      WRITE(6,1000) I,CTX(I),CTY(I)
1000    CONTINUE
300    CONTINUE
1025    FORMAT(5X,I3,6X,F8.3,3X,F8.3)
      FORMAT(///,' ELEMENT NO.      X & Y CENTROIDS',/)
      RETURN
      END
```

C*****
C*
C* SUBROUTINE DCOVL: DETERMINES DISPLACEMENT COVARIANCES
C*
C*****
C*
C* COMMENTS: THIS SUBROUTINE CALCULATES THE COVARIANCE OF
C* VERTICAL DISPLACEMENTS FOR SELECTED NODAL POINTS US-
C*ING THE FIRST TWO TERMS OF A TAYLOR SERIES EXPANSION
C* ABOUT THE EQUILIBRIUM DISPLACEMENT EQUATIONS. THE
C* CORRELATION COEFFICIENT FUNCTION IS AN EXPONENTIAL
C* DECAY FUNCTION (VALUES BETWEEN 0 & 1) TO INDICATE THE
C* DECREASE IN CORRELATION BETWEEN ELEMENT PROPERTIES
C* WITH INCREASING DISTANCE BETWEEN CENTERS. THE SELECT-
C*ION OF 'AN' IS TO ESTABLISH A RATE AT WHICH IT DECAYS.
C* TO NORMALIZE THE EXPONENTIAL RATIO IN THE EXPRESSION
C* 'RO' IS USED. THE LATTER SECTION DETERMINES THE RATIO
C* OF THE NODAL DISPLACEMENT STANDARD DEVIATION (SQUARE
C* ROOT OF VARIANCE) TO THE MEAN DISPLACEMENT (USING
C* MEAN ELASTIC MODULI)
C*

C*****
C*
C* NEP - NUMBER OF NODES CONSIDERED FOR STOCHASTIC ANALYSIS
C* IV(I) - NODE NUMBER FOR NODES CONSIDERED FOR STOCHASTIC ANALYSIS
C* NE(II,2) - NUMBER SIGNIFYING FOR NODE 'II' VERTICAL DEGREE OF FREEDOM (D.F.)
C* XX(*),YY(*) - VECTORS OF GLOBAL COORDINATES FOR ELEMENT NODES
C*
C* X(*),Y(*) - VECTORS OF CENTROIDAL COORDINATES
C* NUMNP - TOTAL NUMBER OF NODAL POINTS
C* NUMEL - TOTAL NUMBER OF ELEMENTS
C* GT(M,N) - MATRIX INDICATING RELATIVE DISTANCE BETWEEN CENTROIDS OF ELEMENTS
C* E(I) - ELASTIC MODULUS FOR ELEMENT 'I'
C* COV - COEFFICIENT OF VARIATION (C.O.V.) OF MATERIAL PROPERTIES EXPRESSED AS A FIXED PERCENTAGE OF THE ELEMENT MODULI
C*
C* STD(I) - STANDARD DEVIATION OF ELASTIC MODULUS FOR ELEMENT 'I'
C*
C* AN - CORRELATION DISTANCE FACTOR (FIXED VALUE)
C* RO - PRODUCT OF CORRELATION DISTANCE FACTOR & DIAMETER OF TANK STRUCTURE (92 METERS)
C* R - COVARIANCE OF ELASTIC MODULI BETWEEN ANY TWO ELEMENTS
C* II, I2 - NE(**,2)
C* DFU(I,J) - GLOBAL MATRIX OF PARTIAL DERIVATIVES OF NODAL DISPLACEMENTS WITH ELASTIC MODULUS FOR D.F. 'I', & ELEMENT 'J' (FROM SUBROUTINE 'DUWH')
C*

C*****

13
=

```

C***** **** C***** **** C***** **** C***** **** C***** ****
C*
C* VAR(I,J)   - SUMMATION OF PRODUCTS OF PARTIAL DERIVA-
C*           TIVES FOR ALL ELEMENTS *
C* VVAR(I,J)   - COVARIANCE OF VERTICAL DISPLACEMENT *
C*           MATRIX BETWEEN NODAL POINTS 'I' & 'J' *
C* U(JJ,2)     - MEAN VERTICAL DISPLACEMENT AT NODE 'JJ' *
C* STAND      - STANDARD DEVIATION OF VERTICAL DISPLA-
C*           MENT FOR NODE 'I' *
C* QCOV       - COEFFICIENT OF VARIATION OF VERT. DISPL. *
C*           - RATIO OF STANDARD DEVIATION TO MEAN VERT. *
C*
C*           DISPLACEMENT *
C***** **** C***** **** C***** **** C***** **** C***** ****

```

```

SUBROUTINE DCOVI(E,PNU,DFU,V,NUMEL,XX,YY,NUMNP,NC,NE
1 ,NEP,IV,NES,IVV,COV,NW,U,SIGM)
DIMENSION X(536),Y(536),STD(536),HE(303,2),IVV(47),
1 U(303,2),XX(303),YY(303),NC(536,5),VAR(35,35),IV(35)
2 ,IV1(35),SIGM(3,536),DFU(538,536),E(536),V(538),
3 PNU(14),VVAR(35,35)
COMMON/GTC/GT(536,536),R0
WRITE(6,950)
WRITE(6,*) (IV(I), I=1,NEP)
DO 700 I=1,NEP
II=IV(I)
IJ=NE(II,2)
IV1(I)=IJ
700 CONTINUE
C***** DETERMINE CENTROID LOCATION FOR ELEMENTS *****
CALL CTRD(XX,YY,NC,X,Y,NUMNP,NUMEL)
DO 400 M=1,NUMEL
DO 400 N=M,NUMEL
400 GT(M,N)=SQRT((X(M)-X(N))**2+(Y(M)-Y(N))**2)
DO 400 I=1,NUMEL
EE=E(I)
STD(I)=EE*COV
40 CONTINUE
AN=0.1*(NW-1.)
R0=92.0*AN
WRITE(6,965) AN
WRITE(6,960)
DO 501 I=1,NEP
DO 501 J=1,NEP
501 VVAR(I,J)=0.
DO 500 M=1,NUMEL
DO 500 N=M,NUMEL
DO 5011 I=1,NEP
DO 5011 J=1,NEP
5011 VAR(I,J)=0.
GETA=GT(M,N)
C***** COVARIANCE OF ELASTIC MODULI *****
R=EXP(-GETA/R0)*STD(M)*STD(N)
DO 600 I=1,NEP

```

```

DO 600 J=1,NEP
I1=IVL(I)
I2=IVL(J)
C***** DIAGONAL TERMS OF MATRIX *****
IF (H.EQ.N) CONST=DFU(I1,H)*DFU(I2,N)
C***** OFF-DIAGONAL TERMS OF MATRIX *****
IF (H.NE.N) CONST=(DFU(I1,H)*DFU(I2,N)+DFU(I1,N)*
1 DFU(I2,M))
C***** SUMMATION OF PRODUCTS OF PARTIAL DERIVATIVES *****
VAR(I,J)=VAR(I,J)+CONST
600 CONTINUE
DO 800 I=1,NEP
DO 800 J=1,NEP
C***** ASSEMBLY OF COVARIANCE OF DISPLACEMENT MATRIX *****
VVAR(I,J)=VVAR(I,J)+VAR(I,J)*R
800 VVAR(J,I)=VVAR(I,J)
500 CONTINUE
DO 100 I=1,NEP
100 WRITE(6,111) IV(I),(VVAR(I,J),J=1,NEP)
111 FORMAT(1X,I3,1.1E11.3/4X,1.1E11.3/4X,1.1E11.3/4X,
1 1.1E11.3)
1111 FORMAT(6,1000)
C***** CALCULATING M.P.O.V. OF Y-DISPLACEMENT *****
DO 120 I=1,NEP
JJ=IV(I)
DISP=U(JJ,2)*1000.0
C***** VVAR(I,I) = VARIANCE FOR VERT. DISPL. AT NODE *****
VVAR(I,I)=STAND*(SQRT(VVAR(I,I)))*1000.0
STAND=SQRT(VVAR(I,I))
QCOV=ABS(STAND/DISP)
WRITE(6,*) JJ,DISP,STAND,QCOV
120 CONTINUE
C***** CALLING SUBROUTINE FOR STOCHASTIC STRESS *****
C ANALYSIS
CALL SCOVE(NE,NC,NUMEL,XX,YY,X,Y,E,PNU,V,DFU,D,STD,
1 NES,IVV,NW,SIGM)
90 CONTINUE
950 FORMAT(1//,' STOCHASTIC ANALYSIS OF SELECTED NODAL
1 POINTS: ',/)
960 FORMAT(1//,' MATRIX OF DISPLACEMENT COVARIANCES: ',/)
965 FORMAT(1//,' RATIO OF CORRELATION DISTANCE TO WIDTH
1 OF FOUNDATION IS ',F7.2)
1000 FORMAT(1//,' NODE NO. VERT.DISP.(mm) STD(mm)
1 C.O.V. ',1/4)
RETURN
END

```

```

*****
C*
C* SUBROUTINE DCOV2: DETERMINES DISPLACEMENT COVARIANCES
C*
C*
C* COMMENTS: THIS SUBROUTINE CALCULATES THE COVARIANCE OF
C* VERTICAL DISPLACEMENTS FOR SELECTED NODAL POINTS US-
C* ING THE FIRST TWO TERMS OF A TAYLOR SERIES EXPANSION
C* ABOUT THE EQUILIBRIUM DISPLACEMENT EQUATIONS. THE
C* CORRELATION COEFFICIENT FUNCTION IS AN EXPONENTIAL
C* DECAY FUNCTION (VALUES BETWEEN 0 & 1) TO INDICATE THE
C* DECREASE IN CORRELATION BETWEEN ELEMENT PROPERTIES
C* WITH INCREASING DISTANCE BETWEEN CENTERS. THE SELECT-
C* ION OF 'AN' IS TO ESTABLISH A RATE AT WHICH IT DECAYS.
C* TO NORMALIZE THE EXPONENTIAL RATIO IN THE EXPRESSION
C* 'RO' IS USED. THE LATTER SECTION DETERMINES THE RATIO
C* OF THE NODAL DISPLACEMENT STANDARD DEVIATION (SQUARE
C* ROOT OF VARIANCE) TO THE MEAN DISPLACEMENT (USING
C* MEAN ELASTIC MODULI). THIS SUBROUTINE DIFFERS FROM
C* 'DCOV1' ONLY IN THE DETERMINATION OF 'RO' DUE TO THE
C* H.A.C. HAVING A DIAMETER OF 110 METERS.
C*
*****

```

C* NEP	NUMBER OF NODES CONSIDERED FOR STOCHASTIC ANALYSIS
C* IV(I)	- NODE NUMBER FOR NODES CONSIDERED FOR STOCHASTIC ANALYSIS
C* NE(II,2)	- NUMBER SIGNIFYING FOR NODE 'II' VERTICAL DEGREE OF FREEDOM (D.F.)
C* XX(*),YY(*)	- VECTORS OF GLOBAL COORDINATES FOR ELEMENT NODES
C* X(*),Y(*)	- VECTORS OF CENTROIDAL COORDINATES
C* NUMNP	- TOTAL NUMBER OF NODAL POINTS
C* NUHEM	- TOTAL NUMBER OF ELEMENTS
C* GT(M,N)	- MATRIX INDICATING RELATIVE DISTANCE BETWEEN CENTROIDS OF ELEMENTS
C* E(I)	- ELASTIC MODULUS FOR ELEMENT 'I'
C* COV	- COEFFICIENT OF VARIATION (C.O.V.) OF MATERIAL PROPERTIES EXPRESSED AS A FIXED PERCENTAGE OF THE ELEMENT MODULI
C* STD(I)	- STANDARD DEVIATION OF ELASTIC MODULUS FOR ELEMENT 'I'
C* AN	- CORRELATION DISTANCE FACTOR (FIXED VALUE)
C* RO	- PRODUCT OF CORRELATION DISTANCE FACTOR & DIAMETER OF CAISSON H.A.C. STRUCTURE (110 METERS)
C* R	- COVARIANCE OF ELASTIC MODULI BETWEEN ANY TWO ELEMENTS
C* II,12	- NE(**,2)

```

C*****
C* DFU(I,J) - GLOBAL MATRIX OF PARTIAL DERIVATIVES OF *
C* NODAL DISPLACEMENTS WITH ELASTIC MODULUS *
C* FOR D.F. 'I' & ELEMENT 'J' (FROM SUBROUT-
C* INE "DUWM")
C* VAR(I,J) - SUMMATION OF PRODUCTS OF PARTIAL DERIVA-
C* TIVES FOR ALL ELEMENTS
C* VVAR(I,J) - COVARIANCE OF VERTICAL DISPLACEMENT
C* MATRIX BETWEEN NODAL POINTS 'I' & 'J'
C* U(JJ,2) - MEAN VERTICAL DISPLACEMENT AT NODE 'JJ'
C* STAND - STANDARD DEVIATION OF VERTICAL DISPLACEMENT
C* QCOV - COEFFICIENT OF VARIATION OF VERT. DISPL.
C* - RATIO OF STANDARD DEVIATION TO MEAN VERT.
C* - DISPLACEMENT
C*
C*****

```

```

SUBROUTINE DCOV2(E,PNU,DFU,V,NUMEL,XX,YY,NUMNP,NC,NE
1 ,NEP,IV,NES,IVV,COV,NW,U,SIGN)
DIMENSION X(536),Y(536),STD(536),NE(303,2),IVV(47),
1 U(303,2),XX(303),YY(303),NC(536,5),VAR(35,35),IV(35)
2 ,IV1(35),SIGN(3,536),DFU(538,536),E(536),V(538),
3 PNU(14),VVAR(35,35)
COMMON/GTC/GT(536,536),RO
WRITE(6,950)
WRITE(6,*) (IV(I),I=1,NEP)
DO 700 I=1,NEP
    II=IV(I)
    IJ=NE(II,2)
    IV1(I)=IJ
CONTINUE
C***** DETERMINE CENTROID LOCATION FOR ELEMENTS *****
CALL CTRD(XX,YY,NC,X,Y,NUMNP,NUMEL)
DO 400 M=1,NUMEL
DO 400 N=M,NUMEL
400 GT(M,N)=SQRT((X(M)-X(N))**2+(Y(M)-Y(N))**2)
DO 40 I=1,NUMEL
    EE=E(I)
    STD(I)=EE*COV
CONTINUE
AN=0.1*(NW-1.)
RO=110.0*AN
WRITE(6,965) AN
WRITE(6,960)
DO 501 I=1,NEP
    DO 501 J=1,NEP
        VVAR(I,J)=0.
        DO 500 M=1,NUMEL
            DO 500 N=M,NUMEL
                DO 5011 I=1,NEP
                    DO 5011 J=1,NEP
5011 VAR(I,J)=0.

```

```

GETA=GT(M,N)
C***** COVARIANCE OF ELASTIC MODULI *****
R=EXP(-GETA/R0)*STD(H)*STD(N)
DO 600 I=1,NEP
DO 600 J=1,NEP
11=IV1(I)
12=IV1(J)
C***** DIAGONAL TERMS OF MATRIX *****
IF (M.EQ.N) CONST=DFU(11,M)*DFU(12,N)
C***** OFF-DIAGONAL TERMS OF MATRIX *****
IF (M.NE.N) CONST=(DFU(11,M)*DFU(12,N)+DFU(11,N)*
1 DFU(12,M))
C***** SUMMATION OF PRODUCTS OF PARTIAL DERIVATIVES *****
600 VAR(I,J)=VAR(I,J)+CONST
CONTINUE
DO 800 I=1,NEP
DO 800 J=1,NEP
C***** ASSEMBLY OF COVARIANCE OF DISPLACEMENT MATRIX *****
VVAR(I,J)=VVAR(I,J)+VAR(I,J)*R
800 VVAR(J,I)=VVAR(I,J)
500 CONTINUE
DO 100 I=1,NEP
100 WRITE(6,111) IV(I),(VVAR(I,J),J=1,NEP)
111 FORMAT(1X,I3,11E11.3/4X,11E11.3/4X,11E11.3/4X,
1 11E11.3)
111 FORMAT(6,1000)
C***** CALCULATING C.O.V. OF Y-DISPLACEMENT *****
DO 120 I=1,NEP
JJ=IV(I)
DISP=U(JJ,2)*1000.0
C***** VVAR(I,I) = VARIANCE FOR VERT. DISPL. AT NODE *****
STAND=(SQRT(VVAR(I,I)))*1000.0
QCOV=ABS(STAND/DISP)
WRITE(6,* ) JJ,DISP,STAND,QCOV
120 CONTINUE
C***** CALLING SUBROUTINE FOR STOCHASTIC STRESS *****
C = ANALYSIS
CALL SCOVE(NE,NC,NUMEL,XX,YY,X,Y,E,PNU,V,DFU,D,STD,
1 NES,IVV,NW,SIGM)
90 CONTINUE
950 FORMAT(//,' STOCHASTIC ANALYSIS OF SELECTED NODAL
1 POINTS: ',/)
960 FORMAT(//,' MATRIX OF DISPLACEMENT COVARIANCES: ',/)
965 FORMAT(/, ' RATIO OF CORRELATION DISTANCE TO WIDTH
1 OF FOUNDATION IS ',F7.2)
1000 FORMAT(//,' NODE NO. VERT.DISP.(mm) STD(mm)
C.O.V. ',//)
RETURN
END

```

```

*****
C* SUBROUTINE DCOV3: DETERMINES DISPLACEMENT COVARIANCES
C*
C* COMMENTS: THIS SUBROUTINE CALCULATES THE COVARIANCE OF
C* VERTICAL DISPLACEMENTS FOR SELECTED NODAL POINTS US-
C* ING THE FIRST TWO TERMS OF A TAYLOR SERIES EXPANSION
C* ABOUT THE EQUILIBRIUM DISPLACEMENT EQUATIONS. THE
C* CORRELATION COEFFICIENT FUNCTION IS AN EXPONENTIAL
C* DECAY FUNCTION (VALUES BETWEEN 0 & 1) TO INDICATE THE
C* DECREASE IN CORRELATION BETWEEN ELEMENT PROPERTIES
C* WITH INCREASING DISTANCE BETWEEN CENTERS. THE SELECT-
C* ION OF 'AN' IS TO ESTABLISH A RATE AT WHICH IT DECAYS.
C* TO NORMALIZE THE EXPONENTIAL RATIO IN THE EXPRESSION
C* 'RO' IS USED. THE LATTER SECTION DETERMINES THE RATIO
C* OF THE NODAL DISPLACEMENT STANDARD DEVIATION (SQUARE
C* ROOT OF VARIANCE) TO THE MEAN DISPLACEMENT (USING
C* MEAN ELASTIC MODULI). THIS SUBROUTINE DIFFERS FROM
C* 'DCOV1' ONLY IN THE DETERMINATION OF 'RO' DUE TO THE
C* M.A.C. HAVING A DIAMETER OF 110 METERS AND IN THE USE
C* OF A PSEUDO-RANDOM NUMBER GENERATOR IN OBTAINING THE
C* STANDARD DEVIATION OF THE ELASTIC MODULI. USING THIS
C* RANDOM STANDARD DEVIATION, A RANDOM STOCHASTIC ANALY-
C* SIS OF DISPLACEMENTS AND STRESSES IS ACHIEVED.
C*
*****
C* NEP      - NUMBER OF NODES CONSIDERED FOR STOCHASTIC
C* IV(I)    - NODE NUMBER FOR NODES CONSIDERED FOR STO-
C* CHASTIC ANALYSIS
C* NE(II,2)  - NUMBER SIGNIFYING FOR NODE 'II' VERTICAL
C*             DEGREE OF FREEDOM (D.F.)
C* XX(*),YY(*) - VECTORS OF GLOBAL COORDINATES FOR ELEMENT
C*             NODES
C* X(*),Y(*)  - VECTORS OF CENTROIDAL COORDINATES
C* NUMNP    - TOTAL NUMBER OF NODAL POINTS
C* NUMEL    - TOTAL NUMBER OF ELEMENTS
C* GT(M,N)   - MATRIX INDICATING RELATIVE DISTANCE BE-
C*             TWEEN CENTROIDS OF ELEMENTS
C* E(I)     - ELASTIC MODULUS FOR ELEMENT 'I'
C* DSEED    - INPUT VARIABLE ASSIGNED AN INTEGER VALUE
C*             IN THE EXCLUSIVE RANGE 1 TO 2147483647
C* RR(I)    - OUTPUT VECTOR OF PSEUDO-RANDOM UNIFORM
C*             DEVIATES WITH VALUES BETWEEN ZERO AND ONE
C*             FOR EACH ELEMENT 'I'
C* COV      - COEFFICIENT OF VARIATION (C.O.V.) OF MAT-
C*             ERIAL PROPERTIES EXPRESSED AS A FIXED
C*             PERCENTAGE OF THE ELEMENT MODULI
C*
*****

```

```

***** C*****
C*
C* STD(I)      - STANDARD DEVIATION OF ELASTIC MODULUS FOR *
C*           ELEMENT 'I' *
C* AN          - CORRELATION DISTANCE FACTOR (FIXED VALUE) *
C* RO          - PRODUCT OF CORRELATION DISTANCE FACTOR & *
C*           DIAMETER OF CAISSON H.A.C. STRUCTURE (110 *
C*           METERS) *
C* R           - COVARIANCE OF ELASTIC MODULI BETWEEN ANY * *
C*           TWO ELEMENTS *
C* I1,I2        - NE(**,2) *
C* DFU(I,J)    - GLOBAL MATRIX OF PARTIAL DERIVATIVES OF * *
C*           NODAL DISPLACEMENTS WITH ELASTIC MODULUS * *
C*           FOR D.F. 'I' & ELEMENT 'J' (FROM SUBROUT- * *
C*           INE 'DUWM') *
C* VAR(I,J)    - SUMMATION OF PRODUCTS OF PARTIAL DERIVA- *
C*           TIVES FOR ALL ELEMENTS *
C* VVAR(I,J)   - COVARIANCE OF VERTICAL DISPLACEMENT *
C*           MATRIX BETWEEN NODAL POINTS 'I' & 'J' *
C* U(JJ,2)      - MEAN VERTICAL DISPLACEMENT AT NODE 'JJ' *
C* STAND       - STANDARD DEVIATION OF VERTICAL DISPLA- *
C*           MENT FOR NODE 'I' *
C* QCOV        - COEFFICIENT OF VARIATION OF VERT. DISPL. *
C* R           - RATIO OF STANDARD DEVIATION TO MEAN VERT. *
C*           DISPLACEMENT *
C* *****
```

```

SUBROUTINE DCOV3(E,PNU,DFU,V,NUMEL,XX,YY,NUMNP,NC,NE
1 ,NEP,IV,NES,IVV,COV,NW,U,SIGM)
DIMENSION X(536),Y(536),STD(536),NE(303,2),IVV(47),
1 U(303,2),XX(303),YY(303),NC(536,5),VAR(35,35),IV(35)
2 ,IV1(35),SIGM(3,536),DFU(538,536),E(536),V(538),
3 PNU(14),VVAR(35,35)
COMMON/GTC/GT(536,536),RO
REAL RR(536)
WRITE(6,950)
WRITE(6,*) (IV(I),I=1,NEP)
DO 700 I=1,NEP
  II=IV(I)
  IJ=NE(II,2)
  IV1(I)=IJ
CONTINUE
700
***** DETERMINE CENTROID LOCATION FOR ELEMENTS *****
CALL CTRD(XX,YY,NC,X,Y,NUMNP,NUMEL)
DO 400 M=1,NUMEL
  DO 400 N=M,NUMEL
    GT(M,N)=SQRT((X(M)-X(N))**2+(Y(M)-Y(N))**2)
    DSSEED=123457.0
    CALL GGUB8(DSSEED,NUMEL,RR)
    DO 400 I=1,NUMEL
      EE=E(I)
      STD(I)=EE*COV*RR(I)
    CONTINUE
400
```

```

AN=0.1*(NW-1.)
RO=110.0*AN
WRITE(6,965) AN
WRITE(6,960)
DO 501 I=1,NEP
DO 501 J=1,NEP
501 VVAR(I,J)=0.
DO 500 M=1,NUMEL
DO 500 N=M,NUMEL
DO' 5011 I=1,NEP
DO' 5011 J=1,NEP
5011 VAR(I,J)=0.
GETA=GT(M,N)
C***** COVARIANCE OF ELASTIC MODULI *****
R=EXP(-GETA/RO)*STD(M)*STD(N)
DO 600 I=1,NEP
DO 600 J=I,NEP
I1=IV1(I)
I2=IV1(J)
C***** DIAGONAL TERMS OF MATRIX *****
IF (M.EQ.N) CONST=DFU(I1,M)*DFU(I2,N)
C***** OFF-DIAGONAL TERMS OF MATRIX *****
IF(M.NE.N) CONST=(DFU(I1,M)*DFU(I2,N)+DFU(I1,N)*
1 DFU(I2,M))
C***** SUMMATION OF PRODUCTS OF PARTIAL DERIVATIVES *****
VAR(I,J)=VAR(I,J)+CONST
600 CONTINUE
DO 800 I=1,NEP
DO 800 J=I,NEP
C***** ASSEMBLY OF COVARIANCE OF DISPLACEMENT MATRIX *****
VVAR(I,J)=VVAR(I,J)+VAR(I,J)*R
800 VVAR(J,I)=VVAR(I,J)
500 CONTINUE
DO 100 I=1,NEP
100 WRITE(6,111) IV(I),(VVAR(I,J),J=1,NEP)
111 FORMAT(1X,I3,1LE11.3/4X,1LE11.3/4X,1LE11.3/4X,
1 1LE11.3)
WRITE(6,1000)
C***** CALCULATING C.O.V. OF Y-DISPLACEMENT *****
DO 120 I=1,NEP
JJ=IV(I)
DISP=U(JJ,2)*1000.0
C***** VVAR(I,I) = VARIANCE FOR VERT. DISPL. AT NODE *****
STAND=(SQRT(VVAR(I,I)))*1000.0
QCOV=ABS(STAND/DISP)
WRITE(6,*), JJ,DISP,STAND,QCOV
120 CONTINUE
C***** CALLING SUBROUTINE FOR STOCHASTIC STRESS *****
C ANALYSIS
CALL SCOVE(NE,NC,NUMEL,XX,YY,X,Y,E,PNU,V,DFU,D,STD,
1 NES,IVV,NW,SIGN)
90 CONTINUE
950 FORMAT(//,' STOCHASTIC ANALYSIS OF SELECTED NODAL
1 POINTS: ',/)
```

```
960    FORMAT(//,' MATRIX OF DISPLACEMENT COVARIANCES:',//)
965    FORMAT(//,' RATIO OF CORRELATION DISTANCE TO WIDTH
1000   1 OF FOUNDATION IS ',F7.2)
      1 FORMAT(//,' NODE NO. VERT.DISP.(mm) STD(mm)
      1          C.O.V. ',//)
      1 RETURN
      1 END
```

C*****
C*
C* SUBROUTINE DCOV4: DETERMINES DISPLACEMENT COVARIANCES
C*
C*****
C*
C* COMMENTS: THIS SUBROUTINE CALCULATES THE COVARIANCE OF
C* VERTICAL DISPLACEMENTS FOR SELECTED NODAL POINTS US-
C*ING THE FIRST TWO TERMS OF A TAYLOR SERIES EXPANSION
C* ABOUT THE EQUILIBRIUM DISPLACEMENT EQUATIONS. THE
C* CORRELATION COEFFICIENT FUNCTION IS AN EXPONENTIAL
C* DECAY FUNCTION (VALUES BETWEEN 0 & 1) TO INDICATE THE
C* DECREASE IN CORRELATION BETWEEN ELEMENT PROPERTIES
C* WITH INCREASING DISTANCE BETWEEN CENTERS. THE SELECT-
C*ION OF 'AN' IS TO ESTABLISH A RATE AT WHICH IT DECAYS.
C* TO NORMALIZE THE EXPONENTIAL RATIO IN THE EXPRESSION
C* 'RO' IS USED. THE LATTER SECTION DETERMINES THE RATIO
C* OF THE NODAL DISPLACEMENT STANDARD DEVIATION (SQUARE
C* ROOT OF VARIANCE) TO THE MEAN DISPLACEMENT (USING
C* MEAN ELASTIC MODULI). THIS SUBROUTINE DIFFERS FROM
C* 'DCOV1' ONLY IN THE USE OF A PSEUDO-RANDOM NUMBER
C* GENERATOR IN OBTAINING THE STANDARD DEVIATION OF THE
C* ELASTIC MODULI. USING THIS RANDOM STANDARD DEVIATION,
C* A RANDOM STOCHASTIC ANALYSIS OF DISPLACEMENTS AND
C* STRESSES IS ACHIEVED.
C*

C*****
C*
C* NEP = NUMBER OF NODES CONSIDERED FOR STOCHASTIC
C* ANALYSIS
C* IV(I) = NODE NUMBER FOR NODES CONSIDERED FOR STO-
C* CHASTIC ANALYSIS
C* NE(II,2) = NUMBER SIGNIFYING FOR NODE 'II' VERTICAL
C* DEGREE OF FREEDOM (D.F.)
C* XX(*),YY(*) = VECTORS OF GLOBAL COORDINATES FOR ELEMENT
C* NODES
C* X(*),Y(*) = VECTORS OF CENTROIDAL COORDINATES
C* NUMNP = TOTAL NUMBER OF NODAL POINTS
C* NUEL = TOTAL NUMBER OF ELEMENTS
C* GT(M,N) = MATRIX INDICATING RELATIVE DISTANCE BE-
C*TWEEN CENTROIDS OF ELEMENTS
C* E(I) = ELASTIC MODULUS FOR ELEMENT 'I'
C* DSEED = INPUT VARIABLE ASSIGNED AN INTEGER VALUE
C* IN THE EXCLUSIVE RANGE 1 TO 2147483647
C* RR(I) = OUTPUT VECTOR OF PSEUDO-RANDOM UNIFORM
C* DEVIATES WITH VALUES BETWEEN ZERO AND ONE
C* FOR EACH ELEMENT 'I'
C* COV = COEFFICIENT OF VARIATION (C.O.V.) OF MAT-
C*ERIAL PROPERTIES EXPRESSED AS A FIXED
C* PERCENTAGE OF THE ELEMENT MODULI
C* STD(I) = STANDARD DEVIATION OF ELASTIC MODULUS FOR
C* ELEMENT 'I'
C*****

```

*****
C*
C* AN      - CORRELATION DISTANCE FACTOR (FIXED VALUE) *
C* RO      - PRODUCT OF CORRELATION DISTANCE FACTOR &   *
C*          DIAMETER OF TANK STRUCTURE (92 METERS)    *
C* R       - COVARIANCE OF ELASTIC MODULI BETWEEN ANY   *
C*          TWO ELEMENTS                                *
C* I1,I2    - NE(**,2)                                 *
C* DFU(I,J) - GLOBAL MATRIX OF PARTIAL DERIVATIVES OF   *
C*          NODAL DISPLACEMENTS WITH ELASTIC MODULUS   *
C*          FOR D.F. 'I' & ELEMENT 'J' (FROM SUBROUT-   *
C*          INE 'DUWM')                                *
C* VAR(I,J) - SUMMATION OF PRODUCTS OF PARTIAL DERIVA-   *
C*          TIVES FOR ALL ELEMENTS                      *
C* YVAR(I,J) - COVARIANCE OF VERTICAL DISPLACEMENT   *
C*          MATRIX BETWEEN NODAL POINTS 'I' & 'J'        *
C* U(JJ,2)   - MEAN VERTICAL DISPLACEMENT AT NODE 'JJ'   *
C* STAND    - STANDARD DEVIATION OF VERTICAL DISPLACE-   *
C*          MENT FOR NODE 'I'                          *
C* QCOV    - COEFFICIENT OF VARIATION OF VERT. DISPL.   *
C*          - RATIO OF STANDARD DEVIATION TO MEAN VERT.   *
C*          DISPLACEMENT                                *
C*
*****
```

```

SUBROUTINE DCOV4(E,PNU,DFU,V,NUMEL,XX,YY,NUMNP,NC,NE
1 ,NEP,IV,NES,IVV,COV,NW,U,SIGH)
DIMENSION X(536),Y(536),STD(536),NE(303,2),IVV(47),
1 U(303,2),XX(303),YY(303),NC(536,5),VAR(35,35),IV(35)
2 ,IV1(35),SIGM(3,536),DFU(538,536),E(536),V(538),
3 PNU(14),VVAR(35,35)
COMMON/GTC/GT(536,536),RO
REAL RR(536)
WRITE(6,950)
WRITE(6,*)(IV(I),I=1,NEP)
DO 700 I=1,NEP
II=IV(I)
IJ=NE(II,2)
IV1(I)=IJ
700 CONTINUE
C***** DETERMINE CENTROID LOCATION FOR ELEMENTS *****
CALL CTRD(XX,YY,NC,X,Y,NUMNP,NUMEL)
DO 400 M=1,NUMEL
DO 400 N=M,NUMEL
400 GT(M,N)=SQRT((X(M)-X(N))**2+(Y(M)-Y(N))**2)
DSEED=123457.0
CALL GGUBS(DSEED,NUMEL,RR)
DO 40 I=1,NUMEL
EE=E(I)
STD(I)=EE*COV*RR(I)
40 CONTINUE
AN=0.1*(NW-1.)
RO=92*0*AN
WRITE(6,965) AN
```

```

      WRITE(6,960)
      DO 501 I=1,NEP
      DO 501 J=1,NEP
 501   VVAR(I,J)=0.
      DO 500 M=1,NUMEL
      DO 500 N=M,NUMEL
      DO 5011 I=1,NEP
      DO 5011 J=1,NEP
 5011   VAR(I,J)=0.
      GETA=GT(M,N)
C***** COVARIANCE OF ELASTIC MODULI *****
      R=EXP(-GETA/RO)*STD(M)*STD(N)
      DO 600 I=1,NEP
      DO 600 J=I,NEP
      I1=IV1(I)
      I2=IV1(J)
C***** DIAGONAL TERMS OF MATRIX *****
      IF (M.EQ.N) CONST=DFU(I1,M)*DFU(I2,N)
C***** OFF-DIAGONAL TERMS OF MATRIX *****
      IF(M.NE.N) CONST=(DFU(I1,M)*DFU(I2,N)+DFU(I1,N)*
      1 DFU(I2,M))
C***** SUMMATION OF PRODUCTS OF PARTIAL DERIVATIVES *****
      VAR(I,J)=VAR(I,J)+CONST
 600   CONTINUE
      DO 800 I=1,NEP
      DO 800 J=I,NEP
C***** ASSEMBLY OF COVARIANCE OF DISPLACEMENT MATRIX *****
      VVAR(I,J)=VVAR(I,J)+VAR(I,J)*R
 800   VVAR(J,I)=VVAR(I,J)
 500   CONTINUE
      DO 100 I=1,NEP
 100   WRITE(6,111) IV(I),(VVAR(I,J),J=1,NEP)
      111   FORMAT(1X,13,11E11.3/4X,11E11.3/4X,11E11.3/4X,
      1 11E11.3)
      WRITE(6,1000)
C***** CALCULATING C.O.V. OF Y-DISPLACEMENT *****
      DO 120 I=1,NEP
      JJ=IV(I)
      DISP=U(JJ,2)*1000.0
      VVAR(I,I) = VARIANCE FOR VERT. DISPL. AT NODE *****
      STAND=(SQRT(VVAR(I,I)))*1000.0
      QCOV=ABS(STAND/QISP)
      WRITE(6,*) JJ,DISP,STAND,QCOV
 120   CONTINUE
C***** CALLING SUBROUTINE FOR STOCHASTIC STRESS *****
C     ANALYSIS
      CALL SCOVE(NE,NC,NUMEL,XX,YY,X,Y,E,PNU,V,DFU,D,STD,
      1 NES,IVV,NW,SIGH)
 90    CONTINUE
 950   FORMAT(////,' STOCHASTIC ANALYSIS OF SELECTED NODAL
      1 POINTS:',/)
 960   FORMAT(//,' MATRIX OF DISPLACEMENT COVARIANCES:',/)
 965   FORMAT(/, ' RATIO OF CORRELATION DISTANCE TO WIDTH
      1 OF FOUNDATION IS ',F7.2)

```

```
1000  FORMAT(///,'    NODE NO. VERT.DISP.(mm)      STD(mm)
1          C.O.V. ',//)
      RETURN
      END
```

```

C*****
C*
C* SUBROUTINE DCOVE: DETERMINES DISPLACEMENT COVARIANCES
C*
C*****
C*
C* COMMENTS: THIS SUBROUTINE CALCULATES THE COVARIANCE OF
C* VERTICAL DISPLACEMENTS FOR SELECTED NODAL POINTS US-
C*ING THE FIRST TWO TERMS OF A TAYLOR SERIES EXPANSION
C* ABOUT THE EQUILIBRIUM DISPLACEMENT EQUATIONS. THE
C* CORRELATION COEFFICIENT FUNCTION IS AN EXPONENTIAL
C* DECAY FUNCTION (VALUES BETWEEN 0 & 1) TO INDICATE THE
C* DECREASE IN CORRELATION BETWEEN ELEMENT PROPERTIES
C* WITH INCREASING DISTANCE BETWEEN CENTERS. THE SELECT-
C*ION OF 'AN' IS TO ESTABLISH A RATE AT WHICH IT DECAYS.
C* TO NORMALIZE THE EXPONENTIAL RATIO IN THE EXPRESSION
C* 'RO' IS USED.
C*
C*****
C*
C* NEP      = NUMBER OF NODES CONSIDERED FOR STOCHASTIC
C* IV(I)    = NODE NUMBER FOR NODES CONSIDERED FOR STO-
C* CHASTIC ANALYSIS
C* NE(II,2)  = NUMBER SIGNIFYING FOR NODE 'II' VERTICAL
C* DEGREE OF FREEDOM (D.F.)
C* XX(*),YY(*) = VECTORS OF GLOBAL COORDINATES FOR ELEMENT
C* NODES
C* X(*),Y(*) = VECTORS OF CENTROIDAL COORDINATES
C* NUMNP   = TOTAL NUMBER OF NODAL POINTS
C* NUMEL   = TOTAL NUMBER OF ELEMENTS
C* GT(M,N) = MATRIX INDICATING RELATIVE DISTANCE BE-
C* TWEEN CENTROIDS OF ELEMENTS
C* E(I)     = ELASTIC MODULUS FOR ELEMENT 'I'
C* COV      = COEFFICIENT OF VARIATION (C.O.V.) OF MAT-
C* ERIAL PROPERTIES EXPRESSED AS A FIXED
C* PERCENTAGE OF THE ELEMENT MODULI
C* STD(I)   = STANDARD DEVIATION OF ELASTIC MODULUS FOR
C* ELEMENT 'I'
C* AN       = CORRELATION DISTANCE FACTOR (FIXED VALUE)
C* RO       = PRODUCT OF CORRELATION DISTANCE FACTOR &
C* DIAMETER OF STRUCTURE (92 METERS)
C* R        = COVARIANCE OF ELASTIC MODULI BETWEEN ANY
C* TWO ELEMENTS
C* II,I2    = NE(**,2)
C* DFU(I,J) = GLOBAL MATRIX OF PARTIAL DERIVATIVES OF
C* NODAL DISPLACEMENTS WITH ELASTIC/MODULUS
C* FOR D.F. 'I' & ELEMENT 'J' (FROM SUBROUT-
C* INE 'DUWM')
C* VAR(I,J) = SUMMATION OF PRODUCTS OF PARTIAL DERIVA-
C* TIVES FOR ALL ELEMENTS
C*
C*****

```

```
*****
C*
C* VVAR(I,J) - COVARIANCE OF VERTICAL DISPLACEMENT *
C* MATRIX BETWEEN NODAL POINTS 'I' & 'J' *
C* VARS(I,J) - VARIANCE OF STRESS MATRIX FOR LOAD STEP *
C* NI - ITERATION NUMBER FOR PIECEWISE LINEAR *
C* ANALYSIS *
C*
*****
```

```
SUBROUTINE DCOVE(E,PNU,DFU,V,NUMEL,XX,YY,NUMNP,NC,NE
1 ,NEP,IV,NES,IVV,COV,NW,VVAR,VARS,NI)
1 DIMENSION X(536),Y(536),STD(536),NE(303,2),IVV(47),
1 XX(303),YY(303),NC(536,5),VAR(47,47),IV(47),PNU(14),
2 IV1(47),DFU(538,536),E(536),V(538),VARS(47,3),
3 VVAR(47,47)
COMMON/GTC/GT(536,536) MRO
*WRITE(6,950)
*WRITE(6,*) (IV(I),I=1,NEP)
DO 700 I=1,NEP
II=IV(I)
IJ=NE(PI,2)
IV1(I)=IJ
700 CONTINUE
C***** DETERMINE CENTROID LOCATION FOR ELEMENTS *****
CALL CTRDD(XX,YY,NC,X,Y,NUMNP,NUMEL,NI)
DO 400 M=1,NUMEL
DO 400 N=M,NUMEL
400 GT(M,N)=SQRT((X(M)-X(N))**2+(Y(M)-Y(N))**2)
DO 400 I=1,NUMEL
EE=E(I)
STD(I)=EE*COV
40 CONTINUE
AN=0.1*(NW-1.)
RO=92.0*AN
WRITE(6,965) AN
WRITE(6,960)
DO 501 I=1,NEP
DO 501 J=1,NEP
501 VVAR(I,J)=0.
DO 500 M=1,NUMEL
DO 500 N=M,NUMEL
DO 5011 I=1,NEP
DO 5011 J=1,NEP
5011 VAR(I,J)=0.
GETA=GT(M,N)
C***** COVARIANCE OF ELASTIC MODULI *****
R=EXP(-GETA/RO)*STD(M)*STD(N)
DO 600 I=1,NEP
DO 600 J=1,NEP
I1=IV1(I)
I2=IV1(J)
C***** DIAGONAL TERMS OF MATRIX *****
IF (M.EQ.N) CONST=DFU(I1,M)*DFU(I2,N)
```

```
-- C***** QFF-DIAGONAL TERMS OF MATRIX *****
      IF(M.NE.N) CONST=(DFU(11,M)*DFU(12,N)+DFU(11,N)*
      1 DFU(12,M))
C***** SUMMATION OF PRODUCTS OF PARTIAL DERIVATIVES *****
      VAR(I,J)=VAR(I,J)+CONST
      600 CONTINUE
      DO 800 I=1,NEP
      DO 800 J=1,NEP
-- C***** ASSEMBLY OF COVARIANCE OF DISPLACEMENT MATRIX *****
      VVAR(I,J)=VVAR(I,J)+VAR(I,J)*R
      800 VVAR(J,I)=VVAR(I,J)
      500 CONTINUE
      DO 100 I=1,NEP
      100 WRITE(6,111) TV(I),(VVAR(I,J),J=1,NEP)
      111 FORMAT(1X,I3,1YE11.3/4X,1YE11.3/4X,1YE11.3/4X,
      1 1YE11.3)
C***** CALLING SUBROUTINE FOR STOCHASTIC STRESS *****
      C ANALYSIS
      CALL SCOVEN(NE,NC,NUMEL,XX,YY,X,Y,E,PNU,V,DFU,D,STD,
      1 NES,IVV,NU,VARS)
      90 CONTINUE
      950 FORMAT(////,' STOCHASTIC ANALYSIS OF SELECTED NODAL
      1 POINTS: /)
      960 FORMAT(//,' MATRIX OF DISPLACEMENT COVARIANCES: /)
      965 FORMAT(/,' RATIO OF CORRELATION DISTANCE TO WIDTH
      1 OF FOUNDATION IS ',F7.2)
      RETURN
      END
```

```

***** C*
C* SUBROUTINE DMAT: GENERATES ELASTIC CONSTITUENT MATRIX *
C* OF MATERIAL PROPERTIES *
C*
***** C*
C* COMMENTS: THIS SUBROUTINE PRESENTS ELASTIC CONSTITUENT *
C* MATRIX FOR A PLANE STRAIN FORMULATION. A DERIVATION *
C* OF THIS CAN BE OBTAINED IN J. S. PRZEMIENIECKI'S *
C* "THEORY OF MATRIX STRUCTURAL ANALYSIS", McGRAW-HILL *
C* BOOK COMPANY (1968), PAGES 18-19. *
C*
***** C*
C* PR = ELEMENTAL POISSON'S RATIO *
C* D(I,J) = ELASTIC CONSTITUENT MATRIX OF ELEMENT MATERIAL *
C* PROPERTIES EXCLUDING MODULUS OF ELASTICITY *
C*
***** C*
SUBROUTINE DMAT(PR,D)
DIMENSION D(3,3)
FA=(1.-PR)/((1.+PR)*(1.-2.*PR))
D(1,1)=FA
D(2,2)=FA
D(1,2)=FA*PR/(1.-PR)
D(2,1)=D(1,2)
D(1,3)=0.
D(2,3)=0.
D(3,1)=0.
D(3,2)=0.
D(3,3)=FA*(1.-2.*PR)/(1.-PR)/2.
RETURN
END

```

```

C*****
C*
C* SUBROUTINE DUWM: DIFFERENTIATES THE DISPLACEMENT WITH
C* RESPECT TO ELASTIC MODULUS AND ARRIVING AT THE COEFF-
C* IENTS TO CALCULATE VARIANCES AND COVARIANCES OF THE
C* NODAL DISPLACEMENTS
C*
C*****
```

C* NUMEL = TOTAL NUMBER OF ELEMENTS
C* NC(***,L) = ELEMENT INFORMATION:
C* NC(***,1) = MEMBER INCIDENCE
C* NC(***,2) = MEMBER INCIDENCE
C* NC(***,3) = MEMBER INCIDENCE
C* NC(***,4) = LAYER NUMBER
C* X(*),Y(*) = VECTORS OF GLOBAL COORDINATES FOR ELEMENT
C* NF = TOTAL NUMBER OF NODAL DEGREES OF FREEDOM
C* PNU(MT) = POISSON'S RATIO FOR LAYER 'MT'
C* E = MODULUS OF ELASTICITY.
C* NODE = NODE NUMBER.
C* NE(NODE,I) = NUMBER SIGNIFYING A PARTICULAR DEGREE OF
FREEDOM (D.F.) AT 'NODE':
C* I = 1, X-DIRECTION D.F.
C* I = 2, Y-DIRECTION D.F.
C* V(***) = SOLUTION VECTOR FOR DISPLACEMENTS OF D.F.
C* DU(IK) = SUMMATION OF PARTIAL DIFFERENTIATION OF
DISPLACEMENTS WITH MODULUS OF ELASTICITY
FOR D.F. 'IK'.
C* SKD(I,J) = LOCAL STIFFNESS MATRIX.
C* DFU(I,NEL) = GLOBAL MATRIX OF PARTIAL DERIVATIVES OF
NODAL DISPLACEMENT WITH ELASTIC MODULUS.
C*

```

SUBROUTINE DUWM(D,DFU,STI,V,XX,YY,PNU,NE,NC,NUMEL,NF
1 ,MB)
1 DIMENSION V(538),XX(303),YY(303),NE(303,2),NC(536,5)
1 ,DU(538),IE(6),B(3,6),SKD(3,6),SKD(6,6),STI(538,32),
1 DFU(538,536),X(3),Y(3),VE(6),D(3,3),PNU(14)
1 DO 100 NEL=1,NUMEL
1 DO 200 L=1,3
1 X(L)=XX(NC(NEL,L))
200 Y(L)=YY(NC(NEL,L))
1 DO 300 I=1,NE
300 DU(I)=0.0
1 MT=NC(NEL,4)
1 PR=PNU(MT)
1 E=1.0
C***** DIFFERENTIATING DISPLACEMENT W.R.T. ELASTIC *****
C* MODULUS MAKES 'E' EQUAL TO 1.0
1 CALL DMAT(PR,D)
1 CALL ELST(SKD,X,Y,E,D)
1 K=1
1 DO 80 I=1,3
```

```
NODE=NC(NEL,I)
IE(K)=NE(NODE,1)
IE(K+1)=NE(NODE,2)
K=K+2
80 CONTINUE
DO 400 I=1,6
IJ=IE(I)
IF (IJ) 90,5100,90
90 VE(I)=V(IJ)
GOTO 400
5100 VE(I)=0.0
400 CONTINUE
DO 3000 I=1,6
IK=IE(I)
IF (IK.EQ.0) GO TO 3000
DO 3001 J=1,6
C***** SUMMATION OF PARTIAL DIFFERENTIATION FOR 'IK' *****
3001 DU(IK)=DU(IK)+SKD(I,J)*VE(J)
3000 CONTINUE
C***** SOLVE FOR PARTIAL DERIVATIVE VECTOR VALUES *****
CALL SYMBOL(2,STL,DU,NF,MB,538)
DO 500 I=1,NF
C***** ASSEMBLY OF GLOBAL MATRIX OF PARTIAL DERIVAT- *****
C LIVES OF NODAL DISPLACEMENT WITH MODULUS
DFU(I,NEL)=DU(I)
500 CONTINUE
100 CONTINUE
RETURN
END
```

```

C*****
C* SUBROUTINE ELST: LOCAL STIFFNESS MATRIX FOR INDIVIDUAL
C* ELEMENT
C*
C*****
C* COMMENTS: THIS SUBROUTINE WILL DETERMINE THE LOCAL
C* STIFFNESS MATRIX 'SK' FOR THE INDIVIDUAL ELEMENTS.
C* THE LOCAL STIFFNESS MATRIX IS OBTAINED BY PRE-MULTI-
C* PLICATION OF THE D-MATRIX BY THE TRANPOSED B-MATRIX
C* AND THE POST-MULTIPLICATION OF THIS PRODUCT BY THE
C* B-MATRIX.
C*
C*           T
C* [SK] = [B] [D] [B]
C*
C*****
C* D(I,J) - ELASTIC CONSTITUENT MATRIX OF ELEMENT
C* MATERIAL PROPERTIES
C* ED(I,J) - ELASTIC CONSTITUENT MATRIX EXCLUDING MODULUS
C* OF ELASTICITY
C* E - ELEMENTAL MODULUS OF ELASTICITY
C* B(I,J) - LOCAL STRAIN DISPLACEMENT MATRIX
C* X,Y - CARTESIAN COORDINATES FOR NODES OF TRIANGULAR
C* ELEMENT (X-AXIS IS POSITIVE TO THE RIGHT AND
C* Y-AXIS IS POSITIVE downwards)
C* A - DETERMINANT OF SYSTEM OF ELEMENT'S
C* INTERPOLATING POLYNOMIALS
C* - TWICE THE AREA OF THE TRIANGULAR ELEMENT
C* SK(I,J) - LOCAL STIFFNESS MATRIX
C*

```

```

SUBROUTINE ELST(SK,X,Y,E,ED)
DIMENSION SK(6,6),D(3,3),B(3,6),X(3),Y(3),ED(3,3),
1   SK(3,6)
      DO 10  I=1,3
      DO 10  J=1,3
10   D(I,J)=ED(I,J)*E
C***** GENERATE B-MATRIX *****
CALL BDEFIN(B,X,Y,A)
      DO 30  I=1,3
      DO 30  J=1,6
      SK(I,J)=0.0
      DO 30  K=1,3
30   SK(I,J)=SK(I,J)+D(I,K)*B(K,J)
      DO 50  I=1,6
      DO 50  J=1,6
      SK(I,J)=0.0
      DO 40  K=1,3
40   SK(I,J)=SK(I,J)+B(K,I)*SKI(K,J)
50   CONTINUE

```

DO 60 I=1,6
DO 60 J=1,6
SK(I,J)=SK(I,J)/A/2.0
60 CONTINUE
RETURN
END

```

*****
C*
C* SUBROUTINE GGEN: GENERATION OF NODES AND ELEMENTS FOR
C* TANK FOUNDATION AND SOIL INTERACTION PROBLEM
C* (TRIANGULAR PLANE STRAIN FORMULATION)
C*
*****
C*
C* COMMENTS: THIS SUBROUTINE GENERATES THE LOCATION AND
C* NUMBERING OF THE NODAL POINTS AND TRIANGULAR ELEMENTS
C* FOR A STANDARD TANK FOUNDATION PROBLEM OVERLYING
C* SEVERAL SOIL LAYERS. IT WILL GENERATE NODAL COORDIN-
C* ATES, ELEMENT MEMBER INCIDENCES, BOUNDARY CONSTRAINTS
C* AND MATERIAL CLASSIFICATION; ALL WITH THE MINIMUM
C* AMOUNT OF INPUT DATA.
C*
*****
C*
C* NX      = NUMBER OF COLUMNS OF NODES
C* XX(I)   = X-COORDINATE FOR EACH COLUMN OF NODES (m)
C*          (X-AXIS IS TAKEN AS POSITIVE TO THE RIGHT)
C* NY      = NUMBER OF ROWS OF NODES
C* YY(I)   = Y-COORDINATE FOR EACH ROW OF NODES (m)
C*          (Y-AXIS IS TAKEN AS POSITIVE IN THE DIRECTION
C*          OF GRAVITY)
C* NX1     = COLUMN NUMBER FOR START OF TANK FOUNDATION
C* NX2     = COLUMN NUMBER FOR END OF TANK FOUNDATION
C* NY      = NUMBER OF LAYERS IN DISCRETIZED FINITE
C*          ELEMENT MODEL
C* NA(I)   = MATERIAL CLASSIFICATION NUMBER FOR LAYER 'I'
C*          (0 = CONCRETE, 1 = SAND, 2 = CLAY)
C* ID(I,J) = BOUNDARY CONSTRAINTS FOR NODAL DEGREES OF
C*          FREEDOM: 0 = FREE
C*          1 = FIXED
C* NODE    = TOTAL NUMBER OF NODAL POINTS
C* NC(I,J) = ELEMENT INFORMATION:
C*          NC(***,1) = MEMBER INCIDENCE
C*          NC(***,2) = MEMBER INCIDENCE
C*          NC(***,3) = MEMBER INCIDENCE
C*          NC(***,4) = LAYER NUMBER
C*          NC(***,5) = MATERIAL CLASSIFICATION
C* NELM    = TOTAL NUMBER OF ELEMENTS
C*
*****

```

```

SUBROUTINE GGEN(X,Y,ID,NC,NODE,NELM)
DIMENSION X(303),Y(303),XX(50),YY(50),IX(50,50),
1 ID(315,2), NA(14),NC(536,5)
READ (1,*) NX,(XX(I),I=1,NX)
READ (1,*) NY,(YY(I),I=1,NY)
READ (1,*) NX1,NX2
NY-NY-1
READ (1,*)(NA(I),I=1,NY)

```

```

DO 1 I=1,NX
DO 1 J=1,NY
1   IX(I,J)=0
NXY=NX*NY
DO 2 I=1,NXY
DO 2 J=1,2
2   ID(I,J)=0
C***** SECTION FOR GENERATING NODAL NUMBERS *****
K=0
DO 10 I=1,NX
C***** STARTING WITH TOP SOIL LAYER *****
NY1=2
C***** BOUNDARY CONDITION OF VERTICAL ROLLER AT ALL *****
C - NODES AT EXTREME LEFT AND RIGHT COLUMNS
IF(I.GE.NX1.AND.I.LE.NX2) NY1=1
DO 20 J=NY1,NY
K=K+1
IF(I.EQ.1.OR.I.EQ.NX) ID(K,1)=1
X(K)=XX(I)
Y(K)=YY(J)
IX(J,I)=K
C***** BOUNDARY CONDITION OF RIGIDLY FIXED ALONG *****
C - LOWEST ROW OF NODES
IF(J.NE.NY) GO TO 20
ID(K,1)=1
ID(K,2)=1
20   CONTINUE
10   CONTINUE
NODE-K
C***** SECTION FOR GENERATING TRIANGULAR ELEMENTS *****
ILY-NY-1
ILX-NX-1
K=0
DO 40 J=1,ILY
DO 30 I=1,ILX
IF(J.EQ.1.AND.I.LT.NX1) GO TO 30
IF(J.EQ.1.AND.I.GE.NX2) GO TO 30
IF(I.GT.ILX/2) GO TO 50
C***** SECTION FOR LEFT HALF GENERATION *****
K=K+1
NM=NA(J)
NC(K,1)=IX(J,I)
NC(K,2)=IX(J,I+1)
NC(K,3)=IX(J+1,I)
NC(K,4)=J
NC(K,5)=NM
K=K+1
NC(K,1)=IX(J,I+1)
NC(K,2)=IX(J+1,I+1)
NC(K,3)=IX(J+1,I)
NC(K,4)=J
NC(K,5)=NM
GO TO 30

```

***** SECTION FOR RIGHT HALF GENERATION *****

346

```
50      K=K+1
      NM=NA(J)
      NC(K,1)=IX(J,I)
      NC(K,2)=IX(J+1,I+1)
      NC(K,3)=IX(J+1,I)
      NC(K,4)=J
      NC(K,5)=NM
      K=K+1
      NC(K,1)=IX(J,I)
      NC(K,2)=IX(J,I+1)
      NC(K,3)=IX(J+1,I+1)
      NC(K,4)=J
      NC(K,5)=NM
30      CONTINUE
40      CONTINUE
      NELM=K
      RETURN
      END
```

```
*****  
C*  
C* SUBROUTINE GGUBS: BASIC UNIFORM (0,1) PSEUDO-RANDOM  
C* NUMBER GENERATOR  
C*  
C*  
C* COMMENTS: THIS SUBROUTINE IS BASED ON A ROUTINE BY THE  
C* SAME NAME 'GGUBS' IN THE ISML PROGRAM LIBRARY. BASED  
C* ON AN ALGORITHM, IT GENERATES A RANDOM SET OF NUMBERS  
C* WITH VALUES IN THE RANGE OF ZERO & UNITY. THE PSEUDO-  
C* RANDOMNESS IS DUE TO THE SAME SET OF RANDOM NUMBERS  
C* BEING GENERATED WHEN 'DSEED' REMAINS UNCHANGED.  
C*  
C*  
C* DSEED = INPUT VARIABLE ASSIGNED AN INTEGER VALUE IN THE  
C* EXCLUSIVE RANGE OF 1 TO 2147483647.  
C* NR = NUMBER OF DEVIATES TO BE GENERATED  
C* R(NR) = OUTPUT VECTOR OF PSEUDO-RANDOM UNIFORM DEVIATES  
C* WITH VALUES BETWEEN ZERO & ONE.  
C*  
C*  
SUBROUTINE GGUBS(DSEED,NR,R)  
INTEGER NR  
REAL R(NR)  
INTEGER I  
DATA D2P31M/2147483647.00/  
DATA D2P31/2147483648.00/  
DO 5 I=1,NR  
DSEED=MOD(16807.0*DSEED,D2P31M)  
R(I)=DSEED/D2P31  
RETURN  
END
```

```

C*****
C*
C* SUBROUTINE LOAD: GENERATES THE LOAD-VECTORS
C*
C*****
C*
C* COMMENTS: THIS SUBROUTINE DETERMINES THE FORCES TO BE
C* APPLIED AT THE NODES OF THE FINITE ELEMENT MODEL. THE
C* FIRST SECTION CALCULATES NODAL FORCES IN THE VERTICAL
C* DIRECTION THAT ARISE FROM THE LOADS PER UNIT AREA
C* ASSUMING MODEL IS ONE METER SLICE THROUGH STRUCTURE.
C* THE LOAD PER ELEMENT IS DIVIDED EQUALLY AND APPLIED
C* TO EACH OF THE THREE NODES OF THE ELEMENT. THIS PROC-
C* EDURE IS REPEATED FOR ALL ELEMENTS. THE SECOND PART
C* OF THE SUBROUTINE APPLIES LOADS OBTAINED IN THE MAIN
C* PROGRAM (FROM INPUT DATA) TO THE APPROPRIATE NODES
C* DIRECTLY. THESE CAN REFER TO EXTERNAL LOADS BOTH
C* HORIZONTAL AND VERTICAL.
C*
C*****
C*
C* FRI, FR2 = FACTORS TO DETERMINE PORTIONS OF TOTAL LOAD
C*             APPLIED: FRI FOR AREA LOADINGS
C*             FR2 FOR NODAL LOADINGS
C*
C* N      = ELEMENT NUMBER
C* MT     = LAYER NUMBER
C* NC(N,L) = MEMBER INCIDENCES WHERE 'L' HAS VALUES OF
C*             1, 2 & 3 INDICATING THE THREE NODES OF THE
C*             TRIANGULAR ELEMENT
C* DENS(MT) = RATE OF GRAVITY LOADING PER UNIT AREA OF
C*             TWO-DIMENSIONAL MODEL FOR LAYER 'MT'
C* X,XX(L)  = X-COORDINATE FOR NODE 'L'
C* Y,YY(L)  = Y-COORDINATE FOR NODE 'L'
C* AREA    = AREA OF TRIANGULAR ELEMENT (REFER TO SUB-
C*             ROUTINE: BDEFIN)
C* WT     = PORTION OF VERTICAL FORCE APPLIED AT NODE
C*             ATTRIBUTED TO ELEMENT'S AREA LOADING
C* IE(***,I) = NUMBER FOR PARTICULAR GLOBAL DEGREE OF
C*             FREEDOM (D.F.): I = 1, HORIZONTAL D.F.
C*                         I = 2, VERTICAL D.F.
C* PLOAD(**) = ACCUMULATED LOAD VECTOR
C* II     = TOTAL NUMBER OF NODES UNDER EXTERNAL LOADS
C* NN(II)  = NODE NUMBER FOR LOCATION OF EXTERNAL LOADS
C* FX(II)  = HORIZONTAL FORCE VECTOR
C* FY(II)  = VERTICAL FORCE VECTOR
C*
C*****

```

```

1 SUBROUTINE LOAD(IE,PLOAD,NUMEL,X,Y,NC,DENS,JJ,NN,FX,
1 FY,FRL,FR2)
1 DIMENSION IE(303, 2),PLOAD(538),X(303),Y(303),NN(18),
1 NC(536, 5),XX(3),YY(3),DENS(14),FX(18),FY(18)
1 DO 10 I=1,538
10 PLOAD(I)=0.0

```

```
      IF(FR1.LE.0.0) GOTO 55
C***** LOADS APPLIED AS FUNCTION OF ELEMENT AREA *****
      DO 50 N=1,NUMEL
      MT=NC(N,4)
      DES=DENS(MT)
      DO 20 L=1,3
      XX(L)=X(NC(N,L))
      YY(L)=Y(NC(N,L))
20    CONTINUE
      AREA=(XX(2)*YY(3)-XX(3)*YY(2)-(XX(1)*YY(3)-XX(3)*
1     YY(1))+(XX(1)*YY(2)-XX(2)*YY(1)))*0.5
      WT=DES*AREA/3.0
      DO 30 L=1,3
      M=NC(N,L)
      N2=IE(M,2)
      PLOAD(N2)=PLOAD(N2)+WT*FR1
30    CONTINUE
50    CONTINUE
55    IF(FR2.LE.0.0) GOTO 70
C***** LOADS APPLIED DIRECTLY TO NODES *****
      DO 60 II=1,JJ
      MM=NN(II)
      N2=IE(MM,2)
      N1=IE(MM,1)
      PLOAD(N1)=PLOAD(N1)+FX(II)*FR2
      PLOAD(N2)=PLOAD(N2)+FY(II)*FR2
60    CONTINUE
70    CONTINUE
      RETURN
      END
```

```

*****
C*
C* SUBROUTINE LOADD: GENERATES THE LOAD VECTORS
C*
*****
C*
C* COMMENTS: THIS SUBROUTINE DETERMINES THE FORCES TO BE
C* APPLIED AT THE NODES OF THE FINITE ELEMENT MODEL. THE
C* FIRST SECTION CALCULATES NODAL FORCES IN THE VERTICAL
C* DIRECTION THAT ARISE FROM THE LOADS PER UNIT AREA
C* ASSUMING MODEL IS ONE METER SLICE THROUGH STRUCTURE.
C* THE LOAD PER ELEMENT IS DIVIDED EQUALLY AND APPLIED
C* TO EACH OF THE THREE NODES OF THE ELEMENT. THIS PROC-
C* EDURE IS REPEATED FOR ALL ELEMENTS. THE SECOND PART
C* OF THE SUBROUTINE APPLIES LOADS OBTAINED IN THE MAIN
C* PROGRAM (FROM INPUT DATA) TO THE APPROPRIATE NODES
C* DIRECTLY. THESE CAN REFER TO EXTERNAL LOADS BOTH
C* HORIZONTAL AND VERTICAL. THIS SECOND SECTION HAS TWO
C* PARTS: ONE TO APPLY THE GRAVITY NODAL LOADS IN STAGES
C* UNTIL IT IS ALL APPLIED; AND THE OTHER, TO APPLY THE
C* "WAVE" FORCE TO THE NODES IN STAGES UNTIL COMPLETED.
C* THE PORTIONS ARE GOVERNED BY THE FACTORS 'FR1' AND
C* 'FR2'. THE STAGES IN THE PIECEWISE LINEAR ANALYSIS IS
C* CONTROLLED BY THE ITERATION NUMBER, 'NI'.
C*
*****
C*
C* FR1,FR2 - FACTORS TO DETERMINE PORTIONS OF TOTAL LOAD
C*           APPLIED: FR1 FOR AREA LOADINGS
C*           FR2 FOR NODAL LOADINGS
C* N - ELEMENT NUMBER
C* MT - LAYER NUMBER
C* NI - ITERATION NUMBER
C* NC(N,L) - MEMBER INCIDENCES WHERE 'L' HAS VALUES OF
C*           1', 2 & 3 INDICATING THE THREE NODES OF THE
C*           TRIANGULAR ELEMENT
C* DENS(MT) - RATE OF GRAVITY LOADING PER UNIT AREA OF
C*           TWO-DIMENSIONAL MODEL FOR LAYER 'MT'
C* X,XX(L) - X-COORDINATE FOR NODE 'L'
C* Y,YY(L) - Y-COORDINATE FOR NODE 'L'
C* AREA - AREA OF TRIANGULAR ELEMENT (REFER TO SUB-
C*           ROUTINE: BDEFIN)
C* WT - PORTION OF VERTICAL FORCE APPLIED AT NODE,
C*           ATTRIBUTED TO ELEMENT'S AREA LOADING
C* IE(***,I) - NUMBER FOR PARTICULAR GLOBAL DEGREE OF
C*           FREEDOM: (D.F.): I = 1, HORIZONTAL D.F.
C*           I = 2, VERTICAL D.F.
C*
C* PLOAD(***) - ACCUMULATED LOAD VECTOR
C* II - TOTAL NUMBER OF NODES UNDER EXTERNAL LOADS
C*
*****

```

```

C***** **** C***** **** C***** **** C***** **** C***** **** C***** ****
C*
C* NN(II)      - NODE NUMBER FOR LOCATION OF EXTERNAL LOADS   *
C* FX(II)       - HORIZONTAL FORCE VECTOR FOR WAVE LOADS    *
C* FY(II)       - VERTICAL FORCE VECTOR FOR WAVE LOADS     *
C* FXG(II)      - HORIZONTAL FORCE VECTOR FOR GRAVITY LOADS *
C* FYG(II)      - VERTICAL FORCE VECTOR FOR GRAVITY LOADS *
C*
C***** **** C***** **** C***** **** C***** **** C***** **** C***** ****

```

```

SUBROUTINE LOADD(IE,PLOAD,NUMEL,X,Y,NC,DENS,NI,JJ,NN
1 ,FX,FY,FR1,FR2,FXG,FYG)
DIMENSION IE(303,2),PLOAD(538),X(303),Y(303),NN(18),
1 NC(536,5),XX(3),YY(3),DENS(14),FX(18),FY(18),FXG(18)
2 ,FYG(18)
DO 10 I=1,538
10 PLOAD(I)=0.0
IF(FR1.LE.0.0) GOTO 55
C***** LOADS APPLIED AS FUNCTION OF ELEMENT AREA *****
DO 50 N=1,NUMEL
MT=NC(N,4)
DES=DENS(MT)
DO 20 L=1,3
XX(L)=X(NC(N,L))
YY(L)=Y(NC(N,L))
20 CONTINUE
AREA=(XX(2)*YY(3)-XX(3)*YY(2)-(XX(1)*YY(3)-XX(3)*
1 YY(1))+(XX(1)*YY(2)-XX(2)*YY(1)))*0.5
WT=DES*AREA/3.0
DO 30 L=1,3
M=NC(N,L)
N2=IE(M,2)
PLOAD(N2)=PLOAD(N2)+WT*FR1
30 CONTINUE
50 CONTINUE
55 IF(FR2.LE.0.0) GOTO 70
C***** LOADS APPLIED DIRECTLY TO NODES *****
IF(NI.GT.21) GOTO 80
C***** SECTION FOR GRAVITY LOADING *****
DO 100 II=1,JJ
MM=NN(II)
N2=IE(MM,2)
N1=IE(MM,1)
PLOAD(N1)=PLOAD(N1)+FXG(II)*FR2
PLOAD(N2)=PLOAD(N2)+FYG(II)*FR2
100 CONTINUE
GOTO 70

```

C***** SECTION FOR WAVE LOADING *****
80 CONTINUE
DO 60 II=1,JJ
MM=NN(II)
N2=IE(MM,2)
N1=IE(MM,1)
PLOAD(N1)=PLOAD(N1)+FX(II)*FR2
PLOAD(N2)=PLOAD(N2)+FY(II)*FR2
60 CONTINUE
70 CONTINUE
RETURN
END

```

***** C*
C* SUBROUTINE MAT: DETERMINES {H} VALUES FOR SELECTED
C* ELEMENTS. ij
C*
C* ***** C*
C* 
$$\{H\}_{ij} = \frac{d[D]}{dE} \{B\}_{ij} \{U\}_j \delta_i + [D]_{ij} \{B\}_{ij} \frac{d\{U\}}{dE}$$

C* i j i j i i j i i dE
C* ***** C*
C* KK - ELEMENT NUMBER SELECTED FOR STOCHASTIC
C* STRESS ANALYSIS
C* PR - POISSON'S RATIO
C* EE - ELASTIC MODULUS
C* NC(KK,4) - LAYER NUMBER FOR ELEMENT 'KK'
C* NC(KK,L) - MEMBER INCIDENCES FOR 'KK' WHERE L = 1,2 & 3
C* X(L) - X-COORDINATE FOR NODES
C* Y(L) - Y-COORDINATE FOR NODES
C* NE(N,L) - NUMBER FOR GLOBAL DEGREE OF FREEDOM (D.F.):
C* L = 1, HORIZONTAL D.F.
C* L = 2, VERTICAL D.F.
C* D(I,K) - ELASTIC CONSTITUENT MATRIX OF MATERIAL PROPERTIES
C* B(K,J) - INTERPOLATION MATRIX
C* A - TWICE AREA OF TRIANGULAR ELEMENT
C* NUMEL - TOTAL NUMBER OF ELEMENTS
C* KODE - KROENECKER DELTA FUNCTION:
C* KODE = 0, M EQUAL TO KK
C* KODE = 1, M NOT EQUAL TO KK
C* ('M' IS ELEM. NO. & 'KK' IS ELEM. SELECTED
C* FROM SUBROUTINE 'SCOVE')
C* DFU(I,J) - MATRIX OF PARTIAL DERIVATIVES OF NODAL DIS-
C* PLACEMENTS W.R.T. ELASTIC MODULUS WHERE:
C* I - D.F.
C* J - ELEMENT NUMBER
C* V(***) - SOLUTION VECTOR FOR DISPLACEMENTS OF D.F.
C* DS(M,I) - {H}_i, PREDEFINED FUNCTION
C* ij
C* ***** C*

```

```

SUBROUTINE MAT(KK,NUMEL,NC,NE,XX,YY,E,PNU,V,DFU,DS,D
1 ,KODE)
1 DIMENSION NC(536,5),NE(303,2),XX(303),YY(303),E(536)
1 ,PNU(14),V(538),DFU(538,536),DS(536,3),D(3,3),B(3,6)
2 ,IE(6),DB(3,6),X(3),Y(3),
MT=NC(KK,4)
PR=PNU(MT)
EE=E(KK)

```

```

***** GENERATE ELASTIC CONSTITUENT MATRIX OF *****
C MATERIAL PROPERTIES
  CALL DMAT(PR,D)
  DO 1 L=1,3
    X(L)=XX(NC(KK,L))
    Y(L)=YY(NC(KK,L))
1 ***** GENERATE INTERPOLATION MATRIX (B-MATRIX) *****
  CALL BDEFIN(B,X,Y,A)
  K=1
  DO 2 I=1,3
    N=NC(KK,I)
    IE(K)=NE(N,1)
    IE(K+1)=NE(N,2)
2   K=K+2
  DO 3 I=1,3
    BO 3 J=1,6
    DB(I,J)=0.0
    DO 3 K=1,3
3   [DB] = [D][B]
C
C   DB(I,J)=DB(I,J)+D(I,K)*B(K,J)/A
DO 300 M=1,NUMEL
  KODE=1
  IF(M.EQ.KK) KODE=0
  IF(KODE.EQ.0) GO TO 100
  DO 4 I=1,3
    DSM=0.0
    DO 4 J=1,6
4   C***** ELEMENT NUMBER IS NOT EQUAL TO ELEMENT SELECTED *****
C FOR STOCHASTIC STRESS ANALYSIS
  DSM=DSM+DB(I,J)*DFU(IE(J),M)*EE
4   DS(M,I)=DSM
  GO TO 300
100  DO 5 I=1,3
    DSM=0.0
    DO 5 J=1,6
5   C***** ELEMENT NUMBER IS EQUAL ELEMENT SELECTED *****
C FOR STOCHASTIC STRESS ANALYSIS
  DSM=DSM+DB(I,J)*(V(IE(J))+DFU(IE(J),M)*EE)
5   DS(H,I)=DSM
300  CONTINUE
      RETURN
      END

```

C*****
C*
C* SUBROUTINE NLIN: SELECTS NONLINEAR (PIECEWISE LINEAR)
C* MODULUS OF ELASTICITY BASED ON SHEAR MODULUS AND
C* PRINCIPAL STRAINS OF EACH ELEMENT
C*
C*****
C*
C* COMMENTS: THIS SUBROUTINE SELECTS THE ELASTIC MODULUS
C* FOR THE ELEMENTS USING A PIECEWISE LINEAR PROCEDURE.
C* USING THE PRINCIPAL STRESSES FROM THE F.E.M. FORMU-
C* LATION, THE PRINCIPAL STRAINS CAN BE CALCULATED.
C* (REFER TO E. P. POPOV'S " MECHANICS OF MATERIALS ",
C* SECOND EDITION, PRENTICE-HALL, INC. (1978), PAGES 47,
C* 263). BASED ON THE SHEAR STRAINS, A SHEAR MODULUS RE-
C* DUCTION FACTOR IS OBTAINED FROM LINEAR INTERPOLATION
C* INTO A TABLE OF FACTORS WITH CORRESPONDING EFFECTIVE
C* STRAIN LEVELS. THERE ARE SETS OF FACTORS FOR BOTH
C* SAND AND CLAY. THIS WORK IS BASED ON THE RESEARCH
C* REPORT BY J. LYSHER, T. UDAKA, H. B. SEED & R. HWANG;
C* " LUSH: A COMPUTER PROGRAM FOR COMPLEX RESPONSE ANAL-
C* YSIS OF SOIL-STRUCTURE SYSTEMS "; REPORT NO. E-E.RTC.
C* 74-4, APRIL 1974, UNIVERSITY OF CALIFORNIA, BERKELEY
C* (PAGE 11). USING THE RELATIONSHIP BETWEEN SHEAR AND
C* ELASTIC MODULI FOR PLANE STRAIN CONDITIONS, A NEW
C* ELASTIC MODULUS 'EE(I)' IS DETERMINED. TAKING AN
C* AVERAGE OF THIS NEW MODULUS AND THE MODULUS OF THE
C* PREVIOUS ITERATION, A CONVERGENCE TEST IS APPLIED.
C* WHEN THE DIFFERENCE BETWEEN THIS AVERAGE AND THE
C* ELASTIC MODULUS FROM THE PREVIOUS ITERATION IS LESS
C* THAN 5.0%, THE ELEMENT MODULUS HAS CONVERGED. THIS
C* VALUE IS STORED UNTIL ALL ELEMENTS HAVE CONVERGED
C* MODULI OR THE ITERATION NUMBER HAS REACHED THE NEXT
C* LOAD STEP. THE ITERATION NUMBERS FOR EACH LOAD STEP
C* ARE SELECTED SUCH THAT ALL ELEMENTS HAVE CONVERGED
C* WITH THE EXCEPTION OF A FEW.
C*
C*****
C*
C* LL = INTEGER TO COUNT NUMBER OF CONVERGED ELE-
C* MENTS IN ITERATION 'NI'
C* NUMEL = TOTAL NUMBER OF ELEMENTS
C* NC(I,4) = LAYER NUMBER FOR ELEMENT 'I'
C* NC(I,5) = MATERIAL CLASSIFICATION: CONCRETE = 0
C* SAND = 1
C* CLAY = 2
C* MINIMUM MODULUS = 3
C* NI = ITERATION NUMBER FOR PIECEWISE LINEAR
C* ANALYSIS
C* STRAIN(I) = TOTAL ACCUMULATED SHEAR STRAIN (PERCENT)
C* GAM(I) = MAXIMUM SHEAR STRAIN (PERCENT) FOR LOAD
C* STAGE BASED ON PREVIOUS ITERATION MODULI
C*

```

*****
C*
C* EY      = ELASTIC MODULUS FROM PREVIOUS ITERATION
C* PR      = POISSON'S RATIO
C* SS1     = MAXIMUM PRINCIPAL STRESS (MPa)
C* SS2     = MINIMUM PRINCIPAL STRESS (MPa)
C* EPS1(I) = MAXIMUM PRINCIPAL STRAIN
C* EPS2(I) = MINIMUM PRINCIPAL STRAIN
C* GAMMA(I) = ACCUMULATED SHEAR STRAIN (PERCENT) USED TO
C*           SELECT REDUCTION FACTOR 'RF'
C* L(I)    = VECTOR TO DETERMINE WHEN MODULUS OF ELEMENT
C*           'I' HAS CONVERGED, DURING EACH LOADING STAGE;
C*           L = 0, UNCONVERGED
C*           L = 1, CONVERGED
C* SM      = INITIAL SHEAR MODULUS OF ELEMENT USING
C*           INITIAL MEAN ELEMENT MODULUS
C* RF1,RF2 = SHEAR MODULUS REDUCTION FACTORS
C* GAM1,GAM2= EFFECTIVE SHEAR STRAIN LEVELS CORRESPONDING
C*           TO SHEAR MODULUS REDUCTION FACTORS
C* RF      = SHEAR MODULUS REDUCTION FACTOR AS ESTIMATED
C*           FROM LINEAR INTERPOLATION FOR 'GAMMA(I)'
C*           VALUE
C* G       = REDUCED SHEAR MODULUS VALUE
C*           PRODUCT OF REDUCTION FACTOR & INITIAL SHEAR
C*           MODULUS
C* EE(I)   = ELASTIC MODULUS VALUE BASED ON REDUCED
C*           SHEAR MODULUS, 'G'
C* E(I)    = AVERAGE OF 'EY' & 'EE(I)' TO MAKE ELEMENT
C*           MODULI CONVERGE FASTER
C* EMIN    = MINIMUM ELASTIC MODULUS ( 20% OF INITIAL
C*           MODULUS )
C* RATIO(I) = CONVERGENCE RATIO
C*           = RATIO OF DIFFERENCE BETWEEN 'EY' & 'E(I)'
C*           TO 'EY'
C*
*****

```

```

SUBROUTINE NLIN(PS1,PS2,NUMEL,EM,PNU,E,NC,NI,L,RATIO
1 ,EE,GAM,STRAIN,LL)
DIMENSION PS1(536),PS2(536),EM(14),PNU(14),E(536),
1 NC(536,5),L(536),RATIO(536),EPS1(536),EPS2(536),
2 STRAIN(536),GAMMA(536),GAM(536),EE(536)
***** IF ALL ELEMENTS HAVE CONVERGED PROCEED TO *****
C* NEXT LOAD STAGE
C* IF(LL.EQ.NUMEL) GOTO 900
DO 100 I=1,NUMEL
C***** FOR CONCRETE ELEMENTS ASSUME LINEAR MODULI *****
IF (NC(1,5).EQ.0) GOTO 200
C***** FOR ELEMENTS THAT HAVE REACHED MINIMUM *****
C* ELASTIC MODULI
IF (NC(1,5).EQ.3) GOTO 210
IF (NI.EQ.1) GOTO 150

```

```

***** ESTABLISHING ITERATION NUMBERS FOR ADVANCING *****
C TO NEXT LOAD STAGE
IF (NI.EQ.7) GOTO 160
IF (NI.EQ.11) GOTO 160
IF (NI.EQ.15) GOTO 160
IF (NI.EQ.19) GOTO 160
IF (NI.EQ.22) GOTO 160
IF (NI.EQ.26) GOTO 160
IF (NI.EQ.29) GOTO 160
GOTO 170
160 CONTINUE
***** ACCUMULATES TOTAL SHEAR STRAIN AFTER EACH LOAD *****
C STAGE IS COMPLETED
STRAIN(I)=STRAIN(I)+ABS(GAM(I)),
170 CONTINUE
EY=E(I)
GOTO 250
150 EY=EM(NC(I,4))
CONTINUE
PR=PNU(NC(I,4))
SS1=PS1(I)
SS2=PS2(I)
EPS1(I)=(SS1-PR*SS2)/EY
EPS2(I)=(SS2-PR*SS1)/EY
***** CALCULATING MAXIMUM SHEAR STRAIN FOR THIS LOAD *****
C PORTION (IN PERCENT)
GAM(I)=50.0*(EPS1(I)-EPS2(I))
***** ACCUMULATED SHEAR STRAIN BASED ON UNCONVERGED *****
C MODULUS VALUES
GAMMA(I)=ABS(GAM(I))+STRAIN(I)
IF (L(I).EQ.1) GOTO 100
SM=EM(NC(I,4))/(2.0*(1.0+PR))
IF (NC(I,5).EQ.2) GOTO 300
C SECTION FOR SHEAR STRAIN DEPENDENT PROPERTY *****
C SELECTION OF SHEAR MODULUS FOR SAND
IF ((GAMMA(I).LE.0.0001)) GOTO 400
IF ((GAMMA(I).LE.0.000316)) GOTO 410
IF ((GAMMA(I).LE.0.001)) GOTO 420
IF ((GAMMA(I).LE.0.00316)) GOTO 430
IF ((GAMMA(I).LE.0.01)) GOTO 440
IF ((GAMMA(I).LE.0.0316)) GOTO 450
IF ((GAMMA(I).LE.0.1)) GOTO 460
IF ((GAMMA(I).LE.0.3)) GOTO 470
RF=0.115
GOTO 550
400 RE=1.0
GOTO 550
410 GAM1=0.0001
RF1=1.0
GAM2=0.000316
RF2=0.984
GOTO 500

```

420 GAM1=0.000316
RF1=0.984
GAM2=0.001
RF2=0.934
GOTO 500

430 GAM1=0.001
RF1=0.934
GAM2=0.000316
RF2=0.826
GOTO 500

440 GAM1=0.000316
RF1=0.826
GAM2=0.01
RF2=0.656
GOTO 500

450 GAM1=0.01
RF1=0.656
GAM2=0.0316
RF2=0.443
GOTO 500

460 GAM1=0.0316
RF1=0.443
GAM2=0.1
RF2=0.246
GOTO 500

470 GAM1=0.1
RF1=0.246
GAM2=0.316
RF2=0.115
GOTO 500

300 CONTINUE

C***** SECTION FOR SHEAR STRAIN DEPENDENT PROPERTY *****
C SELECTION OF SHEAR MODULUS FOR CLAY

IF(GAMMA(I).LE.0.0001) GOTO 600
IF(GAMMA(I).LE.0.000316) GOTO 610
IF(GAMMA(I).LE.0.001) GOTO 620
IF(GAMMA(I).LE.0.00316) GOTO 630
IF(GAMMA(I).LE.0.01) GOTO 640
IF(GAMMA(I).LE.0.0316) GOTO 650
IF(GAMMA(I).LE.0.1) GOTO 660
RF=0.152
GOTO 550

600 RF=1.0
GOTO 550

610 GAM1=0.0001
RF1=1.0
GAM2=0.000316
RF2=0.913
GOTO 500

620 GAM1=0.000316
RF1=0.913
GAM2=0.001
RF2=0.761
GOTO 500

```

630    GAM1=0.001
       RF1=0.761
       GAM2=0.00316
       RF2=0.565
       GOTO 500
640    GAM1=0.00316
       RF1=0.565
       GAM2=0.01
       RF2=0.4
       GOTO 500
650    GAM1=0.01
       RF1=0.4
       GAM2=0.0316
       RF2=0.261
       GOTO 500
660    GAM1=0.0316
       RF1=0.261
       GAM2=0.1
       RF2=0.152
      CONTINUE
C***** LINEAR INTERPOLATION BETWEEN VALUES TO SELECT *****
C   SHEAR MODULUS REDUCTION FACTOR 'RF'
C   RF=RF1+(RF2-RF1)*(GAMMA(I)-GAM1)/(GAM2-GAM1)
550    G=RF*SM
       EE(I)=2.0*G*(1.0+PR)
       E(I)=0.5*(EY+EE(I))
       EMIN=0.2*EM(NC(I,4))
C***** IF ELASTIC MODULUS IS LESS THAN PRE-SELECTED *****
C   MINIMUM VALUE, THEN FIX VALUE AT 20% OF ORIGINAL
C   ELASTIC MODULUS TO AVOID EXCESSIVE LOCAL DEFORMATION
C   AND TO INCORPORATE PLASTIC DEFORMATION
       IF(E(I).LE.EMIN) GOTO 700
       DIFF=EY-E(I)
       RATIO(I)=ABS(DIFF)/EY
C***** CRITERIA FOR CONVERGENCE *****
C   IF THE CHANGE IN ELASTIC MODULUS FOR THE ELEMENT IS
C   LESS THAN 5.0% THEN THE ELEMENT HAS SATISFACTORILY
C   CONVERGED TO A CONSTANT VALUE
       IF(RATIO(I).LE.0.05) GOTO 275
       GOTO 100
700    E(I)=EMIN
       NC(I,5)=3
       RATIO(I)=0.0
       GOTO 100
C***** ELASTIC MODULI FOR CONCRETE ELEMENTS *****
200    E(I)=EM(NC(I,4))
       GOTO 220
C***** MINIMUM ELASTIC MODULUS *****
210    E(I)=0.2*EM(NC(I,4))
220    PR=PNU(EM(NC(I,4)))
       SS1=PS1(I)
       SS2=PS2(I)
       EPS1(I)=(SS1-PR*SS2)/E(I)
       EPS2(I)=(SS2-PR*SS1)/E(I)

```

```
GAM(I)=50.0*(EPS1(I)-EPS2(I))
GAMMA(I)=ABS(GAM(I))+STRAIN(I)
RATIO(I)=0.0
GOTO 100
***** ELEMENT MODULUS HAS CONVERGED *****
275  L(I)=1
      RATIO(I)=0.0
100  CONTINUE
      WRITE(6,1010)
      DO 800 I=1,NUMEL
      IF(RATIO(I).LE.0.0001) GOTO 750
      GOTO 775
750  LL=LL+1
775  WRITE(6,*)
      I,GAMMA(I),E(I),RATIO(I)
800  CONTINUE
900  CONTINUE
1010 FORMAT(//,' ELEM.NO SHEAR STRAIN ELAST.MOD.
1           CONVERGENCE',//)
      RETURN
      END
```

```

C*****
C*
C* SUBROUTINE RDIS: GENERATES THE DISPLACEMENT VECTOR AND
C* THE STRESSES FOR EACH ELEMENT
C*
C*****
C*
C* COMMENTS: THIS SUBROUTINE GENERATES THE OUTPUT FOR THE
C* NODAL DISPLACEMENTS THAT WERE PREVIOUSLY SOLVED IN
C* SECOND PART OF SUBROUTINE 'SYMBOL'. THE SUBROUTINE
C* GENERATES THE NORMAL AND SHEAR STRESS COMPONENTS FOR
C* EACH ELEMENT UTILIZING THE DISPLACEMENT VECTOR TO OBTAIN
C* THE STRAIN VECTOR. MULTIPLYING THE STRAIN VECTOR BY THE D-MATRIX,
C* THE STRESS VECTOR CAN BE ESTABLISHED. THIS PROCEDURE MAY BE FOUND IN J. S. PRZEMIENIECKI'S
C* "THEORY OF MATRIX STRUCTURAL ANALYSIS", McGRAW-HILL BOOK COMPANY (1968), PAGES 84-85. USING THESE NORMAL
C* STRESSES, PRINCIPAL STRESSES AND MAXIMUM SHEAR STRESS CAN BE DETERMINED. THE PROCEDURE FOR THIS IS FOUND IN
C* STRENGTH OF MATERIALS TEXTBOOKS SUCH AS E. P. POPOV'S "MECHANICS OF MATERIALS", (SECOND EDITION) PRENTICE-HALL (1978), PAGES 240-243.
C*
C*****
C*
C* SAI,SA2      - PREDEFINED FUNCTION FOR MAXIMUM/MINIMUM PRINCIPAL STRESSES
C* NUHNP        - TOTAL NUMBER OF NODAL POINTS
C* IE(I,J)      - NUMBER SIGNIFYING A PARTICULAR DEGREE OF FREEDOM (D.F.) AT NODE 'I':
C*                   J = 1, X-DIRECTION D.F.
C*                   J = 2, Y-DIRECTION D.F.
C* V(***)       - SOLUTION VECTOR FOR DISPLACEMENTS OF D.F.
C* U(I,1)        - HORIZONTAL DISPLACEMENT AT NODE 'I'
C* U(I,2)        - VERTICAL DISPLACEMENT AT NODE 'I'
C* NUMEL        - TOTAL NUMBER OF ELEMENTS
C* E(I)          - MODULUS OF ELASTICITY FOR ELEMENT 'I'
C* PNU(***)     - POISSON'S RATIO FOR MATERIAL LAYER
C* IC(I,J)      - ELEMENT INFORMATION:
C*                   NC(***,1) = MEMBER INCIDENCE
C*                   NC(***,2) = MEMBER INCIDENCE
C*                   NC(***,3) = MEMBER INCIDENCE
C*                   NC(***,4) = LAYER NUMBER
C* W(*)          - VECTOR OF THE SIX NODAL DEGREES OF FREEDOM OF A TRIANGULAR ELEMENT
C* X(*),Y(*)    - VECTORS OF GLOBAL COORDINATES FOR ELEMENT
C* SIG(II)       - ELEMENT STRAIN VECTOR
C* B(IL,J)      - LOCAL STRAIN DISPLACEMENT MATRIX
C* D(II,J)      - ELASTIC CONSTITUENT MATRIX OF ELEMENT MATERIAL PROPERTIES EXCLUDING ELASTIC MODULUS
C* A             - TWICE THE AREA OF THE TRIANGULAR ELEMENT
C*
C*****

```

```

C*****
C*
C* SIGMA(II) = NORMAL STRESSES AND SHEAR STRESS FOR
C* ELEMENT: II = 1, SIGMA-X
C* II = 2, SIGMA-Y
C* II = 3, SIGMA-XY
C* SS1 = MAXIMUM PRINCIPAL STRESS
C* SS2 = MINIMUM PRINCIPAL STRESS
C* SS3 = MAXIMUM SHEAR STRESS
C* SIGM(II,I) = GLOBAL NORMAL AND SHEAR STRESS MATRIX
C*
C***** SUBROUTINE RDIS(V,D,SIGM,NUMNP,IE,IC,XX,YY,EM,
1 PNU,E,U)
1 DIMENSION V(538),U(303,2),D(3,3),B(3,6),XX(303),
1 YY(303),IE(303,2)
1 DIMENSION IC(536,5),EM(14),X(3),Y(3),SIG(3),SIGMA(3)
1 ,PNU(14),SIGM(3,536)
1 DIMENSION W(6),E(536)
C***** DEFINE FUNCTIONS FOR PRINCIPAL STRESSES *****
1 SAI(S1,S2,S3)=((S1+S2)/2.)+SQRT(((S1-S2)/2.)**2+S3*
1 S3)
1 SA2(S1,S2,S3)=((S1+S2)/2.)-SQRT(((S1-S2)/2.)**2+S3*
1 S3)
C***** SECTION FOR PRESENTING NODAL DISPLACEMENTS *****
DO 100 I=1,NUMNP
IF (IE(I,1)) 20,30,20
30 U(I,1)=0.0
GOTO 40
20 U(I,1)=V(IE(I,1))
40 IF (IE(I,2)) 50,60,50
60 U(I,2)=0.0
GOTO 100
50 U(I,2)=V(IE(I,2))
100 CONTINUE
WRITE(6,1000)
WRITE(6,2000) (I,U(I,1),U(I,2); I=1,NUMNP)
WRITE(6,3005)
C***** SECTION TO DETERMINE ELEMENT NORMAL STRESSES *****
DO 300 IJ=1,NUMEL
I=IJ
EY=E(I)
PR=PNU(IC(I,4))
I1=IC(I,1)
I2=IC(I,2)
I3=IC(I,3)
W(1)=U(I1,1)
W(2)=U(I1,2)
W(3)=U(I2,1)
W(4)=U(I2,2)
W(5)=U(I3,1)
W(6)=U(I3,2)
X(1)=XX(I1)

```

```
Y(1)=YY(I1)
X(2)=XX(I2)
Y(2)=YY(I2)
X(3)=XX(I3)
Y(3)=YY(I3)
CALL BDEFIN(B,X,Y,A)
CALL DMAT(PR,D)
DO 400 II=1,3
SIGMA(II)=0.0
400
SIG(II)=0.0
DO 500 II=1,3
DO 500 J=1,6
C***** {E} = [B]{U} *****
500 SIG(II)=SIG(II)+B(II,J)*W(J)
DO 600 II=1,3
DO 600 J=1,3
C***** {S} = [D][B]{U} *****
600 SIGMA(II)=SIGMA(II)+D(II,J)*SIG(J)*EY/A
C***** SECTION TO CALCULATE PRINCIPAL STRESSES AND *****
C MAXIMUM SHEAR STRESS
SS1=S1(SIGMA(1),SIGMA(2),SIGMA(3))
SS2=S2(SIGMA(1),SIGMA(2),SIGMA(3))
SS3=(SS1-SS2)/2.
WRITE(6,67) I,(SIGMA(II),II=1,3),SS1,SS2,SS3
DO 700 II=1,3
700 SIGM(II,I)=SIGMA(II)
300 CONTINUE
67 FORMAT(1X,I3,6E12.4)
1000 1 FORMAT('1'/2(6X,'NODE NO.',4X,'X-DISPL',6X,'Y-DISPL
'9/2X,2(4X,10(1H*),2X,9(1H*),4X,9(1H*))//')
2000 FORMAT(2X,2(7X,I3,7X,E9.3,4X,E9.3))
3005 1 FORMAT(///,' ELEM SIGMA-X - SIGMA-Y SIGMA-XY
1 PRINCIPAL STRESSES MAX SHEAR STRESS',/)
RETURN
END
```

```

*****
C*
C* SUBROUTINE RRDIS: GENERATES THE DISPLACEMENT VECTOR AND *
C* THE STRESSES FOR EACH ELEMENT
C*
*****
C*
C* COMMENTS: THIS SUBROUTINE GENERATES THE OUTPUT FOR THE *
C* NODAL DISPLACEMENTS THAT WERE PREVIOUSLY SOLVED IN *
C* SECOND PART OF SUBROUTINE 'SYMBOL'. THE SUBROUTINE *
C* GENERATES THE NORMAL AND SHEAR STRESS COMPONENTS FOR *
C* EACH ELEMENT UTILIZING THE DISPLACEMENT VECTOR TO OBTAIN *
C* THE STRAIN VECTOR. MULTIPLYING THE STRAIN VECTOR BY *
C* THE D-MATRIX, THE STRESS VECTOR CAN BE ESTABLISHED. *
C* THIS PROCEDURE MAY BE FOUND IN J. S. PRZEMIENIECKI'S *
C* "THEORY OF MATRIX STRUCTURAL ANALYSIS", McGRAW-HILL *
C* BOOK COMPANY (1968), PAGES 84-85. USING THESE NORMAL *
C* STRESSES, PRINCIPAL STRESSES AND MAXIMUM SHEAR STRESS *
C* CAN BE DETERMINED. THE PROCEDURE FOR THIS IS FOUND IN *
C* STRENGTH OF MATERIALS TEXTBOOKS SUCH AS E. P. POPOV'S *
C* "MECHANICS OF MATERIALS" (SECOND EDITION) PRENTICE *
C* -HALL (1978), PAGES 240-243.
C*
*****
C*
C* SAI,SA2      = PREDEFINED FUNCTION FOR MAXIMUM/MINIMUM *
C*                 PRINCIPAL STRESSES
C* NUMNP        = TOTAL NUMBER OF NODAL POINTS
C* IE(I,J)      = NUMBER SIGNIFYING A PARTICULAR DEGREE OF,
C*                 FREEDOM (D.F.) AT NODE 'I':
C*                 J = 1, X-DIRECTION D.F.
C*                 J = 2, Y-DIRECTION D.F.
C* V(***)       = SOLUTION VECTOR FOR DISPLACEMENTS OF D.F.
C* U(I,1)        = HORIZONTAL DISPLACEMENT AT NODE 'I'
C* U(I,2)        = VERTICAL DISPLACEMENT AT NODE 'I'
C* NI           = ITERATION NUMBER FOR PIECEWISE LINEAR
C*                 ANALYSIS
C* NUMEL        = TOTAL NUMBER OF ELEMENTS
C* E(I)          = MODULUS OF ELASTICITY FOR ELEMENT 'I'
C* PHU(***)     = POISSON'S RATIO FOR MATERIAL LAYER
C* IC(I,J)      = ELEMENT INFORMATION:
C*                 NC(***,1) = MEMBER INCIDENCE
C*                 NC(***,2) = MEMBER INCIDENCE
C*                 NC(***,3) = MEMBER INCIDENCE
C*                 NC(***,4) = LAYER NUMBER
C* W(*)          = VECTOR OF THE SIX NODAL DEGREES OF FREEDOM
C*                 OF A TRIANGULAR ELEMENT
C* X(*),Y(*)    = VECTORS OF GLOBAL COORDINATES FOR ELEMENT
C* SIG(IL)       = ELEMENT STRAIN VECTOR
C* B(IL,J)      = LOCAL STRAIN DISPLACEMENT MATRIX
C* D(IL,J)      = ELASTIC CONSTITUENT MATRIX OF ELEMENT MAT-
C*                 ERIAL PROPERTIES EXCLUDING ELASTIC MODULUS
C*
*****

```

```

C*****
C* A      = TWICE THE AREA OF THE TRIANGULAR ELEMENT *
C* SIGMA(II) = NORMAL STRESSES AND SHEAR STRESS FOR *
C*           ELEMENT: II = 1, SIGMA-X *
C*           II = 2, SIGMA-Y *
C*           II = 3, SIGMA-XY *
C* SS1,PS1(I) = MAXIMUM PRINCIPAL STRESS (MPa) *
C* SS2,PS2(I) = MINIMUM PRINCIPAL STRESS (MPa) *
C* SS3       = MAXIMUM SHEAR STRESS (MPa) *
C* SIGM(II,I) = GLOBAL NORMAL AND SHEAR STRESS MATRIX *
C*****

```

```

SUBROUTINE RRDIS(V,D,SIGM,NUMEL,NUMNP,IE,IC,XX,YY,EM
1 ,PNU,PS1,PS2,NI,E)
1 DIMENSION V(538),U(303,2),D(3,3),B(3,6),XX(303),
1 YY(303),IE(303,2),IC(536,5),EM(14),X(3),Y(3),SIG(3),
2 SIGMA(3),PNU(14),SIGH(3,536),W(6),E(536),PS1(536),
3 PS2(536)
C***** DEFINE FUNCTIONS FOR PRINCIPAL STRESSES *****
SA1(S1,S2,S3)=((S1+S2)/2.)+SQRT(((S1-S2)/2.)**2+S3*1
1 S3)
SA2(S1,S2,S3)=((S1+S2)/2.)-SQRT(((S1-S2)/2.)**2+S3*1
1 S3)
C***** SECTION FOR PRESENTING NODAL DISPLACEMENTS *****
DO 100 I=1,NUMNP
IF (IE(I,1)) 20,30,20
30 U(I,1)=0.0
GOTO 40
20 U(I,1)=V(IE(I,1))
40 IF (IE(I,2)) 50,60,50
60 U(I,2)=0.0
GOTO 100
50 U(I,2)=V(IE(I,2))
CONTINUE
IF (NI.EQ.1) GOTO 150
GOTO 150
CONTINUE
WRITE(6,1000)
WRITE(6,2000) (I,U(I,1),U(I,2), I=1,NUMNP)
WRITE(6,3005)
175 CONTINUE
C***** SECTION TO DETERMINE ELEMENT NORMAL STRESSES *****
DO 300 IJ=1,NUMEL
I=IJ
IF (NI.EQ.1) GOTO 200
EY=E(I)
GOTO 250
200 EY=EM(IC(I,4))
250 PR=PNU(IC(I,4))
I1=IC(I,1)
I2=IC(I,2)
I3=IC(I,3)

```

```

W(1)=U(I1,1)
W(2)=U(I1,2)
W(3)=U(I2,1)
W(4)=U(I2,2)
W(5)=U(I3,1)
W(6)=U(I3,2)
X(1)=XX(I1)
Y(1)=YY(I1)
X(2)=XX(I2)
Y(2)=YY(I2)
X(3)=XX(I3)
Y(3)=YY(I3)
CALL BDEFIN(B,X,Y,A)
CALL DMAT(PR,D)
DO 400 II=1,3
SIGMA(II)=0.0
400 SIGG(II)=0.0
DO 500 II=1,3
DO 500 J=1,6
C***** {E}=[B]{U} *****
500 SIG(II)=SIG(II)+B(II,J)*W(J)
DO 600 II=1,3
DO 600 J=1,3
C***** [S]=[D][B]{U} *****
600 SIGMA(II)=SIGMA(II)+D(II,J)*SIG(J)*EY/A
C***** SECTION TO CALCULATE PRINCIPAL STRESSES AND *****
C MAXIMUM SHEAR STRESS
SS1=SA1(SIGMA(1),SIGMA(2),SIGMA(3))
PS1(I)=SS1
SS2=SA2(SIGMA(1),SIGMA(2),SIGMA(3))
PS2(I)=SS2
SS3=(SS1-SS2)A2.
IF (NI.EQ.1) GOTO 650
GOTO 675
650 WRITE(6,67) I,(SIGMA(II),II=1,3),SS1,SS2,SS3
675 CONTINUE
DO 700 II=1,3
700 SIGM(II,I)=SIGMA(II)
300 CONTINUE
67 FORMAT(1X,I3,6E12.4)
1000 FORMAT('1'//2(6X,'NODE NO.',4X,'X-DISPL',6X,'Y-DISPL',
      '0/2X;2(4X,10(1H*),2X,9(1H*),4X,9(1H*))//),
2000 FORMAT(2X,2(7X,I3,7X,E9.3,4X,E9.3))
3005 FORMAT(//, ' ELEM SIGMA-X' SIGMA-Y SIGMA-XY
      1 PRINCIPAL STRESSES MAX SHEAR STRESS',/)
      RETURN
END

```

```

*****
C*
C* SUBROUTINE SCOVE: DETERMINES VARIANCES OF STRESSES
C*
C*
C* COMMENTS: THIS SUBROUTINE CALCULATES THE VARIANCES OF
C* STRESSES USING THE FIRST TWO TERMS OF A TAYLOR SERIES
C* EXPANSION ABOUT THE EQUILIBRIUM STRESS EQUATIONS.
C* THIS ANALYSIS IS PERFORMED ON ONLY SELECTED ELEMENTS
C* 'IV', AS INPUT IN THE MAIN PROGRAM. THE LATTER SECT-
C* IONS DETERMINE C.O.V. OF THE STRESSES (HORIZONTAL,
C* VERTICAL OR SHEAR) BY CALCULATING THE RATIO OF THE
C* ELEMENT'S STANDARD DEVIATION (SQUARE ROOT OF VARLANCE)
C* TO THE MEAN STRESS. (USING MEAN ELASTIC MODULI).
C*
*****
C* NES      = NUMBER OF ELEMENTS CONSIDERED FOR STOCHAST-
C* IC STRESS ANALYSIS
C* IV(I)    = ELEMENT NUMBER FOR ELEMENTS CONSIDERED FOR *
C* STOCHASTIC STRESS ANALYSIS
C* AN       = CORRELATION DISTANCE FACTOR (FIXED)
C* NUMEL   = TOTAL NUMBER OF ELEMENTS
C* GT(M,N) = MATRIX INDICATING RELATIVE DISTANCE OF *
C* CENTROIDS OF ELEMENTS
C* RO       = PRODUCT OF CORRELATION DISTANCE FACTOR AND *
C* DIAMETER OF STRUCTURE
C* STD(M)   = STANDARD DEVIATION OF ELASTIC MODULUS FOR *
C* ELEMENT 'M'.
C* R        = COVARIANCE OF ELASTIC MODULI BETWEEN TWO *
C* ELEMENTS
C* DS(M,I)  = PREDEFINED FUNCTION {H} , IN SUBROUTINE
C* 'MAT'
C* VAR(NEL,I) = VARIANCE OF THE THREE STRESSES ASSOCIATED
C* WITH THE ELEMENT 'NEL'
C* SIGM(1,JJ) = MEAN HORIZONTAL STRESS FOR ELEMENT 'JJ'
C* SIGM(2,JJ) = MEAN VERTICAL STRESS FOR ELEMENT 'JJ'
C* SIGM(3,JJ) = MEAN SHEAR STRESS FOR ELEMENT 'JJ'
C* STND     = STANDARD DEVIATION OF STRESS FOR ELEMENT
C* RCOV     = COEFFICIENT OF VARIATION OF STRESS
C* R        = RATIO OF STANDARD DEVIATION TO MEAN STRESS
*****

```

```

SUBROUTINE SCOVE(NE,NC,NUMEL,XX,YY,X,Y,E,PNU,V,DFU,D
1 ,STD,NES,IV,NW,SIGM)
DIMENSION NE(303,2),NC(536,5),X(536),Y(536),XX(303),
1 YY(303),E(536),PNU(14),V(538),DFU(538,536),D(3,3),
2 IV(47),STD(536),VAR(47,3),SIGM(3,536),RVAR(47,3)
DIMENSION DS(536,3)
COMMON/GTC/GT(536,536),RO
WRITE(6,1000)
1000 WRITE(6,*)
2000 WRITE(6,*) (IV(I),I=1,NES)

```

```

AN=0.1*(NW-1.)
WRITE(6,400) AN
WRITE(6,*) 'VARIANCES OF STRESSES:'
WRITE(6,1010)
DO 200 NEL=1,NES
NEE=IV(NEL)

C***** DETERMINES {H} VALUES FOR SELECTED ELEMENTS *****
C          ij
1      CALL MAT(NEE,NUMEL,NC,NE,XX,YY,E,PNU,V,DFU,DS,D,
KODE)
DO 500 I=1,NES
DO 500 J=1,3
VAR(I,J)=0.
500  CONTINUE
DO 600 M=1,NUMEL
DO 600 N=M,NUMEL
GETA=GT(M,N)
R=EXP(-GETA/RO)*STD(M)*STD(N)
DO 300 I=1,3
C***** DIAGONAL TERMS INCLUDED ONCE *****
IF(M.EQ.N)CONST=DS(M,I)*DS(M,I)*R
C***** OFF-DIAGONAL TERMS INCLUDED TWICE DUE TO *****
C      SYMMETRY
IF(M.NE.N)CONST=DS(M,I)*DS(N,I)*R*2.
C***** VARIANCE OF STRESSES *****
300  VAR(NEL,I)=VAR(NEL,I)+CONST
600  CONTINUE
CONTINUE
WRITE(6,*)NEE,VAR(NEL,1),VAR(NEL,2),VAR(NEL,3)
DO 100 II=1,3
RVAR(NEL,II)=VAR(NEL,II)
100  CONTINUE
200  CONTINUE
C***** CALCULATES C.O.V. OF HORIZONTAL STRESS *****
WRITE(6,1015)
DO 700 I=1,NES
JJ=IV(I)
STRESS=SIGM(1,JJ)*1000.0
STND=(SQRT(RVAR(I,1)))*1000.0
RCOV=ABS(STND/STRESS)
WRITE(6,*) JJ,STRESS,STND,RCOV
700  CONTINUE
C***** CALCULATES C.O.V. OF VERTICAL STRESS *****
WRITE(6,1020)
DO 800 I=1,NES
JJ=IV(I)
STRESS=SIGM(2,JJ)*1000.0
STND=(SQRT(RVAR(I,2)))*1000.0
RCOV=ABS(STND/STRESS)
WRITE(6,*) JJ,STRESS,STND,RCOV
800  CONTINUE

```

```
C***** CALCULATES C.O.V. OF SHEAR-STRESS *****
      WRITE(6,1025)
      DO 900 I=1,NES
      JJ=IV(I)
      STRESS=SIGHM(3,JJ)*1000.0
      STND=(SQRT(WAR(I,3)))*1000.0
      RCOV=ABS(STND/STRESS)
      WRITE(6,*) JJ,STRESS,STND,RCOV
900   CONTINUE
400   FORMAT(//,' RATIO OF CORRELATION DISTANCE TO
1    FOUNDATION WIDTH IS ',F7.2,/)
1000  FORMAT(///,' STOCHASTIC ANALYSIS OF SELECTED
1    ELEMENTS:',/)
1010  FORMAT(//,3X,' ELEM. NO.',5X,'SIGMA-X',8X,'SIGMA-Y'
1    ,7X,'SIGMA-XY',/)
1015  FORMAT(//,' ELEM. NO. HORZ-STRESS(kPa) STD(kPa)
1    C.O.V. ',/)
1020  FORMAT(//,' ELEM. NO. VERT-STRESS(kPa) STD(kPa)
1    C.O.V. ',/)
1025  FORMAT(//,' ELEM. NO. SHEAR STRESS(kPa) STD(kPa)
1    C.O.V. ',/)
      RETURN
      END
```

```

C*****
C*
C* SUBROUTINE SCOVEN: DETERMINES VARIANCES OF STRESSES
C*
C*****
C*
C* COMMENTS: THIS SUBROUTINE CALCULATES THE VARIANCES OF
C* STRESSES USING THE FIRST TWO TERMS OF A TAYLOR SERIES
C* EXPANSION ABOUT THE EQUILIBRIUM-STRESS EQUATIONS.
C* THIS ANALYSIS IS PERFORMED ON ONLY SELECTED ELEMENTS
C* 'IV', AS INPUT IN THE MAIN PROGRAM.
C*
C*****
C*
C* NES      - NUMBER OF ELEMENTS CONSIDERED FOR STOCHASTIC STRESS ANALYSIS
C* IV(I)    - ELEMENT NUMBER FOR ELEMENTS CONSIDERED FOR STOCHASTIC STRESS ANALYSIS
C* AN       - CORRELATION DISTANCE FACTOR (FIXED)
C* NUMEL   - TOTAL NUMBER OF ELEMENTS
C* GT(M,N) - MATRIX INDICATING RELATIVE DISTANCE OF CENTROIDS OF ELEMENTS
C* RO       - PRODUCT OF CORRELATION DISTANCE FACTOR AND DIAMETER OF STRUCTURE
C* STD(M)   - STANDARD DEVIATION OF ELASTIC MODULUS FOR ELEMENT 'M'
C* R        - COVARIANCE OF ELASTIC MODULI BETWEEN TWO ELEMENTS
C* DS(M,I)  - PREDEFINED FUNCTION {M}, IN-SUBROUTINE 'MAT' [1]
C* VAR(NEL,I) - VARIANCE OF THE THREE STRESSES ASSOCIATED WITH THE ELEMENT 'NEL'
C* VARS(N,I) - STORED ARRAY OF VARIANCES OF STRESSES FOR THIS LOAD STAGE
C*
C*****

```

```

SUBROUTINE SCOVEN(NE,NC,NUMEL,XX,YY,X,Y,E,PNU,V,DFU,
1 D,STD,NES,IV,NW,VARS)
DIMENSION NE(303,2),NC(536,5),X(536),Y(536),XX(303),
1 YY(303),E(536),PNU(14),V(538),DFU(538,536),D(3,3),
2 IV(47),STD(536),VAR(47,3),VARS(47,3),DS(536,3)
COMMON/GTC/GT(536,536),RO
WRITE(6,1000)
WRITE(6,*) (IV(I),I=1,NES)
AN=0.1*(NW-1.)
WRITE(6,400) AN
WRITE(6,*) 'VARIANCES OF STRESSES:'
WRITE(6,1010)
DO 200 NEL=1,NES
NEE=IV(NEL)

```

```

***** DETERMINES {H} VALUES FOR SELECTED ELEMENTS *****
C
      CALL MAT(NEE,NUMEL,NC,NE,XX,YY,E,PNU,V,DFU,DS,D,
1      KODE)
      DO 500 I=1,NES
      DO 500 J=1,3
      VAR(I,J)=0.
500   CONTINUE
      DO 600 M=1,NUMEL
      DO 600 N=M,NUMEL
      GETA=GT(M,N)
      R=EXP(-GETA/RO)*STD(M)*STD(N)
      DO 300 I=1,3
***** DIAGONAL TERMS INCLUDED ONCE *****
      IF(M.EQ.N)CONST=DS(M,I)*DS(M,I)*R
***** OFF-DIAGONAL TERMS INCLUDED TWICE DUE TO *****
C      SYMMETRY
      IF(M.NE.N)CONST=DS(M,I)*DS(N,I)*R*2.
***** VARIANCE OF STRESSES *****
      VAR(NEL,I)=VAR(NEL,I)+CONST
***** STORE IN NEW ARRAY SINCE 'VAR' IS SET TO *****
C      ZERO FOR EACH LOADING STAGE
      VARS(NEL,I)=VAR(NEL,I)
300   CONTINUE
600   CONTINUE
      WRITE(6,*)NEE,VAR(NEL,1),VAR(NEL,2),VAR(NEL,3)
200   CONTINUE
400   FORMAT(//,' RATIO OF CORRELATION DISTANCE TO
1      FOUNDATION WIDTH IS ',F7.2,/)
1000  FORMAT(//,' STOCHASTIC ANALYSIS OF SELECTED
1      ELEMENTS:',/)
1010  FORMAT(//,3X,' ELEM. NO.',5X,'SIGMA-X',8X,'SIGMA-Z'
1      ,7X,'SIGMA-XY',/)
      RETURN
      END

```

```

C*****
C*
C* SUBROUTINE SYMBOL: DECOMPOSING AND BACK-SUBSTITUTION OF *
C* DEGREES OF FREEDOM
C*
C*****
C*
C* COMMENTS: THIS SUBROUTINE IS COMPOSED OF TWO PARTS: ONE
C* FOR DECOMPOSING THE GLOBAL STIFFNESS MATRIX AND THE
C* OTHER FOR SOLVING THE DEGREES OF FREEDOM (NODAL DIS-
C* PLACEMENTS). SECTION 1 TAKES THE STIFFNESS MATRIX (IN
C* BAND FORM FROM SUBROUTINE 'ASMB') TO DECOMPOSE IT TO
C* AN UPPER TRIANGULAR MATRIX USING THE GAUSSIAN ELIMIN-
C* ATION PROCEDURE. SECTION 2 DECOMPOSES THE LOAD VECTOR
C* 'B' AND SOLVES FOR THE NODAL DISPLACEMENTS USING THE
C* METHOD OF BACKWARD SUBSTITUTION. FURTHER DISCUSSION
C* ON THIS SOLUTION TECHNIQUE FOR BAND MATRICES CAN BE
C* FOUND IN L. J. SEGERLIND'S "APPLIED FINITE ELEMENT
C* ANALYSIS", JOHN WILEY & SONS (1976), PAGES 377-379.
C*
C*****
C* KKK - NUMBER FOR DETERMINING SECTION OF SUBROUTINE
C* ACCESSED: KKK = 1, DECOMPOSING
C* = 2, BACK-SUBSTITUTION
C* A(I,J) - GLOBAL STIFFNESS MATRIX
C* B(I) - INPUT AS LOAD VECTOR/OUTPUT AS SOLUTION VECTOR
C* NN - TOTAL NUMBER OF DEGREES OF FREEDOM (D.F.)
C* MM - SEMI-BANDWIDTH
C* NMAX - NUMBER LIMITING THE MAXIMUM SIZE OF BOTH
C* STIFFNESS MATRIX AND LOAD/SOLUTION VECTORS
C*
C*****

```

```

SUBROUTINE SYMBOL(KKK,A,B,NN,MM,NMAX)
DIMENSION A(NMAX,32),B(NMAX)
GO TO (5,275),KKK
C***** SECTION FOR DECOMPOSING BANDED STIFFNESS MATRIX *****
C* SPACE AND COMPUTATION TIME
5 DO 270 N=1,NN
DO 260 L=2,MM
C=A(N,L)/A(N,1)
I=N+L-1
IF(NN-I) 260,240,240
240 J=0
DO 250 K=L,MM
J=J+1
250 A(I,J)=A(I,J)-C*A(N,K)
260 A(I,L)=C
270 CONTINUE
GO TO 500

```

C***** SECTION FOR BACK-SUBSTITUTION TO OBTAIN SOLUTION *****
C VECTOR FOR ALL D.F. (NODAL DISPLACEMENTS)
275 DO 290 N=1,NR
Y=B(N)
DO 280 L=2,MM
I=N+L-1
IF(NN-I), 290, 280, 280
280 B(I)=B(I)-A(N,L)*Y
290 B(N)=Y/A(N,1)
NN
N=NN
300 N=N-1
IF(N)350,500,350
350 DO 400 K=2,MM
L=N+K-1
IF(NN-L), 400, 370, 370
370 B(N)=B(N)-A(N,K)*B(L)
400 CONTINUE
GO TO 300
500 RETURN
END

APPENDIX V

Gross Moment of Inertia for
Ekofisk's Raft Foundation

To determine the gross moment of inertia about an axis passing through its center, the raft foundation of the Ekofisk Tank is subdivided into regular shapes. These subdivisions are indicated in the plan outline shown in Figure V.1. The subdivided structure consists of:

- i) a main rectangular area denoted as 1,
- ii) two smaller rectangles denoted as 2, and
- iii) four quarter circles denoted as 3.

To simplify computations, these four quarter circles are treated as two semicircles. For each regular shape, section properties are calculated about its own center. Using the parallel axis theorem, the gross moment of inertia, I_{xx} , is determined:

$$I_{xx} = I_{01} + 2(I_{02} + I_{03} + A_2d_2^2 + A_3d_3^2) \dots$$

V.1

where moments of inertia:

$$I_{01} = 34439 \text{ m}^2$$

$$I_{02} = 73970 \text{ m}^2$$

$$I_{03} = 234940 \text{ m}^2$$

area:

$$A_2 = 622.9 \text{ m}^2$$

$$A_3 = 2298.2 \text{ m}^2$$

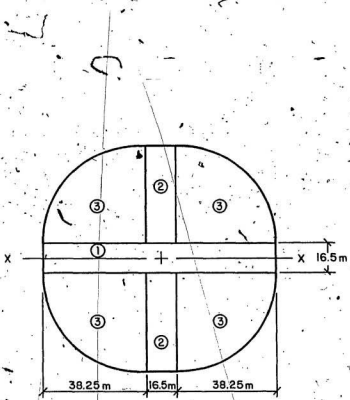


FIGURE V.1 SUBDIVISIONS OF RAFT FOUNDATION

distance from centroid to x-x axis:

$$d_2 = 27.13 \text{ m}$$

$$d_3 = 24.48 \text{ m}$$

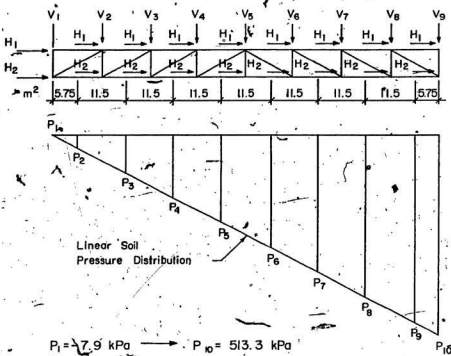
$$\Delta I_{xx} = 4324150 \text{ m}^4$$

APPENDIX VI

Nodal Forces for Combined Gravity
and Wave Loading at Ekofisk

The November 1973 stormy wave conditions have produced a linear pressure distribution beneath the Ekofisk Tank foundation as indicated by Figure VI.1. It has ranged from a minimum of -7.9 kPa (tension) to 513.3 kPa maximum. To equate this loading to nodal forces on a one-metre wide strip, these soil pressures are averaged over the tributary areas to arrive at the vertical node loadings.

Using this vertical load distribution, an overturning moment of 370.5 MN-m for a one-meter wide strip is calculated about the raft foundation's centroid. This moment is 1.512% of the total overturning moment. Since the overturning moment at the base of the gravity structure arises from the eccentricity of the horizontal wave force, the same percentage of the 677 MN total horizontal force is considered acting on the one-metre strip. The net horizontal strip force is estimated at 10.238 MN. Considering this force to be distributed equally over the eighteen nodes of the elements representing the tank, results with a horizontal load of 0.5688 MN per node.



Soil Pressure (kPa)	Averaging	Tributary Area (m^2)	Nodal Force (MN)
P_1 -7.9		5.75	V_1 0.048
P_2 24.7		11.5	V_2 0.6584
P_3 89.6		11.5	V_3 1.4076
P_4 155.0		11.5	V_4 2.1568
P_5 220.1		11.5	V_5 2.9061
P_6 285.3		11.5	V_6 3.6553
P_7 350.4		11.5	V_7 4.4045
P_8 415.6		11.5	V_8 5.1537
P_9 480.7		5.75	V_9 2.8578
P_{10} 513.3			

FIGURE VI:1 VERTICAL NODAL FORCE DERIVATION



